Cranfield
UNIVERSITY

Alessandro Poma

Automatic solid-phase synthesis of molecularly imprinted nanoparticles (MIP NPs)

Cranfield Health

PhD Thesis
Academic Years 2009 - 2012

Supervisors: Prof. Sergey A. Piletsky
Dr. Antonio R. Guerreiro

November 2012

Cranfield

UNIVERSITY

Cranfield Health

PhD Thesis

Academic Years 2009 - 2012

Alessandro Poma

Automatic solid-phase synthesis of molecularly imprinted
nanoparticles (MIP NPs)

Supervisors: Prof. Sergey A. Piletsky
Dr. Antonio R. Guerreiro

November 2012

This thesis is submitted in partial fulfilment of the requirements for
the degree of Doctor of Philosophy

Abstract

Molecularly Imprinted Polymers (MIPs) are potential generic alternatives to antibodies in diagnostics and separations. To compete with biomolecules in these technological niches, MIPs need to share the characteristics of antibodies (solubility, size, specificity and affinity) whilst maintaining the advantages of MIPs (low cost, short development time and high stability). For this reason the interest in preparing MIPs as nanoparticles (MIP NPs) has increased exponentially in the last decade.

This research was aimed at developing an efficient and flexible method for the automatic synthesis of MIP NPs using a solid-phase automated photoreactor. Our approach incorporated a column-cartridge with an immobilised template docked into a thermostatic computer-controllable UV photoreactor, thereby allowing the controlled manufacture of high-affinity MIP NPs with narrow size distributions. The polymerisation was performed through UV-irradiation of the reactor for the desired reaction time. After polymerisation was completed, the column was washed with fresh solvent at a low temperature. At this stage unreacted monomers and other low molecular weight materials were eluted along with low-affinity polymer NPs, leaving the desired high-affinity MIP NPs still bound to the immobilised template phase. These were then collected by increasing the column temperature. Batches of MIP NPs with diameters 30-400 nm and narrow size distributions were prepared for low molecular weight targets including melamine (d = 60 nm, K_D = 6.3 × 10^{-8} M), vancomycin (d = 250 nm, K_D = 3.4 × 10^{-9} M), and a peptide (d = 350 nm, K_D = 4.8 × 10^{-8} M) in less than 3 h/batch. For the first time the reuse of molecular templates in the synthesis of MIPs (≥ 30 batches of MIP NPs) was demonstrated.

For the imprinting of high molecular weight targets such as proteins a second version of automated chemical reactor was developed which was capable of operating in aqueous conditions. It was tested in the preparation of MIP NPs against three protein targets, namely pepsin A, trypsin and α-amylase. The manufacturing cycle took 4 h during which "synthetic antibodies" with 250-300

nm diameter and sub-nanomolar affinity were prepared. All synthesised materials exhibited high specificity towards their respective target compound.

Benefits of the proposed novel approach include: i) uniform binding properties of synthesised MIP NPs, resulting from affinity-based separation on column; ii) eliminating contamination of the product with template; iii) possibility of reusing template; iv) ease of automation and standardisation; v) the final product is obtained in a pure form obviating the need for lengthy post-synthesis purification steps. We believe the developed MIP NPs might be used in diagnostic applications and, in the future, possibly in *in vivo* applications, such as drug delivery, imaging and pharmacological activity.

Keywords:

Acknowledgements

A. P.: "What is my project going to be?"

S. P.: "Well, you could develop an artificial receptor, but it is not really new…OR…You could work on this new challenging project regarding the development of a machine to produce MIP nanoparticles…"

First day at Cranfield University, 11/01/2010

Table of contents

Aims and objectives

The aim of the project presented and discussed in this thesis is to investigate and develop useful tools and strategies to automate the synthesis of MIP NPs able to mimic the characteristics of natural antibodies in terms of size, affinity, and specificity. These approaches should exploit templates immobilised on a convenient solid support (e.g. glass beads), providing a system able to generate MIP nanoparticles with strong affinity and specificity and in good yields and purity, enabling large-scale production for industrial applications.

To achieve this aim, the objectives of this 3-year research have been:

1.   Investigation of suitable solid supports for the immobilisation of different kinds of templates (i.e. small molecules and peptides/proteins);

2.   Investigation of an experimental setup compatible with the automation of the imprinting polymerisation process of NPs;

3.   Research and optimisation of the best experimental conditions to synthesise MIP NPs on solid phase and characterisation of the MIP products in terms of physical and recognition properties;

4.   Adaptation of MIP nanomaterials for sensing, separation or therapeutic purposes;

5.   Dissemination of the results of these studies through presentations at international conferences and preparation of patents and papers for submission to peer-reviewed journals.

List of figures

List of tables

List of equations

List of abbreviations

Symbols

°C	Celsius degree
α	Separation factor
c	Centi (10^{-2})
c_m	Critical monomer concentration
cps	Counts per second, fluorescence
d	Diameter
Da	Dalton, mass
eV	Electron volt, energy
g	Gravitational acceleration (9.81 m/s^2)
g	Gram, mass
h	Hour, time
k	Kilo (10^3)
k_{cat}	Turnover number (M^{-1} s^{-1})
IF	Imprinting factor
λ	Wavelength (nm)
$λ_{em}$	Emission wavelength (nm)
$λ_{ex}$	Excitation wavelength (nm)
L	Litre, volume
K_A	Association constant (L/mol)
K_D	Dissociation constant (mol/L)
μ	Micro (10^{-6})
M	Molar (mol/L), concentration
m	Milli (10^{-3})
m	Metre, length
min	Minute, time
mol	Mole, amount
M_n	Number-average molecular weight
M_w	Weight-average molecular weight
n	Nano (10^{-9})
N_A	Avogadro's number (6.023×10^{23})
π	Pi (3.14)

p	Pico (10^{-12})
Q_{max}	Maximum number of binding sites (mol/g)
ρ	Density (mg/mL or g/cm^3)
r	Radius
rpm	Revolutions per minute
s	Second, time
V	Volt, electric potential
W	Watt, power

Abbreviations

2,4-D	2,4-dichlorophenoxyacetic acid
2-VPy	2-vinylpyridine
4-VPy	4-vinylpyridine
5-FU	5-fluorouracil
AAc	Acrylic acid
AAm	Acrylamide
ABCN	1,1'-azobis-(cyclohexanecarbonitrile)
ACN	Acetonitrile
ACPA	4,4'-azobis-(4-cyanopentanoic acid)
AFM	Atomic force microscopy
AIBN	2,2'-azobis-(2-isobutyronitrile)
AMBN	2,2'-azo(2-methylbutyronitrile)
APBA	3-aminophenylboronic acid
APS	Ammonium persulphate
APTMS	3-aminopropyltrimethyloxysilane
APTES	3-aminopropyltriethoxysilane
ATRP	Atom transfer radical polymerisation
AQ	Antraquinone
BCA	Bicinchonic acid
BFA	L,D-Boc-Phenylalanine anilid
BIS	*N,N'*-methylenebisacrylamide
CaCl$_2$	Calcium chloride
CAFF	Caffeine
CEC	Capillary electro-chromatography

CHO	Chinese hamster ovary
CMMC	7-carboxymethoxy-4-methylcoumarin
CNT(s)	Carbon nanotube(s)
CTA	Chain transfer agent
CV	Cyclic voltammetry
DA	Desisopropylatrazine
DARPin(s)	Designed ankyrin repeat protein(s)
DEDTC	Sodium diethyldithiocarbamate trihydrate
DEHP	(2-ethylhexyl)phthalate
DLS	Dynamic light scattering
DMET	2,4-diamino-6-(methacryloyloxy)-ethyl-1,3,5-triazine
DMF	Dimethylformamide
DMSO	Dimethylsulfoxide
DNA	Desossiribonucleic acid
DPA	D-Phenylalanine
DVB	Divinylbenzene
E2	17β-estradiol
EBP	Engineered binding proteins
E. coli	*Escherichia coli*
EGDMA	Ethylene glycol dimethacrylate
ELISA	Enzyme-linked immunosorbent assay
EtOH	Ethanol
FITC	Fluorescein isothiocyanate
GA	Glutaraldehyde
GPC	Gel permeation chromatography
HCOOH	Formic acid
HEK	Human embryonic kidney
HEMA	2-hydroxyethyl methacrylate
HF	Hydrofluoric acid
HPLC	High-perfomance liquid chromatography
IgG(s)	Immunoglobulin(s) G
Iniferter	*Ini*tiator, trans*fer* agent, *ter*minator
IVD	*In vitro* diagnostics

LPA	ʟ-Phenylalanine
LR	2,4,6-trimethylbenzoylphenyl-phosphinic acid ethyl ester
MAA	Methacrylic acid
mAbs	Monoclonal antibodies
MAm	Methacrylamide
ME	β-mercaptoethanol
MeOH	Methanol
MIP(s)	Molecularly Imprinted Polymer(s)
MMA	Methylmethacrylate
MQD	Methacryloyl quinidine
MQN	Methacryloyl quinine
MSM	Metsulfuron-methyl
NaOH	Sodium hydroxide
NIPAm	*N*-isopropylacrylamide
NH_4HF_2	Ammonium hydrogen fluoride
NIP(s)	Non Imprinted Polymer(s)
NMP	*N*-methyl-2-pyrrolidone
NMR	Nuclear magnetic resonance
NOM(s)	Nanoparticles-on-microsphere(s)
NP(s)	Nanoparticle(s)
OPA	*o*-phtalaldehyde
PAD	Pulsed amperometric detection
PAMAM	Poly(amido amine)
PBS	Phosphate buffered saline
PCR	Polymerase chain reaction
PDA	Polydopamine
PDI	Polydispersity index
PEG	Poly(ethylene glycol)
PET	Poly(ethylene terephthalate)
PGMA-*co*-EGDMA	Poly(glycidyl methacrylate-*co*-ethylene glycol dimethacrylate)
PMMA-*co*-AAc	Poly(methyl methacrylate-*co*-acrylic acid)
POC	Point-of-care
PS	Polystyrene

PSP	Pseudostationary phase
PTFE	Polytetrafluoroethylene
PVA	Poly(vinyl alcohol)
PyS	Pyridinium 12-(4-vinylbenzyloxycarbonyl)dodecanesulphate
QCM	Quartz crystal microbalance
RAFT	Reversible addition–fragmentation chain transfer
RNA	Ribonucleic acid
ROS	Reactive oxygen species
SAM	Self-assembled monolayer
SD	Standard deviation
SDS	Sodium dodecyl sulphate
SELEX	Systemic evolution of ligands by exponential enrichment
SEM	Scanning electron microscopy
SERS	Surface-enhanced Raman spectroscopy
SMO	Sulfamethoxazole
SPE	Solid-phase extraction
SPR	Surface plasmon resonance
St	Styrene
TBAm	*N-tert*-butylacrylamide
TBS	TRIS buffered saline
TEM	Transmission electron microscopy
TEMED	*N,N,N',N'*-tetramethylenethylenediamine
TEOS	Tetraethoxysilane
TFMAA	2-(trifluoromethyl)acrylic acid
THO	Theophylline
TNT	2,4,6-trinitrotoluene
TRIM	Trimethylolpropane trimethacrylate
TyS	Pyridinium 12-(cholesteryloxycarbonyloxy)dodecanesulphate
UV	Ultraviolet
V-70	2,2'-azobis(2,4-dimethylvaleronitrile)

1 Introduction

1.1 Antibodies: "all that glisters is not gold"

Molecular recognition processes are playing an important role in various applications such as diagnostics, chemical catalysis, separation systems, and drug delivery. Natural molecular recognition systems, like enzymes, antibodies and receptors, are widely used in the fundamental study of molecular recognition phenomena as well as in the development of practical therapeutic or diagnostic systems (Yan, 2002).

Antibodies largely dominate in most of the commercial applications. To provide an example, the global monoclonal antibodies (mAbs) market in 2009 was evaluated as $40 Billion, with $30 Billion related to therapeutic applications (RNCOS, 2011; Biocompare Surveys and Reports, 2009). The global in vitro diagnostics (IVD) market, another application area for antibodies and enzymes, has been estimated in 2010 as $44 Billion and is expected to reach $52 Billion by the end of 2013. Among the key constituents of the IVD market, the point-of-care (POC) segment holds the major part, followed by immunochemistry and molecular diagnostics (RNCOS, 2011; Espicom, 2011).

Antibodies are proteins which the immune system synthesises to detect and neutralise "non-self" substances (e.g., bacteria, viruses, and toxins), also known as antigens (Hoshino and Shea, 2011). The most commonly used immunoglobulins G (IgGs) possess a Y-shape resulting from the arrangement of two longer ("heavy") chains and two shorter ("light") chains, all stabilised by disulfide bonds, with an average molecular weight of 150–160 kDa. The lower part of the "Y" is referred to as the Fc region, and its role is to confer stability and drive the interactions with other components of the immune system (e.g., effector mechanisms). The upper part of the "Y" is known as the Fab region and contains the variable domains at which the antigen recognition and binding take place (Ruigrok *et al.*, 2011). The antibody–antigen interaction is driven by a precise combination of electrostatic, hydrogen bonding, van der Waals, and/or

hydrophobic forces, which results in extremely strong affinity (Hoshino and Shea, 2011).

Antibodies are undoubtedly highly specific and selective for several kinds of chemical and biological moieties and can be produced on a large scale (Lavignac *et al.*, 2004). Unfortunately, they also show some disadvantages. Their industrial production relies on the cultivation of modified mammalian cell lines [e.g., those from Chinese-hamster ovary (CHO) and human embryonic kidney (HEK)-2930]. The manufacturing process is logistically difficult and expensive (Ansell, 2004; Shukla and Thömmes, 2010; Ruigrok *et al.*, 2011). Furthermore, antibody production against small molecules requires chemical coupling between haptens and a carrier protein in order to generate an immune response in animals (Lavignac *et al.*, 2004) and their purification involves several steps (especially for applications in therapy), which contribute towards the manufacturing costs up to 50-80% of the total (Roque *et al.*, 2004; Steinmeyer and McCormick, 2008). In addition, antibodies also can give rise to immunogenic adverse reactions, in relation with their production method (Hansel *et al.*, 2010). Moreover, it is difficult to generate antibodies against molecules such as immunosuppressant drugs or toxins, because these chemicals act directly on the immune system and prevent its natural response (Haupt *et al.*, 1998a; Urraca *et al.*, 2007). Additionally, being proteins, the characteristic problems related to their usage are low stability and poor performance in organic solvents, at low and high pH and at high temperature (Szenczi *et al.*, 2006; Piletsky and Turner, 2006; Ahrer *et al.*, 2006). All these factors may alter their recognition properties, thus shortening their shelf-life (Hock *et al.*, 1999; Omersel *et al.*, 2010). Finally, biomolecules may be difficult to immobilise on suitable supports for use in assays and sensors (Butler, 2000; Piletsky and Turner, 2006), which is an extremely important feature for developing diagnostic devices.

For all these reasons, other affinity tools, such as engineered binding proteins, aptamers, and molecularly imprinted polymers (MIPs), have gained interest as potential antibodies substitutes. Their attractive features include enhanced

stability, efficient selection and screening procedures, and cost-effective production methods. In the following sections a brief overview of engineered binding proteins (EBPs) and aptamers is provided, before discussing more thoroughly multiple aspects of the Molecular Imprinting approach to produce a new generation of affinity tools suitable for different applications such as diagnostics, therapeutics and drug delivery, as well as separation and catalysis.

1.1.1 Engineered binding proteins (EBPs)

As already stated above, the recognition ability of antibodies relies on a limited variable region structurally embedded in a more conserved framework. In the same way, proteins capable of binding to a certain target might be selected from a random library, characterised by a constant structural peptide framework and randomised variable binding regions. However, a large amount of peptide derivatives have to be generated and screened to successfully design and engineer a binding protein scaffold. This can be achieved by performing high-throughput screening based on molecular display technology, which establishes a physical link between phenotype and genotype. The most commonly used display technology is phage display in which genes encoding proteins of interest are fused to a gene that encodes a phage coat protein. In this way, phage particles can be made to display peptides of interest on their surface (Paschke, 2006; Sidhu and Koide, 2007). *Escherichia coli (E. coli)* cells are infected with the members of the phage library to produce many copies of each of the library members displaying the variant proteins. This library is screened against the immobilised target molecule and the phages with appropriate specificity and affinity are separated and collected in a process known as biopanning. The collected high-affinity phages are used to re-infect *E. coli* cells and the process is repeated iteratively (usually three to five rounds) using more stringent washing steps. Eventually, monoclonal phages are selected, and the high-affinity protein scaffolds identified by sequencing the DNA of the corresponding phage (Ruigrok *et al.*, 2011). Scaffolds that have good stability are required to have a sufficiently long shelf-life, which is important from a commercial point of view. Among the successful examples of engineered proteins there are

fibronectin type III domain, which has a certain degree of similarity with the structure of an immunoglobulin G variable domain, and designed ankyrin repeat proteins (DARPins) (Hey *et al.*, 2005; Binz *et al.*, 2005; Grönwall and Ståhl, 2009). However, developing scaffolds for a certain application is not easy, in particular due to the unpredictable, costly, and time-consuming nature of the screening procedure, hence the commercialisation of these products is still at early stage (Ruigrok *et al.*, 2011).

1.1.2 Aptamers

Nucleic acids ligands (aptamers) can also be exploited as affinity tools. The term "aptamer" derives from the Latin word "aptus", which means "fitting", and the Greek word "meros", which means "particle". Aptamers are short (15–60 nucleotides) single-stranded nucleic acid (DNA or RNA) oligomers with a specific and complex three-dimensional shape, which allows them to recognise a variety of targets ranging from small organic molecules to large protein complexes (Stoltenburg *et al.*, 2007; Ruigrok *et al.*, 2011). Aptamers can exhibit affinities down to the nanomolar range, but in contrast to mAbs they are produced entirely in vitro through the generation of combinatorial libraries (10^{14}–10^{15} synthetic nucleic acid sequences) and the subsequent stringent selection process with the immobilised target. The selected sequences are amplified by polymerase chain reaction (PCR) and used in several selection/amplification cycles (6–20) with increasingly stringent selection conditions in a process called SELEX (systemic evolution of ligands by exponential enrichment). Eventually, these aptamers are cloned, sequenced, and tested for the intended application (Stoltenburg *et al.*, 2007; Ruigrok *et al.*, 2011).

Aptamers with molecular weight 5–20 kDa are smaller than antibodies and can be used in high-density arrays. Furthermore, thanks to their robustness, aptamers can be chemically modified by, e.g., through biotinylation or by addition of fluorescent labels. They are exploited in ELISA assays or as detection elements in biosensors. Target binding may significantly alter the structure of an aptamer in a reversible way and such an event could be exploited to detect molecules of interest, either fluorescently or

electrochemically. Moreover, unlike antibodies, aptamers are easy to regenerate, either at high temperature or high salt concentration which can be used in affinity purification of proteins. Another important advantage is that aptamers can be generated for virtually any target, even those for which antibodies cannot easily be raised (such as toxins or poorly immunogenic molecules). The SELEX process can also be performed under conditions similar to those used in the assay for which the aptamer has been developed. In this way it can be ensured that the oligonucleotide will retain its structure and recognition ability in the final process for which it was intended (Danielsson, 2007).

SELEX processes are, however, quite lengthy and labour intensive (Mairal *et al.*, 2008). In addition attempts to automate SELEX procedure have so far proved to be unsuccessful. Moreover, despite their claimed robustness, aptamers are prone to degradation. Furthermore, commercialisation of aptamer technology has been hindered by exclusive ownership of IP by a small number of companies (Missailidis and Hardy, 2009; Ruigrok *et al.*, 2011).

1.1.3 Molecularly Imprinted Polymers (MIPs)

Among the alternatives to natural recognition systems, Molecularly Imprinted Polymers (MIPs) have shown high promise. The increasing amount of papers and patents published per annum in this area, which has almost tripled over the last twenty years (Figure 1–1) (Whitcombe, 2012), reflects the potential and broad interest in these materials.
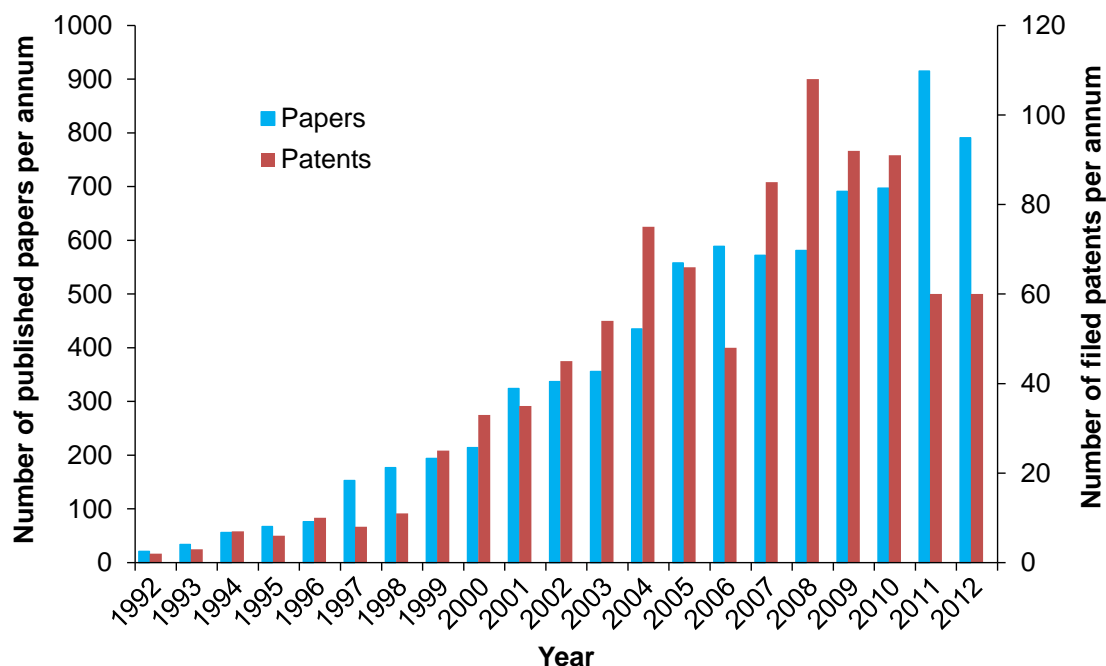
Figure 1–1. Number of published papers and filed patents in the area of molecularly imprinted polymers for the period 1992-2012 (Whitcombe, 2012).

According to the authors of a recent review (Alexander *et al.*, 2006), the first example of molecular imprinting dates back to 1931, in which Polyakov investigated polymerisation process of sodium silicate in water after the addition of ammonium carbonate. He noticed that if the polymerisation process was carried out in presence of an additive (i.e. benzene and toluene), the silica particles produced were able to rebind this additive more than its structural analogues, thus exhibiting a sort of "memory" effect.

However, 40 years more had to pass before the same approach was successfully applied to organic polymers, when Wulff and Sahran (1972) were able to resolve a racemate of glyceric acid by polymerising the vinylphenylboronic ester of the D-enantiomer with divinylbenzene (DVB) and subsequently hydrolysing the ester bonds. During the rebinding process, then, D-glyceric acid reformed a covalent boronate ester bond more than its L-enantiomer, which in turn got more concentrated in solution.

Molecular imprinting, then, has been recently defined as "the construction of ligand selective recognition sites in synthetic polymers where a template (atom,

ion, molecule, complex or a molecular, ionic or macromolecular assembly, including micro-organisms and viruses) is employed in order to facilitate recognition site formation during the covalent assembly of the bulk phase by a polymerisation or polycondensation process, with subsequent removal of some or all of the template being necessary for recognition to occur in the spaces vacated by the templating species" (Alexander *et al.*, 2006). The process is schematically represented in Figure 1–2.
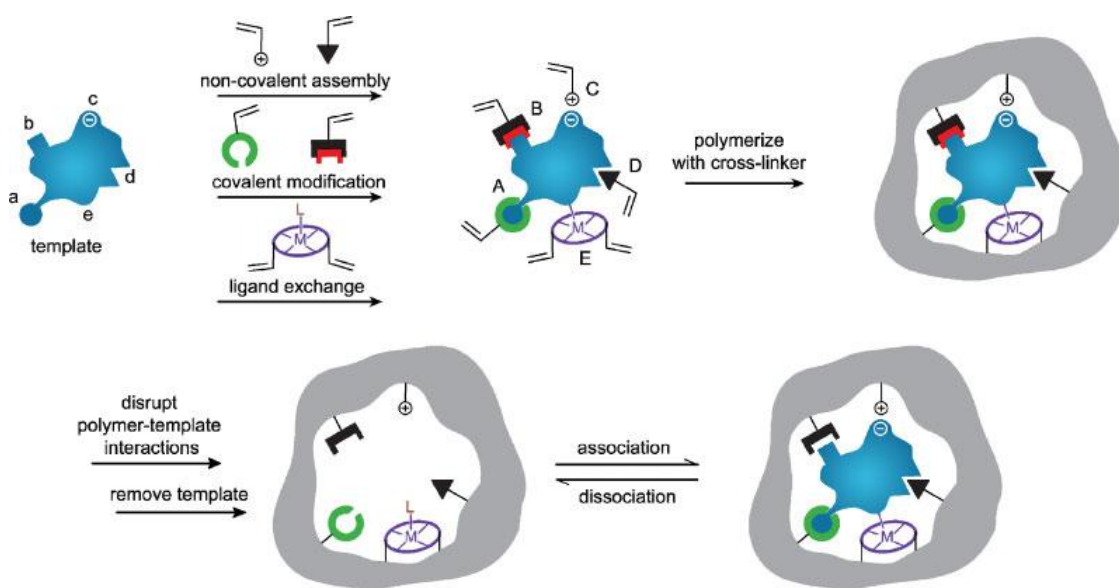
Figure 1–2. Schematic representation molecular imprinting. The template and the functional monomers may interact by: (A) reversible covalent bonds, (B) covalently attached polymerisable binding groups, subsequently activated for non-covalent interaction by template cleavage, (C) electrostatic interactions, (D) hydrophobic or van der Waals interactions, (E) metal-ion mediated interactions. Each one of these is established with complementary functional groups or structural elements of the template (a-e), respectively (adapted from Alexander *et al.*, 2006).

As the figure shows, the synthesis of molecularly imprinted polymers involves one or more types of monomer, which possess functional groups capable of interacting with the target molecule (template), either covalently or through non-covalent interactions. The reaction mixture includes also a cross-linker agent and a porogenic solvent and, after mixing, it is cured, usually thermally or by UV light, thus leading to highly cross-linked polymers with a porous structure. After

this step, the template is usually removed from the imprinted polymer by washing with solvent or through a combination of chemical treatments and washing steps, leaving behind binding sites that are both spatially and chemically complementary to the template molecules, and capable of rebinding either the template or its structural analogues (Alexander *et al.*, 2006, Mayes and Whitcombe, 2005).

In contrast to biomolecules, MIPs are usually stable at low and high pHs, pressures and temperatures (< 150 °C) (Svenson and Nicholls, 2001; Piletsky and Turner, 2006), even if their recognition performance is maximal when the operational parameters used in the rebinding step (i.e. solvent, temperature) match the ones used in the polymerisation process, as it has been demonstrated by Piletsky *et al.* in a series of comprehensive papers regarding the influence of the polymerisation conditions on the performance of MIPs (2002, 2004, 2005, 2006, 2009). In addition, MIPs are able to retain their recognition ability for longer periods of time than natural antibodies or receptors (Svenson and Nicholls, 2001). Moreover, they are less expensive than biomolecules and easier to obtain, and they can be used in organic solvents. Finally, they can be synthesised for diverse classes of substances, such as ions (Esen *et al.*, 2009; Shamsipur *et al.*, 2010), nucleic acids (Ogiso *et al.*, 2007; Diltemiz *et al.*, 2008), proteins (Hoshino *et al.*, 2008; Hoshino *et al.*, 2010b; Zeng *et al.*, 2010), drugs (Puoci *et al.*, 2004; Ciardelli *et al.*, 2004; Cunliffe *et al.*, 2005; Cirillo *et al.*, 2009) and even yeast cells and erythrocytes (Jenik *et al.*, 2009).

However, MIPs are also burdened with some limitations, mainly connected with the methods of their production and the final format of the polymer. For example, they generally exhibit a better performance in organic rather than in aqueous medium, though molecular imprinting in aqueous conditions is feasible. Moreover, they also suffer from lack of a standard common procedure for their preparation (Piletsky and Turner, 2006).

1.2 Molecular imprinting approaches

In terms of imprinting strategies, three main kinds of approaches can be distinguished. They are all classified according to the nature of the bonds established between the template and the functional monomers, and in particular they are indicated as covalent, semi-covalent and non-covalent approaches.

1.2.1 Covalent imprinting

Covalent imprinting approach was pioneered by Wulff and colleagues (1972, 1982) and it involves the covalent modification of the template, which is chemically bound to the functional monomers in a reversible way. This modification is then followed by the polymerisation step, during which the template is still covalently connected to the monomer, now polymerised. Finally, the template is cleaved through a mild chemical reaction (e.g. hydrolysis or reduction), leaving behind the binding cavities. This approach shows very important advantages, such as that thanks to the strong interaction which occurs between the template and the functional monomer, it usually leads to binding sites that are quite homogeneous (Umpleby II *et al.*, 2000). However, both the removal of the chemically bound template and its subsequent rebinding are not simple, because they involve the disruption and the re-establishment of covalent interactions, which in turn make the kinetics of these processes really slow. This latter thing has to be considered, especially in the case of separation applications, in which the presence of a fast rebinding kinetics is important (Zhu *et al.*, 2010). Moreover, the prior derivatisation of the template is not easy with this approach, and is dependent on the chemical nature and the available functional groups of the template (Ye and Mosbach, 2002).

1.2.2 Semi-covalent imprinting

A variation of the above-mentioned method has been developed by Sellergren and Andersson (1990), and consists in carrying out the imprinting step using the polymerisation of the functional monomer bound to the template (usually through an ester bond), while the rebinding process takes place only due to

non-covalent interactions. The template is removed by hydrolysis, allowing the subsequent rebinding step to take place through the establishment of mainly hydrogen and electrostatic bonds. Unfortunately, this process is not as advantageous as it appears, because the template hydrolysis may not be easy to perform due to steric hindrance. Moreover, the same steric aspects might also interfere with the non-covalent interactions in the rebinding step (Mayes and Whitcombe, 2005). In order to overcome these problems the cleavage of the template has been carried out through the reduction of the covalent bond using $LiAlH_4$. With this technique, for example, a hydroxyl group was obtained instead of a carboxylic one (Byström *et al.*, 1993; Ikegami *et al.*, 2004). However, although this cleavage procedure is very strong, it may not allow all the bound template molecules to be removed, even after several reduction steps. This might reduce the amount of binding sites available for the subsequent interactions between the target molecule and the MIP. In a totally different and clever way, Whitcombe and co-workers (1995) connected the functional monomer to the template using a linker group, which was "sacrificed" during the removal of the template. In this first example the carbonyl group of a carbonate ester was used as a spacer group in the imprinting of cholesterol. A 4-vinylphenyl carbonate ester of cholesterol was exploited as a template covalently bound to the monomer; the template can in turn be easily cleaved by hydrolysis, releasing CO_2. After this removal, recognition sites were obtained, which bore a phenolic group able to establish hydrogen bonds with the template. The role of this spacer is to connect the template and the monomer, but also it helps to avoid the steric hindrance which might take place during the rebinding step. This results in the creation of binding sites with higher and narrower homogeneous affinity, and hence with recognition characteristics more similar to true biological receptors (Umpleby II *et al.*, 2000).

1.2.3 Non-covalent imprinting

The third approach is the so-called non-covalent imprinting, which was pioneered by Mosbach and co-workers (1981, 1984, 1990). It exploits several kinds of non-covalent bonds between the template and the monomers, such as

hydrogen, electrostatic and also hydrophobic interactions like van der Waals forces. Since all these types of interactions are not really strong, a way to obtain more stable template-functional monomer complexes is to use an excess of monomers. Unfortunately this choice is far from being free from drawbacks, since it often leads to a broad distribution of heterogeneous binding sites (Umpleby II *et al.*, 2000; Haupt, 2003). The coupling of this approach with semi-covalent imprinting has been recently found to increase the imprinting effect of poorly functionalised molecules (e.g., paracetamol) (Rosengren-Holmberg *et al.*, 2009). However, the prior chemical derivatisation of the template still remains a drawback of these combined approaches. Despite the stated disadvantages, thanks to its simplicity and the faster template removal and rebinding steps, the non-covalent imprinting approach is probably the most widely exploited method to prepare MIPs. It relies on large variety of functional monomers which are commercially available, as well as many others which are tailor-made for specific templates (Alexander *et al.*, 2006).

1.3 Different formats for different applications

1.3.1 Bulk monoliths

MIPs have usually been, and sometimes still are, prepared as monoliths, exploiting 'bulk' polymerisation processes of vinyl monomers. Since this process produces insoluble bulk materials, they require grinding and adequate sieving to obtain a fraction of particles with a narrow range of sizes (typically 5-50 µm), before being useful for various applications. Even if this procedure is simple and convenient, it presents some limitations. First of all, the milling process is time-consuming and it causes a loss of a significant amount of material (up to 80% w/w) (Brüggemann *et al.*, 2000; Pérez-Moral and Mayes, 2006b). Moreover, it might alter or damage the correct orientation of the imprinted sites (Kandimalla and Ju, 2004). In addition, these latter are mostly located in the inner part of the porous matrix. This reduces their accessibility, giving rise to poor mass transfer and slow recognition kinetics. Furthermore, bulk polymerisation is unsuitable for extensive industrial application because of the poor heat dispersal. Free radical addition polymerisation reactions are indeed exothermic and the bulk format prevents efficient heat exchange with the exterior. This can lead to rapid increases in the temperature of the polymerisation mixture up to values at which most solvents may boil, with a consequent increase in pressure within the reaction mixture. This may adversely affect MIP properties and can lead to explosions for anything other than small-scale reactions (Piletsky *et al.*, 2002; Mayes and Whitcombe, 2005; Piletska *et al.*, 2009). Furthermore, after the sieving step, irregularly shaped particles are obtained. This complicates their applications, such as chromatography or solid-phase extraction (SPE) (Mayes and Whitcombe, 2005; Alexander *et al.*, 2006). These latter techniques indeed require micron size spherical beads in order to pursue an efficient packing into columns or cartridges. Monoliths however could be useful for coating of sensor devices, where the format of thin films is quite suitable. Nevertheless, integration of bulk MIPs with sensors and assay protocols has not been very straightforward so far (Mayes and Whitcombe, 2005; Alexander *et al.*, 2006; Piletsky and Turner, 2006). However, probably the main drawback of bulk polymerisation is that it is often difficult to obtain a complete removal of the

template from the bulk MIPs. This in turn could result in the potential for leakage of residual template from the matrix, thus interfering with the intended application, particularly when used for trace analysis (Lorenzo *et al.*, 2011).

To optimise the performance of imprinted polymers, then, it is important to develop a synthetic method which allows them to be obtained in a predefined structural format, appropriate to enhance their properties and make them more suitable with respect to different applications. Several methods have already been developed in order to obtain MIPs under these various formats, like films and membranes, micro- and nanoparticles. Nevertheless, it is not easy to fit the synthetic conditions with the operational parameters required to obtain an adequate imprinting (Pérez-Moral and Mayes, 2006b).

1.3.2 Films and membranes

Two of the most important formats which have been investigated to obtain MIPs, especially when they are meant to be used as responsive layers in sensing devices, are films and membranes. Some of the synthetic approaches tested for these applications include polymerisation in moulds or layers, *in situ* electropolymerisation, and grafting "from" or "to" a support.

Polymerisation in moulds or layers

The first method described has the advantage of obtaining MIP layers and membranes characterised by uniform and very reproducible thickness (Haupt *et al.*, 1999; Cao *et al.*, 2001; Percival *et al.*, 2001; Liu *et al.*, 2006).

It has been used very recently by Sergeyeva and co-workers (2010), who synthesised MIP membranes able to mimic the catalytic properties of the natural enzyme tyrosinase, in order to fabricate biosensors for phenols detection. The membranes were obtained through a thermo-initiated radical polymerisation carried out between two glass slides, used as a mould. MIP membranes exhibited good catalytic activity and selectivity towards catechol, as well as long-term stability. However, the porosity of the material had to be improved by adding a high molecular weight poly(ethylene glycol) (PEG), and the sensitivity was lower than biosensors based on the natural enzyme.

By using the same fabrication method, Wu and his group (2009) created an optical sensor for formaldehyde based on the changes of optical reflective intensity of the MIP film when illuminated by a laser beam in presence of the template. For this reason, the MIP film was directly photopolymerised onto a mirror surface after deposition of the polymerisation mixture and coverage with a cover slip. In this way, a MIP layer about 1 mm thick was obtained, which allowed to achieve good sensitivity and selectivity for the imprinted template. Moreover, the sensor gave consistent responses up to six consecutive tests, but again the porosity of the MIP layer had to be carefully adjusted to guarantee a good level of sensitivity.

In situ electropolymerisation

A very elegant method useful for preparing MIP layers is *in situ* electropolymerisation. It is a very simple and versatile procedure which allows preparing MIP layers with reproducible characteristics (e.g., thickness and porosity) and does not require any initiator or post-processing of the material except from the template removal (Suriyanarayanan *et al.*, 2012). However, only a certain type of redox monomers can be used for this kind of process, which might reduce the possibility to achieve a successful imprinting.

Aghaei and colleagues (2010) exploited the electropolymerisation of 2-mercaptobenzimidazole through cyclic voltammetry (CV) on a gold electrode to fabricate a biosensor for cholesterol based on capacitive detection. To avoid undesirable redox reactions, which might interfere with capacitive measurements, the film-coated electrodes had to be treated with n-dodecanethiol. Alkanethiols are indeed used to fill the defects of the membrane after electropolymerisation, thus increasing the insulating properties of the material. The biosensor produced showed good sensitivity, selectivity and stability, compared to other sensors for cholesterol. Furthermore, as expected, this polymerisation method allowed the authors to obtain a very good control over the film thickness, thus improving the sensitivity of the sensor.

Another good example of MIP films obtained by electropolymerisation has been provided by Choong *et al.* (2009), who performed the electropolymerisation of

caffeine (CAFF)-imprinted polypyrrole thin nanofilms on arrays composed by vertically aligned carbon nanotubes (CNTs) with different densities, which acted as high-surface 3D-scaffolds for the MIP deposition. The sensors produced were analysed using pulsed amperometric detection (PAD) and showed an improved binding capacity with signal up to 15-fold higher than the sensor coated with a conventional MIP thin film. However, despite the increased sensitivity brought by the high-surface CNTs array, the PAD procedure had to be carefully optimised to avoid the formation of dendrites on the tips of CNTs during the measurements.

Grafting approaches

Since it is not easy to generate high-affinity binding sites while controlling the porosity and other features of the materials, a recent trend is to separate the imprinting process from the generation of a material (membrane, particle or sensor) characterised by a precise morphology (Rückert *et al.*, 2002). This last aim can be achieved by grafting MIPs "to" or "from" a support. In particular the "grafting to" approach involves the reaction between the end-functional groups of the polymer chains in solution and suitable functional groups immobilised on the support (usually vinylic ones). Unfortunately, this method usually does not allow depositing a sufficient amount of polymer onto the surface of the support. Moreover, at the same time uncontrolled bulk polymerisation might take place in solution. The "grafting from" technique, instead, requires that the polymerisation process starts from the support using an initiator immobilised on its surface. This usually results in layers characterised by higher amounts of grafted polymer chains, and in turn higher capacity (Sulitzky *et al.*, 2002; Tan and Tong, 2007; Minko, 2008).

An example of this last approach has been given by Piacham *et al.* (2005), who coated the Au electrode on a quartz crystal microbalance (QCM) with a polymer imprinted for *S*-propranolol. The surface of the electrode had been previously treated with 11-mercaptoundecanoic acid, to provide derivatisable carboxylic groups onto the surface of the sensor. These groups were then activated to attach an azo-initiator, 2,2'-azobis(2-amidinopropane) hydrochloride. The MIP

film was then grafted by UV photopolymerisation technique, carried out at 4 °C for 2-4 h (Figure 1–3).
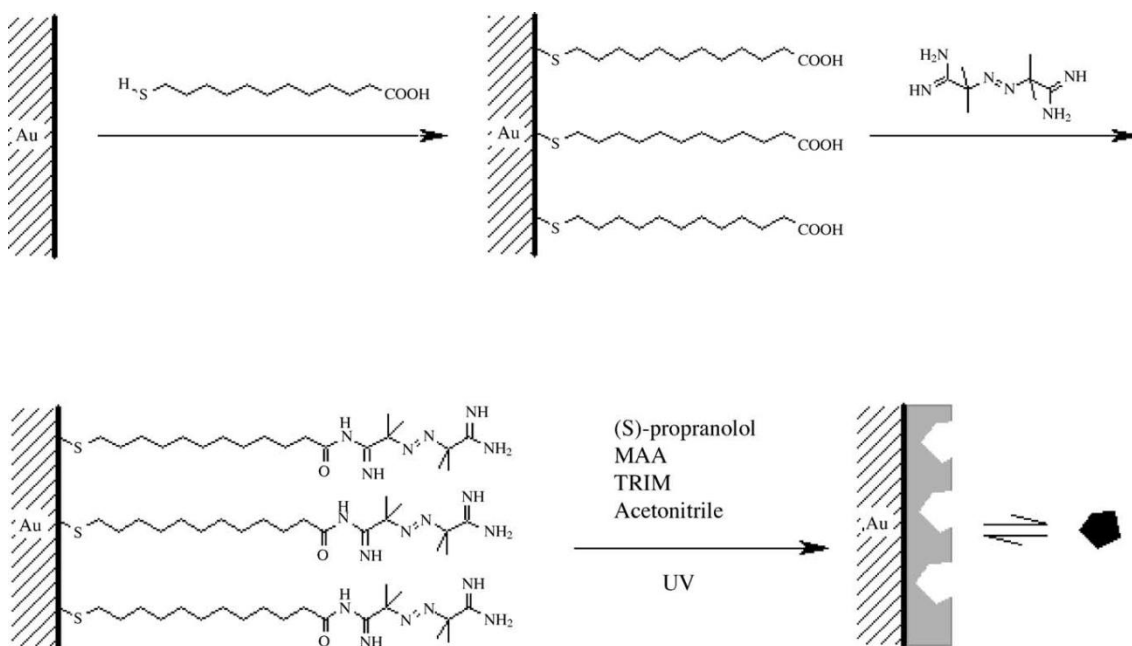
Figure 1–3. Preparation of MIP films using a surface bound photoinitiator (reproduced from Piacham *et al.*, 2005).

The low temperature has been chosen in order to avoid the growing polymer detaching from the sensor surface during the polymerisation reaction. In this way the authors obtained various types of MIP/QCM sensors with ultrathin layers of 30 nm. The sensors exhibited good specific rebinding and response time (< 1 min), thanks to the high binding-site accessibility. However, the detection limit needed to be improved, together with the selectivity of the system, which showed somehow similar response to the template and its analogues. Moreover, even with this kind of approach, gelation and polymerisation processes still might take place in solution (Sulitzky *et al.*, 2002).

This is why new kinds of initiators, known as *iniferters*, are now used. This composite term stands for *ini*tiator, trans*fer* agent and *ter*minator. Initiators of this type decompose reversibly to a pair of free radicals; one of which is the active propagating species, while the second is much less reactive ("dormant"), acting as a transfer agent and terminating the growing polymer chains in solution, reforming a new initiating species in the process (Otsu *et al.*, 1989;

16

Rückert *et al.*, 2002). This results in a better control over the polymerisation process, as well as conferring the possibility to reinitiate the polymerisation process again by simply applying the energy source, which is UV light in most of the cases (Figure 1–4).

Initiation
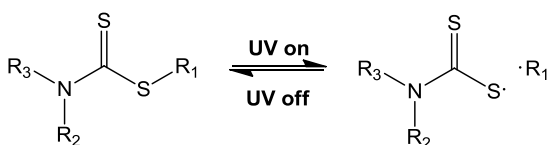
Propagation
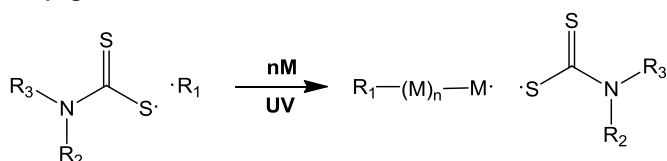
Chain transfer
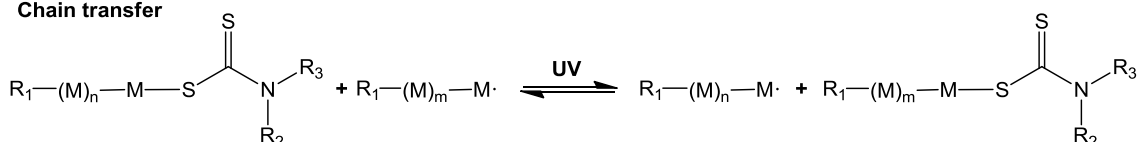
Figure 1–4. Scheme of a general *iniferter* polymerisation mechanism.

On this basis, Lakshmi and co-workers (2009) have prepared an electrochemical sensor for catechols by exploiting iniferters in a grafting "from" approach. First they created a layer of an electrically conducting polymer on the gold electrode surface, through electropolymerisation of *N*-phenylethylene diamine methacrylamide. This monomer bears two orthogonal polymerisable functional groups, an aniline and a methacrylamide function, both independently polymerisable. After this step, the methacrylamide groups on the electropolymerised layer were activated through an iniferter, *N,N*-diethyldithiocarbamic acid benzyl ester. Finally the MIP components, chosen to obtain a mimic of the enzyme tyrosinase, were grafted (Figure 1–5). In this way authors created a catalytic sensor which was able to selectively oxidise catechol and dopamine, even in the presence of an excess of interfering compounds, and with a very good limit of detection (228 nM). However, the number of CV

cycles required to electropolymerise the film had to be tailored to obtain a layer with thickness and morphology suitable to exhibit a good sensitivity.
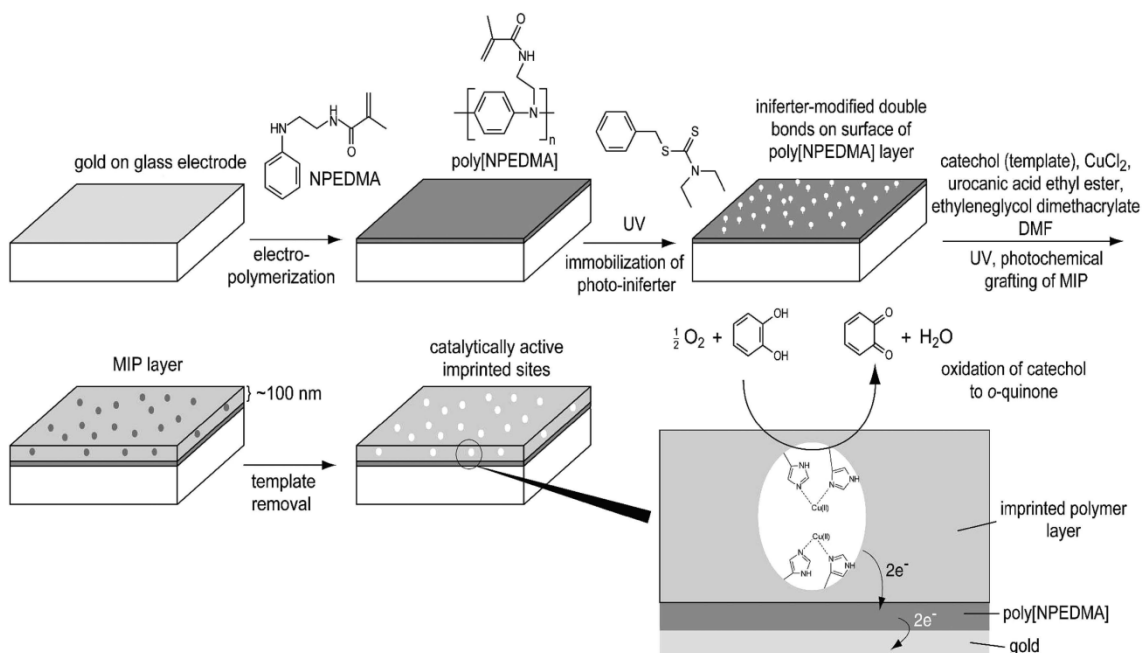
Figure 1–5. Scheme of the preparation of the catalytic MIP-hybrid electrodes imprinted with catechol (adapted from Lakshmi *et al.*, 2009).

1.3.3 Microparticles

As already stated above, molecularly imprinted materials are usually obtained as monoliths, which are then crushed and sieved to obtain MIP particles, but these often have irregular shapes and a broad size distribution. Thus, if they are meant to be used, for example, as stationary phases for chromatography processes, they provide very low column efficiency, together with a heterogeneous distribution of the affinity of binding sites. That is why the attention of researchers has shifted towards obtaining regular-shaped imprinted polymer particles, both of micro- and nano- sizes (Ye and Mosbach, 2002).

Unfortunately, not all the methods which are usually exploited for obtaining monodisperse polymeric particles are suitable for MIPs technology. Aspects such as the cross-linking degree required to obtain stable high-affinity imprints, or the need for very strong interactions between the template and the

monomers, narrow the choice of the synthetic methods which can be used to obtain MIP particles (Sulitzky *et al.*, 2002; Pérez-Moral and Mayes, 2006b).

Micron-sized MIP particles are particularly useful for chromatography and SPE. In these applications, precise flow properties are required to enhance the separation step of the various analytes, whether they are intended for pharmaceutical, biomedical or environmental applications. To date, these kinds of particles have usually been prepared by suspension polymerisation in water, liquid perfluorocarbon or mineral oil, and also by seed polymerisation and dispersion/precipitation polymerisation. Furthermore, two-steps procedures have also been used, which involve the grafting of MIP layers on the surfaces of silica or organic porous materials (grafting imprinting), or filling the pores of silica moulds with MIPs and then dissolving the moulds (hierarchical imprinting, discussed in section *1.6 - Immobilised templates: a new imprinting strategy*).

Suspension polymerisation

The first approach, suspension polymerisation, is known as one of the best methods for preparing micron-sized polymer beads, and it is usually exploited to obtain particles with diameter ranging from 3 µm to 20 µm. It can be carried out in both aqueous and non-aqueous medium. The polymerisation process proceeds in droplets made of polymerisation mixture which are suspended in a continuous phase. This often requires the help of a suspension stabiliser (surfactant) (Pérez-Moral and Mayes, 2006b).

Kotrotsiu and co-workers (2009) have prepared MIP microparticles imprinted with Boc-L-tryptophan using a water suspension polymerisation method. They used several different polymerisation mixtures to investigate the effects of parameters such as the amount of porogen, or different concentrations and types of monomers and cross-linkers on the size, morphology and binding properties of the imprinted particles. Authors have used methacrylic acid (MAA) and methacrylamide (MAm) as functional monomers and ethylene glycol dimethacrylate (EGDMA) and trimethylolpropane trimethacrylate (TRIM) as cross-linkers, while chloroform was chosen as porogen and 2,2'-azobis-(2-isobutyronitrile) (AIBN) as initiator. The particles obtained exhibited good

recognition properties, especially in terms of selectivity, but their affinity strictly depended on the polarity of the solvent. In fact, a highly polar solvent could compete with the template molecule for the binding sites, reducing in this way the specific interactions between MIP functional groups and template molecules. The same thing might happen during the polymerisation step, in which the presence of the polar aqueous continuous phase of the suspension may interfere with the non-covalent interactions between templates and functional monomers, leading to less homogeneous and less specific binding sites. Moreover, depending on operational parameters such as the amount of stabiliser, the size of the obtained particles might be difficult to control, leading to quite polydisperse MIP microparticles.

To overcome these problems, other suspension polymerisation techniques which exploit different continuous phases have been developed. One method has been described by Mayes and Mosbach (1996) and involves the use of liquid perfluorocarbons as dispersing phase. These are mostly immiscible with many organic compounds, thus they represent a good inert phase for suspension polymerisation. To stabilise the droplets, a special perfluorinated polymeric surfactant has been synthesised and used to obtain microparticles with optimal size characteristics. The imprinting mixture, composed of MAA, EGDMA or TRIM, AIBN, porogen solvent (chloroform, toluene or acetone) and Boc-L-Phenylalanine as template, was polymerised using UV irradiation at 366 nm under constant stirring. In this way, the authors were able to obtain MIP microparticles the diameter of which ranged from 5 to 50 μm, depending on the amount of surfactant and the type of porogen. The particles produced performed well in HPLC enantiomeric resolution of the template, especially the 5 μm microparticles in which TRIM was used as cross-linker. These ones exhibited an excellent resolution even at high flow rates. In addition, the fabrication procedure was quite rapid (3 h), hence the operational parameters could be easily adjusted. All the produced microparticles exhibited however more surface defects than usually observed for beads produced by water suspension methods, and only the microparticles obtained using higher amounts of surfactant were narrowly polydisperse. Moreover it is worth noting

that, even if they can be reused after distillation, liquid perfluorocarbons are quite expensive substances.

Two years later (1998), the same authors investigated the possibility of incorporating iron oxide in the preparation, in order to produce magnetic MIP microparticles. Strong magnetic properties indeed enable the particles to be easily recovered with magnetic separation. They also allow MIPs to be applied in magnetic immunoassays. Moreover, magnetic cores allow the particles to be easily concentrated and redispersed after the external magnetic field is removed (Wang *et al.*, 2009). Authors prepared then magnetic microparticles imprinted for *S*-propranolol using this liquid perfluorocarbon suspension approach. However, UV polymerisation could not be used because of the strong adsorption given by the magnetic material, therefore a thermal polymerisation was performed in toluene at 50 °C or 60 °C, with 2,2'-azobis(2,4-dimethylvaleronitrile) (V-70) as initiator. MIP magnetic microparticles exhibited an average diameter of 9.4 μm, specific binding for the template and low cross-reactivity levels also in aqueous medium. Moreover, they could be successfully applied in a radioligand binding assay, providing fast magnetic separation. However, the size distribution of the microparticles was quite broad, and no more than 5% w/w of iron oxide could be incorporated in their bulk, thus resulting in long magnetic separation times. Eventually, MIP microparticles prepared without magnetic properties did not exhibit any or slightly low specific binding, even if a direct comparison with magnetic MIP microparticles could not be made because the cross-linking degree and the polymerisation temperatures for the two products were different.

Suspension polymerisation in liquid perfluorocarbon has also been adapted to achieve the fast synthesis of MIP microparticles directly inside SPE cartridges through UV irradiation (Figure 1–6).
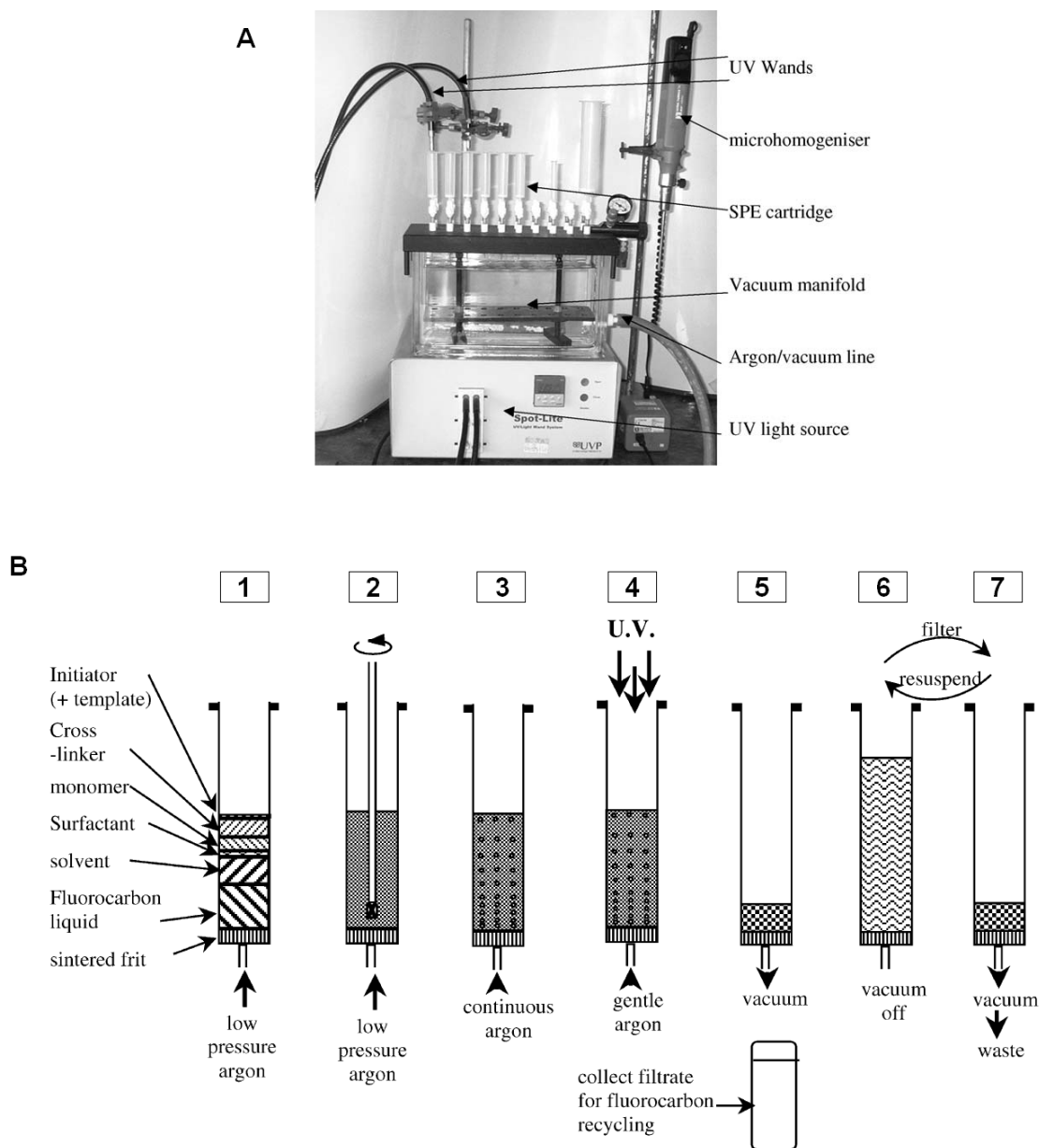
Figure 1–6. A: experimental setup used in the "high-throughput" synthesis. B: scheme of the synthetic process: 1, loading of the polymerisation mixture into an SPE cartridge; 2, homogenisation of the components to create the microdroplets; 3, argon flow to remove oxygen; 4, UV polymerisation for 30 min, with low argon flow to maintain mixing; 5, vacuum applied to remove the solvent and traces of monomers (the solvent can be collected and distilled to be reused); 6 and 7, washing steps to remove template, surfactant and other possible impurities (adapted from Pérez-Moral and Mayes, 2006a).

22

Using this "high-throughput" approach, in a 3-days period, Pérez-Moral and Mayes (2006a) were able to synthesise a total of 12 kinds of MIP microparticles for each of the template tested, propranolol and morphine. They used in fact four different monomers, i.e. MAA, acrylic acid (AAc), 2-hydroxyethyl methacrylate (HEMA) and 2-vinylpyridine (2-VPy), and three different ratios of cross-linker (EGDMA) to functional monomer. MIP microparticles exhibited morphologies similar to the ones prepared with the usual suspension approach, and similar rebinding performances. Moreover, the synthetic setup used could have been easily automated. However, it is worth noting that MIP microparticles synthesised using this system exhibited a broader size distribution than conventional ones, probably because of coalescence phenomena that happened in the SPE cartridge during the synthesis.

Another suspension polymerisation method exploits mineral oil (usually paraffin) as continuous phase for the formation of polymerisation mixture droplets. It has been developed by Kempe and Kempe (2004), who directly mixed the polymerisation mixture with the oil using a special homogenising equipment. In this work the polymerisation mixture was made of MAA, TRIM, 2,2'-azobis(2-methylpropionitrile) as initiator, acetonitrile (ACN) as porogen and propranolol as template and did not contain any surfactant. The droplets were photopolymerised into beads overnight. The fact that no surfactants or other stabilisers are needed for obtaining the droplets is really advantageous but, unfortunately, this method does not allow use of porogen solvents miscible with mineral oils, thus restricting the choice to ACN and a few others. Furthermore the microparticles obtained, despite their regular spherical shape, were not monodisperse and had to be sieved to collect the fraction of interest (between 25 and 50 µm in diameter).

Wang and co-workers (2006) used an original polymerisation approach in silicone oil instead of paraffin to prepare magnetic MIP microparticles imprinted with 2,4-dichlorophenoxyacetic acid (2,4-D). Their choice was driven by the fact that this suspension media is sufficiently viscous to allow the dispersion of polymerisation mixture droplets without using any kind of surfactant, stabiliser or

stirring that might interfere with the template-monomer interactions. They prepared then magnetic nanoparticles coated with methacryloxypropyltrimethoxysilane and dispersed them with the template and 4-vinylpyridine (4-VPy) as functional monomer and EGDMA as cross-linker. UV initiation could not be used because of the opacity of the magnetic material, neither thermal polymerisation because it would have lowered the viscosity of the silicone oil, thus resulting in agglomeration of the MIP product. Authors decided then to use a benzoylperoxide/dimethylaniline redox initiation system, which allowed the polymerisation process to be performed at 10 °C. Even if the size distribution of the particles was not homogeneous, they had a regular spherical shape (20.1 µm in diameter). Moreover, they exhibited good magnetic properties, and 2-fold more affinity than control microparticles. Nevertheless, the preparation procedure was quite long and required several synthetic and purification steps, thus making it impractical for being performed manually.

Both the previous methods (i.e. in liquid perfluorocarbon and in mineral oil) have been recently improved by Zourob and co-workers (2006), who developed a spiral microflowreactor (Figure 1–7a) through which they obtained nearly monodisperse microparticles with an average diameter of 25 µm (coefficient of variation < 2%). The immiscible phase contained liquid perfluorocarbons (Figure 1–7b) or mineral oil (Figure 1–7c). For comparison purposes, they also synthesised microparticles using conventional methods, and the results showed that the binding constants of the MIP particles obtained through the micro-reactor were comparable with those of the particles obtained through conventional methods. However, the size distribution of the latter, as expected, was broader, with coefficients of variation equal to 12% and 67%, respectively for the particles prepared using liquid perfluorocarbons (Figure 1–7d) or mineral oil (Figure 1–7e).
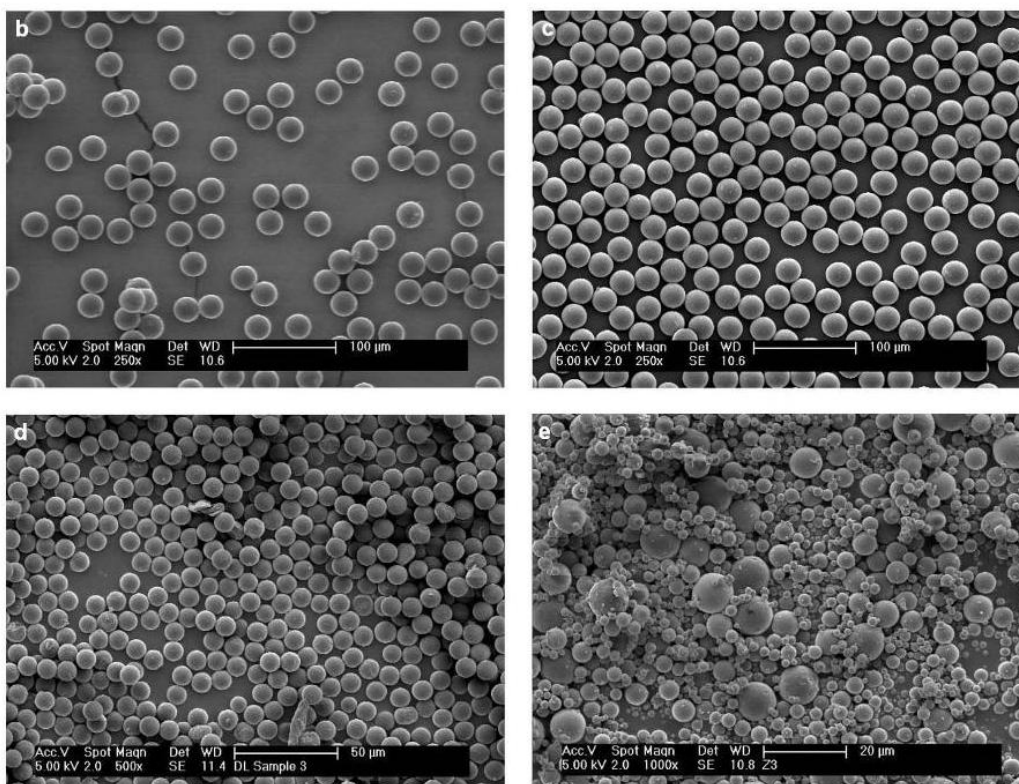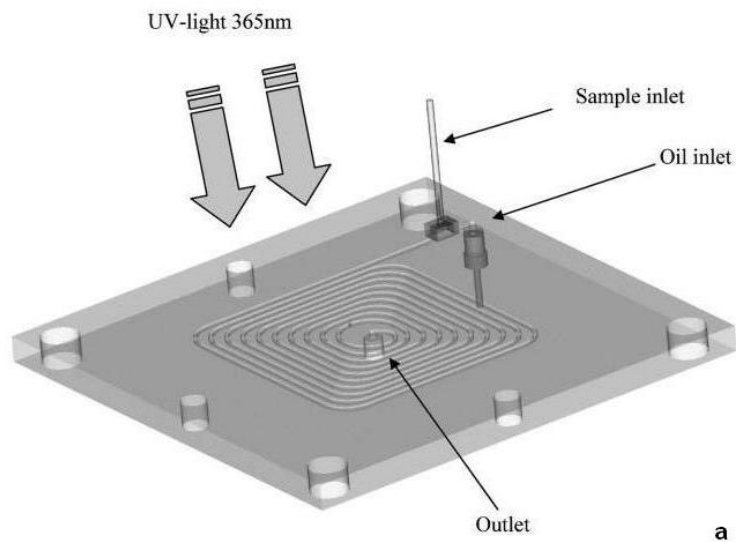
Figure 1–7. Scheme of the spiral microflow-reactor developed by Zourob *et al.* (a) and scanning electron microscopy (SEM) images of the beads produced using the microreactor in liquid perfluorocarbon (b) and in oil (c) and the beads produced using conventional suspension polymerisation in liquid perfluorocarbon (d) and in mineral oil (e) (adapted from Zourob *et al.*, 2006).

25

Seed polymerisation

Another method used for preparing MIP microspheres is the so-called seed polymerisation which has been pioneered by Hosoya *et al.* (1994). It involves the use of particles of a uniform size (mainly made by polystyrene, PS), which act like seeds for the formation of final MIP microparticles. It is usually a multi-step swelling and polymerisation procedure, which implies that the seed particles undergo a first swelling step by micro-emulsion droplets of an activating solvent and, after that, other swelling steps by the polymerisation mixture. At the end of the whole swelling process the polymerisation step takes place thermally or through UV irradiation, resulting in nearly monodisperse MIP microparticles.

Haginaka and colleagues (2008) have recently exploited this method to obtain MIP microparticles imprinted for D-clorphenamine, using different functional monomers (MAA or 2-(trifluoromethyl)acrylic acid, TFMAA) and different porogens (toluene, phenylacetonitrile, benzylacetonitrile or chloroform), with the aim of studying their influence on the morphology and the recognition properties of the MIP particles. The polymerisation process has been thermally performed after three swelling steps using PS seed particles. The MIP microparticles obtained were nearly monodisperse, with an average diameter of 5-6 μm, and they exhibited good porosity and recognition properties. However, the procedure involves the presence of water, which might interfere with the non-covalent interactions between the template and the functional monomers (Haginaka *et al.*, 2008). Moreover, since several synthetic steps are required to produce MIP microspheres with this method, other easier and more straightforward approaches have been usually preferred.

Dispersion/precipitation polymerisation

It is hard actually to distinguish between dispersion and precipitation. The former process in fact implies that primary particles undergo a swelling step in the polymerisation mixture and then the polymerisation takes place inside and on the surface of the same particles, giving rise to spherical-shaped polymer beads. Precipitation polymerisation instead does not include this swelling step,

while the polymerisation process happens directly in the medium (Van Herk and Monteiro, 2003). This polymerisation method is usually exploited to obtain MIP sub-micron particles, so it will be fully described in the following section (*1.3.4 - Nanoparticles and nanogels: true "artificial antibodies"?*). However, by properly adjusting the operational parameters, it can be successfully used also to obtain MIP microparticles.

Puoci and co-workers (2004) exploited this polymerisation approach to produce MIP microparticles as drug delivery systems, imprinted for the pro-drug sulfasalazine. They performed a thermo-initiated precipitation polymerisation using a mixture of MAA, EGDMA and AIBN in ACN/toluene. In this way they obtained MIP and non-imprinted (NIP) microparticles with a diameter of 4 µm and 2 µm, respectively. This shows that the presence of template may influence the particle growth. But the most important result has been obtained after having loaded the particles with the drug and tested their release in simulated gastric fluid for 2 h, and in intestinal fluid for the following 18 h (Figure 1–8). Authors observed that, while the NIP particles had completed the release after 5 h, a controlled release of the drug was achieved for the MIP particles, which slowly released sulfasalazine over 18 h thanks to their imprinting effect.
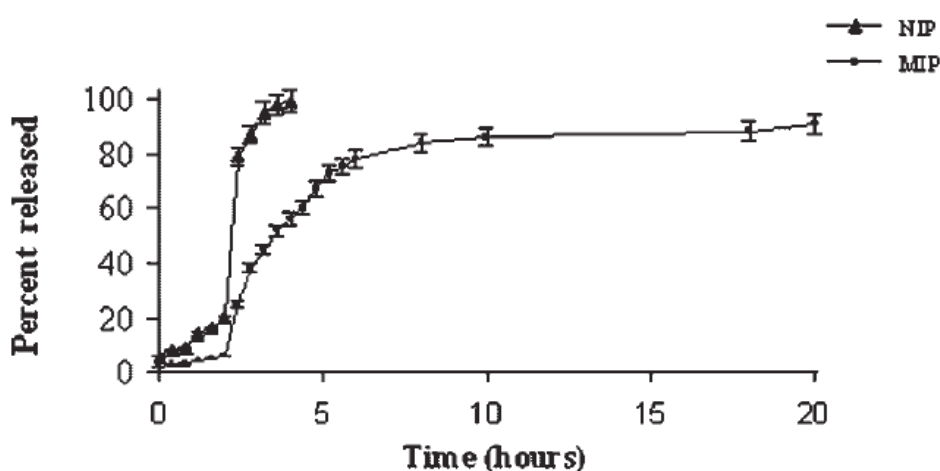
Figure 1–8. Release profile of sulfasalazine from MIP and NIP microparticles in simulated gastric fluid (pH 1, from 0 to 2 h) and in simulated intestinal fluid (pH 6.8, from 2 to 20 h) (adapted from Puoci *et al.*, 2004).

Liu and co-workers (2010) reported the preparation of three different kinds of MIP microparticles, all imprinted for cinchonidine, using precipitation polymerisation. The first two kinds of MIPs were prepared by thermal polymerisation of a mixture of template, MAA, DVB, HEMA and AIBN in ACN/toluene (3:1, v/v). The third type of microparticles has been obtained through two subsequent precipitation polymerisations, both thermo-initiated. The first one resulted in the creation of a DVB core, while the second step gave rise to an imprinted shell made of MAA and DVB. The MIP microparticles obtained through all the three methods had diameters smaller than 5 μm (3.7 ± 0.07 μm, 2.8 ± 0.11 μm and 4.1 ± 0.14 μm) with very good size distributions. Scatchard analysis demonstrated that the binding sites were also homogeneous. Moreover, in a chromatographic evaluation of the synthesised MIP particles, core-shell MIP microparticles had a much higher stereoseparation factor for cinchonidine than MIP microparticles obtained through other methods and tested under the same conditions. Also in this case, the results showed that the presence of the template could influence particle growth, together with the type of functional monomers chosen for the imprinting procedure.

Grafting approaches

A convenient method for preparing MIP microparticles is grafting a thin MIP layer on the surface of prefabricated microparticles. As starting material, beads made of silica or organic polymers are usually utilised. This allows the polymerisation conditions to be adjusted in order to achieve a better imprinting performance, rather than focusing on the best synthetic parameters for obtaining a defined spherical format (Rückert *et al.*, 2002). Moreover, this core-shell strategy results in faster mass-transfer kinetics, which constitute a main issue of bulk polymers.

The extensive work made by Sellergren and his group has led to several developments in this approach (2002). These authors first studied the grafting of MIP layers on silica microparticles with different size and porosity by using the covalent and non-covalent immobilisation of the azo-initiator 4,4'-azobis(4-

cyanopentanoic acid) (ACPA). They subsequently tested the performance of the MIP products in HPLC for the enantiomeric resolution of the template, L,D-Phenylalanine (LPA or DPA). In case of covalent immobilisation, silica surface had to be previously derivatised with amino or epoxy reactive groups to which attach the initiator. The polymerisation mixture was composed by MAA and EGDMA in toluene or dichloromethane and, after the addition of the modified silica particles, the grafting of the MIP layer has been achieved through UV irradiation. Results showed that the grafting rate was directly proportional to the density of immobilised initiator, and that the amount of grafted MIP was dependent also on the reaction time. However, too high initiator density values or reaction times caused a difficult control over the polymerisation, thus resulting in the blockage of the material pores and the loss of any imprinting effect. Moreover, gelation and aggregation phenomena occurred in solution. On the other hand, when coated with a 0.8 nm thick MIP film, the most porous silica used (surface area: 380 m^2/g) could achieve a separation factor (α) of 6.3 for the template racemate with very high efficiency. Non-covalently derivatised supports, as expected, exhibited lower performance and a low quality of the grafted MIP layers.

Zheng and colleagues (2009) have reported the preparation of MIP microbeads with the same approach, but using PS beads as seed particles. MIP microparticles have been obtained in three steps. The first one involved a single-step swelling and polymerisation of PS cores to obtain poly(glycidyl methacrylate-*co*-ethylene glycol dimethacrylate) (PGMA-*co*-EGDMA) microparticles bearing a surface epoxy group. In the second step, ACPA was bound to the surface of PGMA-*co*-EGDMA particles. Finally, the third and last step involved the grafting of a MIP layer imprinted for *S*-naproxen onto the PGMA-*co*-EGDMA particles. The polymerisation reaction involved 2-VPy and EGDMA with chloroform as porogen, and it was thermally initiated. As expected, the amount of initiator bound on the initial particles, together with the grafting reaction time, controlled the mass of grafted MIP. This parameter, in turn, had an important role in defining the morphology and the surface properties of the MIP microparticles, hence their binding properties. In fact, the

highest recognition capabilities were obtained when the MIP content was 16.75% (w/w), with an α of 2.39 between *S*- and *R*-naproxen. This grafting approach then, even if it is time-consuming and not synthetically straightforward, can lead to MIP microparticles in which porosity, morphology and sizes of the beads can be finely controlled by varying the operational parameters.

Nevertheless, to avoid oligomerisation and gelation phenomena in solution, typical of the use of azo-initiators, Rückert and co-workers (2002) tested also the grafting of MIPs on microparticles using immobilised iniferters (see *1.3.2 - Films and membranes*). They immobilised then sodium diethyldithiocarbamate trihydrate (DEDTC) on the surface of chloromethylated PS resin beads or chloromethyl-modified silica beads. Then a MIP layer composed by MAA and EGDMA in toluene was grafted using UV polymerisation, in presence of the templates, LDA or DPA. Also in this case, the mass of grafted MIP could be adjusted by modifying the amount of surface-bound iniferter. However, in the case of PS particles, no imprinting effect was observed. This has been ascribed to the marked decrease in porosity after the grafting of the MIP. Silica particles, instead, exhibited a good imprinting effect after grafting, with an α of 2.4 between the two enantiomers. In addition, they did not exhibit any remarkable change of porosity due to the MIP layer deposit. Moreover, ^{1}H-NMR studies performed on the polymerisation solution after grafting did not show any trace of oligomers, thus confirming that the grafting reaction happened mostly at the surface of iniferter-derivatised microparticles.

1.3.4 Nanoparticles and nanogels: true "artificial antibodies"?

Nanotechnologies are gaining importance in several areas like pharmaceutics, diagnostics and many others. It is not surprising then that many research groups have started developing MIPs in this format. In contrast to bulk monoliths, MIP nanoparticles (MIP NPs) show improved characteristics, which are summarised in Table 1-1.

Table 1-1. Comparison of properties of bulk MIPs and MIP NPs.

Bulk MIPs	MIP NPs
Broad distribution of binding sites with varying affinity, high level of non-specific binding	Similar affinity for all binding sites, 1-2 per particle, 2-3 orders of magnitude difference between specific and non-specific binding
Affinity in the range 10^{-9}-10^{-3} M depending on template	Affinity in the range 10^{-10}-10^{-6} M, possibility of using affinity chromatography for the fractionation of high-performance NPs
Insoluble material, difficult to process	Soluble NPs which can be treated as standard reagents
Substantial batch-to-batch variability	Better control of manufacturing process, using chemical reactors
Possibility of template leaking from the polymer	Traces of template can be relatively easily removed using dialysis or affinity separation
Limited prospects for *in vivo* applications	MIP NPs with biological activity can be produced

MIP NPs have higher surface-to-volume ratio and greater total active surface area per weight unit of polymer. Imprinted cavities are more easily accessible to the templates, which improves binding kinetics and facilitates the template removal process, thus enhancing their overall performance (Tokonami *et al.*, 2009). This is clarified in the scheme elaborated by Gao *et al.* (2007) (Figure 1–9).
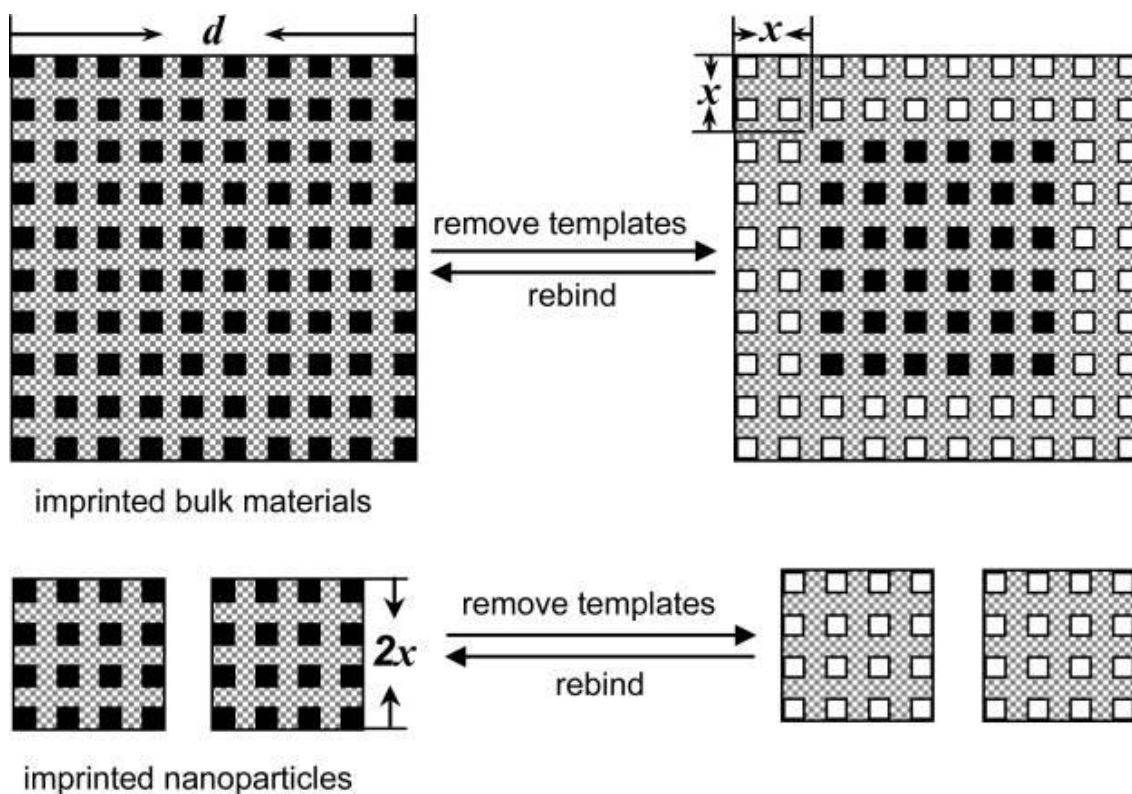
Figure 1–9. Schematic representation of the distribution of effective binding sites in the imprinted bulk materials and MIP NPs after the template removal step (adapted from Gao *et al.*, 2007).

According to this model, for a bulk imprinted polymer with a size of *d*, only the templates which are within *x* nanometres from the surface may be removed, then leaving behind accessible binding sites. If this is the case, the effective volume of imprinted polymer which is able to rebind target analytes is $d^3 - (d - 2x)^3$. If the imprinted materials are prepared as NPs with a scale of *2x* nm, all the sites may be completely accessible and effective for removing and then for rebinding the template molecules.

Additionally, this format fits better with surface-imprinting strategies (Tan and Tong, 2007) allowing *in vitro* assays to be designed using probes conjugated with enzymes, which are usually too bulky to fit into recognition cavities. Moreover, since NPs easily remain in suspension/solution, it is easier to dose them precisely, e.g. for use in ELISA-like tests (Haupt *et al.*, 1998b; Ge and Turner, 2009).

MIP NPs have been synthesised as enzyme substitutes for catalysing chemical reactions (Wulff *et al.*, 2006; Carboni *et al.*, 2008), as drug delivery systems for better controlling and targeting the release of drugs (Ciardelli *et al.*, 2004; Cirillo *et al.*, 2009), as antibody substitutes in binding assays (Ansell, 2004; Lavignac *et al.*, 2004; Yoshimatsu *et al.*, 2007; Ge and Turner, 2009) and for creating stationary phases in capillary electrochromatography (CEC) (Schweitz *et al.*, 2000; Spégel *et al.*, 2003; Nilsson *et al.*, 2007; Priego-Capote *et al.*, 2008), as well as constituents in developing sensors (Piletsky and Turner, 2008; Reimhult *et al.*, 2008; Schirhagl *et al.*, 2010).

Unfortunately, it is not easy to obtain MIP NPs, and several methods have been investigated in recent years. The most popular include precipitation polymerisation and mini- and micro-emulsion polymerisation. Other approaches include core-shell emulsion polymerisation or grafting techniques. Not least, the new living radical polymerisation techniques like ATRP and RAFT are starting to find their use in the production of MIP NPs. Each one of these procedures has its own pros and cons, which will become clearer through the discussion of the various examples in the literature detailed in the following section *1.4 - MIP nanoparticles: manufacturing*.

The applications of MIP NPs, instead will be discussed in detail in section *1.5 - MIP nanoparticles: applications* in an attempt to highlight the advantages and disadvantages arising from the use of MIP NPs for each different purpose.

1.4 MIP nanoparticles: manufacturing

1.4.1 Precipitation polymerisation

The precipitation polymerisation approach for obtaining MIP NPs was first developed in 1999 by Ye and co-workers. This methodology involves formation of the imprinted NPs in an excess of solvent (monomer represents only 2% of the total volume of the reaction mixture). In this system the growing polymer chains do not coagulate but continue to capture oligomers and monomers from solution, and then precipitate when they reach a size which makes them insoluble in the reaction medium. In this way there is no need to use a stabiliser to prevent coalescence of the particles, which is very good for non-covalent imprinting approaches. Furthermore, the technique is easy and less time-consuming than other procedures, offering good yields. Ye and co-workers fabricated NPs imprinted for 17β-estradiol (E2) and theophylline (THO), using both UV and thermal polymerisation methods. MAA was used as functional monomer, TRIM as cross-linker, and the reaction was carried out in ACN with AIBN as initiator. In this way they obtained nearly monodisperse MIP NPs with an average diameter of 200 nm for the THO imprinted nanospheres, and 300 nm for the E2 imprinted ones. Synthesised MIP NPs showed uniform spherical morphologies (Figure 1–10), and were obtained with good yield (85% w/w).
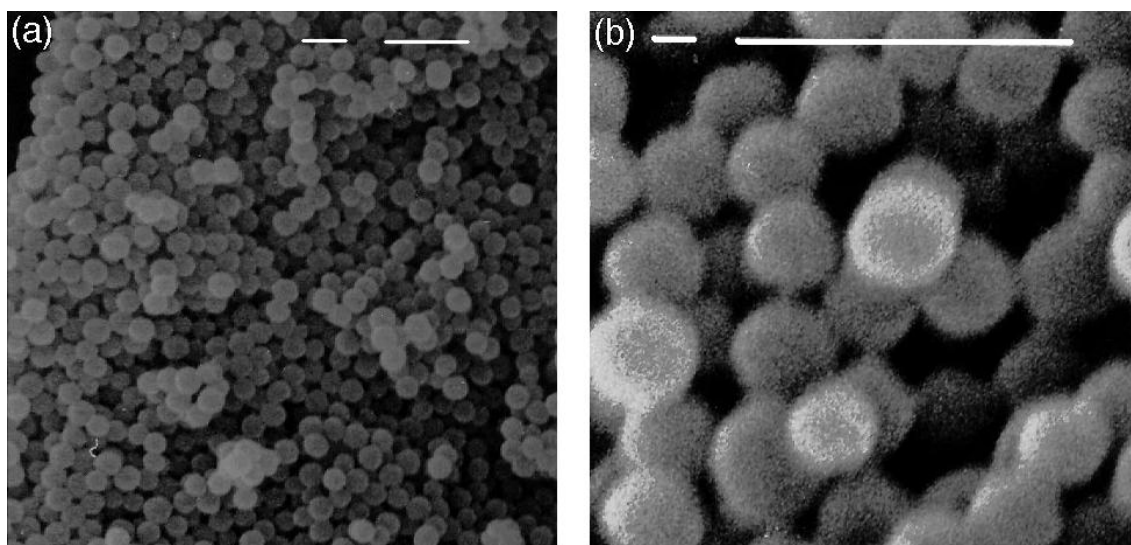
Figure 1–10. SEM images of MIP NPs imprinted for E2 at 7500× of magnification (a) and 30000× of magnification (b). The right hand bar corresponds to 1 μm (adapted from Ye *et al.*, 1999).

Concerning the adsorption properties, MIP NPs were able to bind 3 to 4-fold more template than NIP control particles, and had low cross-reactivity for the template analogues (< 1%). The binding equilibrium for MIP NPs could be achieved in 4 h.

Later (2000), the same authors evaluated the effect of the cross-linking density and of the amount of template on the binding properties of the MIP NPs. They found that, thanks to its high intrinsic cross-linking efficiency, TRIM performed better than EGDMA for obtaining MIP NPs with good binding properties, especially when it was used at a molar ratio 1:2.3 with respect to the functional monomer. Moreover, they noticed an increase in the number of non-specific interactions, together with a slight reduction of the amount of binding sites, when the MIP NPs had been prepared with a reduced amount of template.

The same group one year later exploited this precipitation method to synthesise MIP NPs which incorporated a UV fluorescent scintillation monomer, 4-hydroxymethyl-2,5-diphenyloxazole acrylate, for sensing purposes. This monomer self-distributed together with MAA through the whole MIP NPs matrix. In order to produce the particles, TRIM has been used as cross-linker and AIBN as initiator. The precipitation polymerisation process was carried out in toluene,

and the response was evaluated in the same solvent. The diameter of the imprinted particles ranged from 600 nm to 1 μm, so they were not really monodisperse, but they showed about 2-fold higher response for the template than non-imprinted ones. Nevertheless, the size and morphology of the material would definitely need an improvement to achieve a better performance.

In 2003, Li and his group extensively studied the effects of monomer concentration, polymerisation temperature and types and concentrations of initiators on the size and uniformity of MIP NPs obtained through precipitation polymerisation. Hence, they prepared NPs imprinted for L-2-chloromandelic acid in ACN, using acrylamide (AAm) as functional monomer, 1,4-butanediyl diacrylate as cross-linker and AIBN or 2,4,6-trimethylbenzoylphenyl-phosphinic acid ethyl ester (LR) as initiator. Several polymerisation processes have been thermally performed, using various amounts of solvent, reaction temperatures and concentrations of initiator (either AIBN or LR). In this way they found that decreasing the volume of the solvent (increasing the monomer concentration) resulted in larger particle diameters. In fact, they were able to adjust the diameter of the MIP NPs from 155 to 509 nm by decreasing the solvent volume from 140 to 60 mL. They also found that a low concentration of monomers results in particles with more uniform spherical morphology. In particular, the particles obtained using 100 mL of solvent had very good uniformity and dispersibility (Figure 1–11).
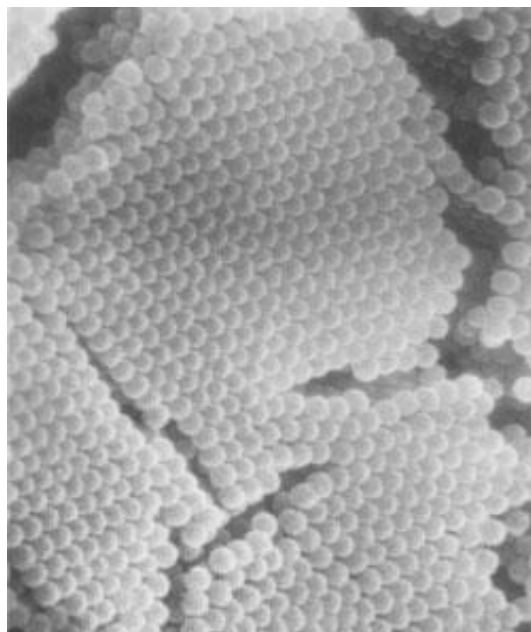
Figure 1–11. Spherical MIP NPs obtained through precipitation polymerisation, arranged on a glass layer (adapted from Li *et al.*, 2003).

The particle size also increased by increasing the reaction temperature (Figure 1–12A). They studied this effect in the temperature range between 50 °C and 95 °C because lower temperatures were not able to initiate the polymerisation process. Too high temperature values strongly interfered with the uniformity of the particles. This is probably due to the fact that higher temperatures result in faster initiation kinetics, i.e. in higher formation of nuclei. In addition, the polymer solubility may increase at higher temperatures. As a consequence, the critical polymer chain length may increase, so reducing the number of polymer particles. Moreover, the viscosity of the system is reduced by an increase in temperature, allowing easier aggregation of the nuclei thanks to the higher diffusion rate. The increase in the amount of initiator also resulted in larger polymer particles (Figure 1–12B).
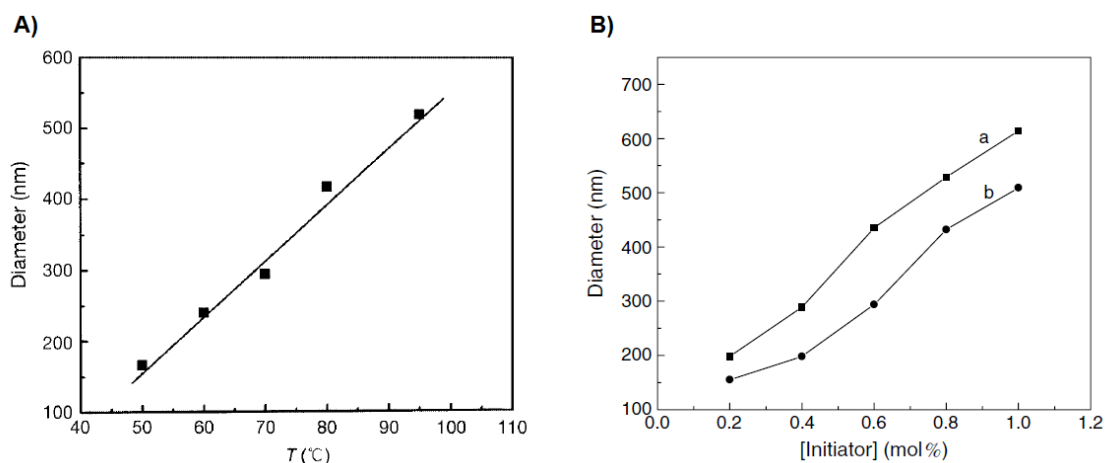
Figure 1–12. Effect of temperature (A) and of initiator concentration (B) on the diameters of spherical MIP NPs obtained by precipitation polymerisation. For the (B) graph, (a) is LR and (b) is AIBN (adapted from Li *et al.*, 2003).

According to the authors, this effect might be explained by considering that an increased amount of initiator results in a higher reaction temperature due to exothermic nature of the initial phase of the polymerisation reaction. In addition, it is worth noting that higher concentration of initiator increases both the creation of radicals and the chain termination and decreases the average molecular weight of the polymer. In order to analyse the binding characteristics, the authors selected the MIP NPs prepared at 70 °C in 100 mL of ACN and with AIBN as initiator. The imprinted NPs showed much higher template adsorption than the non-imprinted ones. Thanks to the higher specific surface area they also showed higher binding capacity and binding rates than MIPs prepared under similar conditions by bulk polymerisation. The authors also evaluated the binding properties through Scatchard analysis, which revealed two classes of binding sites. The dissociation constant (K_D) and the maximum number of binding sites (Q_{max}) were evaluated for both classes, and they were equal to 102.5×10^{-6} M and 75.8×10^{-6} mol/g for the high-affinity binding sites, and 1.7×10^{-3} M and 222.4×10^{-6} mol/g for the low-affinity ones, respectively. This was further confirmed by simulating the interactions between AAm and the template through the software 'Hyperchem'. In fact, two molecular models of two types of monomer-template complexes have been found. They had different calculated

binding energies, which were consistent with the presence of two classes of binding sites.

In a subsequent work (2007), Lai and co-workers produced MIP micro- and nanospheres imprinted for (2-ethylhexyl)phthalate (DEHP) for studying the effects of the use of ACN or cyclohexane as solvents and EGDMA or TRIM as cross-linkers. They also studied the effect of the template on the particles size. Synthesised NPs had an average diameter of 450 nm and a very good binding capacity. Authors found that matching the solubility of the growing polymer chains with that of the porogenic solvent results in larger microparticles, so in order to obtain NPs this parameter has to be carefully optimised. Moreover, results suggested that also the shape of the reactor might have a role in fostering the formation of nano- rather than microparticles. Under the same synthetic conditions, the latter were obtained with a round-bottom flask, while the former by using a conical flask. Probably, the shape of the reactor could influence kinetic parameters such as radial diffusion or local concentration of reactants.

In a later work (2007), Yoshimatsu and co-workers also investigated how to control the size of MIP beads synthesised through precipitation polymerisation. In particular, they focused on the effect that the amount of cross-linker might have on the size and the yield of the beads. They used *R,S*-propranolol as template model, and different polymerisation mixtures composed by MAA as functional monomer, TRIM or DVB as cross-linkers and AIBN as initiator. All the polymerisation processes were performed in ACN by heating the mixtures at 60 °C for 24 h. In this way authors found that, since it is a major reaction component, the cross-linker has a strong effect both on final size and yield of the NPs. In particular, when DVB was used as cross-linker, they obtained MIP particles with a low yield, quite polydisperse (0.6 – 3.1 µm). They reduced the polydispersity by applying a mild agitation (20 rpm). Using TRIM as cross-linker they obtained MIP NPs with diameter 100-300 nm with 90% yield. These particles were uniform in size, and were obtained without agitation. By using combinations of DVB and TRIM, authors were able to tune the size of the

obtained particles. It is worth noting that for the TRIM NPs the presence of the template had a strong influence on their size and uniformity. As can be seen in Figure 1–13, NIP NPs had a size which was 2-fold larger than imprinted ones, both in dry state and after swelling in ACN. This has been explained by considering that without the template MAA exists in solution as monomers and as hydrogen-bonded dimers. When the template is added, another interaction can be established between MAA and propranolol. This might influence the polymer growth, resulting in smaller MIP NPs.
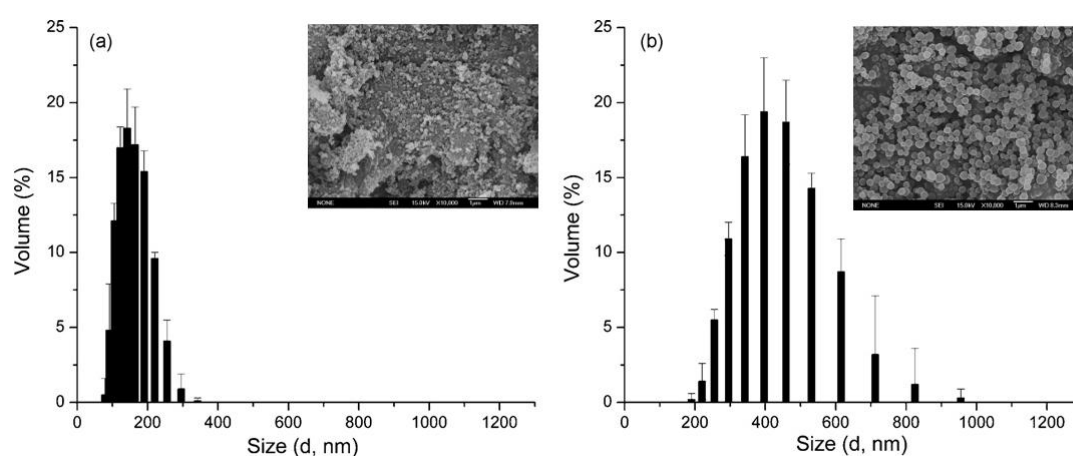
Figure 1–13. Particle size distribution of imprinted (a) and non-imprinted (b) poly(TRIM-*co*-MAA) NPs, measured by photon correlation spectroscopy. Inserts are SEM images of the same NPs (adapted from Yoshimatsu *et al.*, 2007, 2010).

All the obtained MIP beads showed high template rebinding in aqueous buffer, while rebinding levels for non-imprinted particles were negligible. In addition, all the imprinted beads showed low cross-reactivity levels of *S*-propranolol-imprinted sites towards the other enantiomer (below 5%). These values are 6 or 7-fold lower than those obtained for irregular MIP particles prepared by grinding and sieving of MIP monoliths. Once again this highlights the advantages gained by producing MIPs with specific morphologies and sizes.

Also Schweitz *et al.*, in 2000, synthesised MIP NPs for propranolol using precipitation polymerisation. The synthesis was carried out through UV photopolymerisation of MAA, TRIM and AIBN in ACN at -26 °C, to strengthen the interactions between the template and the functional monomer. In this way,

authors obtained MIP NPs of 200-500 nm in diameter, hence quite polydisperse. NIP NPs, on the other hand, had a smaller size (100 nm). These results are in contrast with the ones obtained in the works discussed before (Lai *et al.*, 2007; Yoshimatsu *et al.*, 2007; Yoshimatsu *et al.*, 2010), in which MIP NPs imprinted for propranolol and prepared with the same polymerisation mixture have been found to be smaller than correspondent non-imprinted ones. Maybe in this case the low polymerisation temperature exhibited an effect over the size of the NPs. The details of the application of the MIP NPs produced in this work in CEC are discussed in section *1.5.2 - Capillary Electrochromatography (CEC)*.

Shea and co-workers recently (2008) prepared very small MIP NPs imprinted with a peptide, i.e. melittin. They optimised the composition of the precipitation polymerisation mixture by creating a small combinatorial library composed by: *N*-isopropylacrylamide (NIPAm, backbone monomer), AAm (hydrogen bonding monomer), AAc (negative-charged monomer), *N*-(3-aminopropyl) methacrylamide hydrochloride (positive-charged monomer), *N-tert*-butylacrylamide (TBAm, hydrophobic monomer) and *N,N'*-methylenebisacrylamide (BIS) as cross-linker. To avoid denaturation of the protein, polymerisation processes were carried out without any organic solvent or heating. The authors dissolved the monomers in water or ethanol (EtOH) with the help of a small amount of sodium dodecyl sulphate (SDS) and performed the polymerisation reactions for 15-20 h at 23-25 °C through the addition of ammonium persulphate (APS) and *N,N,N',N'*-tetramethylenethylenediamine (TEMED) as initiating system. From all synthesised NPs only MIPs which contained at least 40% (mol) TBAm and 5% (mol) AAc were able to successfully rebind the peptide. These are important data, considering the effect that the presence of water and surfactant may have in a non-covalent imprinting process. These NPs were also obtained with good yields (80-90% w/w) and uniform diameters of about 54 nm, which is comparable to the size of IgM. The K_D for the obtained nanoparticles was calculated to be about 25 pM and was found comparable to that of natural antibodies for melittin (17 pM). Moreover, no or only slight cross-reactivity with other proteins was observed.

However, the fact that only 2 out of 13 kinds of MIP NPs synthesised in total showed specific binding, once again stresses the importance of the composition of the polymerisation mixture for obtaining MIP NPs with good characteristics. Moreover, considering that the purification of the product involved a 4-days dialysis process, an optimisation of the work-up procedure might be indicated, especially for large-scale production purposes.

Ciardelli *et al.*, in 2004, modified the approach of Ye and colleagues (1999) to investigate if the binding capacity of MIP NPs could be modulated by using a mixture of MAA as functional monomer and methyl methacrylate (MMA) as "non-functional" monomer. Working on this assumption, they synthesised several kinds of MIP NPs for THO with different MMA/MAA ratios. In accordance with the previous results obtained by Ye and co-workers, they found that MIP NPs had smaller diameters than non-imprinted ones. Moreover, they noticed that diameter of the particles decreased from 231 to 202 nm by increasing the amount of MAA, while the rebinding capacity for the template was enhanced. This is an evidence of the stronger template-MAA interactions taking place into the NPs. More detail on the drug release properties of the MIP NPs produced in this work are discussed in section *1.5.1 - Drug delivery*.

Aiming to industrial large-scale production, Yang and his group (2009) applied a distillation-precipitation polymerisation technique for the production of MIP NPs. This method required the precipitation polymerisation process to be performed under refluxing conditions. In this way they synthesised NPs imprinted for *R,S*-propranolol using MAA as functional monomer, BIS or TRIM as cross-linkers and AIBN as initiator. The polymerisation mixtures in ACN were placed in a proper setup and heated up to 115 °C to ensure reflux conditions. For the last 1.5 h, half of the solvent volume was distilled out. The whole process lasted for 3 h, which is a very short time if compared to a conventional precipitation polymerisation procedure. In addition, the reflux of the solvent ensured efficient mixing conditions for the reaction mixture. Interestingly, the distillation did not have any effect on the particles size. In fact, all the synthesised imprinted particles exhibited diameters below 300 nm, reasonably monodisperse. The

same method allowed grafting a hydrophilic AAm shell to MIP NPs in a one-pot reaction, without need to isolate the cores. However, MIP NPs prepared using this distillation-precipitation polymerisation method exhibited a reduction in binding affinity and selectivity, especially in aqueous solvents, as compared to MIP NPs prepared by conventional precipitation polymerisation. This has been ascribed to the high temperature at which the polymerisation process has been carried out, which probably interferes with template-monomer interactions during the imprinting process (Piletsky *et al.*, 2002; Piletsky *et al.*, 2004; Mijangos *et al.*, 2006). Nevertheless, the short reaction time and the suitable setup of the synthesis suggest that this method, if well optimised, might be suitable for large-scale production of MIP NPs.

Another attempt to modify the precipitation polymerisation approach, making it more clean and applicable for industrial large-scale production, has been attempted by Ye *et al.* (2006), who carried out the synthesis of MIP NPs for *S*-propranolol in supercritical CO_2. Authors performed the thermal polymerisation of MAA and DVB as functional monomer and cross-linker, with AIBN as initiator, in presence or in absence of a small volume of ACN as modifier. MIP NPs of about 100 nm in diameter were obtained, and the addition of ACN did not have any effect on the particle morphology. However, it resulted in an increased non-specific binding, while MIP NPs synthesised only in supercritical CO_2 exhibited a specific binding up to 81%. This approach seems quite advantageous because it is easy to scale-up and it reduces the production of organic solvent waste and environmental pollution, since supercritical CO_2 is not toxic. Moreover, this fluid does not interfere with non-covalent interactions between template and functional monomers, which makes it suitable for MIP synthesis. However, supercritical CO_2 is poorly miscible with most of the acrylic cross-linkers used to prepare MIPs, such as EGDMA and TRIM, as well as with highly polar monomers. This strongly limits the choice of functionalities that can be introduced in the imprinting mixture, and might hinder the imprinting process.

From the above, it appears that precipitation polymerisation is a straightforward approach for obtaining MIP NPs; it is quite fast and easy to perform. However,

the fact that high dilutions are required in order to avoid the cross-linking of the NPs represents a limit to this technique, because high amounts of solvents and templates are required. These are not always very cheap or commercially available. Dilution also has negative impact on the strength of the template-monomers interactions. Moreover, this technique requires the characteristics and the composition of the imprinting mixture to be carefully matched with the operating conditions of the system (type of initiation, temperature, shape of the reactor) in order to better control size, shape and imprinting properties of the product.

1.4.2 Mini- and micro-emulsion polymerisation

Another method which has been used to obtain MIP NPs is mini-emulsion polymerisation. Its application to the MIP area is quite recent, and it was first performed by Vaihinger *et al.* (2002), who exploited it to obtain NPs imprinted with L- or D-Boc-Phenylalanine anilid (BFA). Emulsion polymerisation is usually carried out by producing an O/W emulsion in which monomer, cross-linker and template are in the disperse phase, while the initiator is in the continuous aqueous phase. The polymerisation process then is carried out in micelles composed of the polymerisation mixture and stabilised by a proper surfactant. However, this usually gives rise to large microparticles. Mini-emulsion polymerisation is very similar, but it additionally involves a high-shear homogenisation step and the use of a co-surfactant for obtaining particles in the range 50-500 nm (Van Herk and Monteiro, 2003). The co-stabiliser is needed to suppress the diffusion in the aqueous continuous phase and to increase the stability and the homogeneity of the system. In this way it may be possible to obtain nearly full conversion of the nanodroplets into nanoparticles. In the work of Vaihinger and colleagues, the oil phase was composed of MAA as functional monomer and EGDMA as cross-linker, used in different molar ratios in order to study their effect on the particle size. The oil phase also contained hexadecane as co-stabiliser and 2,2'-azo(2-methylbutyronitrile) (AMBN) as initiator, in addition to the aminoacidic template. This phase was then mixed by vigorous stirring with the aqueous continuous phase composed of surfactant SDS

dissolved in water. After that, the mixture was sonicated and polymerised at 80 °C for 16 h. A very high conversion rate (about 98%) of the nanodroplets into MIP NPs was obtained. Moreover, thanks to the use of the hydrophobic initiator AMBN, the polymerisation occurred just into the droplets. The MIP NPs produced also exhibited very good enantio-selectivity, in particular when the monomer-to-cross-linker molar ratio was 1:4. MIP NPs imprinted with L-BFA bound this template 10-fold more efficiently than they bound the D-enantiomer. They also had very good affinity, since NIP NPs bound the template 4-fold less than the MIP. However, these rebinding properties were exhibited only when the amount of template was above 5 µmol, because for lower amounts of template no rebinding differences could be appreciated between MIP and NIP NPs, especially in presence of a higher MAA content. Moreover, despite the particles obtained were regularly spherical, their polidispersity was quite pronounced, since the diameters ranged between 50 and 300 nm (Figure 1–14).
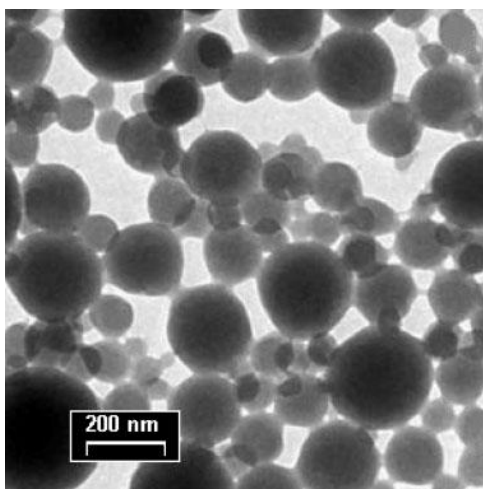
Figure 1–14. Transmission electron microscopy (TEM) image of MIP NPs produced through mini-emulsion polymerisation by Vaihinger *et al.* (2002).

In order to improve the mass transfer of the ligands, a recent trend is to try to control and restrict the location of binding sites mainly onto the surface of the particles. In this way an easier accessibility of the imprinted cavities may be achieved. Priego-Capote and his group in 2008 modified the mini-emulsion polymerisation technique in order to obtain surface-imprinted NPs with a more

homogeneous binding site distribution. Their strategy was to use a polymeric surfactant monomer instead of a conventional one, in order to form more stable micelles and help to locate the template at the surface of the synthesised MIP NPs. In particular, authors used sodium *N*-undecenoyl glycinate as surfactant monomer and EGDMA as cross-linker. These were mixed with hexadecane and AIBN, adding *S*-propranolol as template. This oil phase was emulsified with water under ultrasonication, and then the mini-emulsion was polymerised at 70 °C for 16 h. The synthesised MIP NPs were able to bind 3-fold more template than non-imprinted ones. However, the affinity for the template was lower than the values obtained through other polymerisation methods. In addition the size of the MIP NPs was not really uniform and it ranged from 30 to 150 nm when analysed through dynamic light scattering (DLS) and SEM, confirming the presence of aggregates. Moreover, the composition of the polymerisation mixture had to be carefully optimised in order to avoid stability issues and sedimentation phenomena. Nevertheless, the MIP NPs produced in this work were successfully used in CEC analysis (see section *1.5.2 - Capillary Electrochromatography (CEC)* for more details).

Very recently (2009) Curcio and his group prepared MIP NPs imprinted with glucopyranoside using the same modified mini-emulsion polymerisation approach. They exploited a semi-covalent imprinting technique instead of a non-covalent one in order to force the template to be located on the surface of the MIP NPs. For this purpose, a polymerisable surfactant template was synthesised, with four acrylic ester groups and a lipophilic chain with a polar sulphonated head. This compound was dissolved in styrene (St), chosen as functional monomer, and DVB. Then AMBN and hexadecane were added and this solution was mixed with an aqueous solution of SDS under ultrasonication. The obtained mini-emulsion was thermally polymerised at 80 °C for 20 h, after which the template was removed by alkaline hydrolysis. MIP NPs exhibited good rebinding capacity in comparison with non-imprinted ones, as well as very good selectivity for glucopyranoside rather than galactopyranoside (α = 6.5). Also the rebinding kinetics was quite fast, since it took only 5 h to reach the equilibrium, while for MIPs prepared by bulk polymerisation it usually requires

24 to 48 h. According to the Scatchard analysis, two classes of binding sites with low (K_D = 5780 × 10^{-6} M) and high affinity (K_D = 439 × 10^{-6} M) had been created. However, the use of a semi-covalent imprinting approach did not allow removing all the template from MIP NPs. Moreover, the synthesised MIP NPs did not exhibit a homogeneous size distribution when analysed by TEM (Figure 1–15).
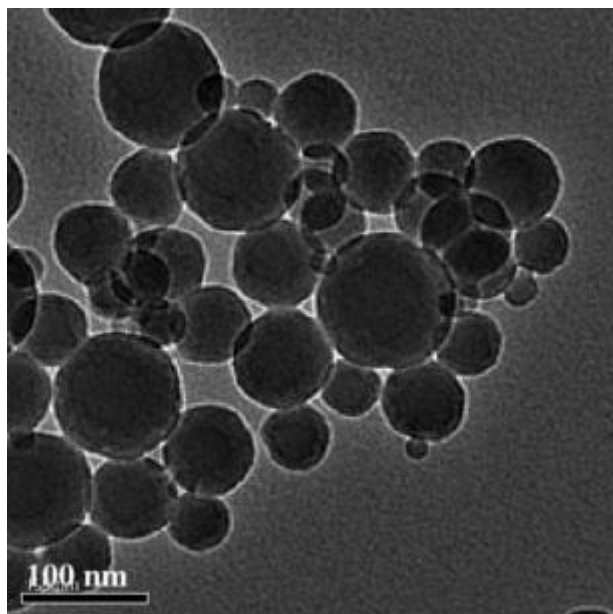
Figure 1–15. TEM image of MIP NPs synthesised by Curcio *et al.* (2009).

Another group (Zeng *et al.*, 2010), very recently used a similar approach to obtain MIP NPs imprinted with a small hydrophilic peptide, GFP-9. They used an inverse micro-emulsion polymerisation, which involves creation of nanodroplets of an aqueous solution of monomers dispersed in an organic continuous phase. Also in this case, a surfactant is required to stabilise the droplets. Authors used GFP-9 peptides coupled with fatty acid chains of different lengths (5, 13 and 15 carbon atoms) as a template. The polymerisation process was performed by dissolving in water AAm and *N,N'*-ethylenebisacrylamide, chosen respectively as monomer and cross-linker. This solution was then dispersed in the oil phase containing surfactants bis(2-ethylhexyl)sulfosuccinate sodium salt and Brij 30, dissolved in hexane. The modified peptides were then added and the mixture was vigorously stirred to form the micro-emulsion. Finally, the polymerisation was started by adding APS

and TEMED and carried out for 2 h. Very small MIP NPs were obtained, about 28 nm in diameter and spherical in shape. Moreover, MIP NPs imprinted with the peptides coupled to acid chains of 13 and 15 carbon atoms exhibited a very strong affinity for the template and good specificity. The calculated K_D ranged between 90 and 900 nM. However, MIP NPs imprinted with the template coupled to the shortest fatty acid chain did not exhibit any relevant imprinting effect. Probably the carbon chain (C_5) was too short to successfully locate the templates onto the surface of the aqueous nanodroplets. Moreover, the affinities of the binding sites were distributed and only a small amount of high-affinity sites had been created. In addition the yields were not very high (50% w/w).

To overcome the presence of water which characterises and disrupts the majority of every mini-emulsion imprinting polymerisation process, Dvorakova and co-workers (2010) recently proposed a non-aqueous mini-emulsion imprinting polymerisation approach which involves the use of a non-ionic, polymeric emulsifier, polyisoprene-block-poly(methyl methacrylate) co-polymer rather than a classic surfactant, and *n*-hexane and DMF respectively as external and internal phase of the emulsion. Authors used MAA and EGDMA as monomer and cross-linker and propranolol as template. These compounds were dispersed in DMF and then emulsified with the external phase containing the co-polymer through ultrasonication. The mini-emulsion was then polymerised thermally at 40 °C for 24 h after the addition of 2,2'-azobis(2,4-dymethylvaleronitrile) as initiator. Monodisperse MIP NPs of 100-120 nm in diameter were obtained, independently from the amount of template used in the preparation. Predictably, both an increase in the amount of emulsifier and a decrease in the volume of internal phase resulted in a decrease in the NPs diameter. MIP NPs exhibited an evident imprinting effect when compared to their NIP counterparts, up to 30% mol of specific template rebinding, with a specific K_A of 1.68×10^6 M^{-1} (about 2 orders of magnitude higher than the K_A calculated for the NIP NPs). Nevertheless, the approach still needs some optimisation because the non-porous rigid nature of the NPs or the shielding effect of the polymeric emulsifier did not allow to remove all the template at the

end of the production process, which could result in potential leakage and contamination in the case of sensing/separation applications.

In summary, the mini-emulsion polymerisation method also suffers from several drawbacks for producing MIP NPs. In fact, even if very small spherical-shaped NPs can be produced, the presence of several chemicals (surfactants, co-stabilisers) might interfere with the imprinting process, thus broadening the affinity distribution of the binding sites. This problem could be limited by using semi-covalent imprinting approaches, but such a strategy is not always applicable, and it depends also on the chemical nature of the template. Moreover, the purification steps required to remove all these substances are quite long and tedious, and they still might not be exhaustive in eliminating all the interfering chemicals.

1.4.3 Core-shell approaches

In order to achieve a surface-imprinting of NPs, core-shell approaches have also been used. These techniques involve the deposition of a MIP layer onto preformed support nanospheres made of various materials such as silica, PS or others. In this way it is also possible to use cores with specific properties, like fluorescence or magnetism, which might improve the whole performance of the imprinted nanosystems (Pérez-Moral and Mayes, 2002; Tan and Tong, 2007).

Core-shell emulsion polymerisation

The most direct technique to produce core-shell MIP NPs is core-shell emulsion polymerisation, which was pioneered by Pérez and co-workers (2000). This approach involves a two-stage process in which the first step requires the production of a latex, which can be prepared from several materials (St, DVB, alkyl acrylate). This latex is usually monodisperse, with diameters ranging from 30 nm to 1 μm. The second stage of the process involves the creation of an imprinted shell on the seed particles, through an emulsion polymerisation process. In this first example, core-shell particles were imprinted for cholesterol using a sacrificial spacer approach. The feasibility of this emulsion polymerisation technique for preparing core-shell MIP NPs was investigated by

using various monomers (MMA or St) and cross-linkers (EGDMA, DVB). Authors first prepared a polymeric latex, which was then swollen in a solution of cross-linker and functional monomer. After this swelling step, an aqueous solution of SDS was added together with APS to initiate the polymerisation of the imprinted shell, which was performed at 60 °C for 24 h. Once the polymerisation was finished, the template was removed by alkaline hydrolysis. All the imprinted NPs exhibited similar sizes, ranging from 50 to 100 nm, and high surface areas (80 ÷ 120 m^2/g) depending on their composition. The best results were obtained with particles bearing EGDMA shells, which exhibited good rebinding capacities and negligible non-specific binding, while MIP NPs produced with DVB shells had poor binding properties. The authors also investigated the possibility of using magnetic cores, thus obtaining superparamagnetic core-shell MIP NPs of 74 nm in diameter and good rebinding characteristics, which underwent a rapid separation (30 s) when a magnetic field was applied. It is worth noting that the same MIP NPs required 75 h to be recovered by sedimentation.

In a subsequent work (2001) the same authors proposed a slightly modified approach in order to improve the imprinting characteristics of the core-shell MIP NPs. Firstly a St/DVB seed latex was produced under the same conditions as in the previous work. In a second stage of the emulsion polymerisation process a mixture of DVB with a tailor-made polymerisable surfactant, pyridinium 12-(4-vinylbenzyloxycarbonyl)dodecanesulphate (PyS), and template surfactant, pyridinium 12-(cholesteryloxycarbonyloxy)dodecanesulphate (TyS) was used. The aim of the authors was to force the template molecules (cholesterol) to be located at the polymer-water interface during the shell formation step, thus creating hydrophobic binding sites preferably on the surfaces of the MIP NPs. The effect of the variation of the TyS/PyS ratio on the morphology and the rebinding properties of the particles was investigated. Authors obtained MIP NPs with relatively uniform morphology and small diameters (60 nm) when the amount of TyS ranged from 0 to 5% (mol), while for greater amounts of TyS polydisperse particles were obtained (Figure 1–16)
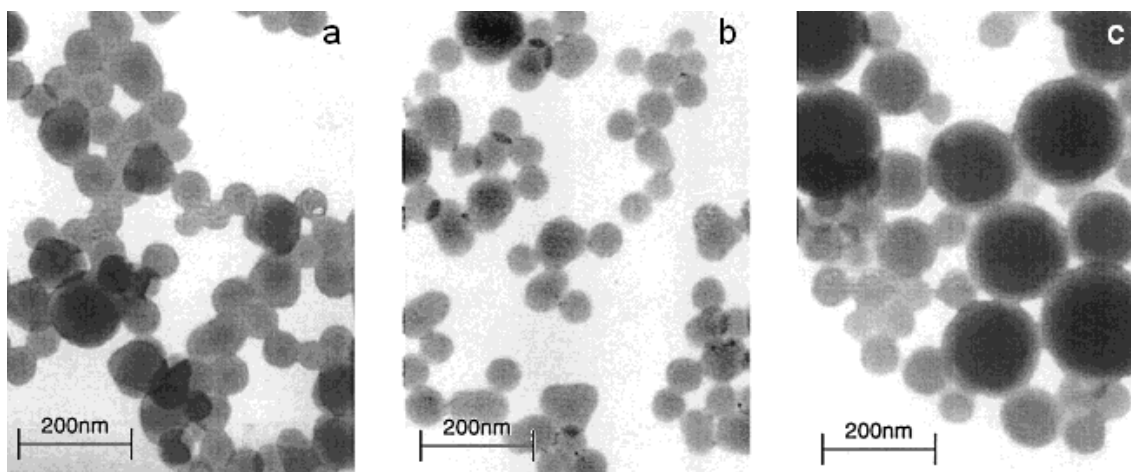
Figure 1–16. TEM images of MIP NPs obtained when the amount (mol) of TyS used was: (a) 0%; (b) 2.5%; (c) 15% (adapted from Pérez *et al.*, 2001).

The cholesterol rebinding reached a maximum when the amount of TyS ranged between 2.5 and 7.5%, but it was lower when higher amounts of TyS were used, probably because the binding sites were no longer isolated from each other. It is worth noting that the use of PyS and TyS, also allowed obtaining MIP NPs with two different surface functionalities (sulphate charged groups or benzyl alcohol groups), thus regulating the hydrophilicity of the particle surfaces. Despite these materials were successfully tested for an "immunoprecipitation-like" reaction (see section *1.5.4 - Sensing applications*), the results of this work suggest that the choice of surfactant, template and monomers has to be carefully tailored to achieve a good imprinting effect on the surfaces of the NPs.

Non-covalent imprinting approaches have also been exploited with the core-shell polymerisation procedure. Pérez-Moral and Mayes (2004) prepared core-shell MIP NPs non-covalently imprinted with propranolol. Authors also studied the effects which the template amount and the presence of the porogen had on the rebinding properties of the NPs. The seed latex was prepared by thermally polymerising an emulsion prepared from an aqueous phase containing $NaHCO_3$ and SDS and an oil phase composed by MMA and EGDMA. The obtained latex, previously mixed with MAA, EGDMA and the template, was then added to an aqueous solution of SDS and the imprinted shell was polymerised by adding

51

APS. The synthesised MIP NPs were recovered with very high yield (98-100%), and their diameters ranged from 60 to 70 nm. The authors found that MIP NPs prepared with more than 6% (mol) of template had increased binding capacity but were not very stable. They also found that the presence of a porogen (toluene in this case) had a strong effect on the shell porosity, making the structure more accessible and thus increasing the surface area and the rebinding capacity of the core-shell MIP NPs. The conditions of the second stage of the polymerisation had to be carefully optimised in order to avoid secondary nucleation phenomena, which were very frequent. Moreover, the presence of the aqueous phase during the non-covalent imprinting resulted in a relatively low imprinting effect, if compared to other polymerisation methods. It is worth noting that the authors of this work also introduced a fluorescent monomer (9-anthrylmethyl methacrylate) into the core of one of the preparations. The obtained MIP NPs did not exhibit any difference in morphology or rebinding characteristics from the ones without the fluorescent core, and might be suitable for sensing applications in diagnostics (see section *1.5.4 - Sensing applications*).

Summarising, core-shell emulsion polymerisation is a good method to obtain surface-imprinted MIP NPs, thus increasing the rebinding capacity and kinetics, as well as the yield of the synthetic process. Moreover, thanks to the heat dispersion, it is more suitable for large-scale applications in industry, especially if compared to the bulk polymerisation method. However, the complexity of the procedure and the presence of surfactants and aqueous phase represent serious drawbacks for standardising the procedure, both in terms of particle dimensions and imprinting effects.

Grafting approaches

Another way to obtain surface-imprinted MIP NPs is represented by grafting approaches (see *1.3.2 - Films and membranes*). In the case of NPs, the support is a suitable spherical monodisperse nanomaterial such as silica, PS or even magnetite (Fe_3O_4).

In 2007, Pérez-Moral and Mayes fabricated core-shell MIP NPs by exploiting a living radical polymerisation process initiated by a dithiocarbamate iniferter immobilised on the surface of polymeric NPs. Authors first synthesised two sets of polymeric seed particles, supposed to act as the core. These particles were composed in one case by MMA/EGDMA, while the other set was made by St/DVB. Both of the particles contained also 20% (mol) of vinylbenzyl chloride, in order to provide the functional groups for immobilisation of the iniferter DEDTC. After the purification of the cores and the immobilisation step, the MIP layers were finally synthesised on the core NPs surfaces by adding monomers, cross-linkers, templates (propranolol, naproxen or morphine) and toluene as porogen solvent. The polymerisation process was performed by UV irradiation for 5-12 h (Figure 1–17).
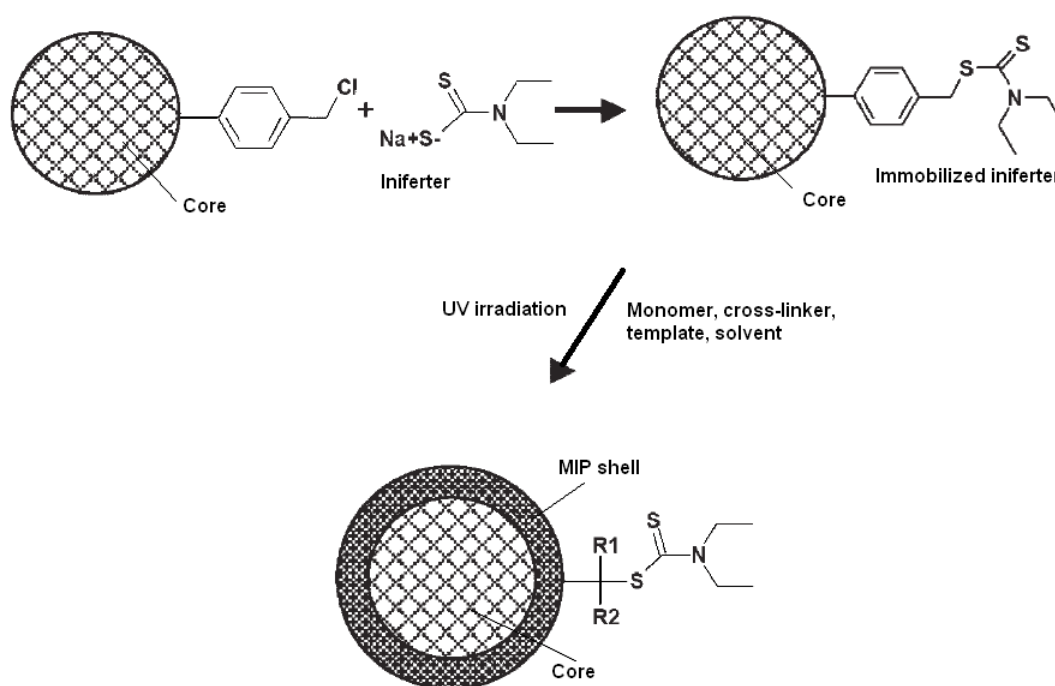
Figure 1–17. Scheme of the immobilisation of the DEDTC iniferter and subsequent application for grafting the MIP shell onto the core surface (adapted from Pérez-Moral and Mayes, 2007).

The synthesised particles showed a clear imprinting effect similar to the one evaluated for MIP NPs prepared by conventional approaches. In addition,

thanks to the absence of water, this method allowed naproxen to be effectively imprinted, while previous attempts to imprint this drug molecule on core-shell MIP NPs were unsuccessful (e.g., by emulsion polymerisation). However, the imprinting of this drug could be confirmed only when the rebinding test was performed in an aqueous environment. The same test carried out in toluene (solvent used in the imprinting process) did not exhibit any imprinting effect for naproxen. These results suggest that the approach still needs to be optimised for different types of templates. Nevertheless, this method is particularly interesting because it allows very thin MIP layers to be deposited on the particles surface. The authors of this work, in fact, were able to build four-component particles, i.e. core and three layers. The first layer was made by MAA/EGDMA and imprinted for propranolol; a second layer was composed of vinylbenzyl chloride and a third one contained an anthracene methacrylic derivative which gave the particles fluorescent properties. The increase of the shell thickness after the addition of each layer slightly affected the amount of specific rebinding, which progressively decreased after each layer addition. However, this approach remains very promising if well optimised, because the living-nature of the radical process is compatible with the formation of multi-layer MIP NPs.

Gao *et al.* in 2007 prepared core-shell MIP NPs imprinted with 2,4,6-trinitrotoluene (TNT) using silica NPs as cores. Authors prepared uniform silica colloidal NPs by hydrolysis of tetraethoxysilane (TEOS). The obtained silica cores with a diameter of 100 nm were subsequently modified by the addition of 3-aminopropyltriethoxysilane (APTES), in order to provide a surface amino group. This latter was needed to introduce acryloyl chloride on their surface, thus obtaining vinyl polymerisable end groups. After this step the imprinted TNT shell was synthesised using AAm as functional monomer, EGDMA as cross-linker and AIBN as initiator. The polymerisation process was performed in ACN through a two-step thermal polymerisation, in order to slow the reaction rate and avoid formation of secondary polymeric particles in solution. In this way core-shell MIP NPs with a diameter of about 125 nm were obtained, nearly

monodisperse (Figure 1–18A). A correlation between shell thickness and particles binding capacity was also found (Figure 1–18B).
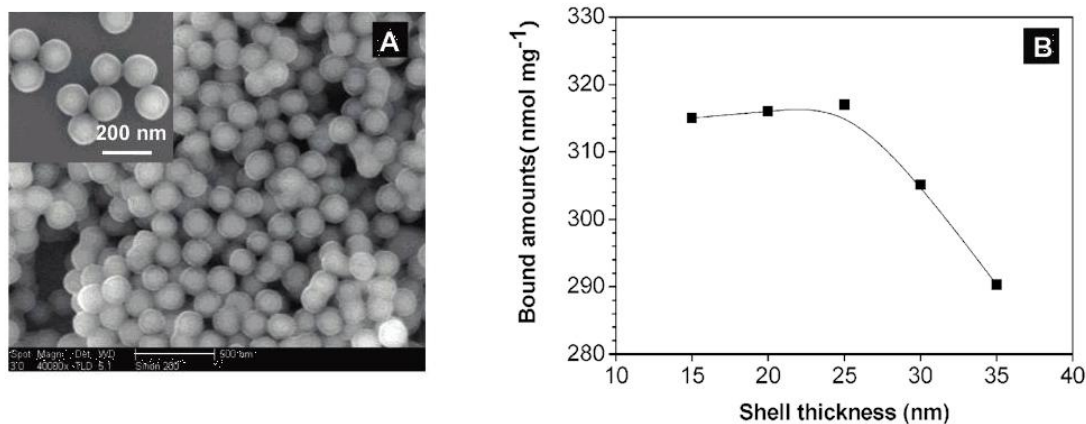
Figure 1–18. A) SEM image of surface-imprinted silica core-shell MIP NPs (the insert is a high-magnification image). B) Evolution of density of effective recognition sites with shell thickness of MIP NPs (adapted from Gao *et al.*, 2007).

Another key point in this work is that the authors exploited the strong charge-transfer interaction established between the nitroaromatic ring of TNT and the residual electron donor amino groups of APTES. In this way the template preferentially located itself onto the particle surface and so increased the density of imprinted sites in the shell, without need to use semi-covalent imprinting approaches or surfactant templates like in other methods. This stresses the importance of the choice of monomers in relation to the chemical nature of the template. Regarding the binding properties, the core-shell MIP NPs produced in this work exhibited a 5-fold higher density of active imprinted binding sites than traditional 2 μm size imprinted particles. These latter were prepared for comparison purposes using precipitation polymerisation. Moreover, the rebinding kinetics of the MIP NPs was 4.5-fold faster than that of conventional microparticles, with very good selectivity. Probably the main drawbacks which emerge from this work are represented by the number of synthetic steps required to obtain the final product, together with the fact that such a thin imprinted shell might not be suitable to successfully imprint bulkier templates. In addition, if the thickness of the shell is not carefully controlled, it could be difficult to avoid the formation of aggregates of NPs. Moreover, it might

be difficult to match other templates and monomers in order to establish such strong interactions during the imprinting process.

More recently, Yao and Zhou (2009) used a similar approach to fabricate surface-imprinted core-shell MIP NPs imprinted for bensulfuron-methyl. Like in the work previously cited, authors first prepared 250 nm size silica core NPs through hydrolysis of TEOS. Then, they modified the surface of these particles with 3-(trimethoxysylil)propylmethacrylate through a one-step ultrasonic procedure. In this way C=C double bonds were introduced faster and more effectively than in the two distinct synthetic steps described in the work of Gao *et al.* Also in this work, the MIP shell was grafted through a step-by-step thermal polymerisation performed in ACN, using MAA as functional monomer, EGDMA as cross-linker and AIBN as initiator. MIP NPs exhibited a uniform 35 nm thick shell and a spherical shape (Figure 1–19A). Their binding properties were compared to 3 μm size MIP microparticles produced by common precipitation polymerisation under the same conditions. The results showed that the rebinding capacity of the surface-imprinted NPs was about 1.5 times higher than traditional microparticles. Moreover, MIP NPs exhibited a 5-fold higher density of effective imprinted sites, probably thanks to the surface-imprinting. They also possessed good rebinding kinetics and selectivity, thanks to the strong interactions occurring between the template and the functional monomer. However, the thermal polymerisation seems to be a key step in the production process of these surface-imprinted nanosystems. If it is not carefully controlled and slowly performed through subsequent steps, it could cause the formation of small particles on the surface of the silica nanobeads (Figure 1–19B), instead of the creation of a grafted MIP shell (Figure 1–19A).
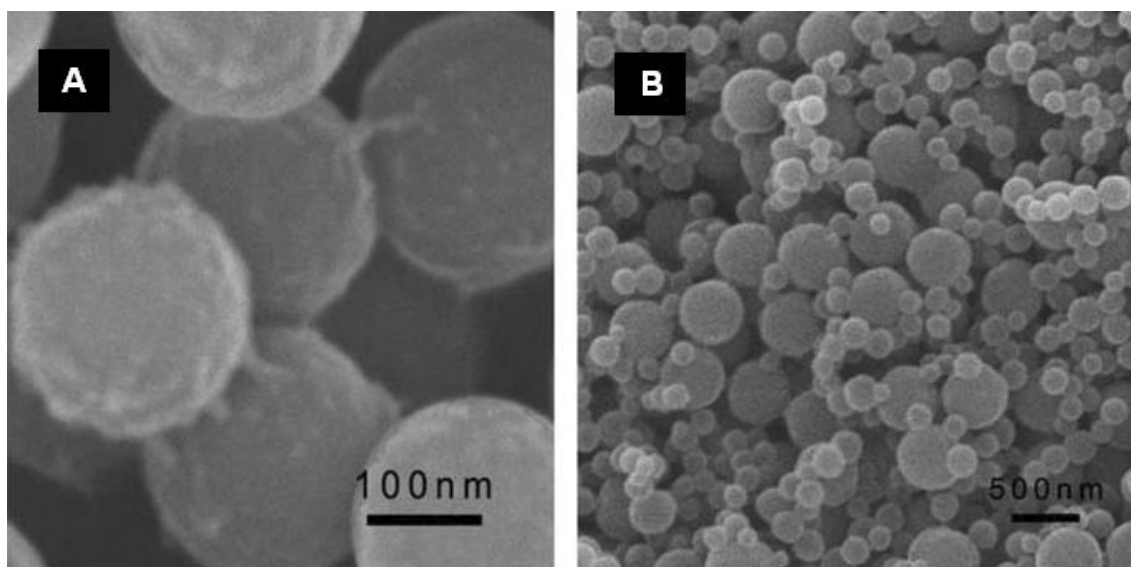
Figure 1–19. SEM images of surface-imprinted silica core-shell MIP NPs obtained through (A) step-by-step polymerisation or (B) directly heating at 80 °C for 3 h. In (B) self-aggregation of particles can be observed (adapted from Yao and Zhou, 2009).

Li and his group (2009) recently prepared surface-imprinted magnetic PS MIP NPs for bovine haemoglobin through a multi-stage core-shell polymerisation process. It involved the use of 3-aminophenylboronic acid (APBA) as functional and cross-linking monomer. In fact, thanks to its water solubility and the variety of reversible interactions which it establishes with amino acids, APBA is particularly suitable for protein imprinting (Bossi *et al.*, 2001). First core magnetite NPs were synthesised with a size smaller than 25 nm in order to achieve superparamagnetic properties. Then these cores were coated with a silica layer using TEOS, and subsequently surface-modified using 3-methacryloxy(propyl)trimethoxysilane. This allowed further introducing a thin PS layer on the surface. Eventually, the MIP layer was created by polymerising APBA on the magnetic PS particles for 14 h, in the presence of the template, using APS as initiator. The final size of the coated particles reached a diameter of 480 nm, in which the MIP film was 15-20 nm thick. TEM analysis did not reveal presence of aggregates, so confirming that each coating step occurred only on the particle surface. Moreover, the core-shell MIP NPs exhibited magnetic properties suitable for an easy separation, also in large scale.

57

Additionally, they had a fast rebinding kinetics (30-120 min). The Scatchard analysis revealed that MIP NPs also had very good specificity (imprinting factor, IF = 2.3) and selectivity (α = 1.98). However the complexity and the amount of time required to execute all the synthetic steps, even if the particles obtained at the end of each step can be recovered through a strong magnet, represent serious drawbacks for the production of this type of MIP NPs on large scale.

Wang and co-workers (2009) prepared Fe_3O_4 magnetic NPs coated with a silica shell imprinted for estrone. Authors chose to use a semi-covalent imprinting approach. The imprinted shell was indeed fabricated by grafting an estrone-silica monomer complex to the magnetic cores, previously coated with silica. To extract the template, MIP NPs were heated at 180 °C in a mixture of dimethylsulfoxide (DMSO) and water for 3 h, causing the cleavage of the urethane bond which connected the template to the shell. Because of the presence of water, the dissociated isocyanato group left behind in the silica shell was hydrolysed to an amino group, allowing non-covalent interactions to be subsequently established with estrone. Relatively monodisperse superparamagnetic MIP NPs (Figure 1–20) of about 150 nm in diameter were obtained.
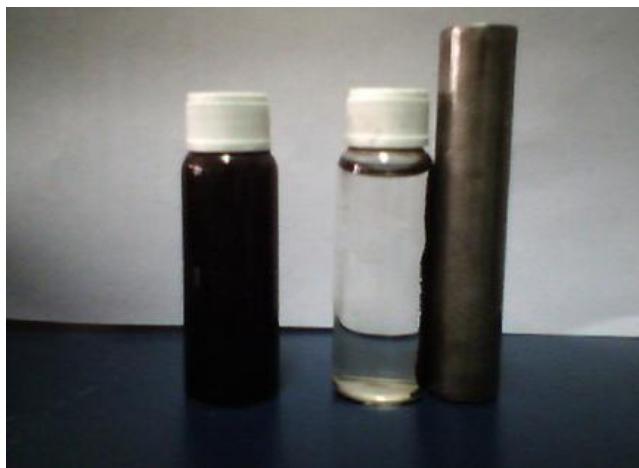
Figure 1–20. Separation of estrone-imprinted magnetic core-shell silica NPs by a magnet (reproduced from Wang *et al.,* 2009).

The linear result of the Scatchard analysis revealed the presence of homogeneous binding sites (R^2 = 0.998). The calculated values of K_D and Q_{max}

were 4.53 mM and 183.4 µmol/g, respectively. MIP NPs rebound estrone about 3.6-fold more than the non-imprinted ones, and 3.2-fold more than they rebound testosterone, thus exhibiting low cross-reactivity. However, even if the semi-covalent imprinting approach used in this work resulted in better rebinding properties, the amount of synthetic and heating steps required for obtaining this kind of products still make these approaches poorly suitable for large-scale processes.

Among the techniques suitable for preparing core-shell MIP NPs, Lu and colleagues (2007) exploited the advantageous reversible addition–fragmentation chain transfer (RAFT) controlled living radical polymerisation approach. RAFT is a versatile and simple polymerisation protocol compatible with several types of monomers. Authors prepared surface-imprinted core-shell MIP NPs imprinted for 2,4-D. They first synthesised silica cores (about 200 nm in diameter), which were then surface-functionalised by grafting trichloro(4-chloromethylphenyl)silane. This was needed to subsequently immobilise the RAFT agent, dithiobenzoate, synthesised *in situ* from CS_2 and phenylmagnesium bromide. The final step involved the production of the MIP shell by mixing the surface-modified silica particles with 4-VPy, EGDMA, AIBN, and the template 2,4-D, in a methanol (MeOH)/water (4:1, v/v) mixture. The polymerisation was then thermally performed for 12 h at 60 °C. TEM analysis revealed the presence of a MIP shell about 25 nm thick and quite uniform, probably thanks to the controlled nature of the RAFT polymerisation technique. Moreover, in presence of the same concentration of 2,4-D, MIP NPs were able to bind 50% of the template, while the non-imprinted ones only 7.9%, thus indicating a higher rebinding capacity resulting from the imprinting procedure. Core-shell MIP NPs also exhibited good selectivity, comparable to bulk MIPs.

More recently (2009), the same group used another living radical polymerisation protocol for preparing surface-imprinted core-shell magnetic MIP NPs. Atom transfer radical polymerisation (ATRP) has indeed proved suitable for grafting polymeric layers from solid supports. Authors first coated Fe_3O_4 core NPs with a protective silica layer, thus obtaining NPs about 300 nm in diameter. The

thickness of the silica layer could be controlled by varying the amount of TEOS initially added. Authors then grafted 3-aminopropyltrimethyloxysilane (APTMS) onto the surface of the particles, in order to introduce an amino group suitable to subsequently immobilise 2-bromoisobutyrylbromide as initiator. The MIP layer was then synthesised by mixing in ACN the surface-modified core NPs with CuBr and pentamethylendiethylentriamine, together with 4-VPy as functional monomer, EGDMA as cross-linker and bisphenol A as template. The final core-shell MIP NPs exhibited a diameter of 370 nm and a uniform MIP shell about 15 nm thick (Figure 1–21).
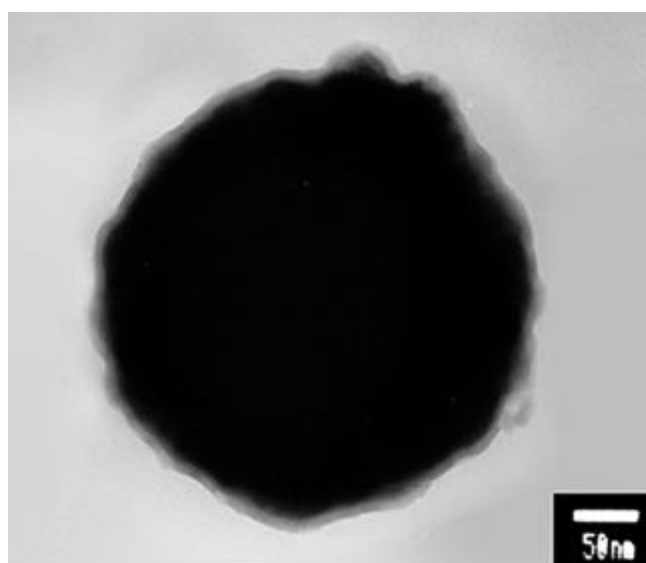
Figure 1–21. TEM image of a core-shell silica-coated magnetic MIP NP (reproduced from Lu *et al.*, 2009).

Moreover, they exhibited high capacity and selectivity, together with a fast rebinding kinetics (60 min to reach the equilibrium, instead of 300 min required by conventional bulk MIPs). In addition, they were successfully applied in separation applications thanks to their superparamagnetic properties (see section *1.5.5 - Separation*). However in this polymerisation approach catalytic complexes formed by the Cu ion and acidic or basic ligands might be disrupted by the template molecules, thus interfering with the polymerisation process. Moreover, the metallic catalyst has to be removed from the final product. This is why usually other living radical polymerisation processes (such as RAFT or iniferter-based approaches) seem to be more suitable for imprinting procedures

(Ye and Mosbach, 2008). However, since their application in molecular imprinting is relatively new, these techniques deserve more studies to better understanding if they can be fully exploited for obtaining MIP nanomaterials.

A modified original core-shell approach has been used by Li and co-workers (2006b) to prepare MIP NPs imprinted for 1-ethyluracil. First, they used ATRP to prepare a diblock co-polymer of *tert*-butyl methacrylate and 2-(trimethylsylyloxy)ethyl methacrylate as monomers. They further modified this co-polymer by derivatising it with 2-acrylamido-6-carboxybutylamidopyridine, in order to introduce a triple-hydrogen bonding moiety and cross-linkable double bonds into the co-polymer. This modified co-polymer was then dissolved in chloroform with the template and thoroughly mixed with cyclohexane to form polymeric micelles, which were subsequently cross-linked in their shell by adding an azo-type initiator (V-65). After the removal of the template, TEM confirmed the creation of uniform core-shell MIP NPs of about 100 nm in diameter. Moreover, the triple-hydrogen bonding moiety ensured good selectivity for the template. In addition, core-shell MIP NPs exhibited 2.4-fold more rebinding capacity than traditional bulk MIPs prepared with the same polymerisation mixture. However, the synthetic complexity of the protocol does not make it particularly suitable for large-scale applications.

Another very interesting approach for preparing core-shell MIP NPs has been recently developed by Zhou and co-workers (2010), who imprinted human haemoglobin on a polydopamine (PDA) layer synthesised on the surface of magnetic Fe_3O_4 NPs. This is an original approach that involves the self-polymerisation process which this catecholamine undergoes when exposed to slightly basic pH values. In particular, the authors first synthesised Fe_3O_4 100 nm size core NPs, and then they coated them by exploiting the self-polymerisation of dopamine in TBS (pH = 8.0) in the presence of haemoglobin. The PDA layer was deposited spontaneously on the surface of the NPs, with an uniform average thickness of 10 nm after 3 h of polymerisation. The synthesised MIP NPs exhibited superparamagnetic properties, suitable to recover them in a short time using a strong magnet. According to the Scatchard

analysis performed in aqueous media, they also exhibited strong recognition affinity towards haemoglobin, with a K_D of 18.13 μg/mL. Moreover, MIP NPs possessed good binding capacity, since the Q_{max} was evaluated as 22.3 μg/mg. In addition, they showed low cross-reactivity, evaluated against proteins such as myoglobin, horseradish peroxidase and cytochrome c, with an IF of 5.01, even in case of competitive rebinding. Given these results, it seems that the use of PDA is particularly suitable for imprinting protein templates, because it is hydrophilic, biocompatible and it has amino and catechol groups which can help in establishing interactions with the macromolecular template. Moreover, the thickness of the PDA layer can be tuned by changing the polymerisation time (Lee *et al.*, 2007), suggesting that this approach might represent a promising innovation in molecular imprinting, especially in case of macromolecules.

1.4.4 Soluble nanogels

The creation of soluble MIP nanosystems, able to properly mimic recognition and catalytic phenomena such the ones proper of enzymes and antibodies, is the real new frontier for the development of MIPs.

Between the approaches tested to produce soluble MIP nanosystems, it is worth noting the work of Zimmerman and co-workers, who extensively studied the possibility of exploiting dendrimers as macromolecular hosts into which imprint a single molecule, thus obtaining a system more similar to natural receptors in terms of number of binding sites. They reported the covalent imprinting of porphyrin molecules (2002), in which these templates were used as starting cores to generate dendrimers. Then, after the subsequent cross-linking of vinyl end-groups of dendrimers through ring closing metathesis, the porphyrin core was removed by hydrolysis. The imprinted cavities exhibited a certain degree of selectivity, since only porphyrins able to establish four binding interactions were complexed.

Subsequently (2004), the same authors also prepared MIP dendrimers imprinted for a smaller template, tris(aminoethyl)amine. Dendrimers also contained a colorimetric reporter group able to signal the template binding by changing the colour. These dendrimers exhibited a K_D of 3×10^{-7} M.

Nevertheless, the fact that complex multi-step organic synthesis is required to prepare these materials, together with the limited availability of templates compatible with this approach, have limited its development in favour of more straightforward procedures.

In this respect, systems such as micro/nanogels might represent a viable alternative. The term "microgel" indicates "unimolecular, cross-linked polymer particles possessing a size comparable to the statistical dimensions of non-cross-linked macromolecules (≈ 100 nm) which can exist as stable solutions in appropriate solvents" (Biffis *et al.*, 2001). They might be considered then as soluble NPs. Hence it is not surprising that the cross-over between this technology and molecular imprinting has been investigated in the recent years, resulting in materials which contain a recognition site built in a soluble polymer particle. The dimensions of these particles, together with their solubility, make them similar to a natural enzyme or antibody.

A first attempt to synthesise water-soluble MIP NPs was performed in 1998 by the group of Piletsky and colleagues, who investigated the possibility to prepare MIP NPs imprinted for the thylakoid membrane D1 protein by extensive grinding and sieving of bulk monoliths. A mixture of urocanic acid as functional monomer and *N,N'*-bisacryloyl piperazine as cross-linker was polymerised in water in presence of the template, after the addition of APS and TEMED as initiating system. Monoliths obtained were then washed with diluted chloridric acid to remove the template and then extensively ground and ultrafiltered during centrifugation. Three fractions of soluble MIP NPs with different M_w (< 5 kDa, 5 ÷ 10 kDa and > 10 kDa) were collected and extensively characterised. Affinity chromatography showed that MIP NPs with M_w ranging from 5 to 10 kDa had a capacity factor almost double if compared to non-imprinted polymers. This demonstrated that the grinding process did not excessively destroy the structure of the binding sites. Moreover, MIP NPs exhibited good selectivity. However, the yield of the NPs synthesised with this method was very low (about 0.2 mg per fraction). Moreover, since it relied on grinding of bulk monoliths, it was not further developed. Nevertheless, this first work represents a milestone in the

production of soluble MIP NPs with biological activity (see section *1.5.6 - The future: biologically active MIP nanoparticles*).

The first proper example of synthesis of MIP microgels has been provided by Biffis *et al.* (2001), who extensively studied the best suitable radical polymerisation conditions to prepare MIP microgels imprinted for α-D-mannopyranoside. They used a covalent imprinting approach which involved the polymerisation of a vinylphenylboronic ester of the template with MMA as co-monomer, AIBN as initiator, and different amounts of either EGDMA, TRIM or 2,5-di-*O*-methacryloyl-1,4;3,6-dianhydro-D-sorbitol as cross-linkers. Several solvents (cyclohexanone, cyclopentanone, dimethylformamide (DMF), tetrahydrofuran, mixtures of toluene/ACN) have been tested and the polymerisation processes have been performed at 80 °C for 4 days. In all the cases, the value of the monomer concentration was always maintained below the critical monomer concentration (c_m), i.e. that concentration value at which microgels growth is no longer stabilised by steric factors and the system evolves towards the formation of a macrogel. This was done to ensure a good solubility of the MIP microgels. Molecular weights and polydispersities (M_w/M_n) have been found to increase at higher monomer concentrations and cross-linking degrees. Also, when the rebinding of the template was tested in a solvent unable to dissolve the product but capable only to swell it (MeOH), MIP microgels prepared in cyclopentanone exhibited the highest selectivity, without any relevant effect due to the monomer concentration used during the preparation. The cross-linking degree, instead, influenced the selectivity values, which reached a maximum when the cross-linking was 70%, while for higher cross-linking degrees the selectivity decreased. This behaviour was independent from the type of cross-linker used, so it was ascribed to the high-dilution of the polymerisation mixture required to obtain MIP microgels, which resulted in a poor imprinting effect. On the other hand, when the same rebinding tests were performed in DMF, solvent able to dissolve the MIP microgels, they rebound much more template. However, in this case the selectivity values were lower than the ones measured in MeOH, for all the synthesised MIP microgels. It is worth noting that also the selectivity values for the control bulk MIPs

dropped in DMF. This suggests that the conditions for the rebinding tests have to be carefully optimised to precisely assess the recognition properties of the MIP microgels.

The same group, some years later (2006), produced soluble MIP nanogels able to catalyse carbonate hydrolysis. Also in this case, they used several preparation methods. A standard preparation procedure involved a radical thermopolymerisation at 80 °C in cyclopentanone for 4 days, using the template complexed with the functional monomer N,N'-diethyl-4-vinylbenzamidine, MMA, EGDMA as cross-linker and AIBN as initiator. However, several variations of this method have been attempted in order to improve the quality of the MIP nanogels, like increasing the cross-linker content or changing it with TRIM, or use a step-by-step polymerisation. Also in this case, authors found that increasing either the amount of monomer or cross-linker resulted in higher molecular weights and higher polydispersities (M_w/M_n). However, it resulted also in an increased catalytic activity. Nevertheless, the concentration of the monomer could be increased only up to 1.5%, which had been evaluated as c_m value for this polymerisation system. The use of a step-by-step thermal polymerisation also improved the characteristics of the product, but the best properties were obtained through a so-called "post-dilution method" developed by the authors. It involved carrying out the polymerisation process at high concentrations of monomer, similar to those used in bulk polymerisation, but with the addition of a large volume of solvent just before the point of macro-gelation. In this way they increased the cross-linking degree and also the catalytic activity of the MIP nanogels with simultaneous reduction of the polydispersity. The use of TRIM instead of EGDMA in this method, as expected, greatly improved the imprinting effect. However, the polydispersity index also increased exponentially (M_w/M_n = 18.6). By reaching a concentration of monomer of 0.1% after dilution, authors obtained MIP nanogels with very low polydispersity (M_w/M_n = 1.54) and particle size between 10 and 20 nm. A more detailed discussion on the catalytic properties of the MIP nanogels produced in this work is given in section *1.5.3 - Enzyme mimics.*

More recently (2009) Guerreiro *et al.* synthesised soluble MIP NPs imprinted for acetoguanamine by using an early termination of iniferter-initated polymerisation. According to these authors, NPs are always formed during the early stages of the MIP synthesis (Figure 1–22a). If the progressive association of polymer chains is allowed to continue, an insoluble MIP will be obtained (Figure 1–22c).
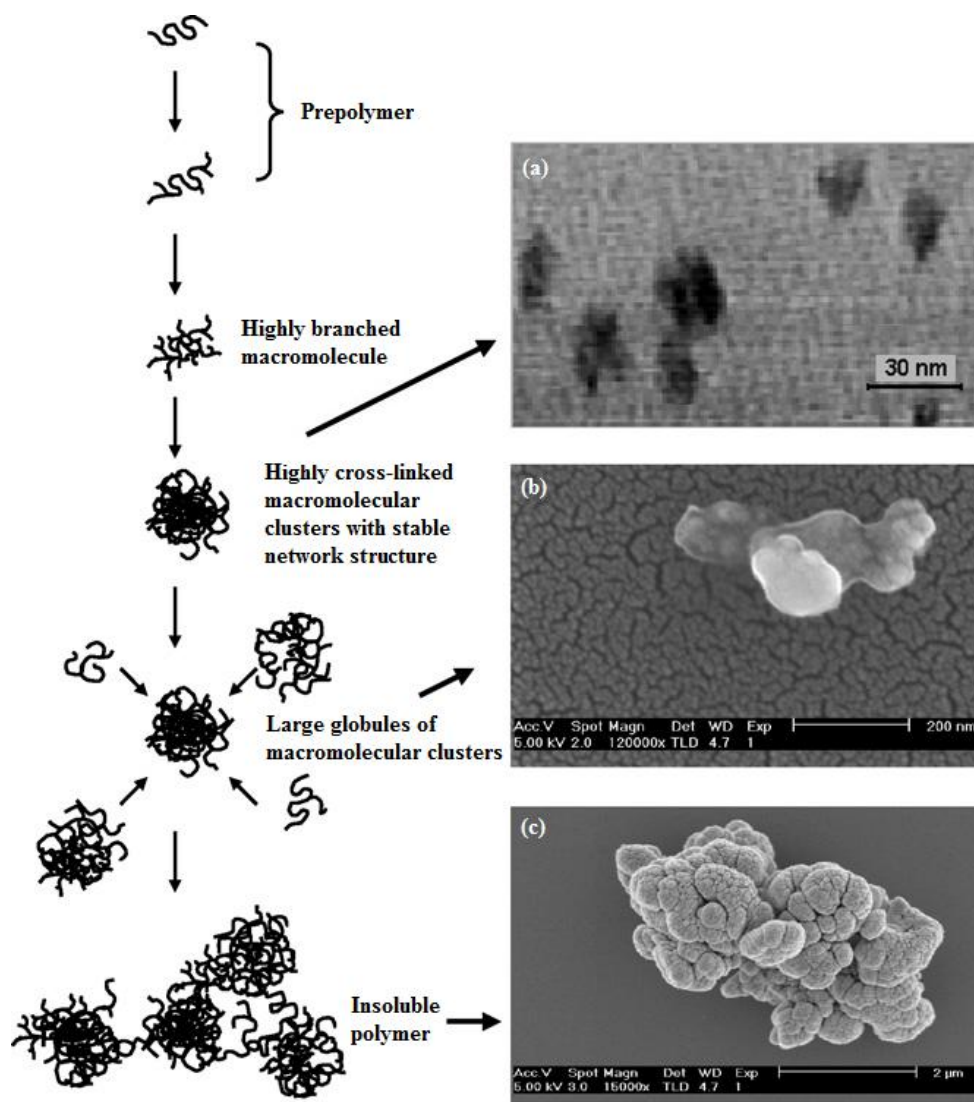
Figure 1–22. Scheme of the chain-growth process. On the right – images of polymer growth representing the three last stages on the scheme. (a) TEM image of NPs formed by UV irradiation for 170 s, magnification 340000×; (b) and (c) SEM images of polymer formed by aggregation of molecular clusters achieved during 180 and 250 s of UV irradiation, respectively (adapted from Guerreiro *et al.*, 2009).

Authors successfully used affinity separation for collecting particles with pseudo-monoclonal binding properties. Differently from the post-dilution method proposed by Wulff and co-workers, they performed polymerisation in the monomer mixture containing high concentration of monomers such as TRIM, EGDMA and MAA in ACN with *N,N*-diethyldithiocarbamic acid benzyl ester as initiator, using UV irradiation applied for 2.5 min. This polymerisation technique has been chosen since at the stage depicted in Figure 1–22a it is not easy to control the size of the particles because the reaction rate is high. The use of iniferter allows the reaction kinetics to be adjusted. Moreover it introduces the possibility to reinitiate the polymerisation later by simply exposing the material to UV irradiation (Otsu *et al.*, 1989; Otsu *et al.*, 1995; Kannurpatti *et al.*, 1996; Otsu, 2000). After the synthesis, NPs of M_w ranging from 3 to 100 kDa were obtained. Then they were divided in fractions of different sizes through gel permeation chromatography (GPC). After this step, an affinity chromatography analysis was performed. Authors found that particles with M_w ranging from 90 to 100 kDa possessed the highest affinity for the template. The authors then exploited the iniferter-moiety still present on the NPs to immobilise them onto the surface of poly(TRIM) microparticles using UV irradiation. After this immobilisation procedure, the binding properties of the NPs could be tested in solution. The K_D of the MIP NPs for the template was evaluated to be equal to 6.6×10^{-8} M. This affinity was comparable to the value reported for monoclonal antibodies for the same template, 3.87×10^{-7} M (Grant *et al.*, 1999) and 9.20×10^{-9} M (Kramer, 2002). At the same time the K_D value was significantly smaller than the K_D values found for non-imprinted NPs and bulk polymers prepared with a similar composition. Moreover, MIP NPs exhibited a clear specificity for acetoguanamine, compared to structurally correlated triazines. This work represents a milestone in the production of high-affinity soluble MIP NPs, because it relies on UV polymerisation instead of a thermal one, which could interfere with the recognition ability of the MIP nanogels (Piletsky *et al.*, 2002, Piletsky *et al.*, 2004, Mijangos *et al.*, 2006). Moreover, it does not involve high-dilution, then ensuring the formation of stronger complexes between template

and functional monomers. Probably, the main drawback of this method was the low yield of the NPs obtained (3% w/w).

Eventually, one of the last innovations achieved in the field of MIP nanogels is the coupling of their recognition properties with the possibility to respond to external stimuli. Chen and his group (2010) recently prepared a water-soluble pH-sensitive catalytic MIP nanogel able to mimic the activity of horseradish peroxidase (see also section *1.5.3 - Enzyme mimics*). It was prepared by polymerising a mixture composed by NIPAm, 4-VPy, hemin and AAm as monomers, EGDMA as cross-linker and homovanillic acid (HVA) as template, using AIBN as initiator and a mixture DMSO/water (7:3, v/v) as solvent. The polymerisation process was performed at 70 °C for 48 h. MIP nanogels were obtained with a narrow size distribution, confirmed by ESEM, DLS and GPC. Moreover, MIP nanogels also showed good affinity and selectivity properties. Despite all these advantages, the low yield (12.5%) and the long times required to purify the product by dialysis, make this process poorly suitable for large-scale applications.

Summarising, the synthesis of soluble nanoMIPs represents a challenge to obtain artificial enzymes, or even "synthetic antibodies". Moreover, they might improve the mass transport issues typical of insoluble MIP materials, resulting in very fast rebinding kinetics. Thanks to the easier synthetic strategies and larger compatibility with the imprinting procedures, MIP micro/nanogels seem to be more promising and feasible than imprinted dendrimers. In addition, compared to traditional MIPs, their characterisation may be easier because they can be investigated using the standard techniques available for soluble macromolecules. However, the synthetic methods available today for these materials need to be improved, especially in terms of yields and purification procedures. Nevertheless, very soon MIP nanogels could provide a viable alternative to the biological molecules used in sensors, separation and catalysis. Even more exciting could be the opportunity to develop these materials for *in vivo* real life applications, such as drug delivery and diagnostics.

These applications are discussed in more detail in the following section *1.5 - MIP nanoparticles: applications*.

1.5 MIP nanoparticles: applications

1.5.1 Drug delivery

The cross-linked nature and affinity properties of MIPs make them intrinsically suitable to act as reservoirs from which achieving a controlled or sustained drug release to enhance pharmacological therapy. This is particularly useful for those drugs with a low therapeutic index (e.g., THO), which might cause adverse effects if their concentration is not kept below a certain threshold value. Similarly, in the case of racemic drugs in which the two enantiomers have different activity levels or effects, MIPs could selectively release the more effective one. Chemically or physically triggered release or targeting properties also can be achieved using MIPs, e.g., when the polymer interacts with the specific imprinted target moiety, like a cell surface receptor overexpressed in a tumor area (Cunliffe *et al.*, 2005). Due to their dimensions and high-surface area, MIP NPs could represent a very interesting solution for these applications.

In a pioneering work by Ciardelli and co-authors (2004), MIP NPs were used as a drug delivery system for the controlled release of THO. Particles of 200 nm average diameter were synthesised using a modification of the precipitation polymerisation approach of Ye and co-authors (1999). However drug release properties of MIP NPs were not so easy to predict and understand. The release pattern depended on the fine balance of the strength of monomers–template interaction, concentration of monomers and polarity of the particles. The slowest release was achieved with MIP NPs in which the ratio MMA/MAA was 75:25 (mol). In all other cases, the release rate was higher. Authors suggested that an optimum amount of MAA can help to bind drug molecules more strongly, while too low or too high amounts of MAA result in NPs capable of establishing only weak interactions with THO, either because of absence of interacting groups or because of too high hydrophilicity of the NPs. This, in turn, would increase the accessibility of the phosphate buffered saline (PBS) used in the release test, thus resulting in a faster release rate. However, while the batch rebinding tests were performed in ACN (the same solvent used for the imprinting process), the release tests were performed in PBS. It might be interesting to assess the

rebinding properties also in PBS, for better understanding the system. Alternatively, the imprinting polymerisation process could be adapted to be performed in aqueous media.

Rather than using directly MIP NPs, Jantarat and co-authors (2008) fabricated composite cellulose membranes embedded with MIP NPs supported on the surface of microspheres (nanoparticles-on-microspheres, NOMs) for the transdermal enantioselective release of racemic propranolol. The *S*-enantiomer of this β-blocker is indeed 100–130 times more potent than its *R*-isomer. Such a delivery system would allow containing the synthetic costs, which can be quite high in case of enantiomerically pure compounds (Barrett and Cullum, 1968). The authors modified the suspension polymerisation method in liquid perfluorocarbons from Mosbach *et al.* (1996), thus obtaining MIP NPs with diameters in the range 300-500 nm directly attached on the surface of of 3-10 µm microspheres. MIP-NOM exhibited enantioselectivity properties, as well as a remarkable imprinting effect in comparison to NIP-NOM when tested in batch rebinding experiments. The corresponding composite membranes, prepared by phase inversion method, exhibited very high surface areas and good robustness. In addition, the release of the *S*-enantiomer from the composite membranes was 1.7 times more rapid than the *R*-enantiomer, and with greater enantioselectivity than other composite membranes prepared with irregular MIP granules or MIP microspheres. This was probably due to the higher surface area and accessibility of the binding sites characteristic of NOMs. Similar results were obtained during *in vitro* permeation studies on rat skin (*S*/*R* flux ratio = 1.3). However, differences between MIP and NIP composite membranes were less remarkable than when NOMs were tested before the incorporation. Probably the effect of the cellulose matrix has to be more carefully evaluated for this approach to be used as a practical method for clinical applications.

The same group (2010) also prepared NOMs imprinted for *S*-omeprazole to be used in the fabrication of an orally administered drug delivery system. Authors exploited polymerisable cinchona alkaloids (methacryloyl quinine, MQN, or methacryloyl quinidine, MQD) as functional monomers, to provide strong

anchoring groups. MIP-NOMs, also in this case, were subsequently embedded in cellulose membranes and additionally covered with polyhydroxyethylmethacrylate and polycaprolactone triol to provide gastroresistant properties. MIP NPs of 50-150 nm were obtained, directly attached on the surface of microspheres of 10-20 μm (Figure 1–23A, B, C). When tested in batch rebinding experiments, MIP-NOMs prepared using MQN exhibited a remarkable imprinting effect as well as interesting enantioselectivity properties in comparison to MQD based systems, probably due to the almost opposite chirality of the two monomers. The corresponding delivery devices exhibited gastroresistant properties and a selective release of *S*-omeprazole with an *S*/*R* enantiomeric ratio of 2, while NIP systems did not exhibit significant enantioselectivity (Figure 1–23D). It might be interesting to investigate the performance of these devices *in vitro* and *in vivo* to assess if they might be suitable for commercialisation.
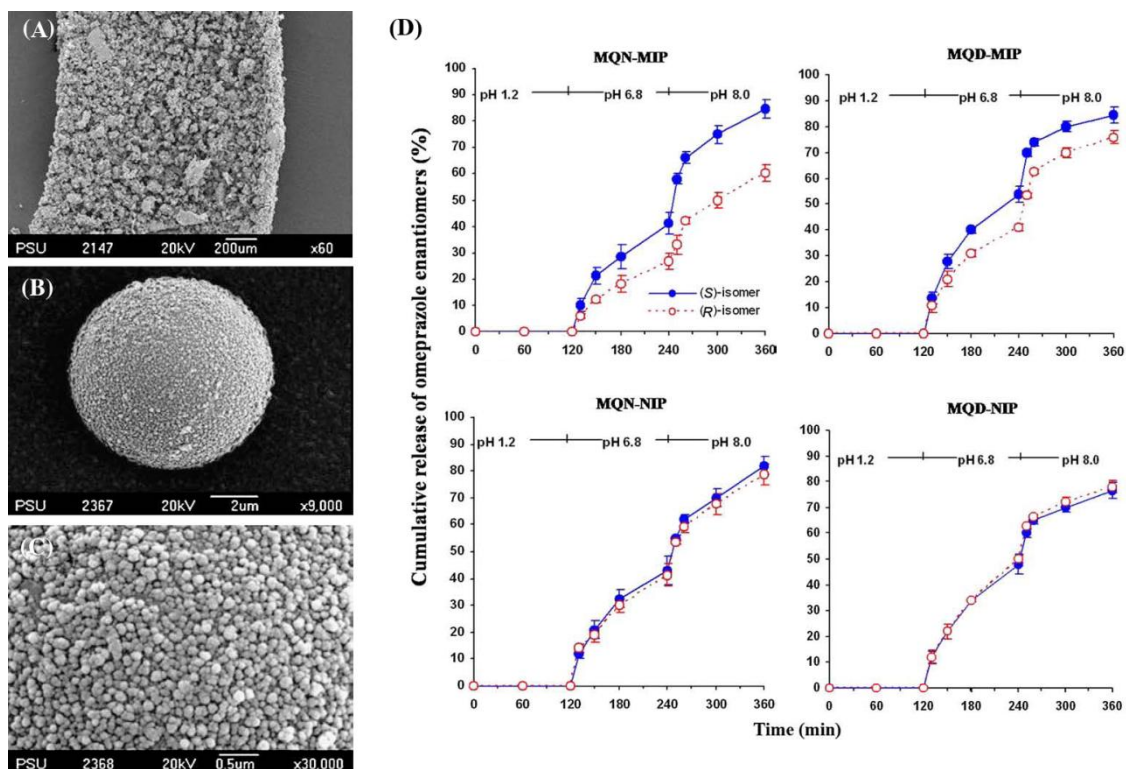
Figure 1–23. (A) SEM image of a cross-section of the controlled delivery device containing the MIP NOMs. (B, C) SEM images of the prepared MIP NOMs at 9000-fold magnification (B) and 30000-fold magnification (C). (D) *In vitro* **dissolution profile of omeprazole enantiomers from MIP- and NIP-loaded delivery systems in dissolution medium changed every 2 h with pH 1.2, 6.8 and 8.0, respectively (mean ± SD,** *n* **= 6) (adapted from Suedee** *et al.***, 2010).**

Very recently (Cirillo *et al.*, 2009), MIP hydrogel nanospheres were prepared by thermo-initiated precipitation polymerisation and used as drug delivery systems for 5-fluorouracil (5-FU). The use of this drug is hampered by its short half-life, hence carefully controlled daily injections are needed to maintain the therapeutic activity. However, this might easily result in severe toxic effects (Johnson *et al.*, 1999). MIP NPs should allow better controlling the drug release profile from the therapeutic system, thus reducing the risks of overdose. The NPs obtained were about 274 nm in diameter, with low polydispersity (Figure 1–24, left). Moreover, the IF evaluated for the imprinted systems versus non-imprinted ones was 4.6 and 3.6, respectively in ACN and in aqueous buffer. This indicates that the MIP NPs obtained here can specifically rebind the target. In addition, MIP NPs exhibited very low cross-reactivity, even for the analogue

73

uracil, which differs from the template only by a hydrogen atom replacing fluorine. Finally, release of 5-FU was tested in simulated plasma fluid and MIP NPs showed a sustained release over 50 h (65% of the total amount of drug loaded), while non-imprinted polymers completed the release after 5 h (Figure 1–24, right).
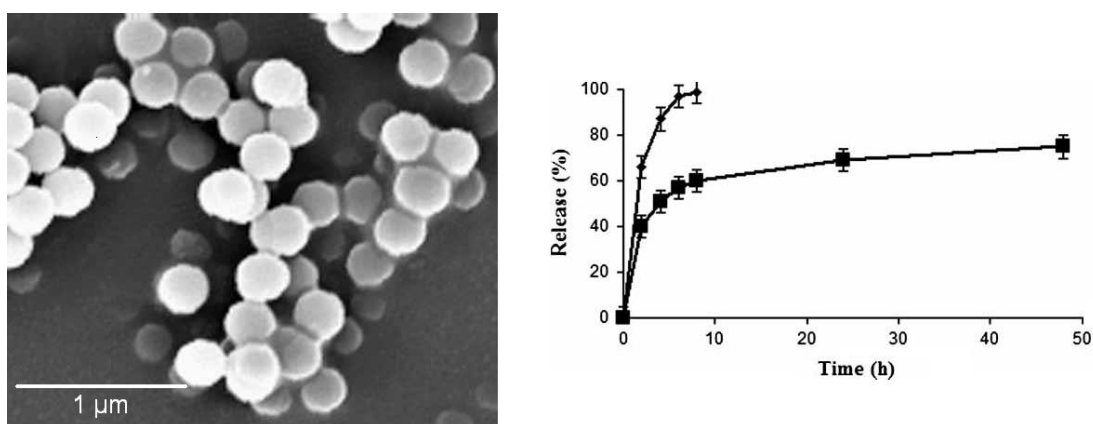
Figure 1–24. On the left, SEM image of MIP NPs. On the right, 5-FU release profile from MIP (■) and NIP (♦) NPs (adapted from Cirillo *et al.*, 2009).

It would be interesting to assess the biocompatibility of these MIP NPs using a suitable *in vitro* model in comparison with the free drug, to verify if they can effectively enhance the therapeutic index of 5-FU.

The first example of magnetic MIP NPs developed as drug delivery systems has been reported by Kan *et al.* (2010), who grafted an aspirin-imprinted MIP shell onto 12 nm diameter silane-modified magnetic cores, thus obtaining 500 diameter MIP NPs. These latter had an IF of 2.4 and exhibited good selectivity for the template in comparison to its structural analogues such as salicylic acid or *o*-aminobenzoic acid. When tested *in vitro,* during the first 2 h magnetic MIPs released about 50% of the loaded drug, while NIP NPs already released about 85%, due to the absence of specific interactions with the template. In addition, thanks to magnetic properties, MIP NPs could be easily separated and manipulated. Theoretically, they could be used to target the drug release towards particular sites in the body by exploiting an external magnetic field (Giri *et al.*, 2005). It might be really interesting to further develop this last application by fabricating magnetic MIP nanosystems below 100 nm in size, i.e. suitable for

passing through altered capillary fenestrations in tissues such as sites of inflammation or tumours.

1.5.2 Capillary Electrochromatography (CEC)

CEC is a hybrid separation technique that combines the high efficiency typical of capillary electrophoresis with the phase selectivity of a high-performance liquid chromatography (HPLC) (Myers and Bartle, 2001). An interesting aspect of this technique is the possibility to use a so-called pseudostationary phase (PSP). Different from a common stationary phase, PSPs are interaction phases that move with (or against) the mobile phase and are continuously replaced, without needing to be packed. In this way, every analysis is performed on a fresh column, thus avoiding stationary phase carry-over effects (Nilsson and Nilsson, 2006). Moreover, since tedious packing procedures are not needed, there is no need also for using frits, which might interfere causing bubbles and peak broadening phenomena (Behnke *et al.*, 2000; Spégel and Nilsson, 2002).

NPs have been used as PSP in CEC (Nilsson *et al.*, 2006). However, to be suitable for this purpose, they have to possess certain properties, such as: i) form stable suspensions and exhibit enough selectivity in the electrolyte solutions used as mobile phases; ii) be charged, in order not to co-elute with the electroosmotic flow; iii) have a uniform velocity to avoid peak broadening; iv) exhibit high surface areas and low mass-transfer resistance; and v) not interfere with the detection mechanism (Göttlicher and Bächmann, 1997).

When MIP NPs have been used in CEC as PSP, a "partial filling" technique has been exploited, whereby a fraction of NPs suspension is injected before the sample (Figure 1–25a). Assuming that the NPs have different mobility than the analytical sample, this latter will pass through the NPs fraction when voltage is applied. During this migration step, analytes will be separated on the MIP NPs (Figure 1–25b) and will arrive at the detection window before the NPs, thus avoiding scattering and absorption phenomena from the PSP during UV detection (Figure 1–25c) (Spégel and Nilsson, 2002; Nilsson *et al.*, 2004; Nilsson and Nilsson, 2006).
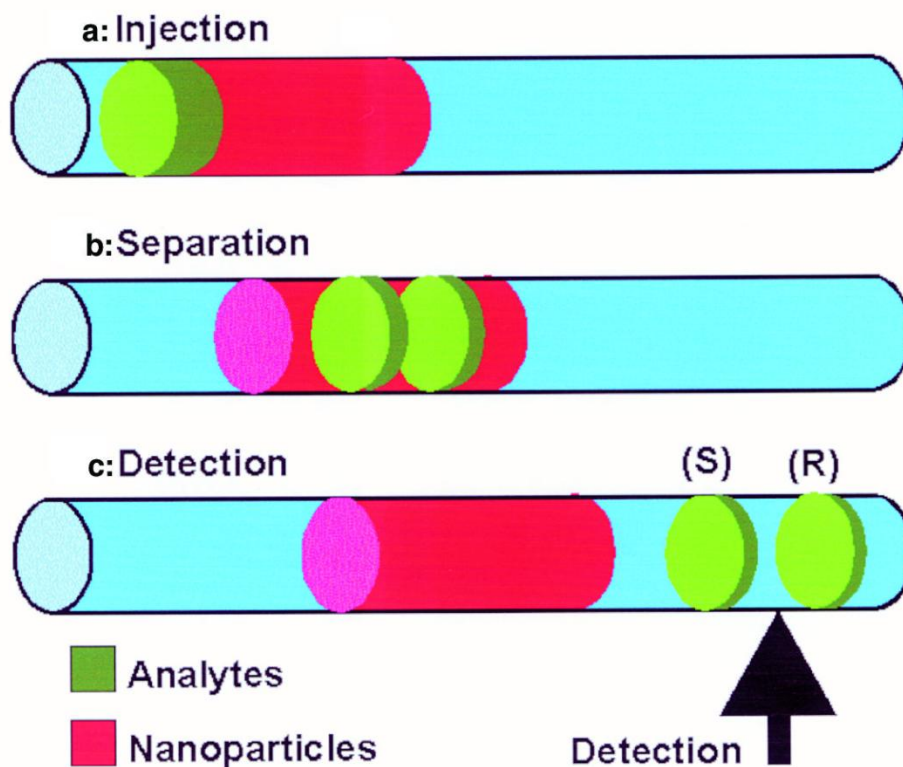
Figure 1–25. Schematic of the partial filling technique (reproduced from Spégel and Nilsson, 2002).

Schweitz *et al.*, in 2000, successfully synthesised and used MIP NPs of 200-500 nm in diameter in CEC separation of propranolol enantiomers. The authors used UV-initiated precipitation polymerisation at -26 °C to strengthen the interactions between the template and the functional monomer. Under optimised conditions, racemic resolution was achieved in slightly more than 1 min, by using the minimum amount of MIP per every run. Moreover, non-imprinted NPs did not exhibit any separation property. Despite some cross-reactivity for propranolol structural analogues was later observed, this was actually exploited to perform multiple separation of racemic mixtures of atenolol, pindolol and propranolol in a single run by sequential injections of the samples (Spégel and Nilsson, 2002).

Encouraged by these results, the same group exploited the versatility and ease of optimisation of the partial filling approach to perform the simultaneous CEC resolution of two different racemic analytes, propranolol and ropivacaine

(Spégel *et al.*, 2003). Authors tried either by injecting two different types of MIP NPs at the same time, or by using MIP NPs which were simultaneously imprinted for the two templates. In the first case it was possible to separate the racemic mixtures of the two different templates in a single run (Figure 1–26), and the optimisation of the separation conditions was quite easy.
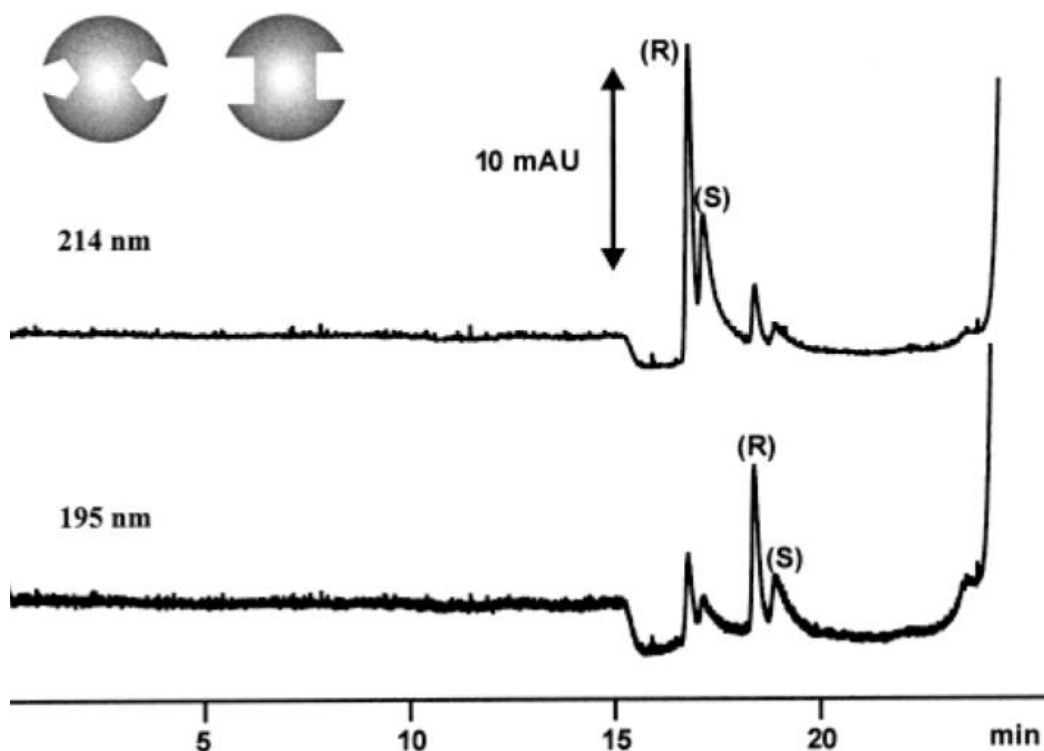
Figure 1–26. Separation of ropivacaine and propranolol enantiomers in CEC by the partial filling technique using a plug composed of *S*-ropivacaine MIP and *S*-propranolol MIP. Detection was performed at 214 (top) and 195 nm (bottom) (reproduced from Spégel *et al.*, 2003).

However, the multi-template imprinting was not so straightforward and careful optimisation of the synthetic conditions and the relative amount of templates was required. In particular, the amount of *S*-propranolol used in the MIP NPs synthesis strongly affected the recognition performance for *S*-ropivacaine, and it had to be decreased down to a template-to-monomer ratio of 1:80 in order to obtain MIP NPs with 2-fold selectivity. It is likely that at higher *S*-propranolol concentrations the interactions between the *S*-propranolol and the functional monomer interfered with the imprinting process of *S*-ropivacaine. Nevertheless,

once optimised, this approach might allow multi-templated MIP NPs to be prepared, suitable for fast CEC analysis.

Since slow mass transfer of the analytes and broad affinity distribution of the binding sites result in peak tailing and bad CEC performance, Priego-Capote and co-authors (2008) exploited a modified mini-emulsion polymerisation technique to try restricting the location of binding sites mainly to the surface of the NPs. In this way an easier accessibility of the imprinted cavities was achieved, together with a more homogeneous binding site distribution. When tested in CEC analysis, for the first time a resolution of a racemic mixture of the template (propranolol) was achieved without evident peak tailing. However, the affinity for the template was only suitable for CEC analysis. In addition, NPs aggregates and bigger particles had to be removed prior being used in CEC. Nevertheless, the fact that the system could be easily tailored for working in aqueous conditions (thanks to its amphiphilic nature) enabled efficient separation of both enantiomers and encourages to further develop and optimise this approach.

Rather than exploting a partial filling technique, Qu and co-authors (2010) recently fabricated and optimised a microfluidic CEC device for resolution of racemic ofloxacin, based on the application of magnetic MIP NPs. Ofloxacin is an antibiotic in which the S-enantiomer is 8–128 times more potent than the R-enantiomer (Hayakawa et $al.$, 1986), hence a fast and efficient enantioseparation method would be useful. A MIP layer was grafted onto the surface of 25 nm diameter magnetic NPs, previously modified with an acryloyl-silane. The obtained MIP NPs of 200 nm in diameter were then pumped into the capillary as a slurry, and packed in a specific region next to magnets. Then, the device assembly was finalised by introducing buffer, sampling and detection reservoirs, as well as electrodes systems to ensure adequate sampling, separation and amperometric detection. Authors thoroughly investigated both polymerisation conditions as well as electrochromatographic parameters on the recognition performance of the CEC microfluidic device. In optimal conditions, a resolution value of 1.46 was achieved in slightly more than 3 min of analysis.

Even if more studies are needed to assess the versatility of the system to analyse different templates, especially in relation to the long time required for optimisation, this approach seems really promising, at least for a fast and very cheap qualitative analysis. The detection limits (5 µM for the template *S*-ofloxacin, and 1 µM for *R*-ofloxacin) are however quantitatively too high compared to conventional chromatographic methods, and hence require further improvement.

1.5.3 Enzyme mimics

Given their small size as well as their dispersibility/solubility characteristics, MIP NPs are very promising candidates for the development of enzyme mimics, especially in the case of low-density MIP microgels (Biffis *et al.*, 2001).

The first example in literature of the synthesis of catalytic MIP NPs has been reported by Markowitz and co-authors (2000), which used micro-emulsion polymerisation to imprint a surfactant-derivative of a transition state analogue (TSA) of α-chimotrypsin. To mimic the enzyme, the authors included in the preparation specific silanes with a structure resembling amino acids of the catalytic triad found in the active site of serine proteases. MIP NPs with diameters in the range 400–600 nm were obtained, which exhibited an enantioselective hydrolysis (10 times faster for the D-enantiomer than for the L-one), especially when high amounts of surfactant-template have been used in the preparation. However, increasing the amount of specific silanes over 5% of the total monomer concentration resulted in a drastic reduction of the catalytic activity, probably because of the establishment of molecular interactions between the monomers themselves rather than with the template molecules.

After this first attempt of catalytic silica MIP NPs, Resmini's group (2004, 2005) presented for the first time soluble MIP catalytic microgels with hydrolytic activity obtained using radical polymerisation in high-dilution conditions. The dimensions of these particles, together with their solubility, make them similar to a natural enzyme or antibody (Biffis *et al.*, 2001). The authors exploited two polymerisable derivatives of tyrosine and arginine as specific catalytic functional monomers in the imprinting of a phosphate-based TSA for the carbonate

79

hydrolysis reaction. Catalytic microgels produced in this way followed a Michaelis-Menten kinetics and exhibited a turnover number (k_{cat}) 530 times higher than the control reaction, together with a remarkable substrate selectivity. Authors found that MIP microgels containing more than 70% of cross-linker exhibited a reduced catalysis rate, even if the values were still higher than the uncatalysed reaction. A lower cross-linking degree probably ensured a sufficient flexibility to the catalytic residues, thus increasing the reaction rate. MIP microgels produced either in absence of the TSA template or in absence of the specific functional monomers exhibited low or no difference with the uncatalysed reaction rate, thus confirming the imprinting effect on the MIP product and the success of the approach.

Wulff and co-workers exploited a similar approach, but rather than using specific monomers mimicking the structure of aminoacids, they prepared highly efficient catalytic MIP NPs by polymerisation of an ionic complex between the diphenyl phosphate TSA and *N,N'*-diethyl-4-vinylbenzamidine as functional monomer (2006). Particular attention was paid in controlling the size of the particles, which is not easy to adjust when using free radical polymerisation processes. Authors obtained the best product in terms of size and catalytic activity through a so called "post-dilution method" (see section *1.4.4 - Soluble nanogels*). The increased degree of cross-linking that resulted from the method was beneficial for the catalytic activity of the synthesised material and for reduced polydispersity. Indeed, monodispersed catalytic MIP nanogels with particle size between 10 and 20 nm were obtained. More importantly, for the first time MIP nanogels with on average one active site per particle were produced. Like in the work of Resmini *et al.*, the catalytic activity of the MIP NPs obeyed Michaelis–Menten kinetics, but in this case the k_{cat} was 3000 times higher than the non-catalysed reaction. It would be interesting also to test the products towards other carbonate substrates, in order to assess their selectivity. In addition, it should be appropriate to rely on the actual amount of active sites present in the catalyst, perhaps by exploiting a titration method like the one recently optimised by Pasetto *et al.* (2009), since knowledge of this parameters

would allow characterising more precisely the catalytic activity of these enzyme mimics and better comparing their performance with other catalysts.

In 2007, Chen *et al.* reported the preparation of peroxidase-mimic MIP microgels for the oxidation of HVA, exploiting hemin groups to create the catalytic sites. Also in this case, the polymerisation process was performed in high-dilution conditions to avoid macro-gelation. Authors obtained microgels of about 200 nm in diameter (as analysed by TEM), with a moderate degree of polydispersity and aggregation. Nevertheless, MIP nanogels were able to specifically increase the oxidation rate of HVA ($k_{cat} = 4.56 \times 10^7$ M^{-1} s^{-1}), 3-fold more than NIP ones. In addition, MIP nanogels exhibited a remarkable selectivity towards the oxidation of template analogues, while simple hemin and NIP nanogels could not distinguish between the different structures. However, 5% of DMSO had to be added to help the solubilisation of the system in buffer media, while higher amounts resulted in a dramatic decrease of the catalytic activity. To improve the water-solubility of the MIP microgels as well as for introducing the possibility for them to respond to external stimuli, the same authors tried introducing a certain amount of NIPAm into the microgel composition (2010). In this way monodispersed MIP microgels were obtained, easily dispersable in water without need for any co-solvent. However, the main interesting aspect of this work is that, by changing the pH of the medium from 2 to 11, both the size and the catalytic activity of the microgels could be modulated (Figure 1–27) with a maximum of activity in correspondence of pH 8.5 and a minimum size (about 250 nm) at the same pH value, very near to the calculated pI for the polymer (7.8).
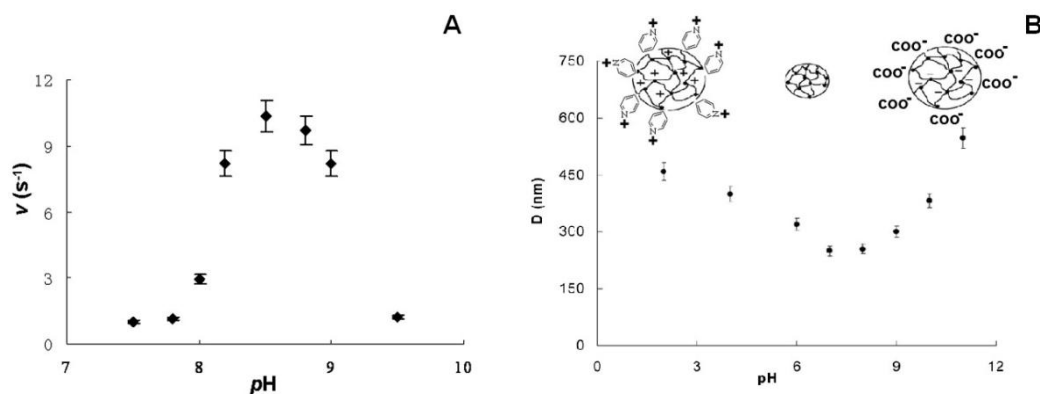
Figure 1–27. pH effect on the catalytic rate in TBS (50 mM) (A) and on the hydrodynamic particle size of imprinted microgels measured by DLS (B) (adapted from Chen *et al.*, 2010).

Such behaviour was attributed, as expected, to the presence of ionic monomers in the polymerisation mixture, which at the isoelectric point of the polymer were electrically neutral and then more hydrophobic. This in turn caused the MIP microgels to shrink and the exclusion of water from the active sites, thus producing an increased catalytic activity. This latter instead dropped when MIP microgels were at too low or too high pH values, conditions in which the polymeric structure was ionised and underwent swelling in aqueous media. In addition to the pH-sensitive catalytic behaviour, which followed a Michaelis-Menten kinetics, MIP microgels retained good affinity and selectivity properties. Despite all these advantages, as already mentioned in section *1.4.4 - Soluble nanogels*, drawbacks such as the low yield (12.5%) and the long purification times, as well as the lack of information about long-term stability should be addressed in order to properly assess the potential commercialisation of these products.

Aiming more at a potential therapeutic application, Huang and co-workers (2008) produced gluthatione peroxidase-mimicking MIP NPs prepared using micro-emulsion polymerisation. In particular they exploited allyl arginine and acryloyloxypropyl 3-hydroxypropyl telluride as specific monomers to mimic the active center of the enzyme, and selectively build it on the surface of polymeric NPs. In this way MIP NPs very regular in shape and size (30-40 nm) were obtained, able to increase the efficiency of the degradation of cumene

82

hydroperoxide of about 600000 times. However, the difference between MIP and NIP NPs was not impressive, and the behaviour of the polymers strictly depended on the ratio between the two functional monomers.

In 2011, the group of Resmini reported the production of a MIP microgel suitable to catalyse Kemp elimination reaction, for which no natural enzymes are currently known to exist. They imprinted an indolic structure as TSA and used 4-VP as basic functional monomer, in a free radical polymerisation reaction performed in high-dilution conditions. MIP NPs were completely soluble in water, and exhibited an optimum activity at pH value 9.4. However, one of the most important aspect of this study is that authors found that the addition of 10% ACN and especially 0.5% surfactant (Tween 20) drastically increased both the catalytic activity as well as the imprinting effect (2-fold more). This could be due to the higher physicochemical stabilisation of the system and better accessibility of the catalytic sites in presence of a small amount of surfactant. Nevertheless, it is the first time that such an effect has been demonstrated on catalytic MIP microgels and undoubtedly it deserves further investigation.

The same group (2008) also reported the first example of MIP microgel capable of catalysing a C–C bond formation reaction, and in particular a cross-aldol reaction between 4-nitrobenzaldeyde and acetone, thus mimicking the enamine-based mechanism of the natural aldolase type I enzymes. In this case a covalent imprinting approach was exploited, bonding a diketone TSA to a polymerisable proline derivative as functional monomer. This latter was chosen by the authors because of the good data available on its catalytic activity and the feasibility of its chemical transformation into a polymerisable derivative. By using high-dilution radical polymerisation, the authors obtained 20 nm MIP NPs with a very low polydispersity (Figure 1–28), while their average molecular weight was evaluated as 260 kDa.
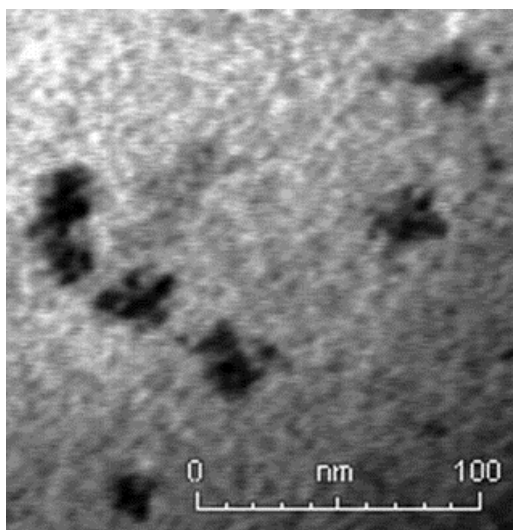
Figure 1–28. TEM image of MIP catalytic nanogels (stained with OsO$_4$) (reproduced from Carboni *et al.,* 2008).

The MIP NPs were not inhibited by product, and the ones containing 10% of functional monomer exhibited 20-fold higher catalytic activity compared to the non-imprinted NPs. In addition, thanks to the chirality of the functional monomer used, the produced nanogels also had good enantioselectivity (62% enantiomeric excess). Moreover, the data showed a homogeneous affinity distribution for the catalytic sites, consistent with the covalent imprinting approach. These results are very exciting and, even if they are still far from the activity values of natural aldolase enzymes, they confirm that MIP catalytic NPs could be used for instance to complement enzymes for those molecules which lack of a natural synthetic system, or in those conditions in which natural enzymes are unstable or very expensive.

1.5.4 Sensing applications

Given their robustness and entirely synthetic nature, MIP NPs are particularly suitable for being immobilised on sensors surfaces or properly labelled for use in assays.

Reimhult and co-authors (2008) produced a QCM sensor by coating its surface with MIP NPs imprinted with *R*- or *S*-propranolol. MIP NPs of 130 nm diameter were synthesised by precipitation polymerisation, then dispersed in a solution of

poly(ethylene terephthalate) (PET) and eventually spin-coated onto the surface of the QCM crystal. This supporting matrix allows the sensor to be used in several solvents, because it has good chemical resistance. Spin-coating, in turn, allows fine adjustment of the thickness of the MIP layer to be achieved (in this case the thickness was below 1 μm), an important aspect to consider in order to guarantee rapid diffusion of the analyte and following sensor response. Nevertheless, while the MIP NPs alone exhibited chiral recognition properties, MIP coated sensors did not. Despite the small thickness of the PET matrix, it is possible that the exposure of the sensors to organic solvents (ACN, in this case) resulted in changes of the rigidity of the PET layer, thus altering the accessibility of MIP binding sites and adversely affecting the polymer recognition properties. Perhaps optimising the spin-coating conditions could improve the performance of the sensor.

Rather than using MIP NPs directly as sensing elements, Schirhagl and co-authors (2010) exploited them as a "secondary template" to transfer their imprints onto a modified QCM wafer. The authors first prepared MIP NPs for IgG raised against human rhino virus 14 by precipitation polymerisation (Figure 1–29a). MIP NPs ranging from 15 to 700 nm were obtained. Following removal of the target IgG (Figure 1–29b), they were deposited on microscope slides and used as stencils to imprint a secondary polymeric layer (made of the same components of the NPs) on a QCM wafer (Figure 1–29c, d). In this way, authors fabricated a chemosensor able to give a response, when exposed to the virus, about 6 times higher than that of the sensor coated with natural antibodies. Despite the polydispersity of the product obtained, this represents a very good example of using MIP NPs not directly as sensing elements, but as stencils to imprint another polymeric structure.
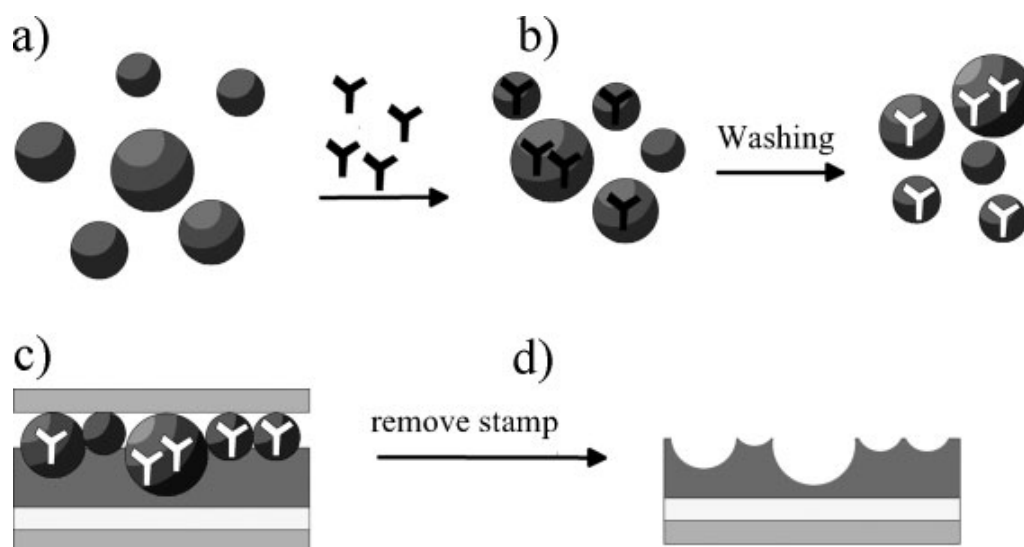
Figure 1–29. Schematic representation of the QCM sensor based on artificial antibody replicas (reproduced from Schirhagl *et al.*, 2010).

The same group later compared the performance of a QCM sensor for atrazine prepared by using natural antibodies, a polymeric bulk layer or MIP NPs embedded in a polymeric matrix (2011). Authors found that the sensor based on natural antibodies exhibited the highest detection limit (0.43 ppm), while polymeric film and MIP NPs allowed reaching 20 and 18 ppb detection limit, respectively. However, while the polymeric film exhibited saturation behaviour at the atrazine concentrations tested, the MIP NPs sensor exhibited a linear response, probably thanks to their higher surface area and less hindered diffusion of the target into the binding sites. This is confirmed by the fact that the QCM sensor prepared with MIP NPs having smaller diameter (45 to 85 nm, hence with higher surface area) exhibited a faster and stronger response than the sensor prepared using larger 200-300 nm MIP NPs. In addition, MIP NPs sensors exhibited the highest selectivity properties when compared to the other two sensors. The sensitivity of this system could be further improved by using devices working at higher frequencies than QCM. Nevertheless, these results are promising enough in relation to the potential use of imprinted NPs in sensing platforms.

Rather than using QCM devices as transduction elements, which often exhibit too low sensitivity, Bompart *et al.* (2009) investigated the possibility of using

micro-Raman spectroscopy to identify and quantify the target molecule adsorbed by MIP NPs. Authors imprinted *R*- or *S*-propranolol on MIP micro- (1 µm diameter) and nanoparticles (200 nm diameter) using precipitation polymerisation. The MIP product tested in batch rebinding experiment exhibited a remarkable imprinting effect. In addition, micro-Raman spectroscopy allowed to perform bulk measurements on a group of MIP NPs pre-equilibrated with the template, allowing to identify and quantify propranolol with good selectivity down to a concentration of 1 µM (K_D = 59 ± 7.7 µM). However, one-particle measurements were not possible because the NPs underwent degradation due to the power of the laser. Furthermore, standardisation of the measurements parameters was difficult and the detection level was not impressive.

To increase the sensitivity of the system the authors used surface-enhanced Raman spectroscopy (SERS) performed on 400 nm composite gold core–shell MIP NPs produced by seeded emulsion polymerisation (2010). This allowed performing target molecule measurements on single MIP NPs, reaching a detection limit of 0.1 µM, while for NIP NPs the detection limit was 100-fold higher. This detection capacity was retained even in presence of a 100-fold excess of interfering compounds such as CAFF or acetylsalicylic acid. In addition, measurements could be performed also in spiked biological samples (diluted equine serum) down to a detection limit of 1 µM. Despite the remarkable improvements, more work needs to be done in order to increase the detection limits of this system. Nevertheless, the possibility of performing multiplexed measurements on several substances by using different MIP NPs is quite attractive and deserves further investigation.

Sener and co-workers (2010) recently assessed the potential of using MIP NPs in sensors for larger protein templates. MIP NPs of 50 nm in diameter imprinted for lysozyme were synthesised by mini-emulsion polymerisation and physically deposited on a QCM crystal by solvent evaporation. Atomic force microscopy (AFM) confirmed the homogeneous deposition of MIP NPs on the QCM wafer surface. In addition, the imprinted sensor exhibited a detection level of 1.2 ng/mL for lysozyme in the analysis of real chicken egg-white samples.

Moreover, the system could be used up to 4 consecutive measurements without loss of detection ability.

The same lysozyme-imprinted MIP NPs were used in a surface plasmon resconance (SPR) sensor (2011). Also in this case the MIP sensor exhibited a selective response in presence of competing proteins, while the non-imprinted one did not show any selectivity. The reproducibility was quite good, up to 5 consecutive measurements without loss of sensitivity, but most importantly the SPR sensor exhibited a response 5 times faster than the QCM sensor, with a 1000-fold lower detection limit. However, the saturation level was remarkably lower (330 nM vs 30 µM in the case of QCM), but this is actually quite interesting because depending on the expected concentration of the target molecule in the sample, a specific sensing platform for high or low concentration levels might be chosen, thus covering a larger range of analytical concentrations.

Another possibility of using MIP NPs for detection and diagnostic purposes is designing a proper assay to detect the analyte either by a change of fluorescent properties, radioactivity, or another measureable property. Most of these assays rely on a displacement mechanism, in which the binding sites of the system are saturated with a labelled template analogue, which is later displaced by an unknown amount of non-labelled target.

One of the first MIP NPs-based assays reported in literature was described by Haupt *et al.* in 1998. The MIP NPs were imprinted with 2,4-D, and used with structurally related fluorescent, chemiluminescent or electrochemical probes to quantify the amount of bound analyte. The detection limit achieved was 100 nM. However, the assay did not perform very well in buffer medium, showing remarkable cross-reactivity with 2,4-D structural analogues in comparison with an antibody-based ELISA assay. Nevertheless, these first results paved the way for the use of MIP NPs in pseudoimmunoassays.

Ye and co-authors synthesised 200–300 nm MIP NPs imprinted with THO and E2 by precipitation polymerisation and used them in a first MIP NPs-based radioimmunoassay (1999, 2001). The authors were able to quantify templates

down to concentrations of 0.1 and 0.01 mg/mL for THO and E2, respectively, even in the presence of competing structural analogues.

However, classical radioimmunoassays always require a separation step between unbound and bound ligand before adding the scintillation media. That is the main reason that led the authors to further improve this assay system by adding a so called "scintillation monomer", 4-hydroxymethyl-2,5-diphenyloxazole acrylate, to the preparation (2001). The binding signal was generated by proximity energy transfer, which arose from the specific binding of a tritium-labelled template (*S*-propranol, in this case). In this way there was no need to remove the unbound labelled ligand, because this latter was too far from the scintillation monomer to generate a signal. MIP NPs exhibited 2-fold higher response than NIP NPs, and discrete enantioselectivity. However, even if these MIP NPs performed well in aromatic solvents, the lack of any aromatic compound in their preparation hampered the generation of the scintillation signal in other media. For this reason, authors also used DVB as cross-linker (2002). This allowed achieving a very good imprinting effect as well as very good enantioselectivity in ACN. However, the same performance could not be obtained in pure citrate buffer, and 50% of ACN had to be added to retain the imprinting effect and selectivity properties. With further development, this approach might lead to a reliable assay technique. Nevertheless, it relies on the use of radioactive materials which are not very easy to handle and dispose.

Systems based on optical detection are easier to handle, even if they are usually more prone to cross-reactivity issues. Surugiu and co-authors (2000) developed an ELISA-like assay based on MIP NPs imprinted with 2,4-D. The target analyte was labeled with tobacco peroxidase as an enzymatic probe and used to detect the template either colorimetrically or by chemiluminescence. In both cases the MIP NPs were suitable to quantify the template down to a concentration of 1 μg/mL, even if a certain percentage of non-specific binding was detected. This was probably due to the higher amount of binding groups present in the enzyme probe, considering that the competition between free

template and analogue was monitored in solution. In addition, cross-reactivity with structural analogues was quite high.

Authors tried to improve this system by making it more similar to a traditional ELISA assay (2001). The same MIP NPs were immobilised on microtiter plate wells using poly(vinyl alcohol) (PVA) as glue, and the detection of chemiluminescence from the competition reaction was performed using a CCD camera. The detection limit of the assay was decreased to 34 nM. As in the previous cases, some cross-reactivity was exhibited, especially when compared to the same assay performed using antibodies. However further optimisation is possible, both in terms of amount of PVA needed for the immobilisation, as well as possible automation of the production of the microplates.

Pérez and co-authors designed an "immunoprecipitation like assay" for cholesterol using surface-imprinted MIP NPs prepared by core–shell emulsion polymerisation (2001). Spherical MIP NPs of 60 nm in diameter were flocculated by the addition of a proper quantity of a multi-ligand template, PEG-bis-cholesterol, while mono-ligand template did not give rise to these effects (Figure 1–30).
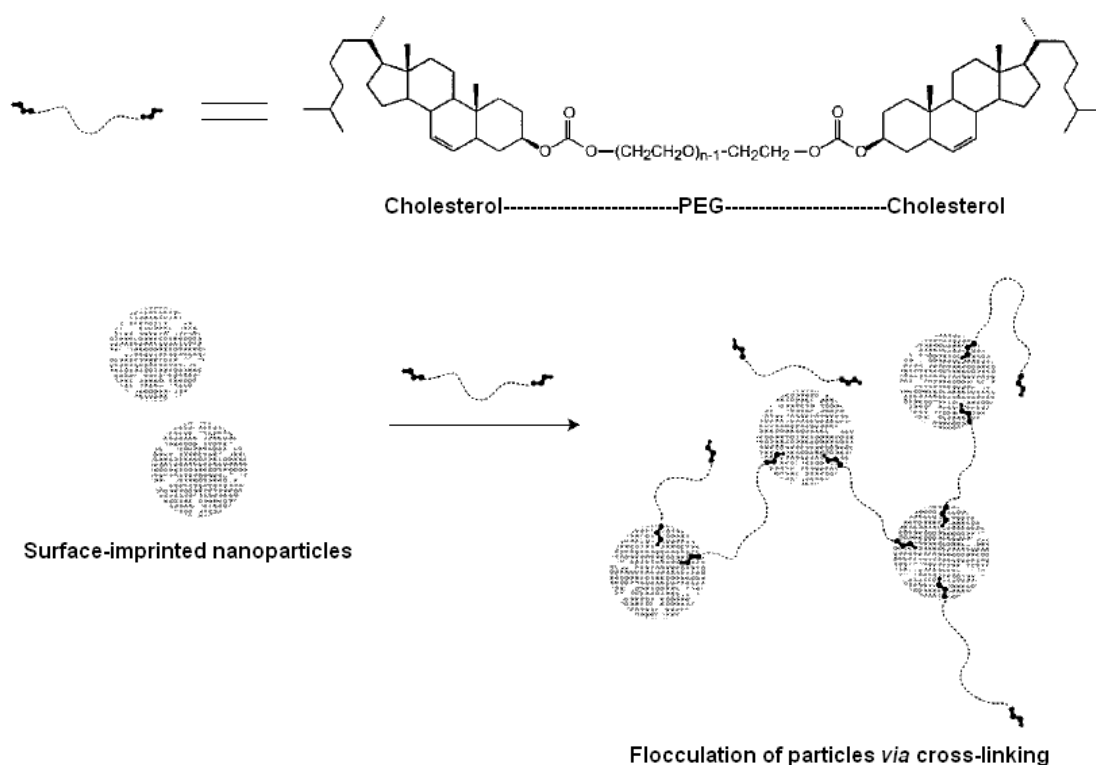
Figure 1–30. "Immunoprecipitation-like" separation of surface-imprinted MIP NPs in the presence of PEG-bis-cholesterol. The addition of the multi-ligand template resulted in flocculation of MIP NPs (adapted from Pérez *et al.*, 2001).

These results encourage undertaking more studies for applying MIP NPs in similar immunoassays. However, it should be noted that the presence of surfactant strongly affected the rebinding properties of synthesised MIP NPs. Maybe a different polymerisation strategy might allow adapting this assay more easily also to other templates with an even better performance.

Another possible strategy to better exploit MIP NPs in such diagnostics assays would be to make them more easily detectable by introducing for example fluorescent probes.

Pérez-Moral *et al.* prepared core-shell MIP NPs either with fluorescent cores (2004), or with multi-layer shells in which one of the layers contained a fluorescent label (2007). In the first case, however, they did not assess nor the binding efficiency or the fluorescent behaviour of the product in dependence of the binding to the template (cholesterol). In the second case, as expected,

addition of several layers onto the imprinted shell caused some reduction of the binding of the template propranolol, but unfortunately also in this case a systematic assessment of the fluorescence of the particles in relation to the template rebinding was beyond the scope of the work.

Rather than using a fluorescent monomer, Diltemiz and co-workers exploited CdS quantum dots as core-labels onto which graft a guanosine-imprinted shell (2008). MIP NPs had an average diameter of 45 nm, and their intrinsic fluorescence was enhanced by the template binding, being proportional to its concentration. MIP NPs also exhibited very high selectivity for guanine and guanosine, while adenosine did not give rise to any change in fluorescence. This is probably due to the recognition mechanism in these MIP NPs, which is based on a ligand-exchange with Pt ions embedded in the polymeric structure. However, to be exploitable for example in the diagnosis of DNA mutations, several studies have to be still undertaken since the binding to double-stranded DNA was quite low.

Purely organic MIP NPs with fluorescent sensing capability were recently synthesised by Ivanova-Mitseva *et al.* (2012) who prepared a fluorescent core by partially modifying the peripheral amino groups of a poly(amido amine) (PAMAM) dendrimer with dansyl residues. The remaining free amino groups were then modified with DEDTC iniferter groups capable of initiating photochemical polymerisation of a MIP shell. The particles had an unusual cube-like shape and were 50 nm in size. The fluorescent MIP NPs (but not blank NPs) showed an enhancement of fluorescence in the presence of the template (acetoguanamine) with a detection limit of 30 nM, but did not respond to relevant structural analogues.

Very recently (2011), Li *et al.* went one step further and developed MIP NPs with a double-layer core-shell structure made of a Fe_3O_4 NPs core, an inner shell of fluorescein isothiocyanate (FITC) and an outer MIP shell, for faster separation and recognition of E2. MIP shell was produced using a controlled living RAFT polymerisation. MIP NPs exhibited a diameter of about 350 nm, with the fluorescent intensity decreasing with increasing concentrations of E2

92

and showing a detection limit of 0.19 µM. A discrete imprinting effect and very good selectivity properties were also achieved, and MIP NPs could be reused up to 5 times after washing. Such a system not only provided a source of fluorescence but also allowed magnetic separation to replace centrifugation and filtration steps during the experimental procedure in a convenient and cost-effective way. Given these advantages, these products could be really interesting especially in the case of high-throughput and automatic detection applications.

1.5.5 Separation

The most popular MIP formats used in separation are membranes and microparticles. Nevertheless MIP NPs with high surface area might offer advantages if they can be integrated with membranes or fibers to improve their performance.

The first example of MIP NPs-containing composite membrane for separation purposes dates back to 2002. In this work Lehmann and co-authors prepared MIP NPs imprinted with L-BFA using mini-emulsion polymerisation, then used them to prepare a composite membrane for enantiomeric separation purposes. Despite MIP NPs exhibited a remarkable imprinting effect and enantioselective properties in batch rebinding tests, the authors did not study the separation performance of the composite membrane, but only its porosity and flow properties.

Silvestri and co-workers (2005) prepared MIP NPs imprinted for THO and for CAFF through precipitation polymerisation, and embedded them in poly(methyl methacrylate-*co*-acrylic acid) (PMMA-*co*-AAc) membranes using a solid-phase inversion method. CAFF-MIP NPs were 174 nm in diameter and performed well in batch rebinding tests, retaining their characteristics after being deposited on the surface of the membranes. Unfortunately THO-MIP NPs (202 to 313 nm in diameter) did not exhibit impressive recognition properties during batch rebinding studies in buffer. However, after being incorporated into the membranes, their recognition properties dramatically improved, since they rebound about 6 times more THO than NIP membranes and 40 times more

THO than control membranes without NPs. Moreover, they exhibited a selectivity factor for THO versus CAFF of 10. According to these results, the membrane structure helped the rebinding process for THO-MIP NPs, probably by improving the establishment of interactions with the template.

The same authors later used this strategy to create composite membranes containing MIP NPs for cholesterol (2006). All the synthesised NPs exhibited specific rebinding capacities for the template both in EtOH and in PBS, even if the materials with lower cross-linking degree performed better (50-60 mg specifically rebound template/g of MIP NPs). This trend was mirrored by the membranes which possessed a specific binding capacity of 14 mg template/g of the composite system. The results of these works are really promising. Nevertheless, further investigation on the mechanism responsible for the modification of the MIP NPs binding properties due to the matrix effect would probably be helpful to further improve the performance of these composite systems.

Chronakis and colleagues (2006) incorporated MIP NPs into composite nanofibers using the electrospinning technique. This is an interesting approach since these materials can constitute well-controlled filtration matrixes, e.g., for SPE applications. MIP NPs imprinted for E2 and THO were prepared using precipitation polymerisation (Ye et al, 1999), suspended in a solution of PET in dicloromethane and trifluoroacetic acid, and electrospun to obtain nanofibers. These latter possessed regular diameters, ranging from 150 to 300 nm, and MIP NPs were clearly still visible inside them (Figure 1–31).
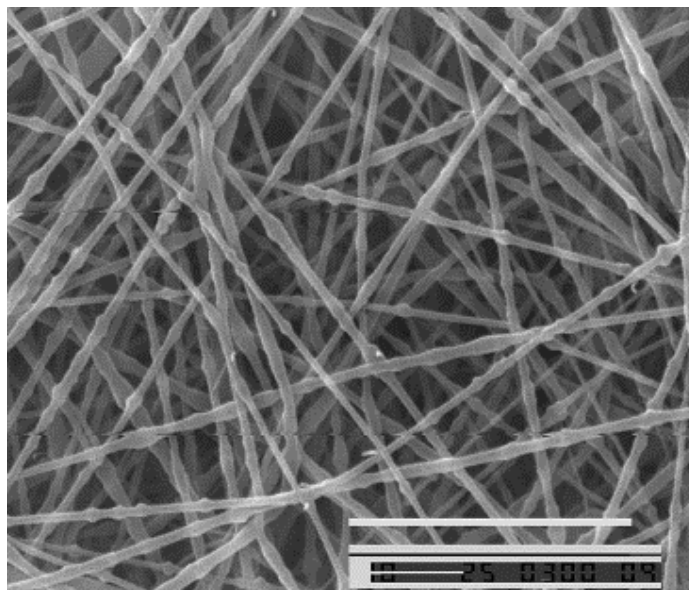
Figure 1–31. SEM image of electrospun PET nanofibers containing 37.5% w/w of MIP-E2 NPs. The scale bar is 10 μm (adapted from Chronakis *et al.*, 2006).

Produced nanofibers were able to accommodate up to 75% (w/w) of NPs, exhibiting excellent binding properties, since MIP nanofibers rebound 2 to 3 times more template than control nanofibers. Moreover, the encapsulation process modified the surface properties of the MIP NPs, making them able to rebind the template in solvents (i.e. toluene) in which they normally gave rise to aggregates. However, the amount of incorporated NPs had to be optimised to avoid direct exposure to the solvent, which caused high non-specific interactions.

The same authors assessed the feasibility of these materials for the analysis of real samples by incorporating MIP NPs imprinted for propranolol into nanofibers prepared using the same electrospinning approach (2008). MIP composite nanofibers were able to rebind 70% of total propranolol, while only 10% was rebound by NIP. In addition, MIP nanofibers mats could be used to specifically extract and concentrate propranolol from spiked tap water samples even in presence of other β-blockers, while in the same conditions the non-specific recovery from NIP nanofibers was about 30%. Some cross-reactivity with the structural related compounds was observed, but if it represents a group specificity this could actually be an advantage since these molecules could be

extracted all with a single SPE process. This material was stable for up to 10 consecutive extractions without showing any loss neither of NPs nor of binding properties. However, some issues need to be addressed in these MIP composite nanofibers, such as the amount and the size of incorporated MIP NPs. This has to be optimised to avoid aggregation phenomena and direct exposure of the particles to the solvent, which result in non-specific interactions.

Rather than using PET, Piperno and co-workers (2011) exploited the cross-linking of PVA to create more stable and water-compatible electrospun nanofibers impregnated with MIP NPs imprinted with dansyl-L-Phenylalanine. The 400 nm MIP NPs were produced by precipitation polymerisation, and were able to rebind 2-fold more template than non-imprinted ones, exhibiting good enantioselectivity. Electrospun materials with diameters between 80 and 350 nm were not able to encapsulate MIP NPs completely, thus leaving them able to interact and rebind the template with micromolar affinity (K_D = 21 µM) and enantioselectively. Most importantly, the fibers retained their recognition activity even after multiple adsorption/desorption cycles, thus highlighting their stability and possibility to be used as SPE media. However, all the rebinding tests were performed in ACN. Given the water-compatibility of PVA, it would have been interesting to verify the rebinding properties of these materials also in buffer.

Instead of supporting NPs on membranes or fibers, Zhu *et al.* (2010) synthesised core-shell silica MIP NPs to be used directly in SPE applications for bisphenol A. A 50 nm MIP silica shell was produced onto the surface of 400 nm silica NPs by exploiting a sol-gel process. MIP NPs had an adsorption capacity 2.5-fold higher than NIP ones, with a very fast rebinding kinetics, probably thanks to the binding sites located mostly at their surface. In addition, they recovered close to 100% of the template, even in presence of an excess of structural analogues. Eventually, when assessed for SPE extraction of true cosmetic samples spiked with bisphenol A, MIP NPs performed better than commercial silica, thus decreasing the level of noise in the subsequent HPLC quantification.

The same group (2010) also synthesised 300–400 nm core–shell MIP NPs for SPE of the herbicide metsulfuron-methyl (MSM). A MIP layer was thermally grafted to silica cores modified with an acryloyl silane. The optimised MIP NPs had a maximum adsorption capacity 3.4 times higher than NIP NPs and 3.8 times higher than conventional C_{18} silica. In addition, rapid rebinding kinetics could be obtained. In the SPE extraction of samples of soil or from crops spiked with the template and its structural analogues, MIP NPs allowed pre-concentrating MSM to a much higher level than commercial silica or non-imprinted NPs, thus allowing the subsequent HPLC quantification to be performed with minimal noise. However, some cross reactivity with analogue herbicides was observed, even if it should not be a major issue for the application of this material. For a practical application, the amount of polymerisable double bonds on the surface of silica cores, as well as the conditions of the thermal polymerisation process and the composition of the polymerisation mixture had to be carefully adjusted to optimise the rebinding conditions.

In a similar way, Gao *et al.* prepared core-shell MIP NPs imprinted with sulfamethoxazole (SMO) to be used in SPE applications (2010). As in their previous work (2007), authors exploited the strong interaction established between the template and the acrylamide moiety on the core-surface to increase the density of imprinted sites in the shell. Core-shell MIP NPs rebound 3-fold more SMO than bulk MIPs or NIP NPs, reaching the adsorption equilibrium in about 45 min. Moreover, MIP NPs exhibited high selectivity for the template (IF = 21) when compared to the binding of five other sulfonamidic structural analogues (IFs between 2 and 4). When assessed for the SPE pre-concentration of real eggs and milk samples spiked with sulphonamides, the recoveries ranged from 73.2 to 89.1% with relative standard deviations below 7.5%, allowing detection of SMO and of another structural analogue, sulfadiazine, through HPLC analysis of the concentrates.

Even ions have been imprinted onto MIP NPs for subsequent separation purposes. Shamsipur *et al.* (2010) prepared MIP NPs with an antraquinone (AQ) derivative as specific complexing monomer for the extraction of copper ion from water. MIP NPs of 60-100 nm with a slight irregular shape were obtained. Under optimised adsorption conditions the synthesised material exhibited a binding capacity of 73.8 µmol/g, as well as very good selectivity in the presence of other ions. In addition MIP NPs could be reused to bind and desorb Cu^{+2} up to 20 consecutive times, without any loss of affinity. Futhermore, when tested with real well and tap water samples spiked with Cu^{+2}, MIP NPs recovered 95 to 105% of the ions present, thus highlighting the possibility of using this materials for purification or preconcentration purposes.

With a similar aim, the group of Prasada Rao (2011) prepared core-shell MIP NPs imprinted for uranyl ions for water purification. The authors first prepared functionalised silica cores bearing an amino silane for the immobilisation of quinoline-8-ol to improve the specific interaction with the uranyl ions. Then, an imprinted shell was prepared by precipitation polymerisation, giving rise to MIP NPs of 50-80 nm diameter. Under optimised rebinding conditions, MIP NPs were able to selectively remove 500 to 1000 ppb of uranyl ions from water samples, about 25% more than non-imprinted materials. Moreover, when tested with real water spiked samples, the recovery performance was almost around 94% for ground water. However, for salt water samples, the recovery was lower (70%). Maybe the high concentration of sodium chloride present disrupted the specific interactions between the template and the binding sites.

Li and his group (2009) recently prepared surface-imprinted magnetic polystyrene NPs for bovine haemoglobin through a multi-stage core-shell polymerisation process. It involved the use of APBA as functional and cross-linking monomer, which is particularly suitable for protein imprinting (Bossi *et al.*, 2001). Magnetite core NPs of 25 nm in diameter were coated with several layers and eventually the MIP shell was created by polymerising APBA in the presence of the template. The final size of the coated particles reached a diameter of 480 nm, in which the MIP film was 15-20 nm thick. Moreover, the

core-shell MIP NPs exhibited superparamagnetic properties suitable for an easy separation, also in large scale. Additionally, they showed a fast rebinding kinetics (30-120 min), good specificity and selectivity for the template, as well as a very high adsorption capacity of about 45.5 mg/g. Such a high capacity is unusual for this kind of material and together with their magnetic properties makes these MIP NPs very attractive for enrichment of low-concentration proteins in proteomics.

1.5.6 The future: biologically active MIP nanoparticles

Undoubtedly the most interesting development for MIPs and MIP NPs is the creation of biologically active systems that can be used as drugs, antibody, or enzyme substitutes *in vivo*.

The first example of water-soluble MIP NPs demonstrating biological activity dates back to 1998, when Piletsky and co-authors investigated the possibility to modify the photosynthetic reaction catalysed by thylakoid membrane D1 protein, either by disrupting the electron acceptor site or interacting with the cytosolic site of the photosystem. For this purpose MIP and NIP bulk monoliths were prepared in water and extensively ground to produce MIP NPs. Affinity chromatography on immobilised D1 protein showed that 5–10 kDa MIP NPs had increased binding affinity to this protein as compared to non-imprinted polymers. In addition, MIP NPs were able to increase the activity of the D1 protein up to 45%, data consistent with a binding at the cytosolic site of the photosystem. However, this example remained isolated in literature because of the production method and the low yield. Nevertheless, this first work represents a milestone in the production of soluble MIP NPs with biological activity.

A different approach was followed by Haupt and his group who recently synthesised water-soluble MIP microgels capable to inhibit the enzymatic activity of trypsin (2009). Their method exploited the synthesis of a tailor-made "anchoring monomer", methacryloylaminobenzamidine (a polymerisable derivative of benzamidine), to complex the template with high affinity and locate the synthesis of the MIP nanogels preferably at the surface of the enzyme.

Benzamidine is indeed a well-known low molecular weight competitive inhibitor of trypsin. Differently from Piletsky and co-workers, authors synthesised water-soluble MIP nanogels through a precipitation polymerisation from a highly diluted solution. Apart from the anchoring monomer, several water-soluble monomers and cross-linkers with different molar ratios were tested. The best imprinting effects were obtained when HEMA and MAm were used as functional monomers (IF respectively of 2.8 and 2.5). Authors found that the presence of the anchoring monomer is a key factor for obtaining MIP nanogels with high inhibition capacity for trypsin. Despite the not so high affinity, calculated inhibition constant (K_i) for the imprinted nanogels was indeed 79 nM. This value is much lower than the K_i value for free benzamidine (18.9 µM), which proved the effectiveness of this imprinting strategy. Moreover, imprinted nanogels exhibited selectivity properties for trypsin, because negligible inhibition activity was found for trypsin-related enzymes such as chimo-trypsin or kallikrein.

Shea and co-workers recently prepared MIP NPs by precipitation polymerisation for the bee venom peptide melittin (2008) (see *1.4.1 - Precipitation polymerisation* for more details on NPs production and characterisation). MIP NPs were tested *in vitro* on fibrosarcoma cells and did not show any toxic effect (2010). Particles were then injected intravenously in mice (dose: 30 mg/kg) 20 s after the administration of a lethal dose of melittin (4.5 mg/kg). Authors found that MIP NPs halved the mortality in mice treated with the toxin, while mice treated with NIP NPs and untreated mice showed a mortality of 80% and 100%, respectively. Moreover, mice treated with MIP NPs exhibited reduced common toxic effects caused by melittin, such as peritoneal phlogosis and weight loss. Authors also investigated the biodistribution of fluorescently marked MIP NPs and melittin during time. They found that while melittin alone distributes extensively into the body through the bloodstream, the administration of MIP NPs results in a concentration of melittin in the liver. This is followed by the removal of the MIP-melittin complexes through the mononuclear phagocytic system (Figure 1–32).
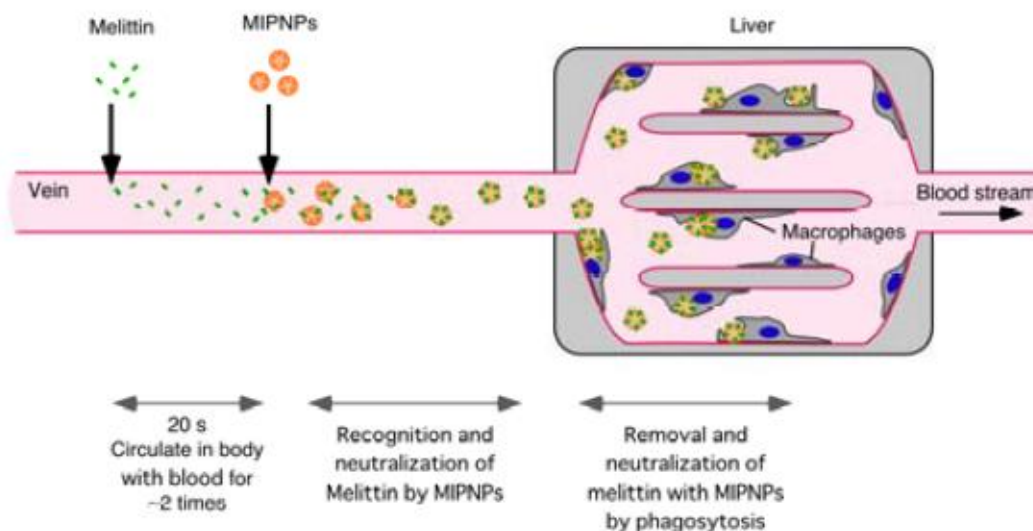
Figure 1–32. Scheme of function of MIP NPs *in vivo* (reproduced from Hoshino *et al.*, 2010b).

These results are undoubtedly very interesting, and once again they testify the broad range of applicability of MIP NPs. However, it would be interesting to test also anti-melittin antibodies *in vivo* under the same conditions to compare the efficacy of these MIP NPs in respect of their natural counterparts. It is known that nanoparticles could cause an increased production of reactive oxygen species (ROS), i.e. increased oxidative stress of cells with possible subsequent inflammation. In addition, once in the blood flow, they can distribute virtually to every organ of the human body, with hardly predictable translocation rates (Oberdörster *et al.*, 2005; Borm *et al.*, 2006; Jones and Grainger, 2009). Finally, they can interact with proteins, altering their structure or function, and could accumulate in excretion organs such as kidney or liver, physically blocking filtration pores and thus causing the organ failure (Oberdörster *et al.*, 2005). Thus the toxicological properties of MIP NPs need to be carefully investigated to assess the risks deriving from the use of these nanomaterials prior to their application in humans.

1.6 Immobilised templates: a new imprinting strategy

Many of the perceived disadvantages of MIPs and MIP NPs can be traced to the way how soluble templates behave in the polymerisation reaction. Soluble templates are in motion, both translational and rotational, during the critical stages of the formation of the recognition sites. The accessibility of these latter into porous polymeric matrixes is also a matter of chance, ranging from partial sites on the inner surface of micro- or macro-pores to complete encapsulation, with an ideal situation lying somewhere in between (Sellergren and Hall, 2000). These factors are major contributors to the problems of binding site heterogeneity and accessibility, and therefore responsible for the "polyclonal" nature of traditional MIPs. However, during the last decade, some examples of MIPs synthesised by using a template covalently immobilised on a suitable support have been reported, thus opening the way to a new strategy of MIP polymerisation at the interphase between liquid and solid. Immobilisation of templates might address some drawbacks typical of MIP polymerised in solution. First of all this approach allows substances that are not soluble in the polymerisation mixtures to be imprinted, thus expanding the range of solvents that can be used in imprinting. The addition of surfactants or co-solvents as solubilising agents can be avoided as well, since these substances indeed might interfere with the interactions between the monomer and the template. In addition, template-template interactions which might occur in solution are suppressed. Moreover, immobilised templates possess a reduced numbers of degrees of freedom and the formation of the polymer at the interface with the template support means that the imprinted sites will always be accessible. This would facilitate also the template removal and the rebinding kinetics (Yilmaz *et al.*, 2000; Tan and Tong, 2007), avoiding complicated strategies involving the synthesis of surfactant templates (Pérez *et al.*, 2001; Priego-Capote *et al.*, 2008; Curcio *et al.*, 2009). Immobilisation also allows the orientation of the template to be controlled (Liu *et al.*, 2012) hence creating more homogeneous binding sites in MIPs. Finally, so far the synthesis of every batch of MIP product has always required a new batch of template molecules which, if expensive,

might represent an important economical drawback for scaling up the production process.

The first example of MIPs synthesised using an immobilised template has been performed by Yilmaz *et al.* (2000), who synthesised a MIP imprinted for THO by immobilising its 8-carboxypropyl derivative through an amide bond on aminopropyl silica gel, chosen as solid support. After the immobilisation, the authors blocked the remaining aminopropyl groups by using acetic anhydride, to avoid interference in the imprinting procedure. The synthesis of MIP was performed using thermal polymerisation at 45 °C of TFMAA as functional monomer and DVB as cross-linker, with V-70 as initiator. The monolith has been mildly wet-milled and the silica solid support with the immobilised template removed by treatment with aqueous hydrofluoric acid (HF) (Figure 1–33). This imprinting strategy that involves the dissolution of the solid support with the template has been given the name of "hierarchical imprinting".
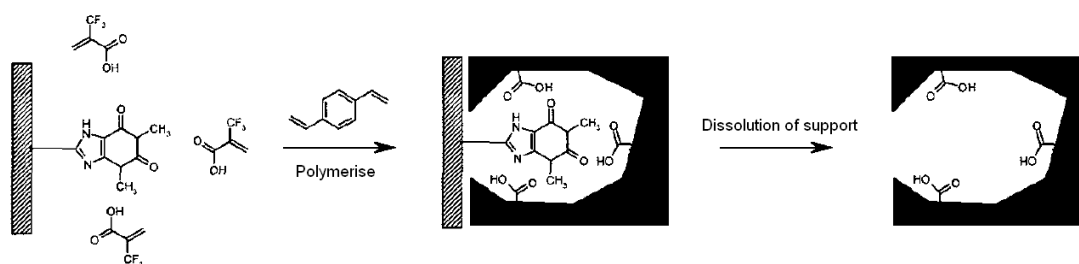
Figure 1–33. Molecular imprinting using immobilised template and subsequent dissolution of the support, better known as "hierarchical imprinting" (adapted from Yilmaz *et al.*, 2000).

The MIP exhibited an evident imprinting effect compared to the control polymer, which bound 5 times less analyte. However, MIPs synthesised using free THO in solution exhibited a higher rebinding capacity, even if they had less uniform binding sites.

Using the same approach, Titirici and co-workers (2002) fabricated microparticles imprinted for adenine or triaminopyrimidine to be exploited in HPLC applications. Authors immobilised the halogenated template precursors on porous silica microparticles previously derivatised with APTES and, after

blocking the remaining aminopropyl groups, performed the synthesis using thermopolymerisation at 60 °C of a mixture of MAA and EGDMA, with AIBN as initiator. The silica has been removed by treatment with aqueous ammonium hydrogen fluoride (NH_4HF_2). After this treatment, porous microparticles with a diameter similar to the starting silica ones have been obtained. They exhibited a homogeneous pore distribution and performed well in HPLC analysis of purine and pyrimidine DNA bases. However, the removal of the support with the template required 4 days to be completed. In addition, the correspondent MIP fabricated using the free template exhibited higher selectivity values. This has been ascribed to the steric hindrance which takes place at the surface of the silica, which in turn might hamper the monomer-template interactions. Probably the use of a spacer group to covalently bind the templates on the silica surface might help avoiding the hindrance problems.

In a later work (2004), the same authors combined this hierarchical imprinting procedure with an epitope imprinting approach. This latter refers to the imprinting of a small peptide sequence (i.e. an epitope) instead of a whole target protein, which can be subsequently recognised and bound to the imprinted cavity thanks to this peptide moiety (Ge and Turner, 2008). Authors synthesised peptide sequences directly on the surface of silica microparticles and prepared MIP microparticles using this approach. When tested in HPLC separation, some of the polymers exhibited higher capacity and selectivity values than the correspondent MIP fabricated in presence of free template in solution, even in the case of separation of larger peptide sequences that contained the epitope moiety.

The hierarchical imprinting approach has also been investigated to prepare catalytic MIPs. In 2004, Lettau *et al.* prepared MIPs able to catalyse the hydrolysis of esters. The TSA for an esterolytic reaction, (4-aminobenzyl)-phosphoramidic acid-4-nitrophenylester was immobilised on aminopropyl silica gel by coupling with succinic anhydride and *N,N'*-diisopropylcarbodiimide. After blocking the residual carboxylic groups, MIP synthesis has been carried out thermally in MeOH for a total of 95 h, by using 4-vinylimidazole as functional

monomer and DVB as cross-linker, with AIBN as initiator. After this the silica has been removed by treatment with HF, leaving behind particles in high yield and very similar in morphology to the starting silica gel. MIPs exhibited higher activity than control polymers (3.5-fold higher), and similar or higher activity than correspondent MIPs synthesised with free TSA in solution. Moreover, MIPs obeyed to Michaelis-Menten kinetics. Nevertheless, the synthesis still relied on the removal of the silica support, and it was quite time-consuming.

An innovative hierarchical-approach has been recently reported by Shen and Ye (2011), who synthesised hydrophilic surface-imprinted MIP microparticles imprinted for a β-blocker moiety by exploiting an unconventional polymerisation process carried out in Pickering emulsion. Unlike conventional emulsions, which are stabilised by the use of surfactants or polymeric emulsifiers, Pickering emulsions are stabilised by solid particles, which prevent instability phenomena by locating themselves at the interphase between the two immiscible liquids. In this particular approach, the authors used template-modified silica NPs as emulsion stabilisers, thus obtaining regular spherical MIP microparticles imprinted only on their surface. The synthesised material exhibited a remarkable specificity in water, thanks to the surface-imprinting which concentrated the hydrophilic COOH groups from the functional monomer MAA on the microparticles surface. The rebinding kinetics was also quite impressive, since MIP microparticles incubated with the template reached the equilibrium in 20 min. Nevertheless also in this case the removal of the template was performed by dissolution of the silica NPs in HF for 12 h. Moreover, despite the use of the immobilised template, additional washing steps were required to remove polyMAA chains, thus making the synthetic process even more time-consuming.

In the field of nanostructures, the formation of MIP nanowires synthesised by immobilising the template on the surface of a nanoporous alumina membrane was reported (Yang *et al.*, 2005). Authors first coated the membrane pores with silica, then they immobilised trimethoxysilylpropylaldehyde to provide aldehyde groups able to bind the template, glutamic acid, through an imino bond. The

modified membranes were immersed in a solution of pyrrole (functional monomer) and then mixed with an oxidant agent to start the polymerisation. MIP nanowires have been collected by dissolving first the alumina membrane, and subsequently removing the silica layer by exploiting the usual treatment with HF. The imprinted products exhibited higher capacity than the non-imprinted ones, and also very good selectivity. Moreover they also showed a fast rebinding kinetics, thanks to the imprinting effect preferably at the surface of the MIP nanowires.

The same group later applied this approach to synthesise MIP nanowires imprinted for whole proteins (2006). Instead of using pyrrole as monomer, they used AAm and BIS as monomer and cross-linker, respectively, thus imprinting bovine serum albumin, bovine cytochrome c and horseradish peroxidase. Authors found that the cross-linking degree of the MIP strongly affects its shape and its capacity, and could result in a too rigid material from which the template removal is too difficult to achieve, despite its high surface area. Nevertheless, imprinted nanowires exhibited about 5 times higher capacity for their templates than control ones. Moreover, MIP nanowires showed good specificity, even in case of very similar proteins. A serious drawback, however, is the fact that the synthetic procedures were quite complex and time-consuming, and still involved the dissolution of both the alumina and the silica supports.

Shea and co-workers, in 2006, reported the synthesis of a MIP film imprinted with cytochrome c, alcohol dehydrogenase or bovine serum albumin by using an epitope approach combined with the immobilisation of peptide moieties for these proteins on a suitable support, either silica or glass. Each support has been previously treated with 7-octenyltrichlorosilane to provide a spacer. This latter has been subsequently oxidised to carboxylic group in order to immobilise the target peptides through an amide bond (Figure 1–34A). The MIP film has been synthesised by depositing the polymerisation mixture formed by AAm, BIS, PEG 200-diacrylate and 2-hydroxy-4'-(2-hydroxyethoxy)-2-methylpropiophenone as photoinitiator onto the derivatised surface. The mixture was subsequently photopolymerised for 10 min using UV irradiation. The

support then has been detached from the MIP film by soaking it in PBS (Figure 1–34B) without any dissolution step. The MIP films were able to selectively rebind all the imprinted proteins (Figure 1–34C) with good capacity and affinity. For instance, the calculated K_D between the MIP film imprinted for cytochrome c and the protein was 72.6 nM.
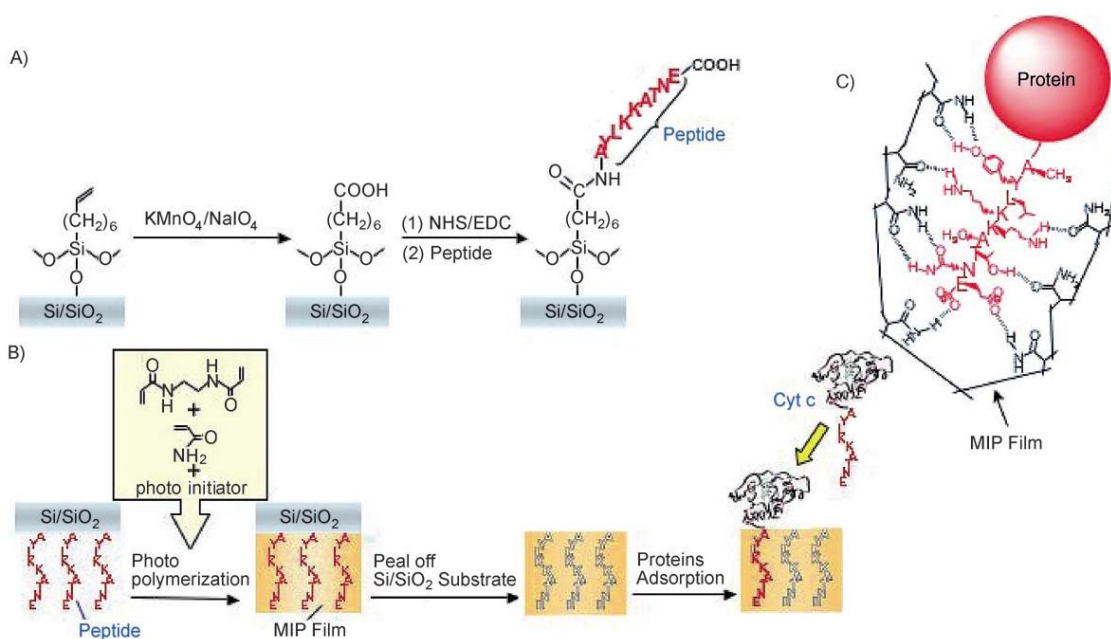
Figure 1–34. Protocol for template imprinting with protein epitopes. A) Glass modification and peptide attachment. B) Photopolymerisation and support removal. C) Target protein recognition (adapted from Nishino *et al.*, 2006).

In summary, despite the advantages stated here, the hierarchical imprinting approach does not provide benefits from an economical and synthetic point of view when compared with a normal imprinting procedure with a free template in solution. The template molecules are still discarded at the end of the MIP synthesis, together with the silica support, which requires long and harsh treatments for its dissolution (3-4 days for dissolution of the silica in concentrated HF or NH_4HF_2). The last described approach seems more promising, since the separation between the solid support and the MIP product was much milder and faster (one night) than the classical hierarchical imprinting. However, the authors did not test the feasibility of synthesising MIPs in different formats.

1.7 Conclusion and future outlook

In recent years we have witnessed a growth of activity in the development of alternative affinity materials to antibodies such as aptamers, EBPs and MIPs. A general overview of these alternatives, with particular emphasis on MIPs, imprinting approaches and different MIP formats has been provided. Recent developments in the synthesis and applications of MIP NPs are particularly encouraging. The feasibility of developing MIP NPs has been analysed in depth, using several examples taken from the recent literature. Several polymerisation methods for MIP NPs have been reviewed, noting their pros and cons and their compatibility with molecular imprinting procedures. A number of interesting practical applications for such materials were also described and discussed in the present review, as well as the most recent progress made in the synthesis of MIPs by using immobilised templates.

It is clear that the process of replacing natural antibodies with their synthetic analogues is mainly hindered by the lack of suitable low-cost protocols for large-scale manufacturing of such materials together with the "polyclonal" nature of synthesised MIPs. Given the importance of MIP NPs as antibody substitutes, and considering their improved properties when compared to larger size MIPs, the automation of their production is an area that really needs to be explored and investigated. To date, there are only few companies that produce MIP micromaterials to be used in SPE applications, i.e. the Swedish company *Biotage* and the French *PolyIntell*. A more recent entry is the US company *Raptor*, which produces MIP-coated wipes for the detection of explosives (Haupt, 2012). Following further advances in polymer and synthetic chemistry, as well as in screening tools, this situation is set to change, motivating companies to put more investment into the development of novel synthetic receptors, thus leading to a new generation of superior affinity materials, readily available for routine diagnostic and industrial applications. New synthetic approaches for MIP preparation can be expected in the next years, which will allow MIPs to be obtained directly in the form of nanoparticles. Hopefully this will allow producing MIPs on a commercial scale for a full range of novel applications.

2 Materials and methods

2.1 Chemicals

Formic acid (HCOOH), boric acid, melamine, vancomycin, desisopropylatrazine (DA), ethylene glycol dimethacrylate (EGDMA), methacrylic acid (MAA), trimethylolpropane trimethacrylate (TRIM), 3-aminopropyltrimethyloxysilane (APTMS), 1,1'-azobis-(cyclohexanecarbonitrile) (ABCN), β-mercaptoethanol (ME), *o*-phtalaldehyde (OPA), glutaraldehyde (GA), phosphate buffered saline (PBS), TRIS buffered saline (TBS), dimethylformamide (DMF), *N*-methyl-2-pyrrolidone (NMP), pentaerythritol-tetrakis-(3-mercaptopropionate), *N*-isopropylacrylamide (NIPAm), acrylic acid (AAc), *N,N'*-methylene-bis-acrylamide (BIS), *N-tert*-butylacrylamide (TBAm), *N,N,N',N'*-tetramethylethylenediamine (TEMED), ammonium persulphate (APS), calcium chloride (CaCl$_2$), cysteamine, α-amylase, pepsin A, methanol (MeOH), ethanol (EtOH), toluene and acetone were purchased from Sigma-Aldrich, UK. Trypsin and bicinchonic acid (BCA) Protein Assay Kit were purchased from Thermo Scientific (UK). Acetonitrile (ACN) and sodium hydroxide (NaOH) were obtained from Fisher Scientific (UK). Poly(ethylene glycol) (PEG) 35000 was purchased from Fluka (Germany). *N,N*-diethyldithiocarbamic acid benzyl ester was obtained from TCI Europe (Belgium). Polymerisable derivative 2,4-diamino-6-(methacryloyloxy)-ethyl-1,3,5-triazine (DMET) from Wako (Japan). Double-distilled ultrapure water, obtained from a Millipore Direct-Q 3 Ultrapure Water Systems (Watford, UK) fitted with a Millipak-20 Express 0.22 μm non-sterile filter, was used for analysis. All chemicals and solvents were analytical or HPLC grade and were used without further purification. The peptide TATTSVLG-NH$_2$ was synthesised and kindly provided by The National Physical Laboratory (UK).

2.2 Preparation of solid-phase affinity media for MIP NPs synthesis

2.2.1 Preparation of polymeric resin as affinity media

Polymeric resin for MIP NPs synthesis was prepared by mixing 5 g DMF, 5 g EGDMA (2.52×10^{-2} mol, $M_w = 198.22$ g/mol), 0.3 g DMET (polymerisable derivative of melamine) (1.29×10^{-3} mol, $M_w = 233.23$ g/mol), 0.1 g ABCN (4.09×10^{-4} mol, $M_w = 244.34$ g/mol) and 0.3 g of PEG 35000 (1.43×10^{-5} mol, $M_w = 35000$ g/mol). This mixture was purged with N_2 for 2 min and then polymerised under UV light for 20 min (UVAPRINT 100 CVI UV source with 0.163 W/cm^2 intensity, Dr. Hönle) in a closed 20 mL glass vial. The obtained white monolith was initially manually ground in smaller pieces in a mortar and then mechanically ground using a Retsch Ultra Centrifugal Mill ZM 200 (Retsch, Germany) at 14000 rpm. The fine powder obtained was wet sieved in MeOH and polymer particles with size 25-63 µm were collected and washed overnight in a Soxhlet extractor with MeOH. Particles were then dried overnight at 80 °C in an oven before use. The procedure has been adapted from Guerreiro *et al.* (2009).

2.2.2 Preparation of template-derivatised glass beads as affinity media

Glass beads were purchased from Sigma-Aldrich, UK (9-13 µm or 75 µm in diameter) or from Blagden Chemicals, UK (Spheriglass® 2429, 53-90 µm diameter). The latter beads had a silane surface coating, which was removed prior to any further treatment by vibrating them with abrasive ceramic beads on a Retsch Vibratory Sieve Shaker AS 200 basic (Retsch, Germany) for 5 h with a 70% amplitude. Glass beads to be used in the photoreactor were activated by boiling in 4 M NaOH for 10 min, while in the case of the aqueous reactor the activation was performed in 1 M NaOH for 1 min. The glass beads were then washed with double-distilled water at 60 °C, followed by acetone and finally dried at 80 °C in an oven. They were then incubated in 150 mL of a 2% v/v solution of APTMS in toluene overnight, then thoroughly washed with acetone and subsequently incubated in 150 mL of a 7% v/v GA solution in PBS 0.01 M

pH 7.2 for 2 h. After this step, the glass beads were rinsed with double-distilled water. The surface immobilisation of the template was performed by incubating beads with 150 mL of a template solution in PBS 0.01 M pH 7.2 overnight at 4 °C. The concentration of template used was 5 mg/mL in the case of melamine; 0.05 mg/mL in the case of peptide TATTSVLG-NH$_2$; 0.5 mg/mL in the case of vancomycin, pepsin A, α-amylase or trypsin (Piletsky *et al.*, 2011). In the case of trypsin, the immobilisation was performed in TBS 0.05 M, pH 8.0 with 0.02 M CaCl$_2$ at 4 °C (Rocha *et al.*, 2005). In the case of melamine, NMP (10% v/v) was also added as co-solvent. Finally, the glass beads were thoroughly washed with double-distilled water and dried under vacuum at room temperature, then stored at 4 °C (melamine, peptide or vancomycin glass beads) or at -18 °C (pepsin A, trypsin or α-amylase glass beads) until used. The procedure was adapted from Piletsky *et al.* (2011).

OPA fluorimetry test of melamine-derivatised glass beads

The reaction between OPA, ME and free amino groups of melamine was exploited to confirm the surface derivatisation of glass beads by analysing the fluorescence of the isoindole adduct. The assay protocol was adapted from Piletska *et al.* (2001). Briefly, 3 mg of 75 µm glass beads, either bare or derivatised with melamine or APTMS, were suspended in 2.3 mL of freshly prepared borate buffer 0.1 M pH 9.5. To this suspension, 300 µL of a 5 mM aqueous solution of OPA and 300 µL of a 5 mM aqueous solution of ME were added. The emission spectrum was recorded after 1 h (excitation wavelength, λ_{ex} = 355 nm) in a 3 cm^3 quartz cuvette using a FluoroMax-2 fluorimeter (ISA Instruments S.A (UK) Ltd., Jobin Yvon-Spex, Middlesex, England).

Elemental analysis of melamine-derivatised glass beads

Elemental analyses of 75 µm glass beads which were either bare, derivatised with APTMS or derivatised with melamine were carried out by MEDAC LTD (Surrey, UK). The accuracy of the analyses was ± 0.30% absolute and the detection limit was 0.1%.

HPLC-MS quantification of template (melamine) on the glass beads

An aliquot of 23.5 g of 75 µm glass beads derivatised with GA was placed in a SPE cartridge equipped with a polypropylene frit (porosity: 20 µm) and incubated with 15 mL of a solution of the template in the same conditions as during the preparation. At the end of the incubation, the supernatant was collected and the solid phase washed with 6 volumes of double-distilled water. The washings were included with the supernatant and the amount of free melamine quantified by HPLC-MS. HPLC separation was conducted using a Waters 2975 HPLC system equipped with Luna C_{18} (2) column (50 × 3 mm, 3 µm, Phenomenex). Mobile phase: MeOH with 0.1% (v/v) HCOOH. The flow rate was 0.2 µL/min, the injection volume was 10 µL and the column temperature was 25 ºC. Fragments of melamine m/z 85 were detected using a mass-spectrometric detector Micromass Quattro Micro (Waters, UK) equipped with an ESI interface in positive ion mode. The detector parameters were the following: desolvation gas: 850 L/h; cone gas: 50 L/h; capillary: 3.5 kV; cone: 35 V; collision energy: 19 eV; source temperature: 120 ºC; desolvation temperature: 350 ºC; multiplier: 650 V. The amount of template immobilised was determined by measuring the difference between the initial amount of melamine incubated and the unbound melamine present in the solution after the immobilisation process.

BCA assay of protein-derivatised glass beads

Immobilisation of protein templates was confirmed by performing a BCA Protein Assay with an aliquot of 75 µm derivatised glass beads, according to the specifications of the manufacturer. Briefly, an aliquot of 150 mg of protein-derivatised glass beads was suspended in 2 mL of freshly prepared working reagent and then incubated at 60 °C for 30 min. A purple colour change confirmed the presence of proteins.

Spectrophotometric quantification of the template on protein-derivatised glass beads

An aliquot of 1.5 g of 75 µm glass beads derivatised with GA was put into a SPE cartridge equipped with a polypropylene frit (porosity: 20 µm) and incubated with 1 mL of a solution of the template in the same conditions as during the preparation. After the end of the incubation, the supernatant was collected and the solid phase washed with 6 volumes of double-distilled water. The washings were added to the supernatant and the amount of free protein in this solution was determined spectrophotometrically ($\lambda = 280$ nm) using a UV-1800 spectrophotometer (Schimadzu, Japan). The amount of protein immobilised was determined by measuring the difference between the initial amount of protein incubated and the free protein present in the solution after the immobilisation process.

2.3 Automatic solid-phase photoreactor for MIP NPs

2.3.1 Feasibility studies: photopolymerisation conditions and reactor setup

Reactor setup

The reactor setup was optimised by performing the synthesis of MIP NPs either within a "short" (4 mm internal diameter, 70 mm length) or a "long" (4 mm internal diameter, 150 mm length) glass column (Soham Scientific, UK). The column was packed with the affinity media under vacuum. For polymeric resin and 9-13 µm derivatised glass beads the packing was performed by producing a slurry of the affinity media in ACN. In all other cases, the dry material was loaded into the column, and then acetone and ACN added under vacuum to pack the glass beads. Custom-cut SPE frits (Sigma Aldrich, UK) were positioned at each end of the column. The column was then fitted into two PEEK™ adapters 10-32 TO M6 (0.020 inch. hole, Sigma-Aldrich, UK), previously modified with a drill and equipped with a custom-made rubber gasket to fit the glass columns. Eventually, the column was mounted on a custom-made aluminium frame and connected to the HPLC system through polytetrafluoroethylene (PTFE) flexible tubes (Phenomenex, UK).

General photopolymerisation and selection conditions

A typical polymerisation mixture was prepared by mixing 0.32 g MAA (3.72×10^{-3} mol, M_w = 86.06 g/mol) as functional monomer, 0.36 g TRIM (1.06×10^{-3} mol, M_w = 338.40 g/mol) and 0.36 g EGDMA (1.82×10^{-3} mol, M_w = 198.22 g/mol) as cross-linkers, 0.087 g *N,N*-diethyldithiocarbamic acid benzyl ester (3.63×10^{-4} mol, M_w = 239.40 g/mol) as iniferter and 0.02 g pentaerythritol tetrakis(3-mercaptopropionate) (4.09×10^{-5} mol, M_w = 488.66 g/mol) as chain transfer agent (CTA) in 1.17 g ACN (Table 2-1, k). The composition was adapted from that used for the preparation of MIP NPs formed under homogeneous conditions (Guerreiro *et al.*, 2009). These conditions were used to perform the first set of experiments discussed in section *3.2.2 - Optimisation of the polymerisation/elution conditions.* After the experimental setup was established,

all polymerisation conditions listed in Table 2-1 were tested to assess the influence of the different parameters on the yield of the synthesised NPs (see the following subsection *Effect of UV irradiation time and composition of the polymerisation mixture on the synthesis of MIP NPs*). In all cases the polymerisation mixture was prepared in a 20 mL glass vial and then purged with N_2 for 2 min. Then 500 μL of the mixture, previously filtered through 0.22 μm PTFE syringe filter (Cronus, Jaytee, UK), were injected into the column packed with the affinity media, and then polymerised under UV irradiation (Philips HB 171/A facial tanning lamp, 4 × 15 W power with 0.09 W/cm^2 intensity, Philips) for a varying time period (Table 2-1). After the polymerisation, the column was connected to the HPLC system (Agilent 1100 Series HPLC or an HPLC system equipped with a Gilson 305 pump (Anachem, UK) and a WATERS Millipore Lambda-max 481 LC spectrophotometric detector).

The elution step to select and collect MIP NPs was performed according to the optimal conditions (*3.2.2 - Optimisation of the polymerisation/elution conditions*). The elution was performed at a flow rate of 1 mL/min with UV detection at 220 nm. For the first 90 min ACN was used as the mobile phase while the column was held at 0 °C using an ice bath. Then for 45 min the mobile phase was switched to ACN with 10 mM HCOOH (used as additive) and the temperature raised to 25 °C, and finally for 35 min the same mobile phase was used but the column was heated to 60 °C in a water bath.

Effect of UV irradiation time and composition of the polymerisation mixture on the synthesis of MIP NPs

The effects of UV irradiation time, concentrations of monomers, CTA and iniferter on the synthesis of MIP NPs were evaluated according to the polymerisation conditions listed in Table 2-1.

Table 2-1. Polymerisation conditions tested during the feasibility study of the automatic synthesis system for the production of MIP NPs.

Set of polymerisation conditions	UV irradiation time (min)	Amount of iniferter (g)	Amount of CTA (g)	Monomer concentration (% w/v)*
a	1	0.044	-	70%
b	1	0.044	0.01	70%
c	1	0.044	0.02	70%
d	2	0.044	-	70%
e	2	0.044	0.01	70%
f	2	0.044	0.02	70%
g	1	0.087	0.01	70%
h	1	0.087	0.02	70%
i	1	0.087	0.04	70%
j	2	0.087	0.01	70%
k	2	0.087	0.02	70%
l	2	0.087	0.04	70%
m	1	0.131	0.01	70%
n	3	0.087	0.02	70%
o	2	0.087	0.02	52.5%
p	2	0.087	0.02	87.5%
q	2	0.087	0.02	140%

*expressed as % ratio between the total amount (g) of MAA, EGDMA and TRIM and the total amount (mL) of ACN added.

The area of the chromatographic peak of the fraction collected during the heating step at 60 °C was chosen as the main parameter to assess the impact of varying polymerisation conditions on the yield of NPs. Corresponding elutions without UV irradiation were performed as a control for the conditions listed in Table 2-1. To calculate the yield, the fraction collected during the heating phase of the elution was evaporated and weighed, and the yield was expressed in terms of % w/w in relation to the weight of the initial monomers.

2.3.2 Automatic solid-phase photoreactor prototype design

Applying the data obtained from the preliminary results, an automated flow photoreactor system was designed using components purchased from HEL Ltd. (UK). Standard components which were used "off the shelf" included:

- Multiple liquid feed: 2 × HEL Dual V6 automated syringe pumps, suitable to provide 4 independently controlled liquid feeds with auto-refill function, and PTFE feed lines constructed of 1/8" internal diameter. An automated switching valve allows each liquid reagent to flow sequentially into the column with a programmable flow rate (mL/min) using the supplied control software. Each syringe pump can be fitted with either a 10 mL, 25 mL, 50 mL or 100 mL glass syringe;

- UV light source: the complete column and column temperature controller is housed in a UV light chamber (W × H × D: 45 × 30 × 32 cm) which can be manually switched on/off as required. The UV light source is composed by 2 × 8 W lamps used to initiate photopolymerisation processes;

- Column temperature controller: the reaction column accommodates the affinity media and is located within a jacketed glass sleeve. The sleeve is connected to a circulator to provide even cooling around the entire column. Inside the column a rod heater provides rapid heating of the column. This allows the rapid changing of temperature within the column from 4 °C to 60 °C;

- Reaction column: the reaction column is constructed of borosilicate glass (main body) and PEEK™ (end piece), with the following dimensions: 6.6 mm internal diameter × 150 mm length. These materials provide stability at temperatures ranging from 4 °C up to 150 °C, and pH values from 1 to 14. The column is also resistant to aqueous solutions and solvents commonly used in liquid chromatography;

- Separation of product and waste: a 6-ways valve enables the separation of product from waste. After the polymerisation, the product deriving from the affinity separation step performed at low temperature is discarded using the waste line, while at high temperatures the remaining five lines allow the collection of the high-affinity fractions of the MIP NPs;

- Control system: individual feed-rates of each solution and solvent as well as reactor temperature are controlled by HEL's proprietary software WinISO, which is installed on a PC. The software enables the logging and control of all reaction parameters in real-time, with reaction procedures being designed, saved, reloaded and edited using this system. All data are displayed on screen in real-time, and also saved automatically in a Windows^{TM} compatible data-file for off-line analysis. The software also provides integral safety parameters with audible and visual alarms, warnings and shutdown states adjustable by the user.

2.3.3 Solid-phase automated photochemical synthesis of MIP NPs for melamine, vancomycin and a model peptide

For melamine MIP NPs, the polymerisation mixture was prepared by mixing 0.96 g MAA (1.12×10^{-2} mol, M_w = 86.06 g/mol) as functional monomer, 1.08 g TRIM (3.18×10^{-3} mol, M_w = 338.40 g/mol) and 1.08 g EGDMA (5.46×10^{-3} mol, M_w = 198.22 g/mol) as cross-linkers, 0.261 g *N,N*-diethyldithiocarbamic acid benzyl ester (1.09×10^{-3} mol, M_w = 239.40 g/mol) as iniferter and 0.06 g pentaerythritol-tetrakis-(3-mercaptopropionate) (1.23×10^{-4} mol, M_w = 488.66 g/mol) as CTA in 3.51 g ACN (total monomer concentration: 70% w/v). The mixture was placed in a 20 mL glass vials and purged with N_2 for 10 min. Then 4 mL of the mixture were automatically injected into the column packed with the immobilised template phase and polymerised under UV irradiation for 3.5 min at 4 °C. After polymerisation, the reactor was maintained at 4 °C and flushed with 120 mL ACN (flow rate: 2 mL/min). Then the temperature was raised to 25 °C, after which 45 mL ACN with 10 mM HCOOH (used as additive) were eluted. Finally, 40 mL of the same mobile phase were eluted at 60 °C to collect the high-affinity MIP NPs. When used continuously in full-automatic mode, the column was flushed (flow rate: 2 mL/min) at 60 °C with 80 mL ACN with 10 mM HCOOH, and then at 20 °C with 30 mL ACN between the cycles. Absence of template in the MIP NPs fraction has been confirmed by HPLC-MS, performed according to the conditions described above in the subsection *HPLC-MS quantification of template (melamine) on the glass beads*.

For vancomycin and peptide MIP NPs, the polymerisation mixture was prepared by mixing 0.936 g NIPAm (8.27×10^{-3} mol, 53% mol, M_w = 113.16 g/mol) as monomer, 0.048 g BIS (3.11×10^{-4} mol, 2% mol, M_w = 154.17 g/mol) as cross-linker, 0.8 g TBAm (6.29×10^{-3} mol, 40% mol, M_w = 127.19 g/mol) as hydrophobic functional monomer, 56.8 µL AAc (8.28×10^{-4} mol, 5% mol, M_w = 72.06 g/mol, ρ = 1.051 g/mL) as negatively-charged functional monomer and 0.152 g *N,N*-diethyldithiocarbamic acid benzyl ester (1.09×10^{-3} mol, M_w = 239.40 g/mol) as iniferter in 7.87 g ACN (total monomer concentration: 18% w/v). The composition was adapted from that used by Hoshino *et al.* (2008). The mixture was placed in a 20 mL glass vials and purged with N_2 for 10 min. Then 4 mL of the mixture were automatically injected into the column packed with the immobilised template solid-phase and then polymerised under UV irradiation for 3.5 min at 20 °C. After polymerisation, the reactor was maintained at 20 °C and flushed with 60 mL ACN (flow rate: 2 mL/min). Then the temperature was raised to 25 °C, after which 45 mL ACN with 10 mM HCOOH (used as additive) were eluted. Finally, 40 mL of the same mobile phase were eluted at 60 °C to collect the high-affinity MIP NPs.

The resulting yield has been expressed in mg of MIP NPs produced. Apparent molarities of the analysed NPs fractions were calculated using the Equation 2-1 (Hoshino *et al.*, 2008) and used for the calculation of dissociation constants:

$$[NPs] = \frac{6}{\pi N_A d^3 \rho} X \qquad \textbf{Equation 2-1}$$

where N_A is Avogadro's constant, d is the hydrodynamic diameter of particles found by DLS (nm), ρ is polymer density of particles (g/cm^3) and X is NPs weight concentration (mg/mL). For the NPs imprinted for melamine, a ρ value of 1 g/cm^3 has been assumed (Ivanova-Mitseva *et al.*, 2012). In the case of NPs imprinted for vancomycin and the model peptide, the ρ value for NPs with a similar composition ranges from 0.08 to 0.27 g/cm^3 (Debord and Lyon, 2003; Hoshino *et al.*, 2008)

2.3.4 Effect of irradiation time on size, yield and affinity of MIP NPs

To study the effect of irradiation time on size, yield and affinity of MIP NPs, melamine MIP NPs were synthesised using three different UV irradiation times (2.5, 3.5 and 4.5 min) in the presence of a constant amount of polymerisation mixture (4 mL). At the end of each cycle, the yield of the MIP NPs fractions was evaluated by drying each solution and then reported in mg of MIP NPs produced. Their size has been evaluated by SEM, TEM and DLS, and their affinity and specificity has been tested on melamine and DA-derivatised BIAcore gold chips using a BIAcore 3000 SPR instrument. The detailed experimental conditions used for SEM, TEM, DLS and SPR are reported in the section *2.5 - Characterisation of MIP NPs*.

2.4 Automatic solid-phase chemical reactor for MIP nanoparticles

2.4.1 Automatic solid-phase chemical reactor prototype design

An additional module designed to operate in aqueous conditions using a mild persulphate-initiated polymerisation performed at room temperature was developed. All system components were purchased from HEL Ltd. (UK). Standard components which were used "off the shelf" included:

- Multiple liquid feed: 2 × HEL Dual V6 automated syringe pumps, capable of providing 4 independently controlled liquid feeds with auto-refill function, and PTFE feed lines constructed of 1/8" internal diameter. An automated switching valve allows each liquid reagent to flow sequentially into the column with a programmable flow rate (mL/min) using the supplied control software. Each syringe pump can be fitted with either a 1 mL, 10 mL, 25 mL, 50 mL or 100 mL glass syringe;

- Column temperature controller: the reaction vessel accommodates the affinity media and is located inside a jacketed glass sleeve. The sleeve is connected to a circulator to provide even cooling/heating around the entire column. This guarantees a control over the temperature in a range from 4 °C to 60 °C;

- Reaction vessel: the reaction column is constructed of borosilicate glass (main body) and PEEK™ (end piece), with the following dimensions: 25 mm internal diameter × 205 mm length (≈ 100 mL capacity). It is equipped with a polypropylene SPE frit (porosity: 20 μm) and a rubber gasket at the bottom to retain the solid phase, which is pre-loaded before assembly onto the stand. These materials provide stability at temperatures ranging from 4 °C up to 150 °C, and pH values from 1 to 14. The column is also resistant to aqueous solutions and solvents commonly used in liquid chromatography;

- Reactor stand: the reactor stand includes a motor connected to a shaking system through a rubber belt for the homogenisation of the reactor contents. The shaft of the motor is interchangeable, thus the shaking frequency can be adjusted depending on the size of the shaft used;

- Gas line: an additional inlet at the top of the reactor provides for flushing N_2 (or another inert gas) to remove oxygen and to pump out the reactor contents;

- Separation of product and waste: a 6-ways valve allows for separation of product and waste. After the polymerisation, the product deriving from the affinity separation step performed at low temperature is discarded using the waste line, while at high temperatures the remaining five lines allow the collection of the high-affinity fractions of the MIP product;

- Control system: individual feed-rates of each liquid feed and reactor temperature are controlled by HEL's proprietary software WinISO, which is installed on a PC. The software enables the logging and control of all reaction parameters in real-time, with reaction procedures being designed, saved, reloaded and edited even once a reaction has started. All data are displayed on screen in real-time, and also saved automatically in a Windows™ compatible data-file for off-line analysis. The software also provides integral safety parameters with audible and visual alarms, warnings and shutdown states adjustable by the user.

2.4.2 Solid-phase automated chemical synthesis of MIP NPs for pepsin A, trypsin and α-amylase

This procedure was adapted from Hoshino *et al.* (2008). In 100 mL double-distilled water, the following monomers were dissolved: 39 mg NIPAm (3.44×10^{-4} mol, 53% mol, M_w = 113.16 g/mol) as backbone monomer, 2 mg BIS (1.26×10^{-5} mol, 2% mol, M_w = 154.17 g/mol) as cross-linker, 33 mg TBAm (2.60×10^{-4} mol, 40% mol, M_w = 127.19 g/mol) as hydrophobic functional monomer and 2.2 µL AAc (3.24×10^{-5} mol, 5% mol, M_w = 72.06 g/mol, ρ = 1.051 g/mL) as negatively-charged functional monomer. TBAm was dissolved in 2 mL EtOH and then added to the aqueous solution. The total monomer concentration was 6.5 mM. The solution was degassed under vacuum and ultrasonication for 10 min, and then purged with N_2 for 30 min. After this time, the container with the polymerisation mixture was connected to one of the pumps of the automatic synthesiser and 80 mL of it injected in the reactor vessel containing 60 g of

template-derivatised glass beads. The polymerisation was started by injecting 800 µL of an APS aqueous solution (60 mg/mL, M_w = 228.20 g/mol) and 24 µL of TEMED (9.36 × 10^{-5} mol, M_w = 198.22 g/mol, ρ = 0.775 g/mL), after which the solution was drawn through the bulk of glass beads under pressure down to a total active polymerisation volume of 25 mL. The polymerisation was carried out at room temperature for 2 h. After this the reactor temperature was adjusted to 15 °C and the remaining polymerisation mixture washed out with two fractions of 50 mL of double-distilled water (flow rate: 2 mL/min). The high-affinity MIP NPs were eluted from the affinity media by passing three fractions of 50 mL of double-distilled water at 60 °C (delivery flow rate: 2 mL/min). The yield of the NPs fractions was evaluated by freeze-drying an aliquot (13 mL) of each solution. Apparent molarities of the analysed NPs fractions were calculated using the Equation 2-1 (Hoshino *et al.*, 2008) and used for the calculation of dissociation constants. The ρ value for non-swollen particles with a similar composition ranges from 0.08 to 0.27 g/cm^3 (Debord and Lyon, 2003; Hoshino *et al.*, 2008). Absence of the protein template in the MIP NPs fraction was confirmed by BCA Protein Assay performed on the NPs solutions according to the specifications of the manufacturer.

2.4.3 Effect of the amount of derivatised glass beads on yield and size of MIP NPs

To study effect of the amount of derivatised glass beads on the yield of MIP NPs four different amounts of template-derivatised glass beads (20 g, 40 g, 60 g and 80 g) were tested in the presence of a constant amount of polymerisation mixture (25 mL). At the end of each cycle, the yields of the MIP NPs fractions were evaluated by freeze-drying 13 mL of each solution, and reported in weight percentage of the total amount of monomers present in the active polymerisation mixture. The MIP NPs size was evaluated by DLS (see *2.5.1 - Dynamic Light Scattering (DLS) size analysis of MIP NPs*). All the results were corrected by subtracting the amount of material obtained after a blank run performed with just double-distilled water on the same amount of derivatised glass beads.

2.5 Characterisation of MIP NPs

2.5.1 Dynamic Light Scattering (DLS) size analysis of MIP NPs

To verify the size of the synthesised MIP NPs, the eluted fractions were ultrasonicated for 20 min, then filtered through 1.2 µm glass fibre syringe filters (Cronus, Jaytee, UK) and analysed either in a 3 cm^3 glass cuvette (for organic solutions) or in disposable polystyrene cuvettes (for aqueous solutions) at 25 °C using a Zetasizer Nano (Nano-S) from Malvern Instruments Ltd (Malvern, UK). The instrument was allowed to automatically select the attenuator position, the measurement duration and the number of runs. A minimum of 5 measurements per sample were made.

2.5.2 Scanning Electron Microscopy (SEM) and Transmission Electron Microscopy (TEM) of MIP NPs

SEM images of MIP NPs were taken using a Philips XL-30 Scanning Electron Microscope. Samples for were prepared by depositing 5 µL of each MIP NPs solution, previously filtered through a 1.2 µm glass fibre syringe filters (Cronus, Jaytee, UK), onto a silicon chip attached to a SEM holder before leaving to dry overnight in a desiccator. Prior to SEM analysis, the samples were plasma-coated with gold using a Polaron Equipment E5100 SEM plasma coater.

TEM images of MIP NPs were taken using a Philips CM20 Transmission Electron Microscope. Samples for analysis were prepared by depositing 5 µL of each MIP NPs solution, previously filtered through a 1.2 µm glass fibre syringe filters (Cronus, Jaytee, UK), in a carbon coated copper grid before leaving to dry overnight in a desiccator.

2.5.3 Preparation of template-derivatised BIAcore gold chips

Au-coated chips (SIA Kit Au, BIAcore) were cleaned by immersion in Piranha solution (H_2SO_4/H_2O_2, 3:1 v/v) for 5 min. Caution! This mixture is highly corrosive, hence extreme care is required during this process. The chips were thoroughly rinsed with double-distilled water and left in EtOH overnight. The immobilisation of the templates was performed by incubating the chips in a 0.2 mg/mL solution of cysteamine in EtOH at 4 °C for 24 h, after which they were

washed with EtOH and incubated in a 7% v/v solution of GA in PBS 0.01 M pH 7.2 for 2 h. After this step, the chips were washed with double-distilled water and immersed in a 1.2 mg/mL solution of each template in PBS 0.01 M pH 7.2 for 24 h at 4 °C (Jiang *et al.*, 2003). In the case of melamine and DA, 20% v/v of MeOH was added as co-solvent. In the case of trypsin the immobilisation was performed in TBS 0.05 M, pH 8.0 with 0.02 M $CaCl_2$ (Rocha *et al.*, 2005). Once the immobilisation was completed, the chips were washed with double-distilled water, dried in a stream of N_2 and assembled on their holders. These were then stored under Ar at 4 °C until required. In the case of protein-derivatised chips, they were used within the following 24 h. To confirm the validity of the immobilisation strategy, the modification of the surface of the gold chips with melamine and DA was confirmed by performing sessile water contact angle measurements using a Cam 100 optical Angle Meter (KSV Instruments Ltd., Finland) along with the software provided.

2.5.4 Surface Plasmon Resonance (SPR) affinity analysis of MIP NPs

Affinity analysis was performed using a BIAcore 3000 SPR system (BIAcore, Sweden). Au-chips with the relevant template immobilised on the surface were used for the experiments. A volume of 10 mL of solution of MIP NPs was washed and concentrated down to a final volume of 1-2 mL through centrifugal membrane filter units (Amicon Centriplus®, 30 kDa MWCO, Millipore, UK) in PBS 0.01 M pH 7.4. In the case of MIP NPs in ACN, the NPs solutions were diluted with PBS 0.01 M pH 7.4 down to an ACN concentration of 10% v/v before loading onto the filtration devices. Each filtration was carried out according to the specifics of the filter manufacturer using a Sigma 3-16P bench-top centrifuge fitted with a swing-bucket rotor, at 2500 *g* for 2.5-3 min. The solutions obtained in PBS were ultrasonicated for 30 min and used as stocks. In the case of melamine, vancomycin and peptide MIP NPs, 5 dilutions were prepared from 1/2 to 1/32 (stock concentrations: melamine MIP NPs: 330 nM; peptide MIP NPs: 1094 nM; vancomycin MIP NPs: 135 nM). In the case of the protein-imprinted MIP NPs, 7 dilutions were prepared, from 1/10 to 1/10[7] (stock concentration: 0.4 nM). All the affinity experiments were performed in PBS 0.01

M pH 7.4 as mobile phase at a flow rate of 35 μL/min. Measurements were made at 25 °C for melamine, vancomycin and protein MIP NPs, while for the peptide MIP NPs the temperature was set to 18 °C. From each dilution, 100 μL were sequentially injected in order of increasing concentration and the sensor response was analysed for 2 min after every injection. Kinetic data were fitted using BIAEvaluation Software v4.1 (BIAcore, Sweden) which assumes a Langmuir isotherm model. If required, a baseline drifting correction was applied.

3 Automatic solid-phase photoreactor for MIP NPs – Results and discussion

As stated in the introduction, MIP NPs offer substantial advantages with comparison to natural antibodies. Nevertheless their production is not straightforward and there are no protocols available for large-scale manufacturing.

The majority of polymerisation processes described in the literature require at least 12 h for completion (Pérez-Moral and Mayes, 2007; Yoshimatsu *et al.*, 2007; Hoshino *et al.*, 2008). Even more time-consuming are the purification procedures for removing templates and non-reacted monomers, which require multiple washing steps (Ciardelli *et al.*, 2004; Yoshimatsu *et al.*, 2007), ultrafiltration (Pérez *et al.*, 2000; Pérez-Moral and Mayes, 2004), Soxhlet extraction (Cirillo *et al.*, 2009), or dialysis (Hoshino *et al.*, 2008; Hoshino *et al.*, 2010b; Zeng *et al.*, 2010).

Furthermore, each batch of MIP product has required a new batch of template molecules which, if expensive, might represent an important economical drawback for scaling up the production process.

Recently, Guerreiro and co-workers have successfully produced soluble MIP NPs imprinted with a triazine derivative (acetoguanamine) which were purified by affinity chromatography using a stationary phase derivatised with the template (2009). Hoshino *et al.* (2010) separated different fractions of non-imprinted NPs using the affinity separation approach reported by Piletsky's group.

Solid-phase synthesis approaches for the preparation of nucleic acids and peptides are now fully established (Merrifield, 2012; Horvath *et al.*, 1987; Kent *et al.*, 1984) and automatic synthesisers are commercially available, allowing the automatic synthesis of the same peptides and nucleic acids to be performed more reproducibly, more cheaply and more rapidly than ever before (Hunkapiller and Hood, 1980; Kambara *et al.*, 1988).

The aim of the present work was to study whether solid-phase synthesis could be used for preparing MIP NPs. Solid phases with immobilised templates (see section *1.6 - Immobilised templates: a new imprinting strategy*) have not previously been used in the preparation of soluble MIP NPs. Successfully addressing this issue would offer interesting scientific challenges and great opportunities for development and commercialisation. Taking all of these challenges into account, the development of a solid-phase synthetic strategy for MIP NPs, compatible with automation, was investigated.

The first stage involved the synthesis of several types of template-derivatised solid phases. This was done to assess the feasibility of obtaining MIP NPs using a solid-phase platform and to verify which material would have the greatest potential for use within an automatic reactor. Melamine was chosen as the model template during these feasibility experiments for the reasons detailed in the following sections.

3.1 Preparation of the affinity media for MIP NPs synthesis

Two types of affinity media were prepared and tested to verify their suitability for the synthesis and purification of high-affinity MIP NPs on a solid-phase support: these were a polymeric resin bearing the template moieties within its porous structure or non-porous glass beads (of different sizes) where the template was immobilised on their surface.

3.1.1 Preparation of polymeric resin as affinity media

The first affinity media tested for use in the production of MIP NPs was prepared according to a procedure adapted from Guerreiro *et al.* (2009). A polymerisable analogue of the melamine template, DMET (Figure 3–1a) was co-polymerised with EGDMA under UV irradiation to produce a resin in which the template moiety is randomly present within the polymeric matrix.

a   b
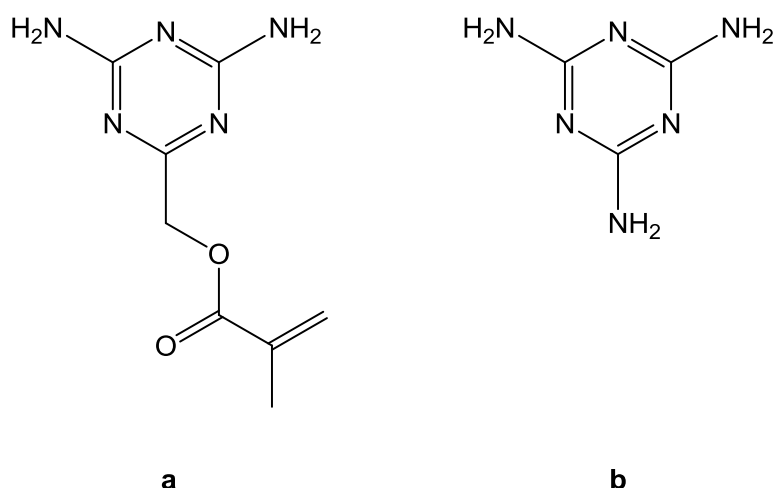
Figure 3–1. Structures of DMET (a) and melamine (b).

The porosity of the matrix was guaranteed by the presence of PEG 35000 as a porogen, which after removal leaves behind macroporous cavities necessary for the formation and subsequent elution of the synthesised NPs (Barral *et al.*, 2010). After washing, this material was suspended in ACN and packed in a glass column to be tested for its suitability for use as the solid phase during the synthesis of MIP NPs (see *3.2.2 - Optimisation of the polymerisation/elution conditions*).

3.1.2 Preparation of template-derivatised glass beads as affinity media

Glass beads were tested as a potential solid phase because they are easy to handle and inexpensive. The surface modification of glass can be easily performed using silane-based chemistry (Arslan *et al.*, 2006; Bossi *et al.*, 2010). The immobilisation procedure used was adapted from Piletsky *et al.* (2011). This protocol is well established for the immobilisation of antibodies, proteins or other compounds which bear a primary amino group (Jiang *et al.*, 2003; Shiomi *et al.*, 2005; Yang *et al.*, 2005; Li *et al.*, 2006a; Bonini *et al.*, 2007). The activation of the glass beads by refluxing in concentrated NaOH increases the amount of reactive silanol groups ($-Si-OH$) available on their surface (Liu *et al.*, 2002), ensuring that the following silanisation reaction with APTMS produces a good coverage of the surface with primary amino groups. In the following steps GA acts as a linker between the two primary amino groups (one on the glass surface, the other on the template molecule) through the formation of Schiff base bonds (Figure 3–2).
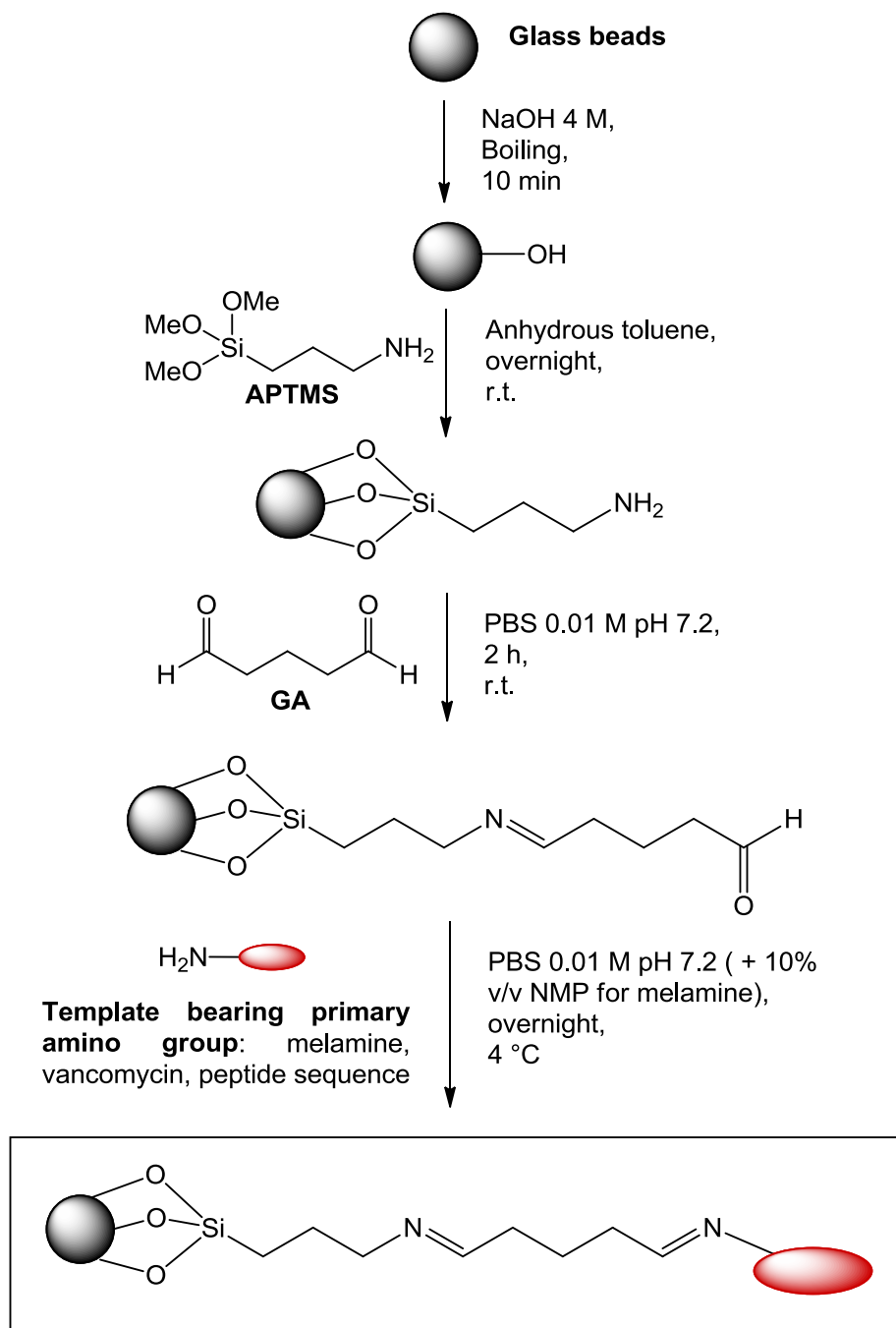
Figure 3–2. Synthetic protocol for the immobilisation of template on the glass beads surface for use in photoreactor.

Additionally, the APTMS and GA act as a spacer between the surface of the glass beads and the template, thus allowing the subsequent polymerisation reaction to take place without steric hindrance or interference due to the overcrowding of template molecules (Titirici *et al.*, 2002). In the case of the

immobilisation of melamine, the addition of NMP as co-solvent is necessary due to the low solubility of this molecule in water.

Qualitative and quantitative analysis of melamine-derivatisation of glass beads

In order to confirm the surface derivatisation of the glass beads with melamine, the reaction between OPA, ME and free primary amino groups of melamine was exploited. The nucleophile addition of ME to OPA forms a thioacetal intermediate that reacts with free primary amino groups, thus giving rise to the fluorescent adduct (Figure 3–3).

| OPA | ME | Hemithioacetale | Primary amines | Fluorescent isoindole |
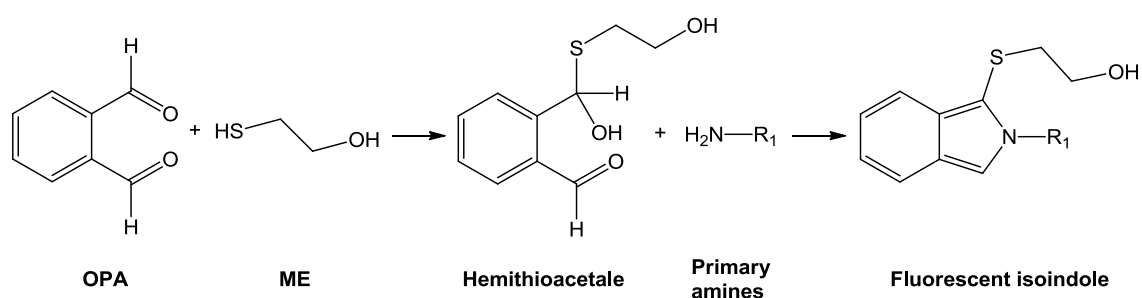
Figure 3–3. Reaction scheme of the OPA assay. OPA undergoes a nucleophilic attack by the thiol group of ME to form a hemithioacetale, which in turn promptly reacts with primary amino groups (such as melamine ones) to provide a fluorescent isoindole.

This protocol was adapted from Piletska *et al.* (2001). The fluorescence was measured after 1 h and before each reading thorough mixing was applied using a pipette directly inside the cuvette, to achieve better homogeneity of the suspension. The excitation and emission maximums are at 355 nm and 450 nm, respectively. The presence of melamine on the surface of glass beads resulted in an increased emission intensity at 450 nm, about 2.3-fold more than the bare glass beads and 2-fold more than the APTMS-derivatised glass beads (Figure 3–4), thus qualitatively confirming the immobilisation of melamine on the surface.
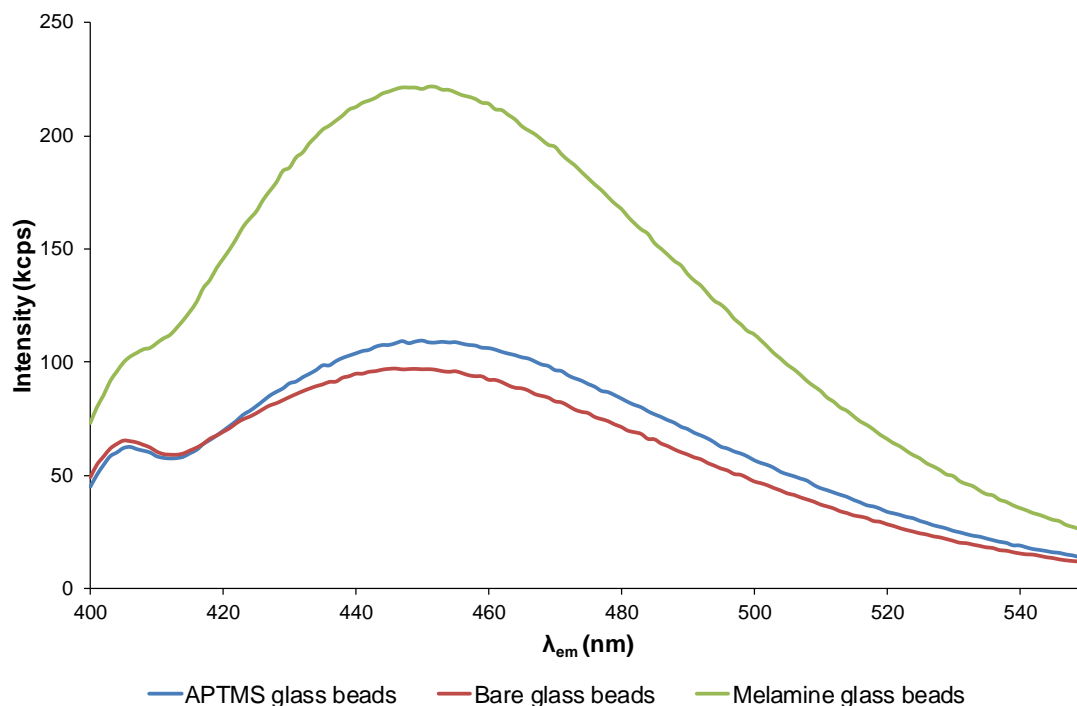
Figure 3–4. Fluorescence emission spectra of ME, OPA and glass beads (bare or derivatised, either with melamine or APTMS) in borate buffer 0.1 M pH 9.5.

Quantification of the amount of melamine immobilised on the surface of the glass beads was attempted by performing elemental analysis on samples of bare, APTMS-derivatised and melamine-derivatised glass beads. The results, however, were inconclusive because the quantity of C, H, and N in APTMS and melamine-derivatised glass beads was relatively low and below the limit of detection (Table 3-1).

Table 3-1. Elemental analysis of 75 µm bare, APTMS-derivatised and melamine-derivatised glass beads.

Glass beads	Element		
	C	**H**	**N**
Bare	0.77%	<0.10%	<0.10%
APTMS-derivatised	0.61%	<0.10%	<0.10%
Melamine-derivatised	0.37%	<0.10%	<0.10%

For this reason, rather than a direct method, an indirect quantification of the immobilised melamine was attempted by performing an HPLC-MS analysis on

the residual solution of the template after incubation with GA-activated glass beads to assess the amount of free template still present. The aqueous solution was analysed by injection into an HPLC-MS. The method enabled the evaluation of the amount of immobilised melamine, which resulted to be 0.29 mg (2.3×10^{-6} mol, M_w = 126.11 g/mol) per gram of glass beads.

3.2 Feasibility studies: photopolymerisation conditions and reactor setup

3.2.1 General solid-phase synthesis of melamine MIP NPs

Melamine was used as a model template in the majority of feasibility experiments performed here (Figure 3–1b). This aminotriazine can be used as an industrial chemical in the production of melamine-formaldehyde polymer resins for several applications (laminates and coatings, adhesives, plastics and even flame-retardants). Due to its high nitrogen content, however, unethical manufacturers have recently adulterated food products with it to increase the nitrogen level while reducing the costs (Chan *et al.*, 2008; Sun *et al.*, 2010). This sadly resulted in the occurrence of kidney stones in thousands of infants across China in 2008, who had consumed infant formula adulterated with melamine, leading in some cases to renal failure, and ultimately death (Chan *et al.*, 2008; BBC News, 2010).

The main concept behind this project involved the possibility of exploiting a solid phase with an immobilised template, packed inside a glass column, to perform both the synthesis and the selection of high-affinity MIP NPs. The immobilised template on the solid phase should act as the template for the imprinting process during a first UV-initiated polymerisation step and then act as an immobilised ligand in a subsequent affinity chromatography for the removal of the low-affinity MIP fraction (including non-polymerised material) from the high-affinity MIP NPs.

To imprint melamine a polymerisation mixture adapted from Guerreiro *et al.* (2009) was used (Figure 3–5).
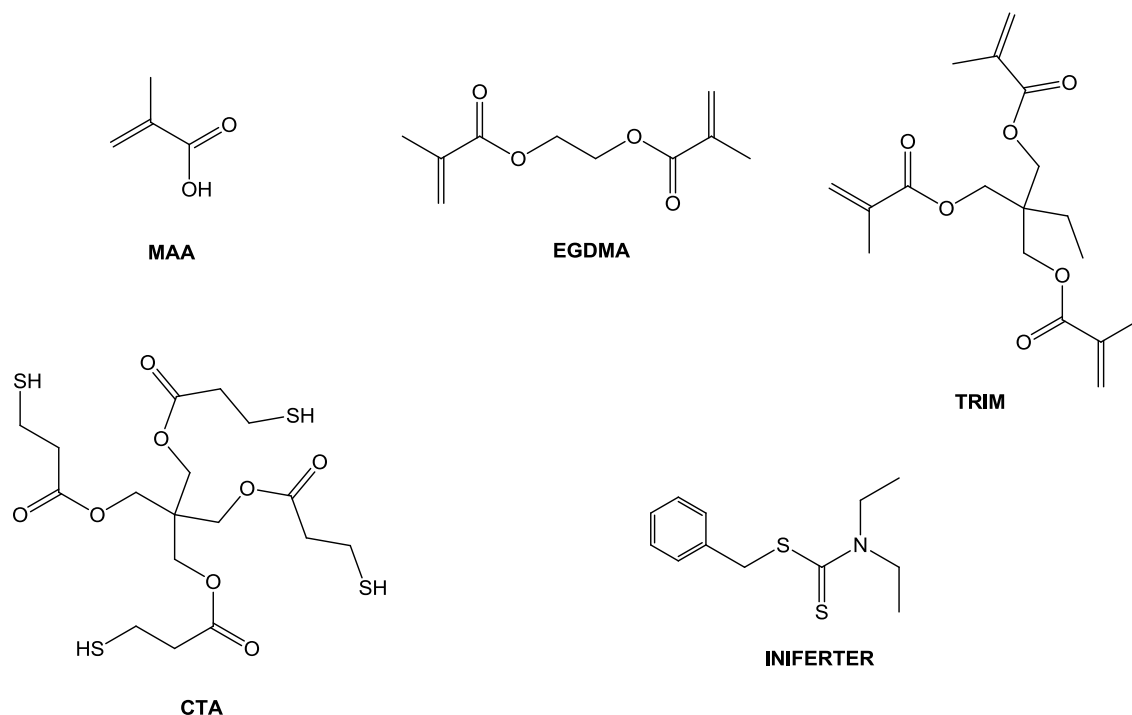
Figure 3–5. Polymerisation mixture used for imprinting melamine through UV photopolymerisation.

Aminotriazine-based structures have been successfully imprinted previously (Matsui *et al.*, 1995; Muldoon and Stanker, 1995; Muldoon and Stanker, 1997; Li *et al.*, 2010b). The molecular recognition in these systems occurs through the strong hydrogen interactions that are established between the template molecule and the functional monomer, MAA. The carboxylic group of MAA can act both as hydrogen bond acceptor and donor, as well as the amino groups and the nitrogen atoms of the triazine aromatic ring (Figure 3–6) (Welhouse and Bleam, 1993; Matsui *et al.*, 1995; Li *et al.*, 2010b).
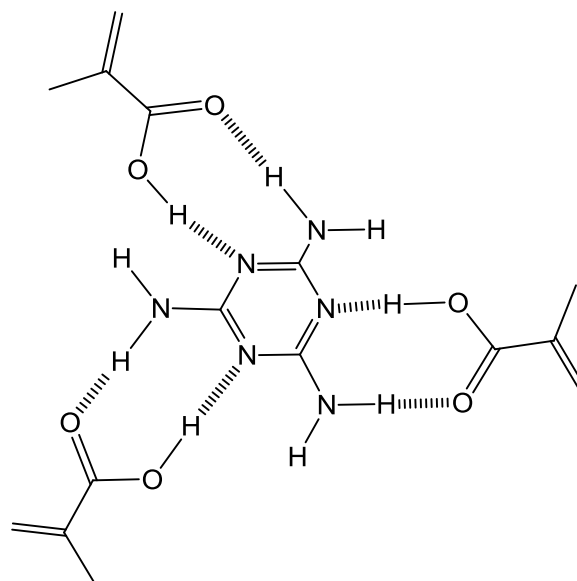
Figure 3–6. Scheme of the hydrogen bonds between MAA and melamine.

The polymerisation protocol based on the early termination of an iniferter-initiated UV polymerisation (Guerreiro *et al.,* 2009) allows the maintainance of a high concentration of functional monomers, beneficial for the formation of stable pre-polymerisation complexes (Haupt, 2003; Guerreiro *et al.*, 2009). Moreover, the short UV-irradiation times reported should ensure the temperature of the polymerisation mixture remains low during the imprinting process, thus enhancing the affinity of the synthesised material (Piletsky *et al.*, 2002; Piletsky *et al.*, 2004; Mijangos *et al.*, 2006; Guerreiro *et al.*, 2009). Short-time UV irradiation should also favour the synthesis of polymers with relatively uniform low molecular weight, required for the production of MIP NPs. To further improve control over the living polymerisation process, pentaerythritol tetrakis(3-mercaptopropionate) (Figure 3–5) has been added as a CTA (Choi *et al.*, 2002; Odian, 2004).

When considering photochemical initiation methods, living polymerisation based on iniferter-type initiators, such as *N,N*-diethyldithiocarbamic acid benzyl ester (Figure 3–5), is a useful approach (Pérez-Moral and Mayes, 2007; Li *et al.*, 2010a). The use of an iniferter allows better control over the reaction kinetics, and provides a living character to the polymerisation process, thus avoiding the high polymerisation rate and the autoacceleration effect typical of non-living

radical polymerisation (Kannurpatti *et al.*, 1996). Of crucial importance is the capacity to initiate polymerisation under mild conditions by this approach using near UV irradiation and to terminate it by ceasing the irradiation (Guerreiro *et al.*, 2009). An additional valuable feature is the possibility to reinitiate the polymerisation from the macroiniferters on the NPs surface by UV irradiation, to allow post-functionalisation of the MIP NPs with fluorescein or other labels (Otsu *et al.*, 1989; Otsu *et al.*, 1995; Otsu, 2000).

A mixture of two cross-linkers, EGDMA and TRIM (Figure 3–5), was used to provide the correct balance of rigidity/flexibility which is markedly important to ensure the molecular recognition properties in MIP NPs (Guerreiro *et al.*, 2009).

The high-affinity fraction of MIP NPs was purified immediately after the polymerisation step by performing temperature-controlled affinity chromatography in the same glass column. The experiments that led to the optimisation of conditions of the synthetic setup and elution are described in the next section (*3.2.2 - Optimisation of the polymerisation/elution conditions*).

3.2.2 Optimisation of the polymerisation/elution conditions

In a typical affinity chromatography process, a raw mixture of molecules (usually proteins) is loaded into a column packed with an immobilised affinity ligand. Only the molecules able to recognise the immobilised ligand with high affinity are retained, and all the others are washed out using mild elution conditions. After this step the molecule of interest is eluted by using stronger elution conditions, e.g. changing the pH or the ionic strength, or adding surfactants (Hage, 1998). The change of temperature is not frequently exploited to promote the elution of the retained target molecule since in most cases targets such as proteins may undergo denaturation at high temperatures. This is not the case for stable MIP NPs, however, which can be eluted at elevated temperature without detrimental effect on their recognition properties.

The first part of the elution process undertaken within this work was performed at a low temperature, which facilitates the interactions between the high-affinity fraction of MIP NPs and the immobilised template, whilst monomers, oligomers

and other material with low or no affinity are flushed from the system. The temperature of the column and solvent was then increased to disrupt the non-covalent interactions between the template and the high-affinity MIP NPs, thus allowing pure fraction of particles free of residual template and monomers to be collected.

The difference between the two chromatograms performed in the presence and in the absence of irradiation was demonstrated with the appearance of a new peak corresponding to the polymeric fraction. The increase in the polymeric fraction peak area was used as one of the criteria to assess the feasibility of the synthetic conditions. The first set of experiments was performed on a "short" glass column (4 mm internal diameter, 70 mm length) (Figure 3–7) packed with the polymeric resin as affinity media and connected to an Agilent 1100 Series HPLC system.
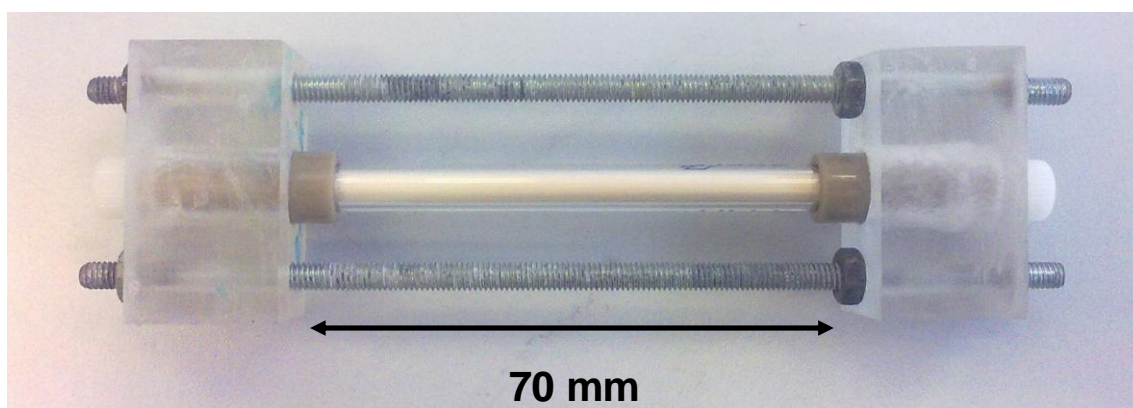
70 mm

Figure 3–7. "Short" glass column (4 mm internal diameter, 70 mm length) packed with affinity media (either polymeric resin or 9-13 μm melamine-derivatised glass beads).

These conditions were applied first because the affinity separation of MIP NPs had been already successfully accomplished using this affinity media (Guerreiro *et al.*, 2009). Unfortunately, the use of this material did not allow the occurrence of high flow rates when packed into the glass column (no higher than 0.25 mL/min) due to the high back pressure caused by irregular (and swellable) polymer particles. Nevertheless several elution conditions (different temperatures, use of 100 mM HCOOH as additive to the mobile phase ACN)

were tested for separating non-polymerised material and the low-affinity fraction of MIP NPs from the high-affinity product. The chromatograms obtained both with or without irradiation did not, however, show any difference (Figure 3–8). It is possible that the opaque polymeric resin was preventing the penetration of the UV light into the bulk of the affinity media, thus hindering the polymerisation process.
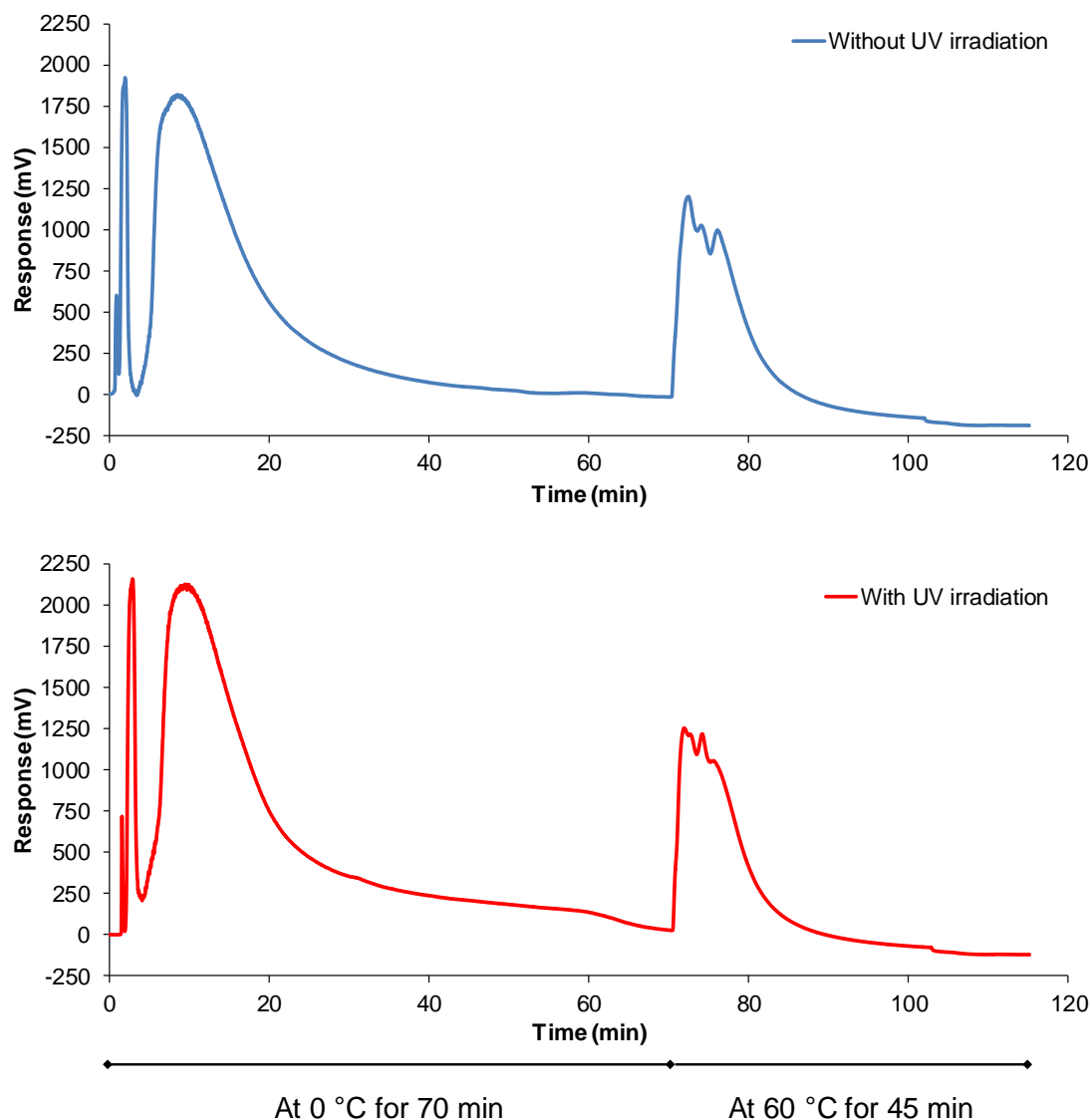
Figure 3–8. Example of comparison between two chromatograms obtained without (blue) or with (red) UV irradiation using polymeric resin as affinity media. The first 70 min of the elution are performed by keeping the column in an ice bath at 0 °C, while for the following 45 min the column is placed in a water bath at 60 °C. Mobile phase: ACN; flow rate: 0.25 mL/min; UV detection at 220 nm. The areas of the peaks after heating are nearly identical.

For this reason, the affinity media was switched from ground and sieved polymeric resin to glass beads derivatised with the template on their surface, with the hypothesis that i) the more regular shape of this material should improve the synthetic and separation conditions of the MIP NPs, and ii) glass

beads should allow better penetration and reflection of the UV light, thus facilitating the polymerisation process.

In the first instance, melamine-derivatised hollow glass beads with 9-13 µm in diameter were used, packed within the same glass column and connected to an Agilent 1100 Series HPLC system. The more regular shape of the stationary phase allowed the flow rate to increase up to 0.5 mL/min, hence the flow properties were partially improved. In addition different elution conditions were tested for their capacity to successfully separate non-polymerised material and the low-affinity fraction of MIP NPs from the high-affinity product. These conditions were: three different elution temperatures (0 °C, 25 °C and 60 °C) and the addition of 10 mM HCOOH to the mobile phase after the first low-temperature elution step. Nevertheless, the chromatograms obtained without or with irradiation did not show significant differences (Figure 3–9).

Figure 3–9. Example of comparison between two chromatograms obtained without (blue) or with (red) UV irradiation using 9-13 µm melamine-derivatised glass beads as affinity media. The first 120 min of the elution are performed by keeping the column in an ice bath at 0 °C, using ACN as mobile phase. The following 73 min of the elution are performed at 25 °C, using ACN + HCOOH (10 mM) as mobile phase, while the last 83 min are performed using the same solvent but putting the column in a water bath at 60 °C. Flow rate: 0.5 mL/min; UV detection at 220 nm. The areas of the peaks after heating are nearly identical.

Surface area and template exposure were then sacrificed in favour of better flow properties by using larger but more uniform non-porous melamine-

derivatised glass beads (75 µm in diameter), coupled with the use of a "long" glass column (4 mm internal diameter, 150 mm length) (Figure 3–10).
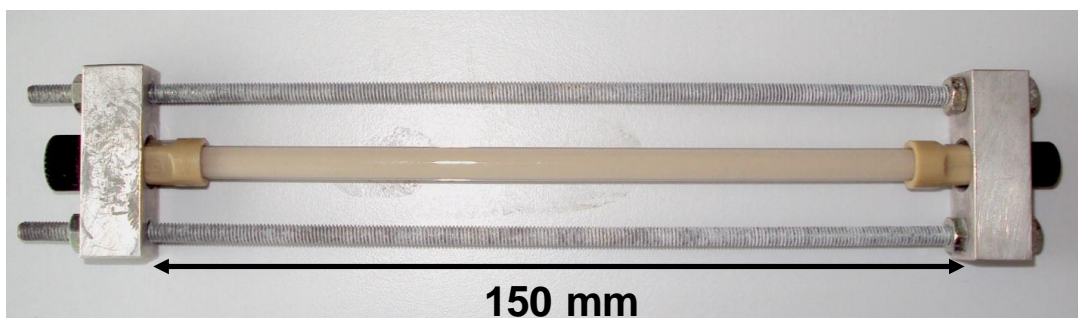
Figure 3–10. "Long" glass column (4 mm internal diameter, 150 mm length) chosen for the experimental setup, packed with 75 µm melamine-derivatised glass beads as affinity media. The column is assembled through tailor-made fitters (green plastic parts) and mounted on a custom-made aluminium frame.

After packing, the column was connected to an Agilent 1100 Series HPLC system. With this material, flow rate could be increased up to 1 mL/min. The elution was performed for 90 min with ACN while the column was kept in an ice bath at 0 °C. Elution continued then for 45 min with HCOOH 10 mM in ACN at 25 °C, and eventually for 35 min with the same solvent but heating the column in a water bath to 60 °C. The results gained from this experimental setup demonstrated a difference between the chromatograms performed in the presence or in the absence of polymerisation due to UV irradiation (Figure 3–11).
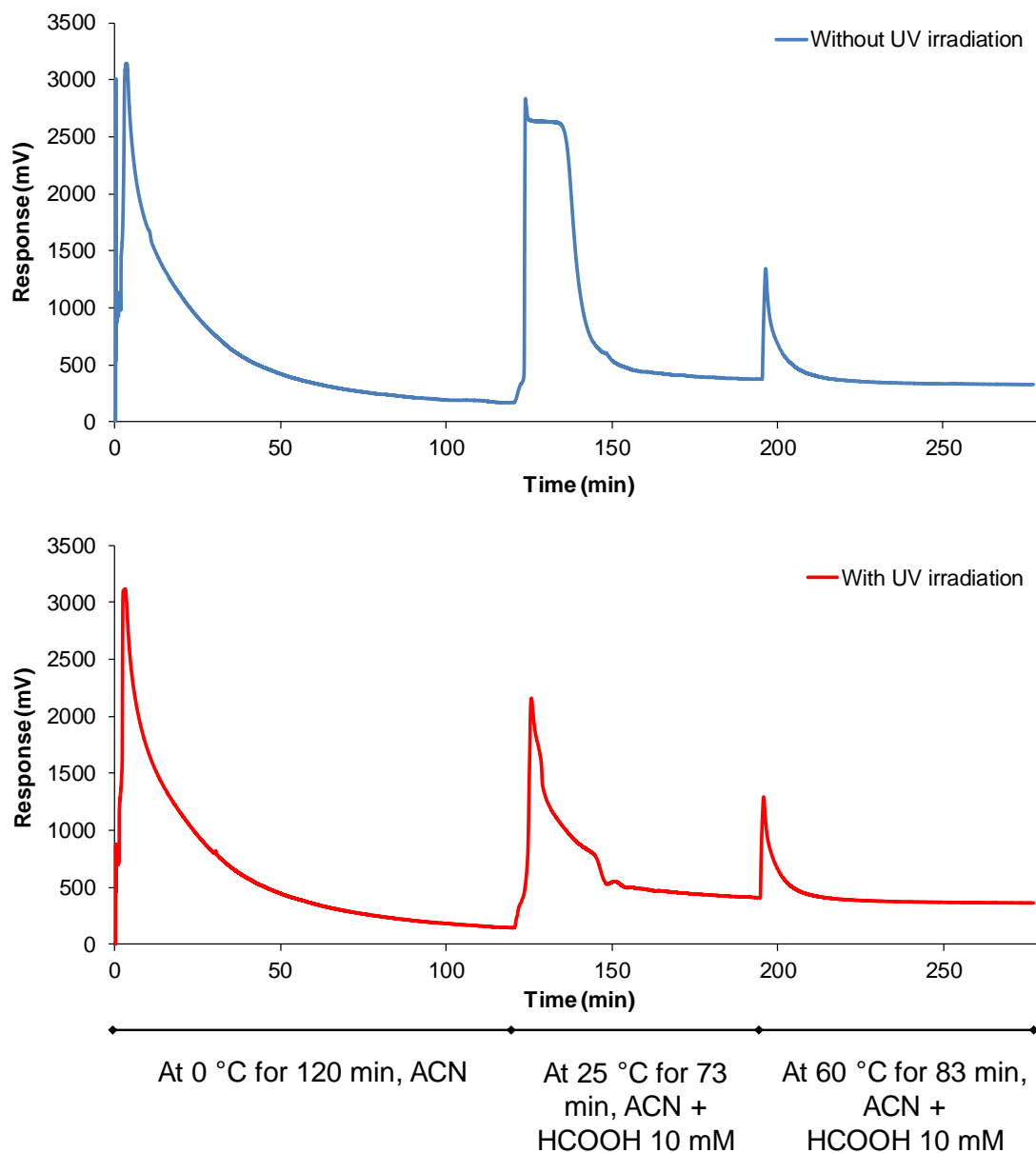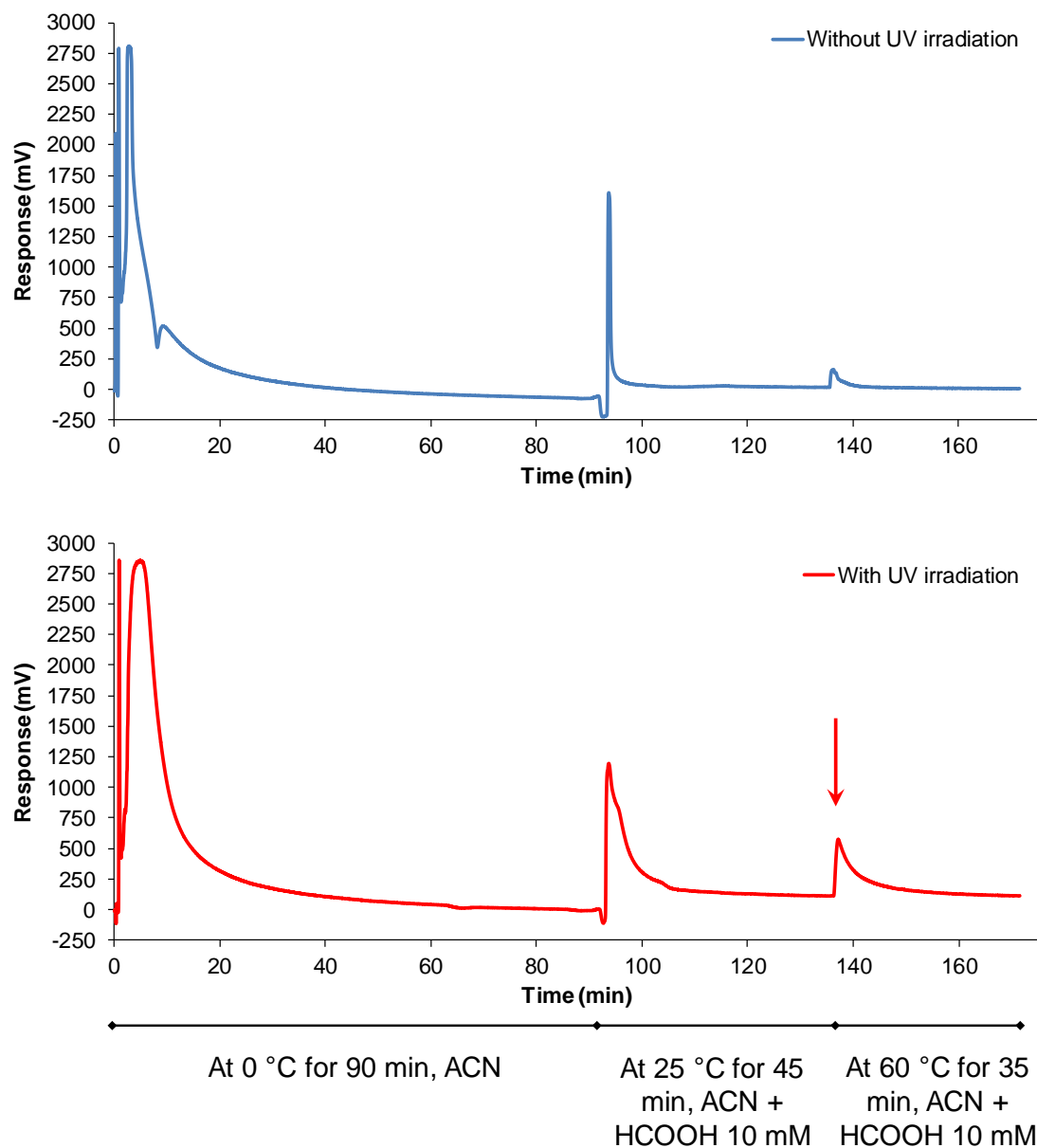
Figure 3–11. Example of comparison between two chromatograms obtained without (blue) or with (red) UV irradiation using 75 μm derivatised glass beads as affinity media. The first 90 min of the elution are performed by keeping the column in an ice bath at 0 °C, using ACN as mobile phase. The following 45 min of the elution are performed at 25 °C, using ACN + HCOOH (10 mM) as mobile phase, while the last 35 min are performed using the same solvent but putting the column in a water bath at 60 °C. Flow rate: 1 mL/min; UV detection at 220 nm. The areas of the peaks after heating (90 min and 135 min) are considerably different; the ratio between the area of the ones with UV irradiation and the ones without are about 4:1 and 8:1, respectively for the peaks at 90 and 135 min.

In particular, the peak of the chromatogram after polymerisation, during the heating step at 60 °C (Figure 3–11, red arrow), exhibited an area of about 160000 mV*s, about 8-fold higher than the corresponding peak of the chromatogram performed without polymerisation (20-25000 mV*s). This configuration (Figure 3–12) and these elution conditions were then selected to perform the subsequent experiments.
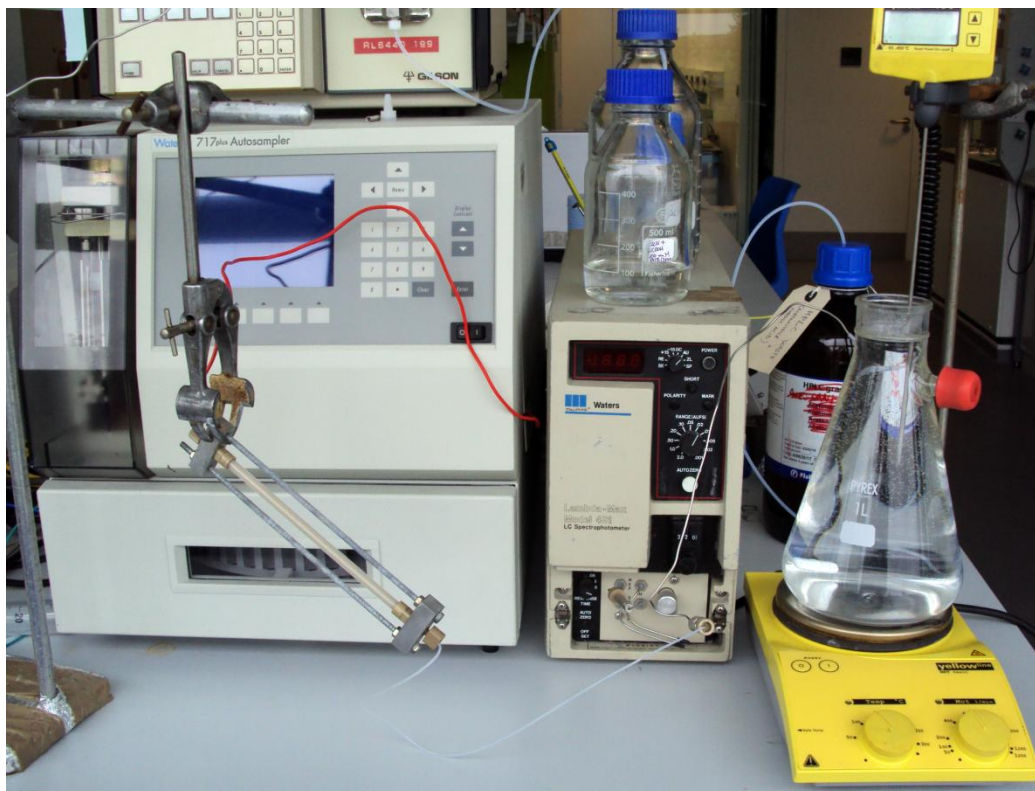
Figure 3–12. "Long" glass column in its aluminium frame connected to the HPLC system through PTFE tubes. During the heating phase of the elution process, the column is vertically put in the water bath at 60 °C (Erlenmeyer's flask, on the right).

3.2.3 Effect of UV irradiation time and composition of the polymerisation mixture on the synthesis of MIP NPs

After having established an appropriate experimental setup and elution conditions promising for obtaining a polymeric material on solid phase, different compositions of the polymerisation mixture and synthetic conditions (see Table 2-1) were tested to assess the effect of UV irradiation time, amount of CTA,

amount of iniferter and the monomer concentration on the synthetic process performed using this system. The aim of these feasibility experiments was to establish the boundaries for possible changes of the operational parameters for further studies. The area of the chromatographic peak after the heating step at 60 °C has been chosen as the defining parameter to assess the outcome of the modification of these different conditions, as this can be related to the yield of the high-affinity MIP NPs.

In all the conditions tested, when no irradiation was applied, the area of the peak after heating varied between 20000 and 30000 mV*s but, after evaporation of the solvent from the collected fraction, no dry residue was found. A possible explanation is that these peaks were mainly due to the presence of HCOOH (contained in the mobile phase) which was released from the immobilised melamine following the increase of temperature. This hypothesis was subsequently confirmed using DLS on the fractions collected after the elution without irradiation, which did not show the presence of any particles.

Initially two different irradiation times (1 and 2 min) were cross-tested with three different amounts of iniferter (0.044, 0.087 and 0.131 g) and four different amounts of CTA (0, 0.01, 0.02 and 0.04 g), to assess their effect on the outcome of the process. These correspond to the polymerisation conditions listed in Table 2-1 (a to m). In all these experiments the monomer concentration was kept constant at 70% w/v. The outcomes of these experiments are plotted in Figure 3–13, which correspond to 1 min (A) or 2 min (B) of UV irradiation, respectively.
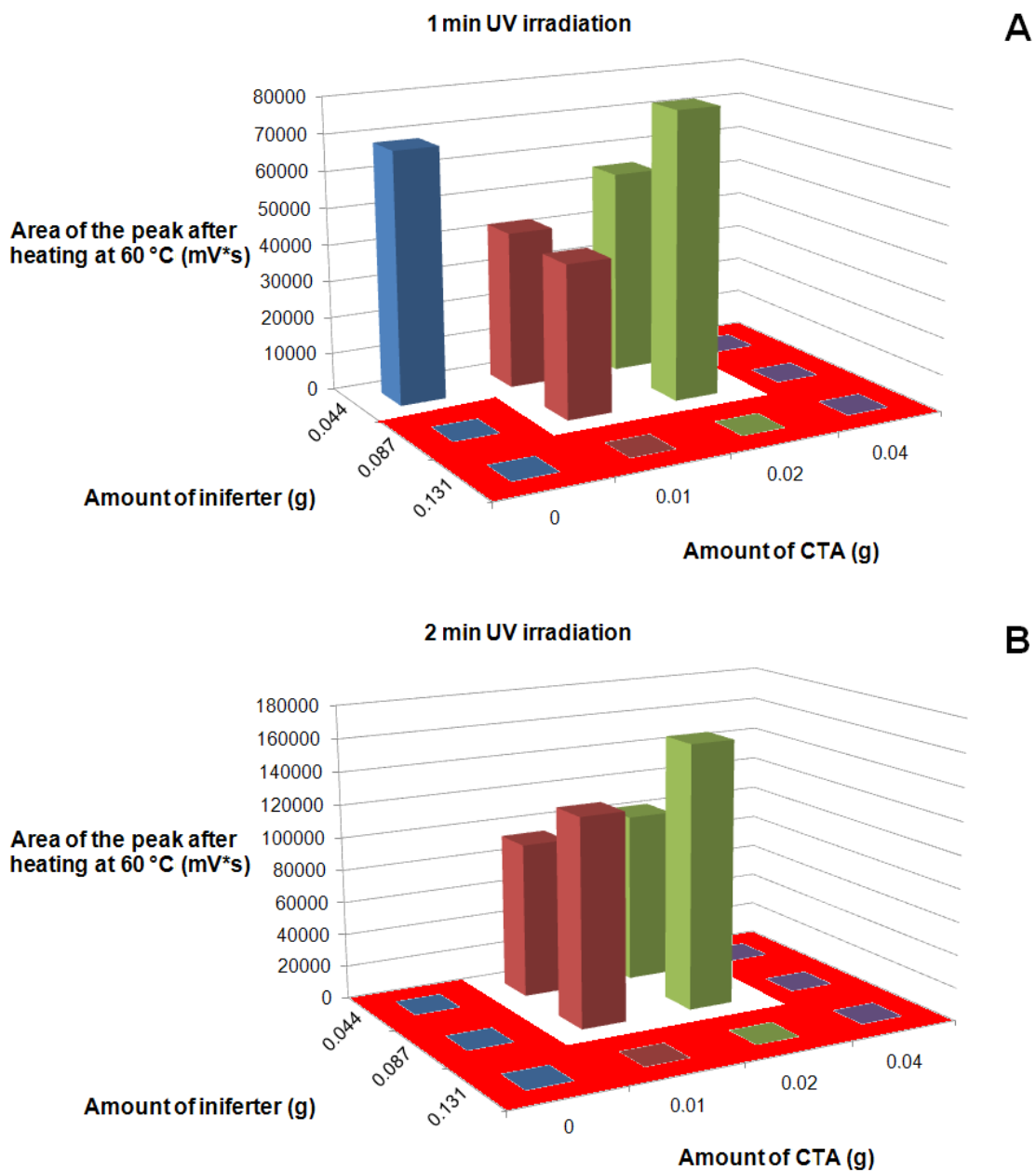
Figure 3–13. Dependence of the yield of the product on UV irradiation time (1 min in graph A and 2 min in graph B), amount of CTA and amount of iniferter. The bars at zero correspond to the boundaries of the system (scarlet red zone), i.e. experiments in which a monolith was obtained inside the column during polymerisation.

The shorter irradiation time should theoretically result in a reduced polymerisation and thus in a reduced yield of MIP NPs. This was demonstrated

to be the case, since most of the area values after 1 min of UV irradiation are much lower than the ones obtained after 2 min of UV irradiation (Figure 3–13).

As expected, increasing the concentration of iniferter generally resulted in an increase of the peak area (Figure 3–13). Even with the lowest irradiation time tested (1 min), however, the high concentration of initiator (0.131 g) caused the creation of a white monolith inside the column (Figure 3–14 and Figure 3–15) rather than MIP NPs.
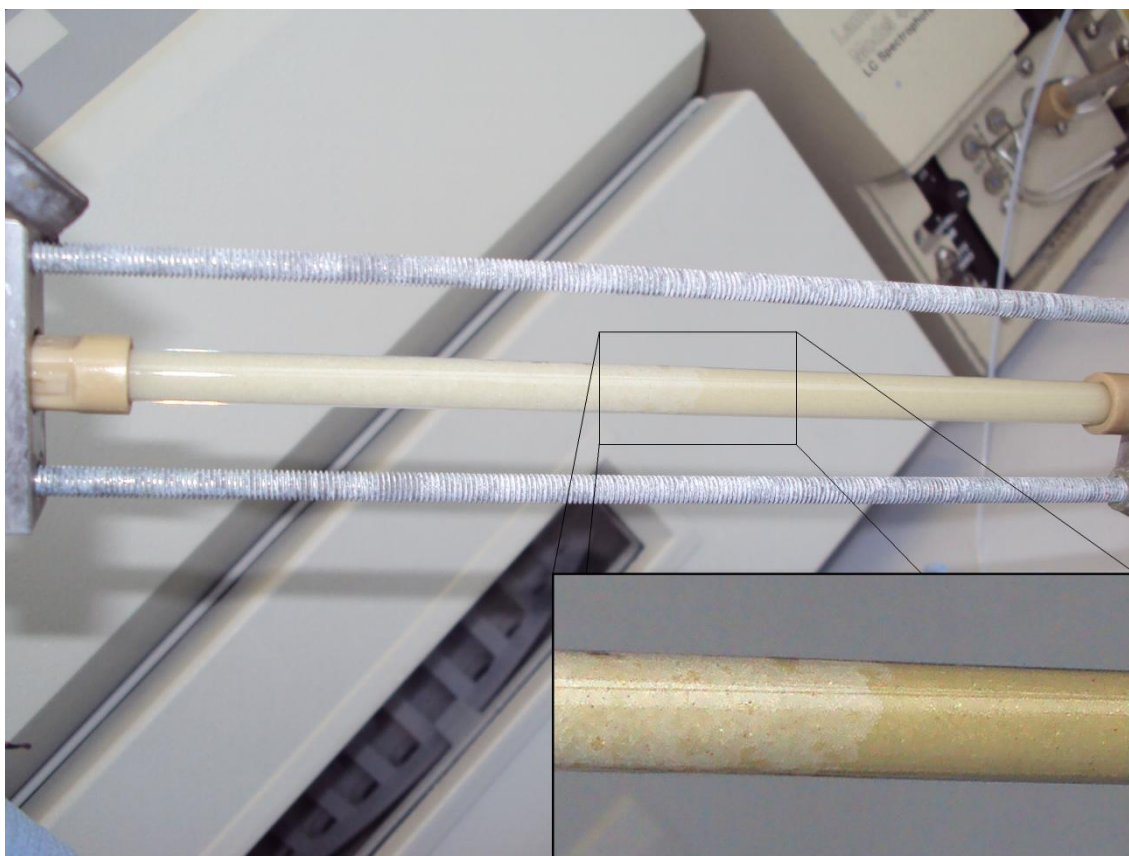
Figure 3–14. Visual assessment of the presence of a white monolith inside the packed glass column. The inset is a magnified view of the column in correspondence of the end of the monolithic layer.
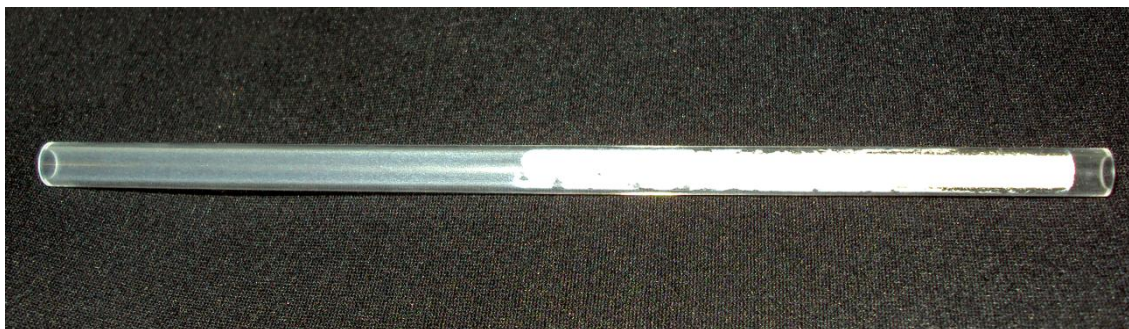
Figure 3–15. Presence of the white polymeric monolith on the inner wall of the glass column after unpacking.

The first time this occurred, the column required unpacking and cleaning. From the results obtained, it became evident that the CTA is required to obtain a suitable control over the polymerisation behaviour within the column (Figure 3–13). The polymerisation performed for 1 min without CTA and 0.044 g of iniferter gave an area almost twice as high as the one obtained in the same conditions but with the addition of 0.01 g of CTA (Figure 3–13A). Increasing the irradiation time to 2 min resulted again in the creation of the monolith inside the column. Results also show, however, that a high concentration of CTA (0.04 g) produces bulk material inside the column (Figure 3–13A). This may be explained by the fact that this tetrathiol at high concentrations may increase the polymerisation rate (Cramer *et al.*, 2003; Hoyle *et al.*, 2004). Moreover, the presence of four thiol groups could potentially result in cross-linking of the synthesised particles. This means that the type and the amount of CTA need to be properly managed in order to obtain high-quality MIP NPs.

The best polymerisation conditions found include the use of 0.087 g iniferter and 0.02 g CTA (Figure 3–13B). An increase in the irradiation time to 3 min (Table 2-1, n) then was attempted to assess if the yield could be further increased. In this case a polymer monolith was also produced inside the column.

These conditions, with 2 min of irradiation, were then kept constant and the effect of different monomer concentrations was evaluated (Table 2-1, k, o, p, q). The results are plotted in Figure 3–16.
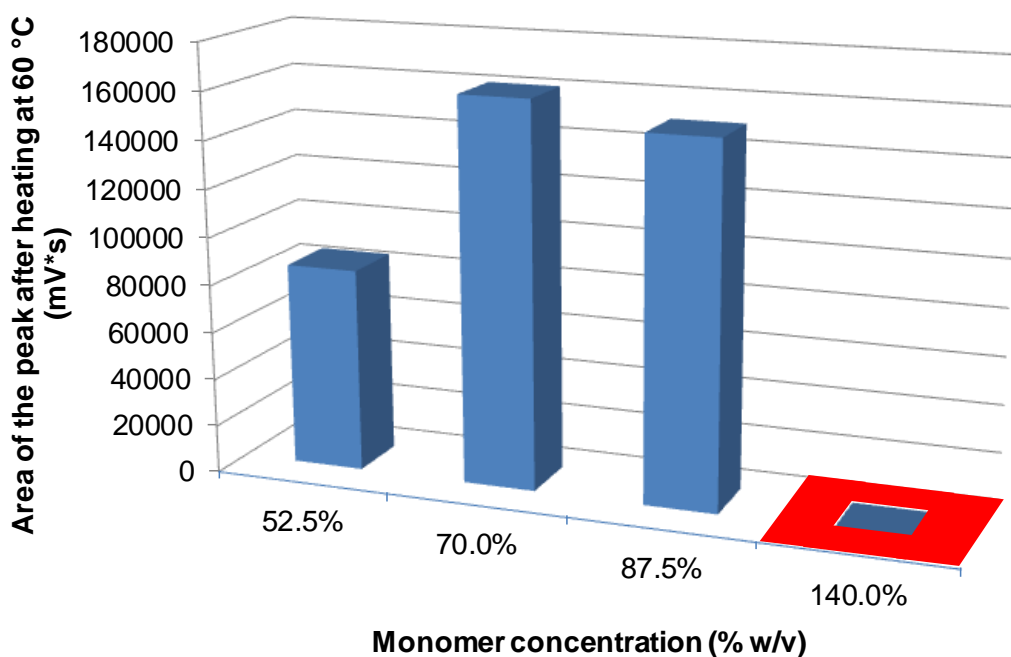
Figure 3–16. Dependence of the yield of the product on monomer concentration (% w/v of the monomer-solvent mixture) (UV irradiation time: 2 min; 0.087 g iniferter; 0.02 g CTA). At 140.0% monomer concentration the reaction could not be performed due to high column pressure.

Reduction of the monomer concentration from 70.0% to 52.5% w/v resulted in a considerable reduction of the peak area and a low yield of high-affinity product. It could be speculated that these conditions are not ideal for the formation of strong complexes between the monomers and template. A yield of NPs at 140.0% w/v concentration of monomers could not be assessed due to high back-pressure in the system. In this case the high pressure was not a result of bulk polymerisation in the column but most likely caused by the high viscosity of the polymerisation mixture.

According to the results, the optimal polymerisation conditions tested required 0.087 g initiator, 0.02 g CTA, a concentration of monomers equal to 70.0% w/w and 2 min of UV irradiation (Table 2-1, k). More subtle adjustments around the boundaries of these conditions might lead to further improvements in the yield and quality of the NPs.

MIP NPs produced using these optimum conditions exhibited a good size distribution (Figure 3–17) and spherical morphology (Figure 3–18).
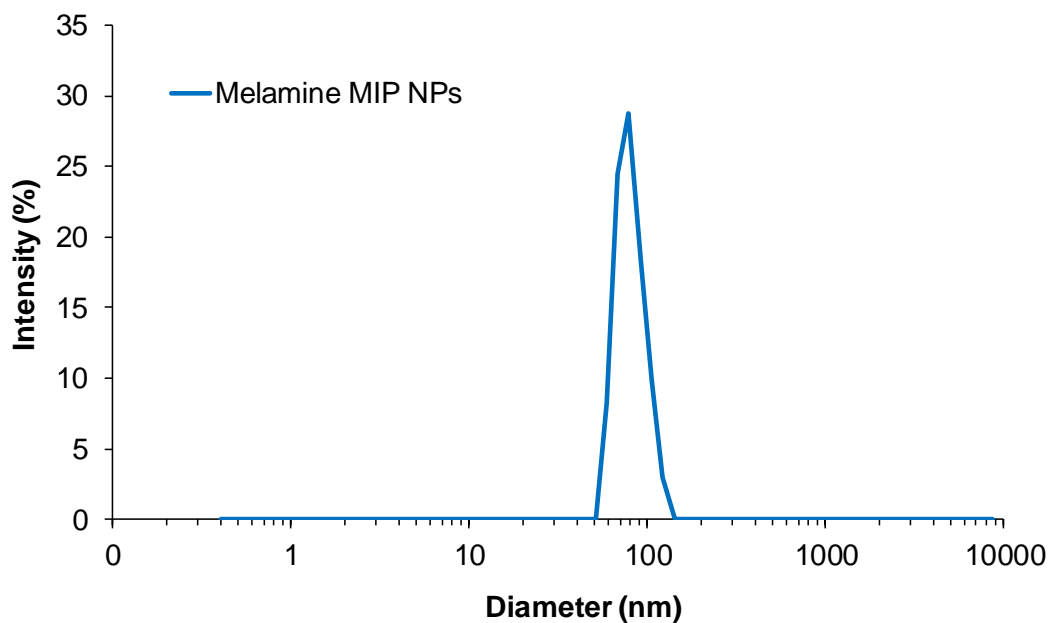
Figure 3–17. DLS size distribution of melamine MIP NPs produced in optimum conditions.
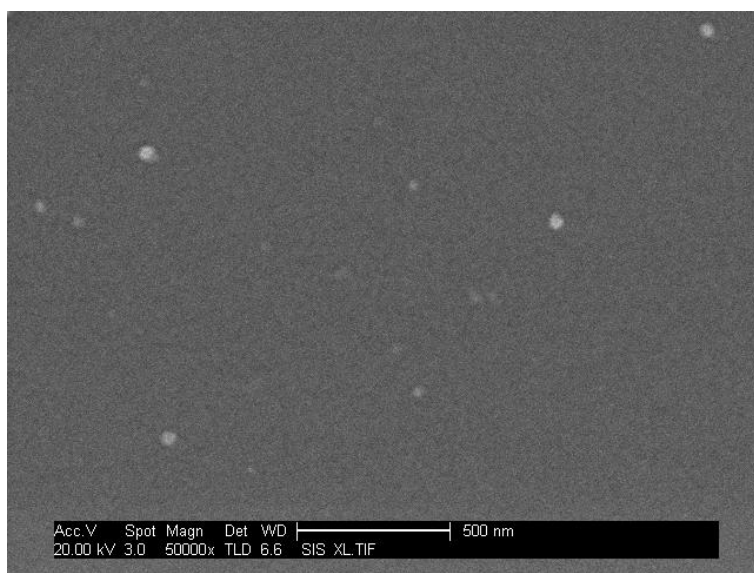
Figure 3–18. SEM image of the melamine MIP NPs produced in optimum conditions. The scale bar is 500 nm.

The yield of the NPs produced in these conditions was equal to 0.22% w/w of the initial mass of monomers. This was evaluated by weighing the dry residue of the evaporated fraction eluted during the heating step. This value corresponded to the MIP NPs fraction with the highest affinity.

Considering that the results of these feasibility experiments were quite encouraging, an automated photoreactor was designed and assembled in accordance to our specification by HEL, Ltd. The details of the design of the photoreactor prototype and the subsequent experiments conducted with it are discussed in the following sections.

3.3 Automatic solid-phase photoreactor: prototype design

A new fully automated synthesiser which uses the immobilised solid-phase template approach was then developed. The following considerations were taken into account during the design phase:

•   MIP synthesis should be performed at a moderately low temperature (−30 °C to +10 °C) in an appropriate organic solvent to favour complex formation between monomers and template (Allender *et al.*, 1997; Piletsky *et al.*, 2002).

•   The requirement for using low temperatures is best met by initiating the polymerisation reaction through photochemical means, since it can be performed at or below room temperature (O'Shannessy *et al.*, 1989; Mijangos *et al.*, 2006).

•   The synthesis of MIP NPs should be performed under controlled conditions to prevent polymer precipitation (Bompart and Haupt, 2009; Gonzato *et al.*, 2011).

•   The template should be immobilised to prevent contamination of the synthesised particles (Lorenzo *et al.*, 2011).

•   Ideally the template should be capable of being recycled to reduce manufacturing costs.

•   A mechanism for the separation of high-affinity MIP NPs from low-affinity materials and unreacted monomers should be integrated into the reactor design (Guerreiro *et al.*, 2009; Hoshino *et al.*, 2010a).

A schematic of the new reactor design is presented in Figure 3–19 and a picture of the reactor is in Figure 3–20. The experimental setup for the automated synthesis of MIP NPs was developed with the aim of controlling the column temperature, delivery of the monomer mixture and washing solvents, UV-irradiation time and yield of the synthesised material. The system comprises a computer-controlled instrument consisting of a custom-made fluid-jacketed glass reactor (which will accommodate the solid phase with the immobilised

template) with internal heating element, connected to pumps which deliver the reaction mixture, wash and elution solvents. The column is housed within a light-tight box fitted with a UV source that can be activated under software control for a predetermined time to perform the polymerisation. The fluid-handling system also employs a multi-way valve post-column to direct the high-affinity MIP NPs to a collection vessel or wash solutions to waste.

The control software is very intuitive and allows for a specific control over the single components of the reactor in real time, as well as programming, saving and executing reaction protocols automatically with the minimum operator intervention (Figure 3–21).
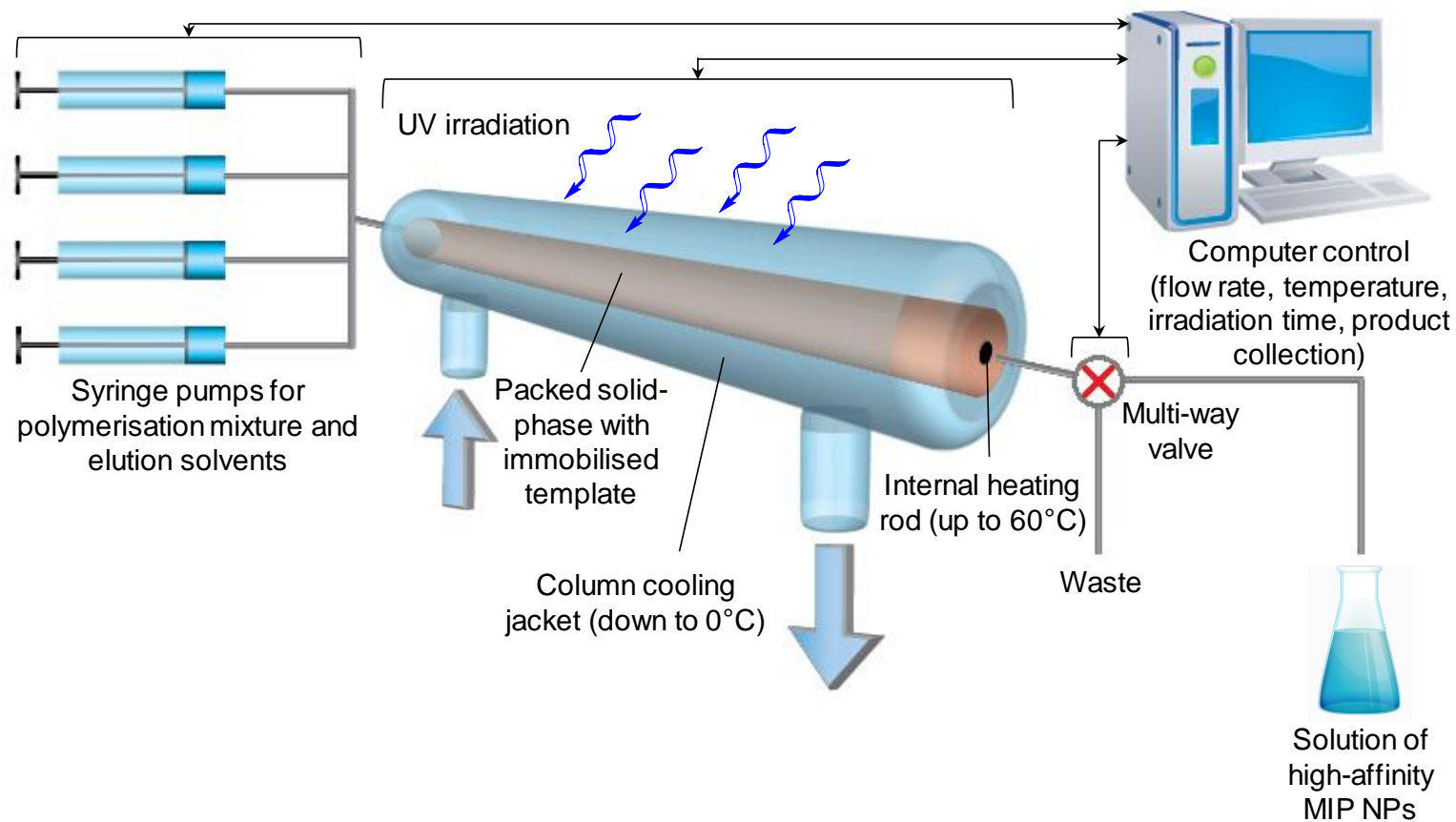
Figure 3–19. Schematic diagram showing the mode of operation of the automated solid-phase MIP NPs photoreactor. Typical operational parameters using melamine as the immobilised target are: operation time: 3 h per cycle; yield of high-affinity fraction: 6.6 ± 0.65 mg per cycle; column capacity: 23.5 g derivatised glass beads (solid phase).

Figure 3–20. Picture of the automated solid-phase MIP NPs photoreactor.
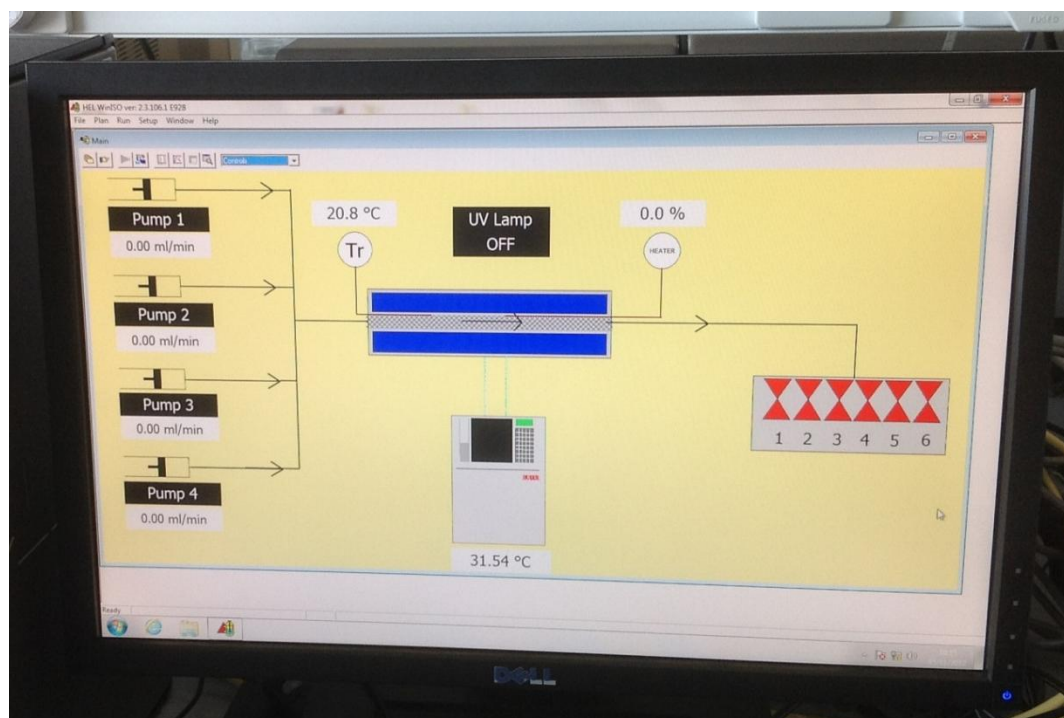
Figure 3–21. Control graphic-interface of the HEL's proprietary software WinISO for the automatic solid-phase MIP NPs photoreactor.

A schematic of a generic automated solid-phase synthesis and purification of MIP NPs is represented in Figure 3–22. The procedure by which all experimental work was undertaken using this automated reactor is as described below. The first step involved loading of the monomer/initiator mixture, dissolved in a suitable solvent, onto the temperature controlled column reactor containing the template already immobilised onto a solid support (Figure 3–22, 1). Once the temperature has reached a pre-determined set point, thus favouring the formation of the pre-polymerisation complexes between immobilised template and functional monomer (Figure 3–22, 2), polymerisation was initiated by UV-irradiation of the reactor for the required reaction time (Figure 3–22, 3). After polymerisation was arrested, the column was washed with fresh solvent at a low temperature. At this stage unreacted monomers and other low molecular weight materials were eluted along with those polymer NPs with the lowest affinity (Figure 3–22, 4). The desired high-affinity MIP NPs remain bound to the immobilised template phase. A second washing step was subsequently performed at a slightly elevated column temperature, with the possibility of utilising an auxiliary additive, such as HCOOH, to remove low-affinity MIP NPs from the reactor (Figure 3–22, 5). Finally, the temperature of the column was increased once more and, with the inclusion of additional reagents such as HCOOH, high-affinity MIP NPs were collected (Figure 3–22, 6). Raising the temperature increased the rate of exchange between the particles and the template phase, which assists in eluting the particles, as well as potentially reducing the strength of the association.

Polymerisation mixture in ACN

Solid-phase with immobilised template

Formation of pre-polymerisation complexes

159
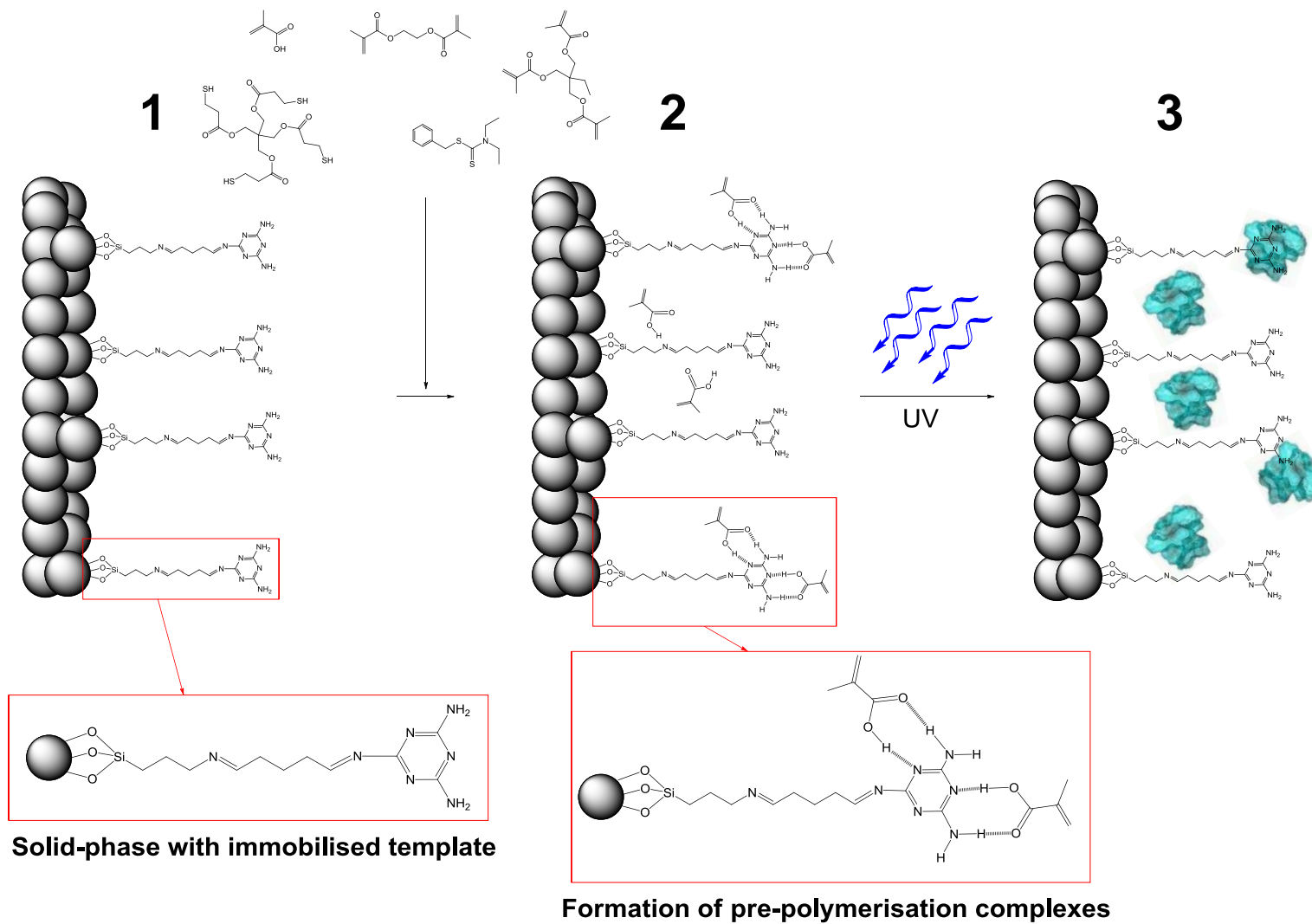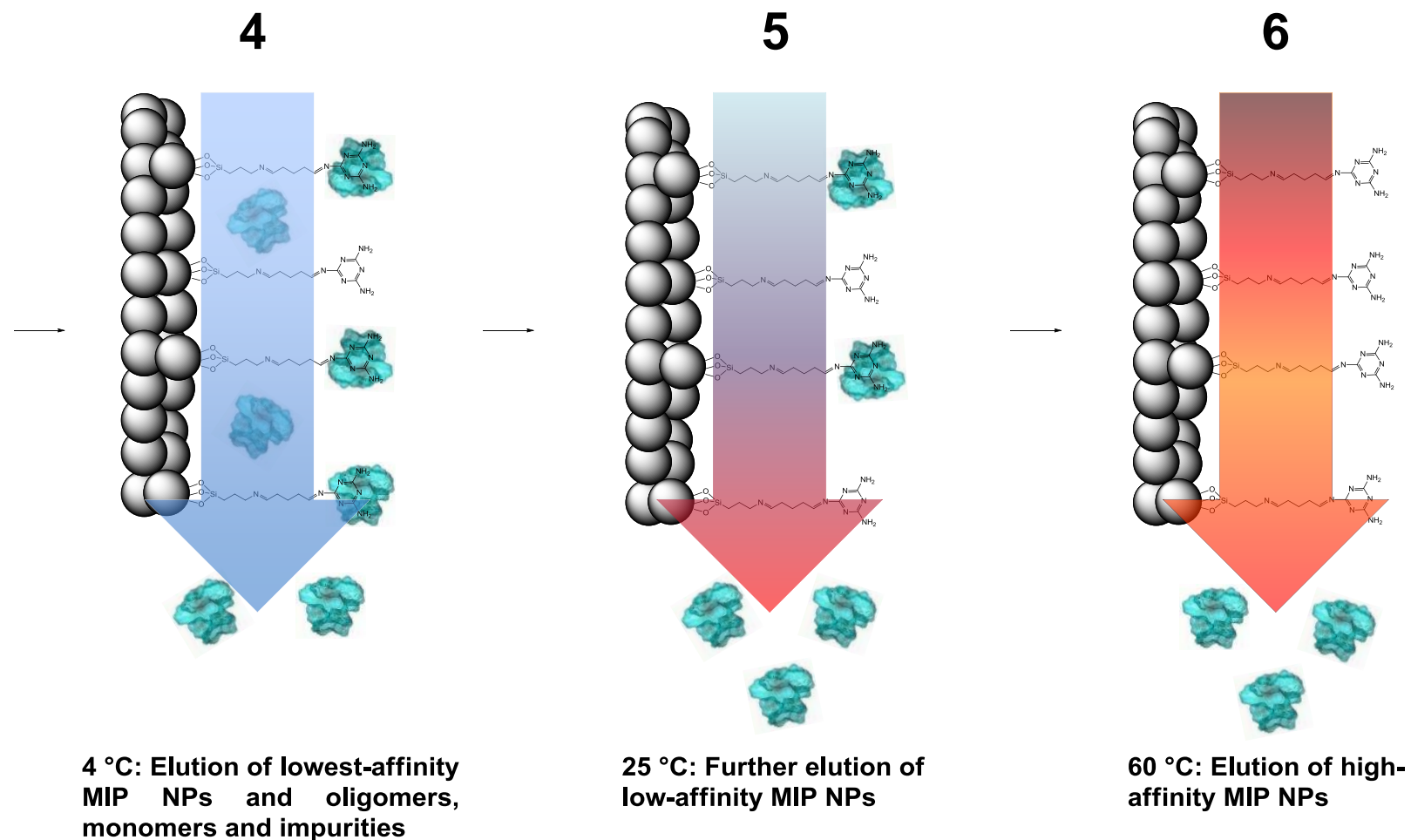
Figure 3–22. Schematic representation of the solid-phase synthesis of MIP NPs in the automatic photoreactor. A detailed description is reported in the main text.

The benefits of this approach included: i) uniform binding properties, resulting from affinity-based separation on column (Guerreiro *et al.*, 2009); ii) eliminating contamination of the product with template; iii) possibility of template reuse; iv) ease of standardisation; v) the final product is obtained in a pure form obviating the need for lengthy post-synthesis purification steps; vi) imprint sites are only formed on one surface of the particle.

3.4 Optimisation of the system: automatic solid-phase synthesis and characterisation of MIP NPs imprinted for melamine

For the same reasons previously discussed (see *3.2.1 - General solid-phase synthesis of melamine MIP NPs*) melamine was chosen as the model template for demonstration of the solid-phase synthesis of MIP NPs with this newly designed automatic system.

Optimisation of the reaction conditions was performed by varying the irradiation time, followed by measuring the resulting yield and properties of the synthesised MIP NPs. As expected, there was a direct correlation between irradiation time and the yield and diameter of the MIP NPs formed (Figure 3–23). This trend continued up to a point when the insoluble polymer was precipitated in the column reactor. The significant decrease in power of the UV lamps of the automated instrument can explain the variation between those results gained in previous sections (see *3.2.3 - Effect of UV irradiation time and composition of the polymerisation mixture on the synthesis of MIP NPs*) and those gained within this section of work with respect to the length of irradiation time before precipitation occurs within the reactor.
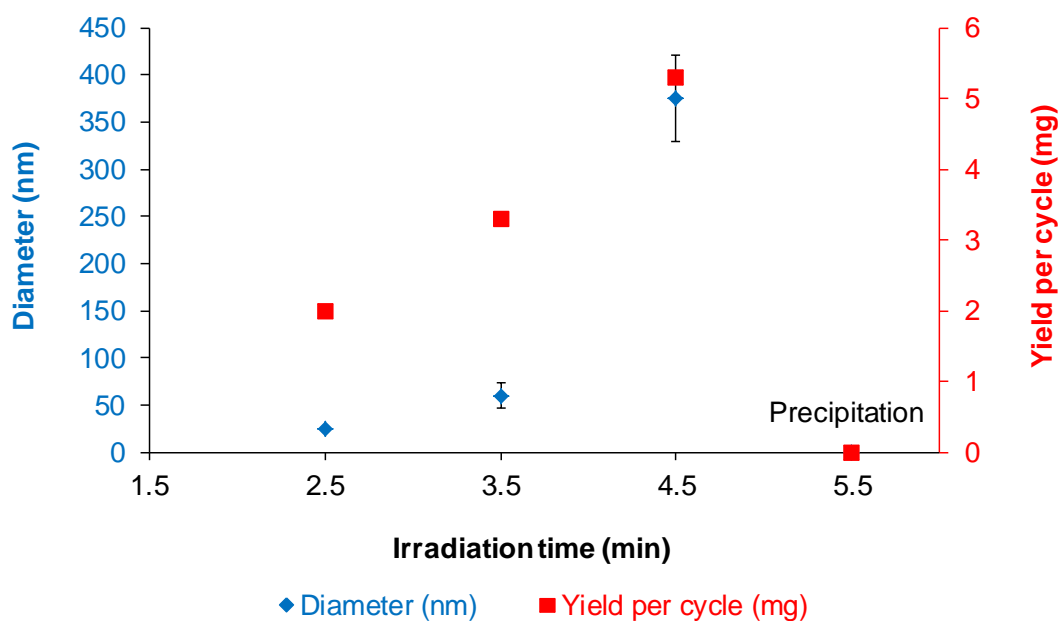
Figure 3–23. Influence of the irradiation time on the yield and size of synthesised MIP NPs. Error bars represent SD ($n \geq 7$).

The binding properties (affinity and selectivity) of MIP NPs were assessed by SPR experiments (BIAcore) using SPR sensor chips modified with the template melamine or its structural analogue, DA (Ivanova-Mitseva *et al.*, 2012). This immobilisation was carried out as illustrated in Figure 3–24.

163
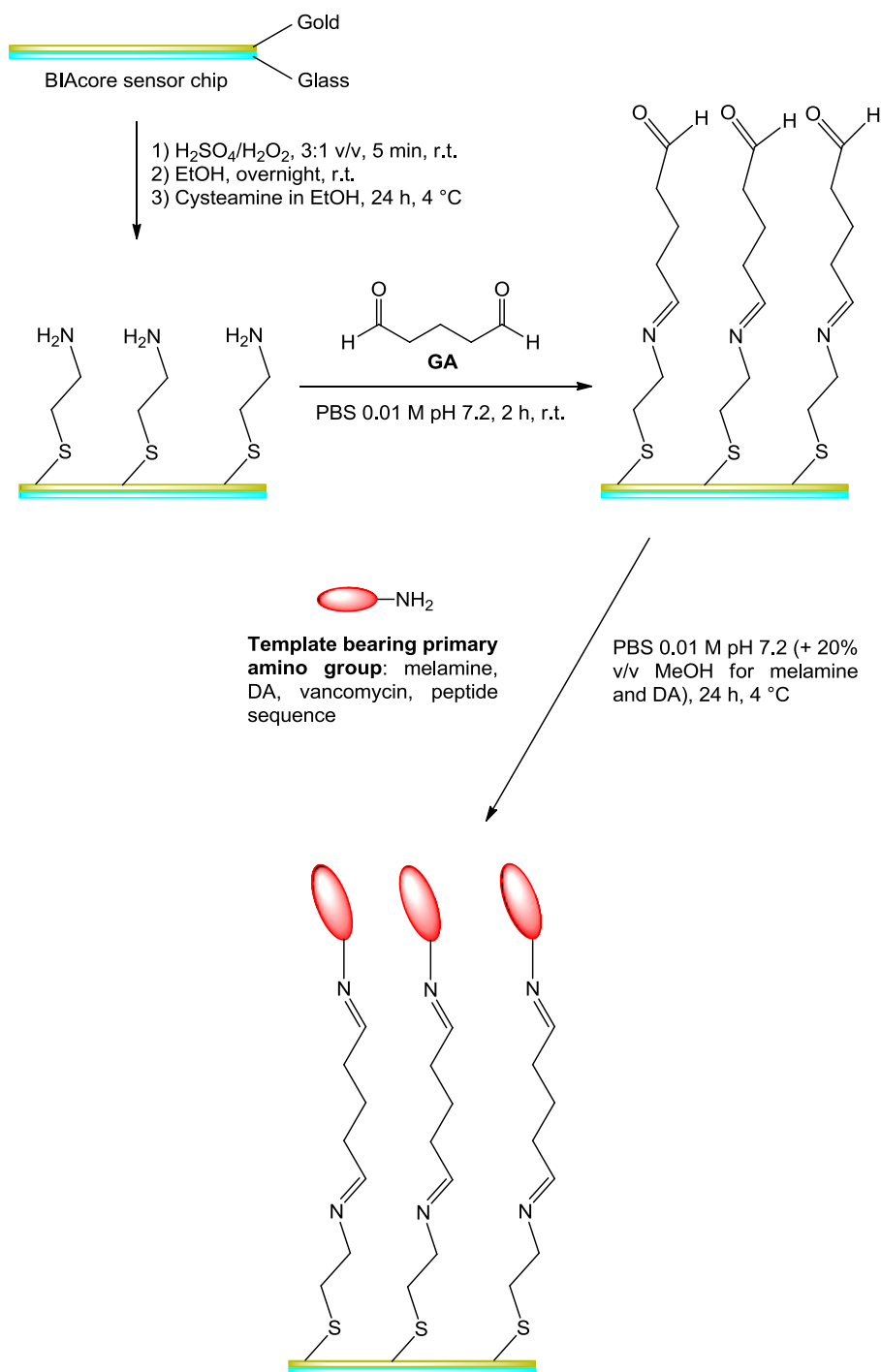
Figure 3–24. Synthetic protocol for the immobilisation of template on the gold surface of BIAcore sensor chips for use in SPR analysis of MIP NPs.

First a self-assembled monolayer (SAM) of cysteamine was created exploiting the capacity of thiols to form SAMs onto gold surfaces (Jiang *et al.*, 2003). Following this first step, the immobilisation procedure involved a GA-based amino-coupling similar to that used during the immobilisation procedure for the

glass beads. The validity of the immobilisation procedure onto the gold SPR sensor chips was confirmed by static contact angle measurements of the surface (Table 3-2).

Table 3-2. Static water contact angle measurements for surface-modified BIAcore SPR sensor chips ($n = 3$).

Surface	Contact angle (degrees, ± SD)
Bare gold	75.85 ± 0.65
Cysteamine	55.41 ± 1.38
Melamine	80.96 ± 0.34
DA	75.41 ± 1.34

The highest affinity was achieved with particles exhibiting 60 nm in diameter (80 nm when measured in ACN) (Figure 3–25, Figure 3–26). The inferior performance of small particles may be due to insufficient rigidity caused by low levels of cross-linking, or because such small MIP NPs lack the bulk required for maintaining the structure of specific binding sites. Particles ≥ 240 nm in diameter may be prevented from forming effective interactions with the immobilised template due to steric effects, resulting in a reduction of their measured affinity. This is in agreement with the results obtained by Piletska and Piletsky (2010), in which the high-affinity interaction between biotin and streptavidin was found to be strictly dependent on the size of the two interacting ligands.
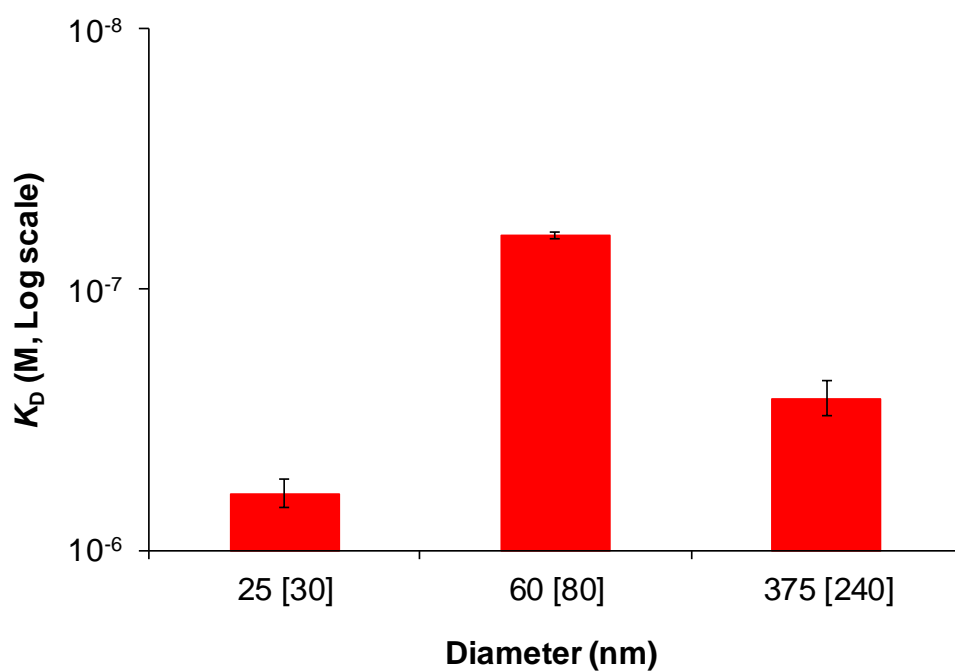
Figure 3–25. Influence of the size of the MIP NPs on their affinity (apparent dissociation constant) as determined by SPR. Dry size, measured by SEM/TEM, and size in ACN (in square brackets) measured by DLS. Error bars represent SD ($n \geq 3$).
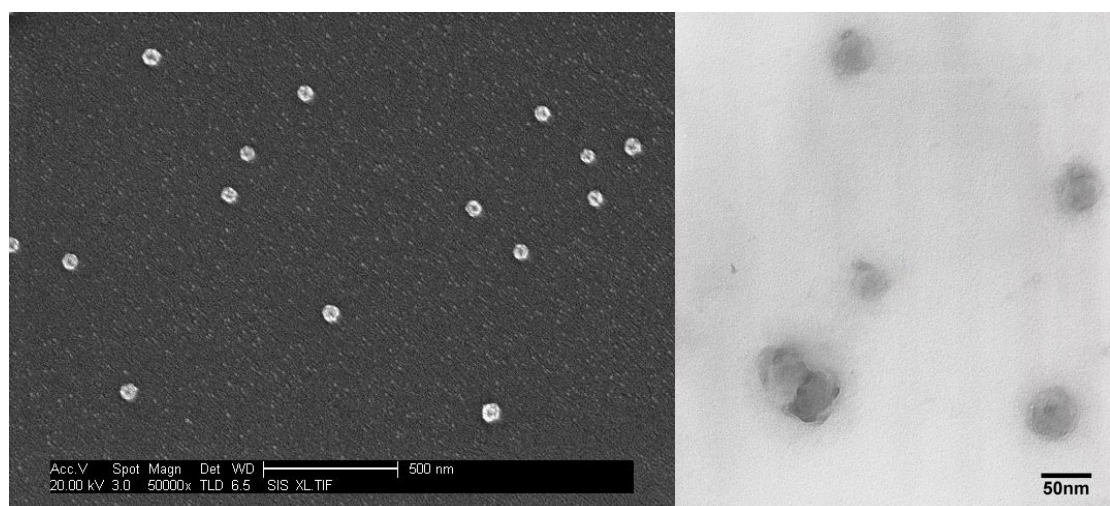
Figure 3–26. SEM image (left, scale bar: 500 nm) and TEM image (right, scale bar: 50 nm) of the 60 nm diameter MIP NPs.

A typical sensorgram of 60 nm MIP NPs is showed in Figure 3–27.
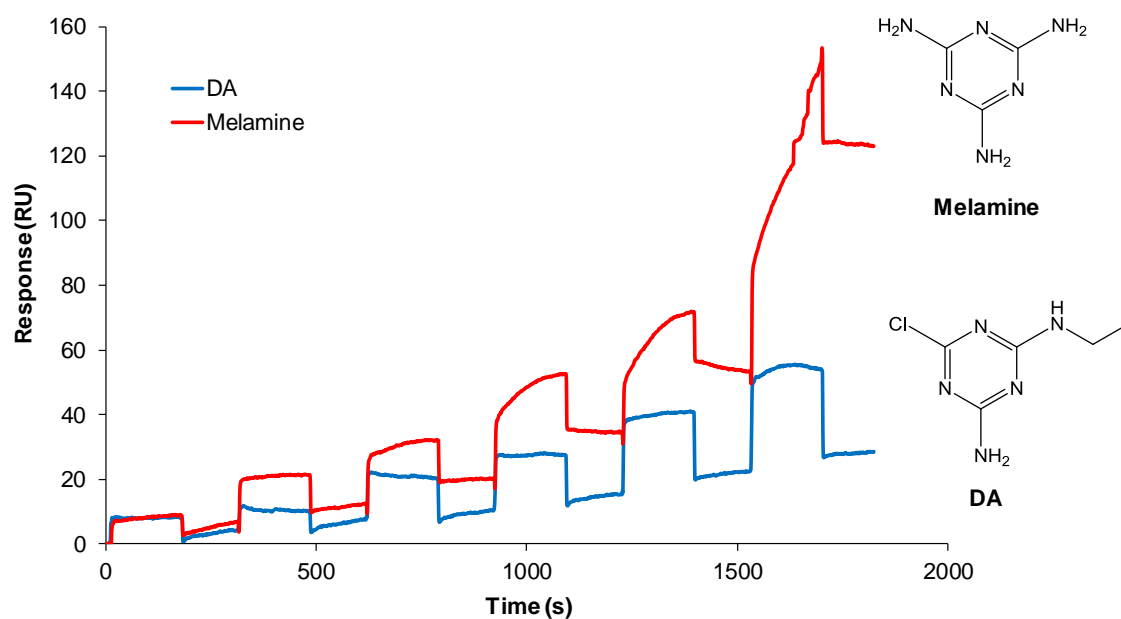
Figure 3–27. SPR sensograms (BIAcore 3000) showing time-dependent binding of 60 nm melamine MIP NPs onto BIAcore sensor chips bearing the specific (melamine) and non-specific (DA) molecules. The solution of melamine MIP NPs at a concentration of 330 nM was sonicated for 30 min and used as stock to prepare 5 further 2-fold dilutions (from 1/2 to 1/32). Injections were made in order of increasing concentration, using PBS buffer 0.01 M pH 7.4 as mobile phase. The sensorgrams show specific binding and target selectivity.

The SPR response of the melamine-imprinted MIP NPs to DA was similar to the response for the solvent alone (less than 6 RU for all concentrations of NPs) and so did not allow for the calculation of the dissociation constant. Conversely a preferential binding to the specific surface was clearly demonstrated, hence confirming both the selective properties and the affinity of the MIP NPs produced.

It is normal practice in MIP research to prepare a non-imprinted polymer or "blank", prepared under identical conditions as the MIP but in the absence of template as an experimental control. Even in the case of traditional "bulk" MIPs this is not ideal, since changes in surface area and morphology are often evident when the template is excluded, making the comparison with non-imprinted controls a compromise at best (Yoshimatsu *et al.*, 2007; Hoshino *et al.*, 2008; Yoshimatsu *et al.*, 2010). The problem that occurred with the current

167

work was that, without a template, there was no retention of material on the column following the low-temperature elution step; hence, it was not possible to prepare a comparable blank polymer. Separation of non-imprinted particles from the cold fraction was complicated by the presence of a high concentration of monomers and the potential presence of a range of lower-affinity imprinted particles and oligomeric material which made it impractical to attempt.

Optimum conditions for the synthesis of high-performance MIP NPs for melamine were determined as follows: UV irradiation for 3.5 min applied to a polymerisation solution containing 70% monomer mixture (w/v). When the synthesiser was run over six days in automatic mode using these conditions, five batches of MIP NPs per day were produced with an essentially identical yield (20 ± 2 mg per day) and very similar binding properties (K_D = 6.3 × 10^{-8} ± 1.7 × 10^{-9} M), for a total of 30 batches of MIP NPs from a single batch of template-immobilised solid phase. In terms of affinity, these results were comparable to those obtained with monoclonal antibodies produced for haptens similar to melamine (Grant *et al.*, 1999; Kramer, 2002).

The fractions containing high-affinity MIP NPs were analysed for the presence of residual template by LC-MS. The template concentration was below the limit of detection for this method; this confirmed that the recycling of the template immobilised on the solid phase did not result in the detrimental degradation and subsequent leakage of the template from the solid phase into the product.

From the calculation of the density of immobilised template versus the quantity of MIP NPs produced in one cycle it was possible to deduce that approximately 560 melamine molecules were required to generate one high-affinity MIP NP. The yield of MIP NPs was limited by the available surface area of the template phase (since the template is the limiting reagent in the system) but could be further increased by either optimising the morphology of the solid support, using several synthesisers in parallel, or eventually increasing the size of the reactor.

Theoretically the number of binding sites per NP is proportional to the concentration of template used in MIP preparation. Considering that the template species in this approach were present only at the surface of the solid

phase, it follows that the selective binding sites would only be formed in the MIP at the point of contact with the surface. The silanisation of glass surfaces measured by other authors gave probe densities of between 1×10^{12} and 2.6×10^{13} functional units per cm^2 (0.01 – 0.26 sites/nm^3) for (3-mercaptopropyl)trimethoxysilane (Halliwell and Cass, 2001) and GA-modified APTMS (Sheng and Ye, 2009) (as used in this work). Assuming that a similar degree of coverage was achieved in the melamine-modified glass beads, then in theory, it is likely that the MIP NPs with diameter 30-80 nm would contain only 1-5 binding sites per particle, localised in one region of the nanoparticle surface. This number is in agreement with previously obtained data for MIP NPs synthesised in solution (Guerreiro *et al.*, 2009).

In terms of stability, dispersions of MIP NPs in ACN were stable for at least one year when stored at 4 °C in the dark. When stored in PBS, some aggregation and sedimentation was observed; this may be solved, however, by the introduction of a more hydrophilic shell (e.g., HEMA or PEG) on the NPs surface by exploiting the living nature of the polymerisation process.

3.5 A versatile system: automatic solid-phase synthesis of MIP NPs imprinted for vancomycin and a model peptide

MIP NPs were also imprinted with different templates, to demonstrate that the reported approach is generic in nature (suitable for small to medium molecular weight organic molecules and peptides etc.). MIP NPs were therefore prepared for other targets, including vancomycin (Figure 3–28) (M_w = 1449.3 g/mol) and a model peptide (TATTSVLG-NH$_2$, M_w = 747.9 g/mol) using the reported automatic solid-phase photoreactor.
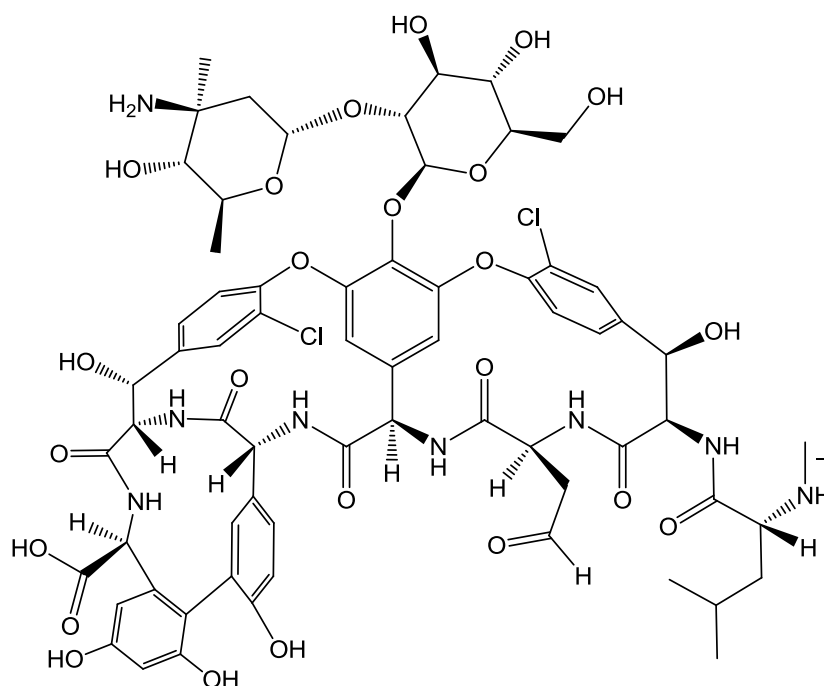
Figure 3–28. Structure of the antibiotic vancomycin.

The first template, vancomycin, is a branched tricyclic glycosylated peptide antibiotic used in the prophylaxis and treatment of infections caused by Gram-positive bacteria. Vancomycin acts by inhibiting proper cell wall synthesis in these bacteria by binding to the D-Ala-D-Ala moieties of the pentapeptides of the peptidoglycan monomers, N-acetylmuramic acid (NAM) and N-acetylglucosamine (NAG). This results in two effects: i) it prevents the synthesis of the long polymers of NAM and NAG that form the backbone strands of the bacterial cell wall, and ii) it prevents the backbone polymers that do manage to form from cross-linking with each other. This weakens the cell wall and

damages the underlying cell membrane, causing its lysis (Small and Chambers, 1990).

The second template is a model peptide sequence (TATTSVLG-NH$_2$). As already stated above, epitope imprinting refers to the imprinting of a small peptide sequence (i.e. an epitope) instead of a whole target protein, and it is a very promising approach in protein imprinting (Ge and Turner, 2008). The aim of these experiments was to prove that MIP NPs could be developed for peptides using the automatic photoreactor.

The polymerisation conditions were identical to those used for the manufacture of MIP NPs for melamine, with the exception of the monomer mixture. The composition of the monomer mixture used to prepare MIPs for vancomycin and for the peptide was based on a published protocol (Hoshino *et al.*, 2008) (Figure 3–29).
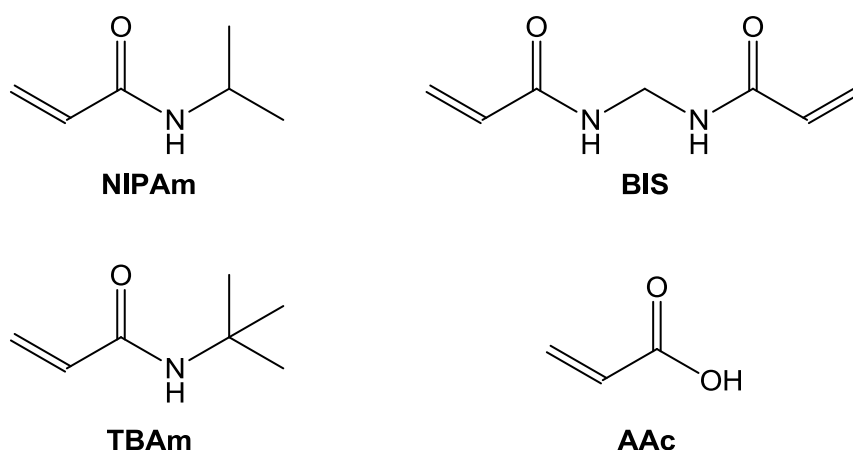
Figure 3–29. Monomers used to prepare MIP NPs for vancomycin and for the peptide sequence.

Although Hoshino's protocol was optimised for imprinting in an aqueous-based solvent, it was modified for use in ACN with good results.

The binding properties of the synthesised MIP NPs were analysed by SPR experiments (BIAcore) using chips with immobilised templates (Figure 3–30, Figure 3–31).
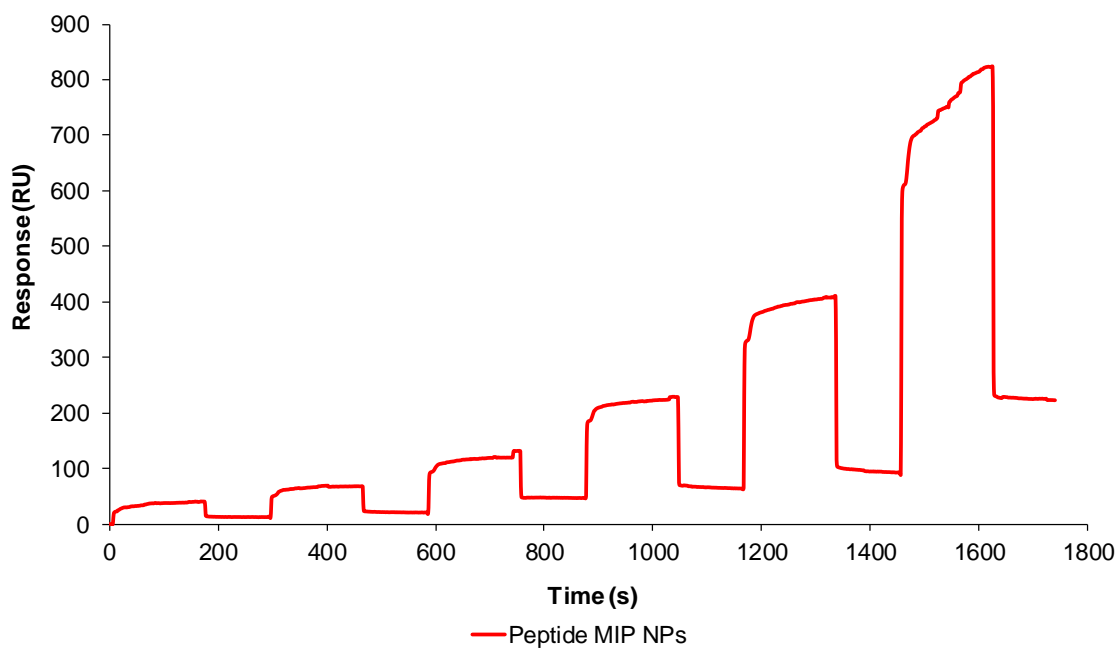
Figure 3–30. SPR sensogram (BIAcore 3000) showing time-dependent binding of peptide MIP NPs onto BIAcore sensor chips bearing the template. The solution of peptide MIP NPs at a concentration of 1094 nM was sonicated for 30 min and used as stock to prepare 5 further 2-fold dilutions (from 1/2 to 1/32). Injections were made in order of increasing concentration, using PBS buffer 0.01 M pH 7.4 as mobile phase. The sensorgram shows affinity for the specific target.
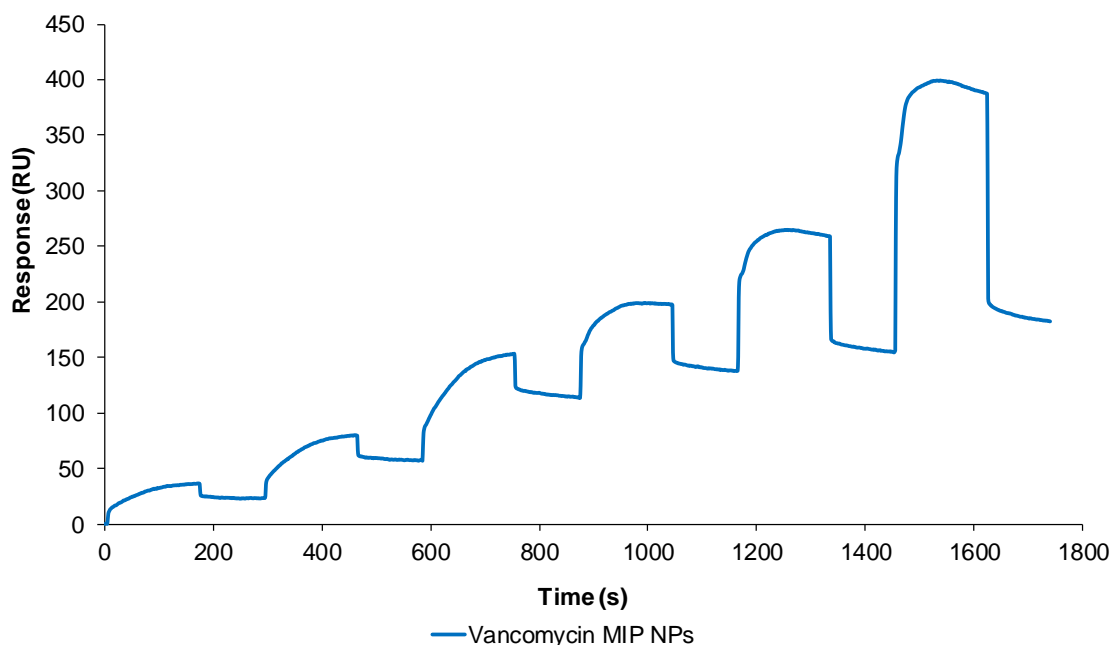
Figure 3–31. SPR sensogram (BIAcore 3000) showing time-dependent binding of vancomycin MIP NPs onto BIAcore sensor chips bearing the template. The solution of vancomycin MIP NPs at a concentration of 135 nM was sonicated for 30 min and used as stock to prepare 5 further 2-fold dilutions (from 1/2 to 1/32). Injections were made in order of increasing concentration, using PBS buffer 0.01 M pH 7.4 as mobile phase. The sensorgram shows affinity for the specific target.

The sensorgrams have shown that MIP NPs exhibited affinity for their respective templates. The calculated apparent dissociation constants vancomycin and peptide MIP NPs were $K_D = 3.4 \times 10^{-9}$ M and $K_D = 4.8 \times 10^{-8}$ M, respectively.

Hydrodynamic diameter of the MIP NPs measured by DLS was 250 nm for vancomycin MIP NPs and 350 nm for peptide MIP NPs (as measured in ACN, Figure 3–32), with a narrow size distribution.
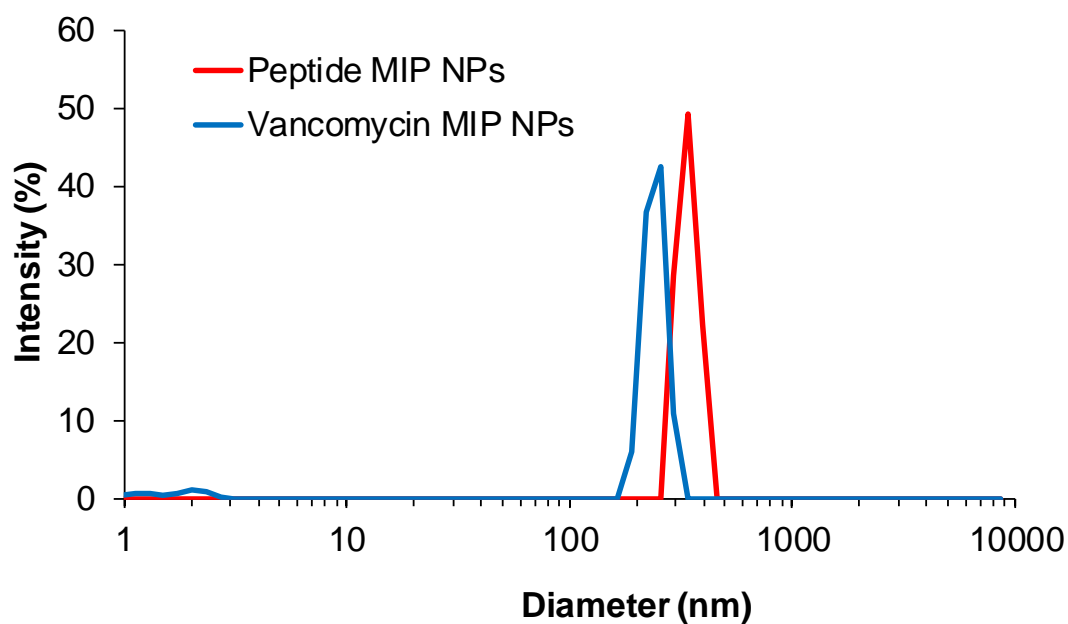
Figure 3–32. DLS size distribution of peptide MIP NPs (red) and vancomycin MIP NPs (blue) in ACN, produced with the automatic solid-phase photoreactor.

These experiments have confirmed that the automatic solid-phase photoreactor is a versatile and flexible tool for the production of high-quality MIP NPs imprinted with low molecular weight templates (up to 1500 Da). The affinity properties of the MIP NPs produced in this work resembled, in practical terms, natural antibodies.

4 Automatic solid-phase chemical reactor of MIP nanoparticles: results and discussion

In the previous chapter the development of the first successful example of an automatic solid-phase photoreactor for MIP NPs which explores iniferter living-polymerisation chemistry was discussed. The polymerisation was performed in organic solvent under UV irradiation – conditions which are favourable for the imprinting of small molecules.

Imprinting of high molecular weight targets such as proteins, polysaccharides and nucleic acids, however, requires an aqueous environment to assure preserving the native structure of these biological molecules during the polymerisation process (Whitcombe *et al.*, 2011; Kryscio and Peppas, 2012). Due to their structural complexity, as well as their low compatibility with the classical preparation methods of MIP NPs, these substances have represented a historical challenge in imprinting.

To address these issues, the solid-phase reactor design for MIP NPs preparation described in the previous chapter was adapted to perform a persulphate-initiated polymerisation in water – conditions developed specifically for protein targets (Hoshino *et al.*, 2008). In this case, much less optimisation was required because the polymerisation procedure was already well-known and established in literature, and the expertise gained by optimising the first reactor allowed a quick and efficient adaptation of the solid-phase synthesis to the aqueous environment required for protein imprinting.

For clarity, within this chapter the expression "chemical polymerisation" has been used to indicate a polymerisation process performed in water and initiated by the addition of ammonium persulphate, and "chemical reactor" has been used to describe the automatic reactor where the polymerisation process is carried out. Although these expressions are not entirely correct, since all the polymerisation processes are chemical (even if initiated by UV irradiation or temperature), they were used here to differentiate the automatic reactor

described in the previous chapter from the new machine which relies on persulfate-initiated polymerisation.

4.1 Preparation of protein-derivatised glass beads as affinity media

The same immobilisation procedure described earlier was used to immobilise the protein templates on the surface of the glass beads (see *3.1.2 - Preparation of template-derivatised glass beads as affinity media*). However, in this case the activation in NaOH was performed in milder conditions than for the glass beads used in the photoreactor (1 M for 1 min rather than 4 M for 10 min) because a high density of functional groups was not required for the immobilisation of large protein molecules. The immobilisation of trypsin was carried out in TBS 0.05 M, pH 8.0 with 0.02 M $CaCl_2$ to inhibit the auto-digestion of the enzyme (Rocha *et al.*, 2005).
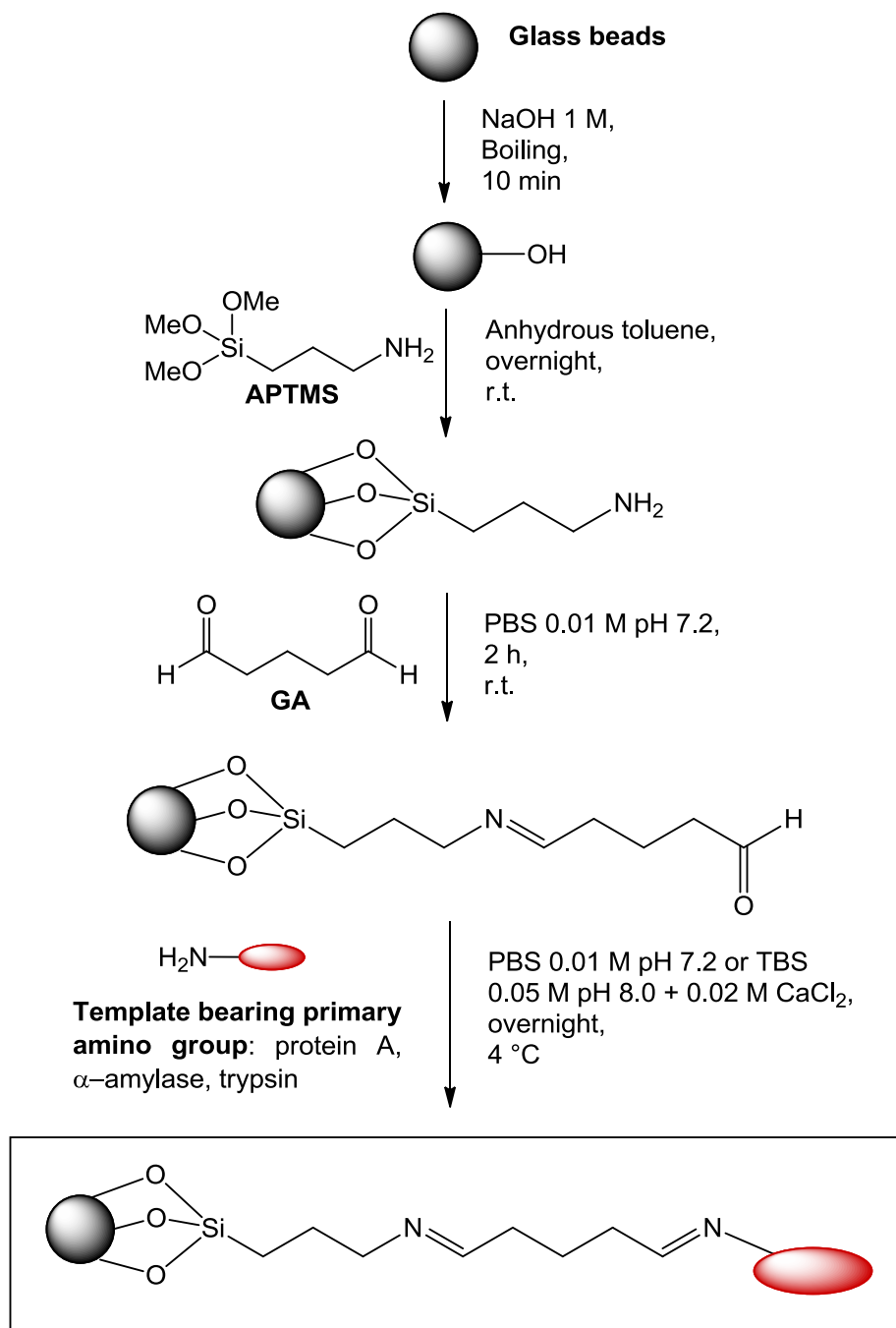
Figure 4–1. Synthetic protocol for the immobilisation of template on the glass beads surface for use in chemical reactor.

Qualitative and quantitative analysis of protein-derivatisation of glass beads

In order to qualitatively confirm the surface derivatisation of glass beads with proteins, a BCA Protein Assay was performed. This method combines the reduction of Cu^{+2} to Cu^{+1} by proteins in an alkaline medium (the biuret reaction)

with the highly sensitive and selective colorimetric detection of the cuprous cation (Cu^{+1}) using a reagent containing BCA (Smith *et al.*, 1985). The purple-colored reaction product of this assay is formed by the chelation of two molecules of BCA with one cuprous ion (Figure 4–2).

Step 1

$$Protein + Cu^{+2} \xrightarrow{\ OH^{-}\ } Cu^{+1}$$

Step 2

$$Cu^{+1} + 2$$

BCA

BCA Cu^{+1} complex (purple)
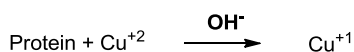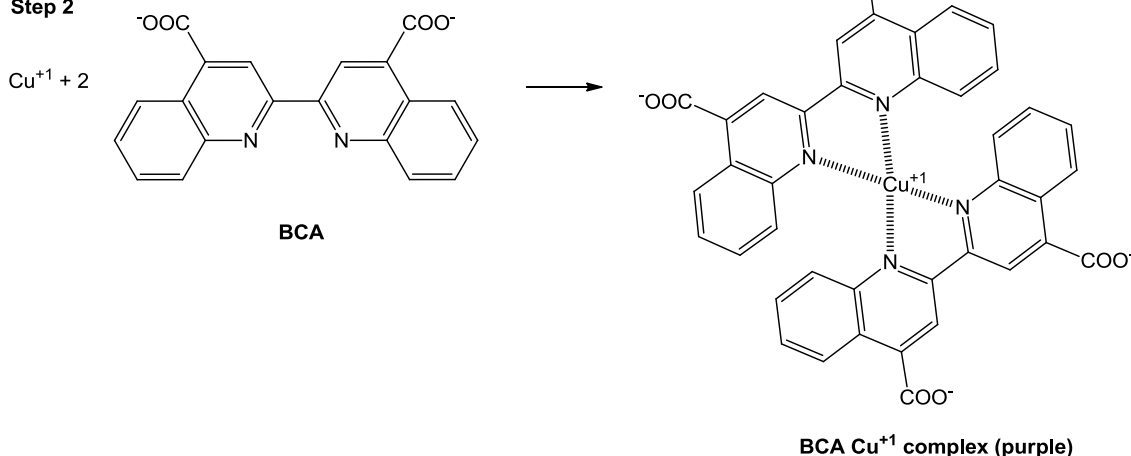
Figure 4–2. Reaction scheme of the BCA Protein Assay.

This water-soluble complex can exhibit a strong absorbance at 562 nm that is nearly linear with increasing protein concentrations over a broad working range (20-2000 µg/mL).

The absorbance was measured by UV after 30 min of incubation at 60 °C. As expected, it was found that the presence of protein on the surface of the glass beads resulted in the development of an intense purple colour in solution, thus qualitatively confirming the immobilisation of the protein templates on the surface.

Quantification of the amount of protein immobilised on the surface of the glass beads was performed indirectly by measuring the UV absorbance at $\lambda = 280$ nm on the residual solution of each protein template after incubation with the GA-activated glass beads. In this instance, the experiment was performed directly inside a SPE cartridge to facilitate the separation and collection of the

supernatant and the washings from the glass beads. Once a calibration curve had been established, this technique enabled the evaluation of the amount of immobilised proteins, which was 0.05 mg protein/g beads for trypsin (2.2×10^{-9} mol, M_w = 23.3 kDa), 0.098 mg protein/g beads for pepsin A (2.8×10^{-9} mol, M_w = 34.6 kDa) and 0.15 mg protein/g beads for α-amylase (2.9×10^{-9} mol, M_w = 52.5 kDa).

4.2 Automatic solid-phase chemical reactor: prototype design
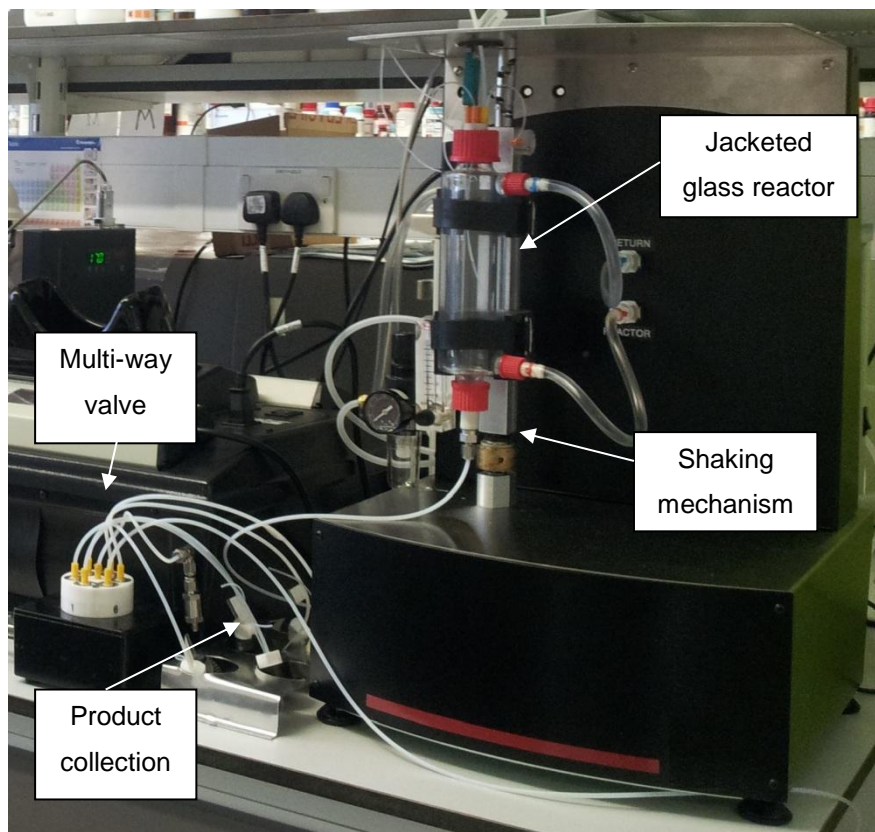
Figure 4–3. The automatic reactor setup developed and used for the synthesis of protein-imprinted MIP NPs on solid phase. Typical operational parameters using proteins as the immobilised targets are: operation time: 4 h per cycle; yield of high-affinity fraction: 8.2 ± 0.5 mg per cycle with 60 g of derivatised glass beads (solid phase).

The developed prototype (Figure 4–3) consists of a temperature-controlled reactor, which is filled with immobilised template and fitted on a stand with a shaking mechanism to ensure adequate homogenisation of the polymerisation mixture. The shaking frequency can be adjusted by changing the motor shaft. A set of pumps is responsible for delivering the monomer mixture, initiator and washing and elution solvents, while the outlet of the reactor is connected to a fraction collector to separate waste streams from high-affinity product fractions. The machine also includes a N_2 inlet to flush the reactor before polymerisation. This N_2 line is also used to force out the liquid and empty the reactor under pressure.

All the parameters and components of the reactor are controlled by a computer-software which allows programming, saving and executing reaction protocols automatically with the minimum operator intervention.
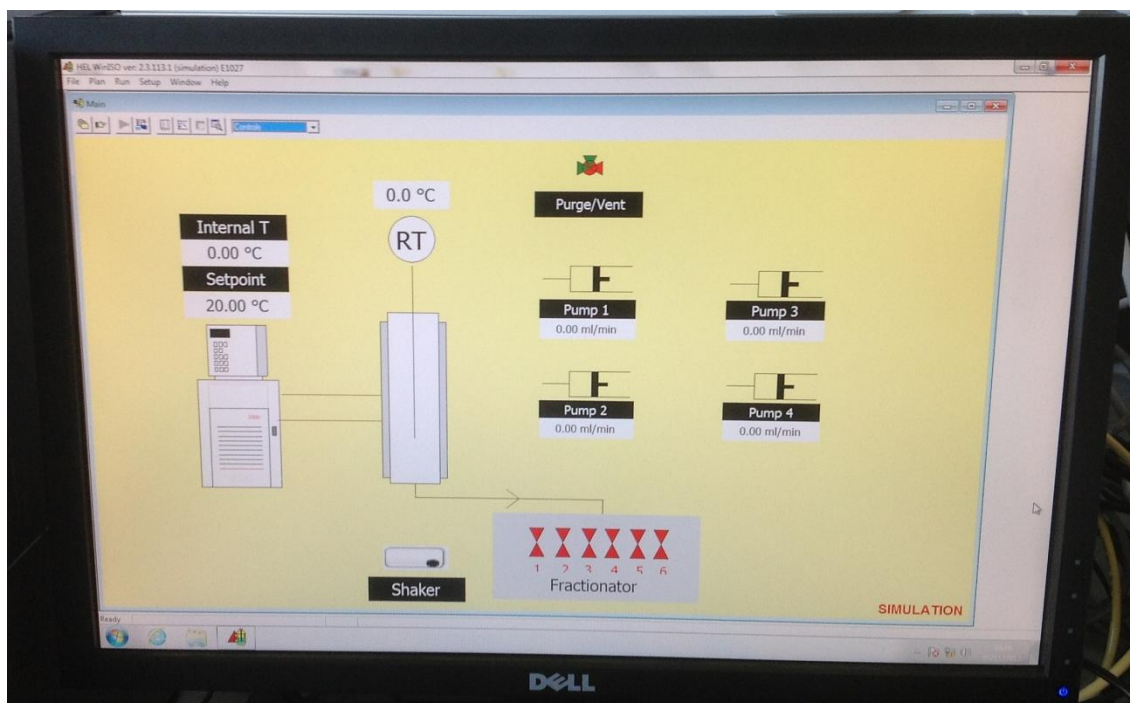
Figure 4–4. Control graphic-interface of the HEL's proprietary software WinISO for the automatic solid-phase MIP NPs chemical reactor.

4.3 Solid-phase chemical synthesis of MIP NPs imprinted for α-amylase, trypsin and pepsin A

As model templates, three enzymes with different molecular weights were chosen: trypsin (M_w = 23.3 kDa), pepsin A (M_w = 34.6 kDa) and α-amylase (M_w = 52.5 kDa). Trypsin and pepsin A are proteolitic enzymes and, more specifically, trypsin is produced in the pancreas while pepsin A is produced in the stomach. In both cases the enzymes are produced and secreted as pro-enzymes, which are then activated *in situ* via other enzymes or the environmental pH. The third imprinted enzyme, α-amylase, catalyses the cleavage of starch into smaller saccharide units, and is present in the saliva as well as in the pancreas (Casella and Taglietti, 1993).

The following generic protocol was applied for the automated synthesis and purification of MIP NPs for proteins: the first step involved loading the monomer mixture dissolved in water into the temperature controlled reactor containing the template-derivatised affinity media. A mild polymerisation process was then initiated by APS and TEMED and carried on for the desired reaction time. The polymerisation mixture was adapted from Hoshino *et al.* (2008), who developed it for the imprinting of proteins. The template-derivatised glass beads also acted as the affinity media for the subsequent purification of the synthesised NPs. At the end of the polymerisation process, the reactor temperature was kept at 15 °C to allow the removal of all the unreacted monomers and other low molecular weight materials while the high-affinity MIP NPs remained attached to the immobilised template. After this step high-affinity MIP NPs were removed by washing the reactor at 60 °C (Figure 4–5). The increase in temperature disrupts the interactions between the immobilised target and the high-affinity MIP NPs, thus assisting in their elution and collection.
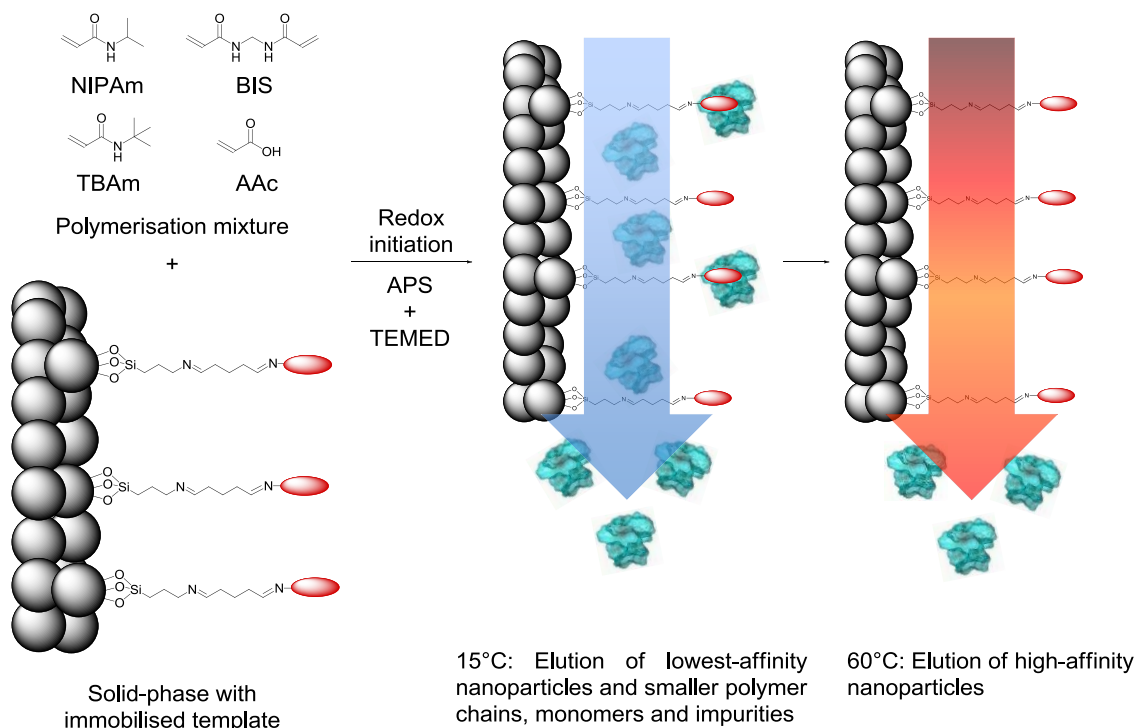
Figure 4–5. Schematic representation of the solid-phase synthesis and purification of the high-affinity MIP NPs exploiting the different interaction strength at different temperatures. The monomer mixture is injected onto the column reactor with the immobilised template and polymerisation is initiated by APS and TEMED. The low-affinity MIP NPs, as well as unreacted monomers, are washed out at a relatively low temperature. The temperature is then increased and high-affinity MIP NPs are eluted from the solid phase for collection.

The whole procedure lasted about 4 h, after which an average yield of 43 ± 2.8 % w/w of high-affinity product with respect to initial monomer mass was obtained. This value refers to a 60 g quantity of affinity media used in the preparation.

Advantages of this process include high binding site accessibility due to the surface-imprinting procedure (Gao *et al.*, 2007; Tan and Tong, 2007) and the option of imprinting whole proteins as well as synthetic epitope peptides (Ge and Turner, 2008). Furthermore, as already mentioned, this solid-phase imprinting approach ensured the formation of a template-free product, as confirmed by the BCA Protein Assay performed on the high-affinity NP fractions, which did not show any protein contamination.

184

Since proteins are not particularly stable molecules and can be easily denatured, the templates were not reused following MIP NPs preparation. Thus the proposed protocol would be useful predominantly for research purposes and for the imprinting of inexpensive protein targets such as trypsin. It is, however, possible to use this approach in imprinting protein epitopes which may offer a convenient way to synthesise large quantities of protein-specific MIP NPs where the template can be recycled. The potential for recycling the template in MIP NPs preparation was demonstrated in the previous chapter.

4.4 Effect of amount of template-derivatised solid-phase on the yield and size of MIP NPs

Optimisation experiments were performed to assess the effect the amount of glass beads has on the yield and size of MIP NPs, using trypsin as the immobilised template. The results showed that the amount of product increased proportionally with the amount of derivatised solid-phase used in the synthesis. The diameter of the MIP NPs remained fairly constant in a range of 240-290 nm (Figure 4–6) and, therefore, did not appear to be dependent on the amount of template-derivatised solid-phase used in the synthesis.
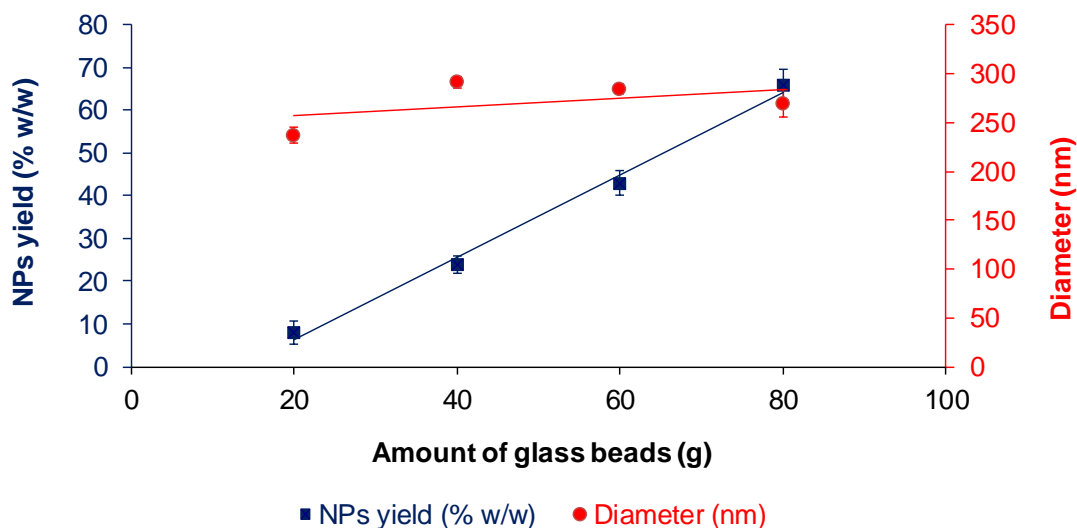
Figure 4–6. Effect of the amount of template-derivatised glass beads on MIP NPs yield and size. Yield is expressed as % of mass of NPs produced per mass of monomers. The template used was trypsin. Error bars represent SD ($n \geq 3$).

Under these conditions, the limiting factor appeared to be the volume of polymerisation mixture and the quantity of beads used in the reactor. With this experimental setup, the maximum dry weight of high-affinity material that could be produced per cycle was 12.5 mg (with 66% yield and 80 g of affinity media). Increasing the volume of the reactor and the quantity of the template-derivatised glass beads should considerably increase the yield of the product, an important aspect to be considered for scaling up the procedure for industrial and commercial purposes. Other potential strategies might be the use of a solid

support with a different morphology and surface area or running several synthesisers in parallel.

4.5 Characterisation of enzyme-imprinted MIP NPs

4.5.1 DLS size analysis

The results of DLS analyses on the MIP NPs synthesised for the different enzymes discussed above are shown in Table 4-1.

Table 4-1. Hydrodynamic diameter and polydispersity index (PDI) of synthesised MIP NPs ($n \geq 5$).

Template	Diameter (nm, ± SD)	PDI
Pepsin A	259 ± 4	0.325
Trypsin	284 ± 5	0.223
α-amylase	285 ± 13	0.349

As can be seen from these values, all synthesised MIP NPs had diameters within the range from 260 to 285 nm. The different sizes of the templates did not exhibit an evident influence on the size of the MIP NPs. The MIP NPs synthesised in this work were, however, 5-6 times larger than those synthesised by Hoshino *et al.* using a similar monomer mixture (Hoshino *et al.*, 2008; Hoshino *et al.*, 2010a; Hoshino *et al.*, 2010b). A possible explanation to this could be related to the effect the solid phase might have on the concentration and aggregation of monomers and particles during the phase separation stage which resulted in these larger particles. Another important aspect to be considered is that in the work of Hoshino *et al.* 10% w/w ionic surfactant was used to stabilise the growing NPs. In this protocol the use of surfactants was excluded since their addition interfered with the affinity analysis performed on SPR, which resulted in NPs with apparent lower affinity.

4.5.2 SEM and TEM imaging

Despite the low focus of the images, due to issues related to the low resistance of the organic polymer within the electron beam, SEM and TEM measurements have confirmed that the MIP NPs exhibited a size of about 100-150 nm and a spherical shape (Figure 4–7).
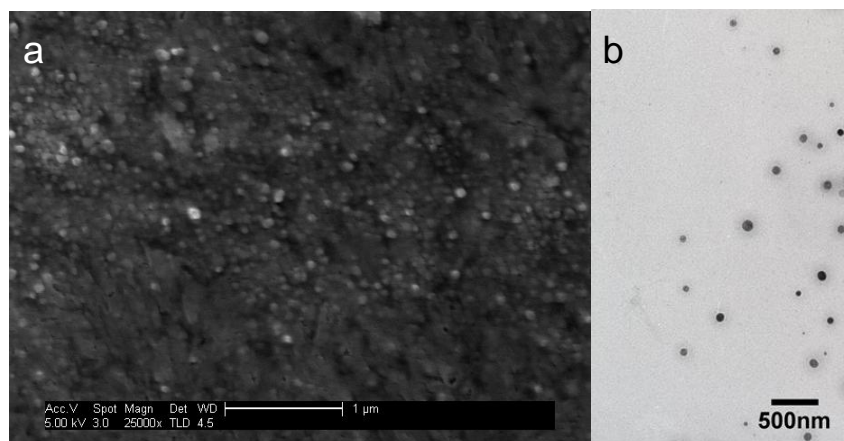
Figure 4–7. Typical sample images of MIP NPs made for proteins: a) SEM image of pepsin A MIP NPs (scale bar: 1 μm); b) TEM image of pepsin A MIP NPs (scale bar: 500 nm).

The higher diameter values obtained by DLS measurements could be attributed to the swelling of the low cross-linked MIP NPs in water, which would be expected with this type of polymer.

4.5.3 SPR affinity and specificity analysis

The affinity and specificity of trypsin, α-amylase and pepsin A MIP NPs were investigated using BIAcore 3000 SPR system by immobilising each template onto the surface of the gold sensors. The immobilisation strategy has already been discussed in section *3.4 - Optimisation of the system: automatic solid-phase synthesis and characterisation of MIP NPs imprinted for melamine.* However, a slight modification was made in the last step for trypsin immobilisation to avoid the auto-digestion of the enzyme (Rocha *et al.*, 2005) (Figure 4–8). For this, $CaCl_2$ was added to the solution of the protein used during the immobilisation stage.
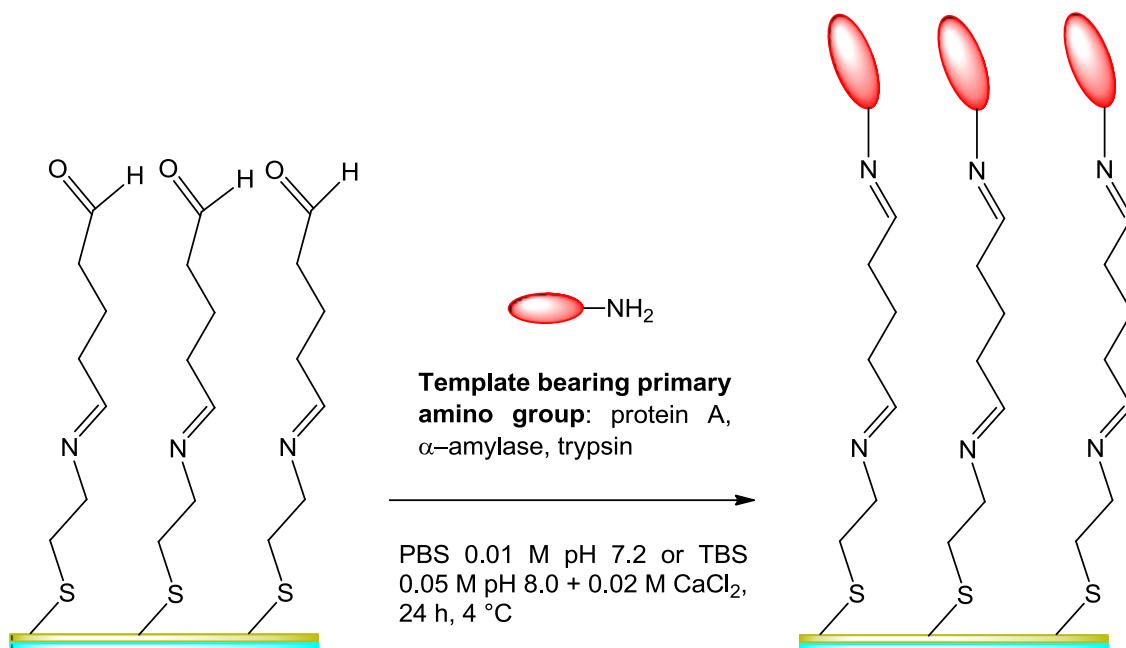
Figure 4–8. Synthetic protocol of the last step for the immobilisation of protein templates on the gold surface of BIAcore sensor chips for use in SPR analysis of MIP NPs.

Several dilutions of the high-affinity fraction of MIP NPs (from 1/10 to $1/10^7$) were sequentially injected (from the lowest to the highest concentration) on each chip bearing one of the templates, and their binding behaviour was recorded.

As previously mentioned (section *3.4 - Optimisation of the system: automatic solid-phase synthesis and characterisation of MIP NPs imprinted for melamine*), non-imprinted NPs were not synthesised and tested since their preparation and collection in the absence of template could not be performed using the existing protocol. Instead of this, the specificity of MIP NPs was assessed in a cross-reactivity study of the MIP NPs towards the proteins which were not used in imprinting (e.g., trypsin MIP NPs were also injected onto the pepsin A and α-amylase-derivatised chips). The results of this study are shown in Figure 4–9 (a, b and c).

a) **Trypsin MIP NPs**

b) **Pepsin A MIP NPs**

191
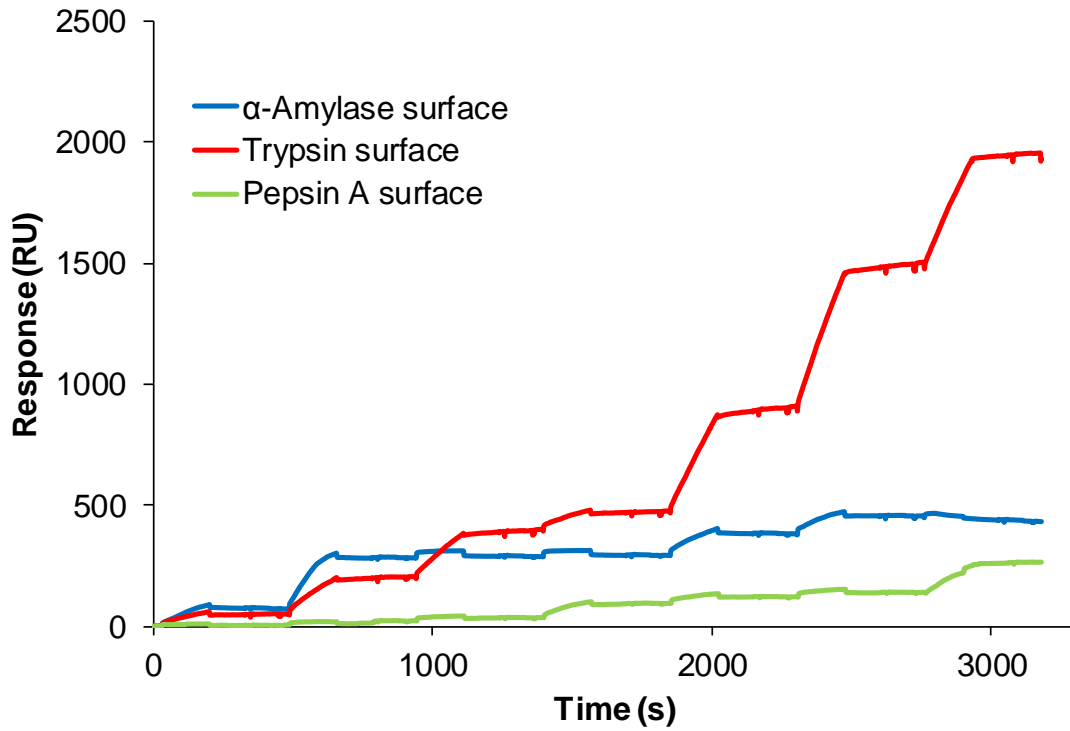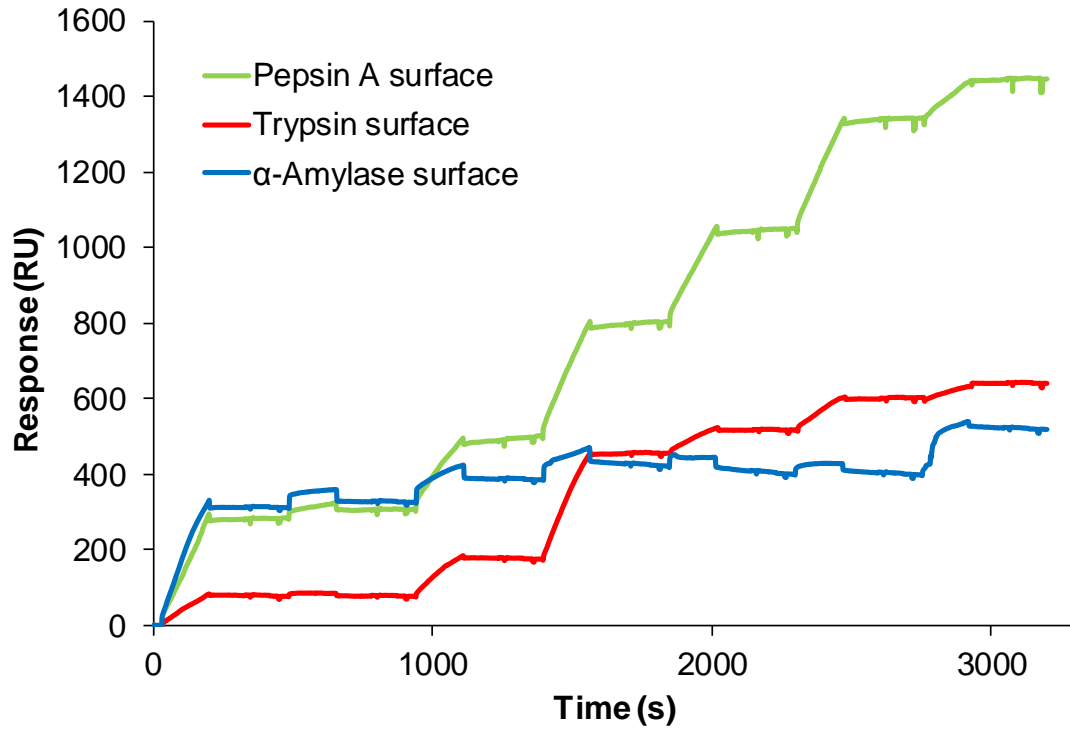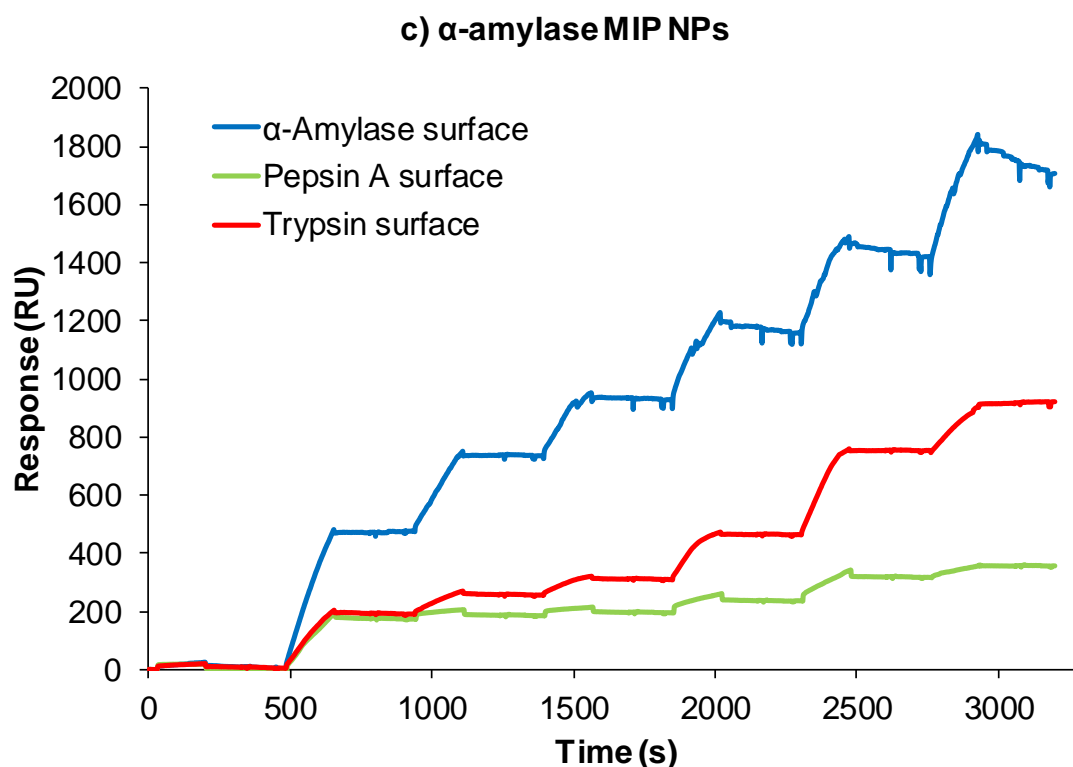
c) α-amylase MIP NPs

Figure 4–9. SPR sensorgrams (BIAcore 3000) showing time-dependent binding of increasing concentrations of: (a) trypsin MIP NPs; (b) pepsin A MIP NPs; (c) α-amylase MIP NPs onto BIAcore sensor chips bearing each of the templates tested. Cross-reactivity has been assessed by injecting MIP NPs onto surfaces bearing the proteins which were not used in the imprinting. Solutions of trypsin, pepsin A and α-amylase MIP NPs at a concentration of 0.4 nM were sonicated for 30 min and used as stocks to prepare 6 further 10-fold dilutions (from 1/10 to $1/10^7$). Injections were made in order of increasing concentration, using PBS buffer 0.01 M pH 7.4 as mobile phase. The sensorgrams show affinity and selectivity for the specific targets.

The sensorgrams presented here show the ability of all the MIP NPs synthesised for each template to specifically recognise and bind their target. Apparent K_Ds of 1.7×10^{-11} M, 4.1×10^{-11} M 3.4×10^{-10} M were calculated for pepsin A, trypsin and α-amylase MIP NPs, respectively. Analysis of the specific interactions of the MIP NPs with their targets was performed using the BIAevaluation software supplied by BIAcore. Despite some non-specific interactions, these analyses resulted in apparent non-specific K_D values about 2

orders of magnitude higher than the K_D values of the MIP NPs assessed with their corresponding BIAcore chip, thus confirming the specific nature of the interactions between MIP NPs and their respective targets.

These experiments confirmed that the automatic solid-phase chemical reactor is a versatile and flexible tool for the production of high-quality MIP NPs imprinted for high molecular weight templates (up to 54 kDa). Also in this case, the affinity properties of the MIP NPs produced here resemble, in practical terms, natural antibodies.

5 Conclusions and future work

5.1 Conclusions

The first example of automated solid-phase synthesis of MIP NPs was reported. Two different types of automatic solid-phase reactor were produced: a photoreactor, suitable for the synthesis of MIP NPs imprinted for relatively small molecules, and a second module specifically designed to prepare MIP NPs in water for high molecular weight templates using mild chemical polymerisation conditions. Automation allowed the reactors to operate continuously, eliminating human error and operator fatigue and ensuring precisely controlled batch-to-batch reproducibility. Moreover, for the first time the multiple reuse of molecular templates in the formation of imprinted polymers (30 times without loss of performance) was achieved through the use of an immobilised template approach. This could be of great advantage in relation to templates which are in short supply or are expensive to obtain. The only other reports of template recycling in the creation of imprinted polymers involved the "double imprinting" of immunoglobulin-imprinted NPs, which can be used as "stamps" to imprint sensor chips (Schirhagl *et al.*, 2010; Schirhagl *et al.*, 2011; Schirhagl *et al.*, 2012). In addition, this solid-phase synthesis strategy offers significant advantages when compared to traditional approaches which rely on imprinting free template in solution, such as full automation and short synthesis/purification times, thus making it suitable for industrial applications. Moreover, hydrophilic high molecular weight targets have been demonstrated to be imprinted in a relatively gentle aqueous environment. There has been only one automatic method for MIP synthesis reported in the literature (Zourob *et al.*, 2006), and this was related to the fabrication of MIP microparticles using a microflow reactor.

Batches of MIP NPs with diameters 30-400 nm and narrow size distributions were prepared using the photoreactor for low molecular weight targets including melamine (d = 60 nm, K_D = 6.3 × 10^{-8} M), vancomycin (d = 250 nm, K_D = 3.4 × 10^{-9} M), and a model peptide (d = 350 nm, K_D = 4.8 × 10^{-8} M). Their recognition properties were similar to MIP NPs prepared in similar conditions using free

template in solution (Guerreiro *et al.*, 2009), but the automatic solid-phase synthesis was performed in less than 3 h/batch.

In the case of the automated chemical reactor, MIP NPs specific for three different proteins were successfully produced: pepsin A (d = 259 nm, K_D = 1.7 × 10^{-11} M), trypsin (d = 284 nm, K_D = 4.1 × 10^{-11} M), and α-amylase (d = 285 nm, K_D = 3.4 × 10^{-10} M). The affinity properties recorded were consistent with those of MIP NPs prepared using similar polymerisation procedures but involving free template in solution (Hoshino *et al.*, 2008; Zeng *et al.*, 2010; Cutivet *et al.*, 2009). However, the automatic solid-phase synthesis and purification of MIP NPs was performed in 4 h/batch, in comparison to the lengthy synthesis and purification procedures reported in the other works.
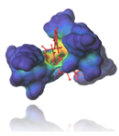
The size and yield of MIP NPs synthesised with the photoreactor were directly proportional to the irradiation time, and the boundary of the system was identified as the irradiation time which caused precipitation of an insoluble polymer. In the case of MIP NPs synthesised using the chemical reactor, there was a direct correlation between amount of solid-phase and yield, without a significant effect on the size of the MIP NPs.

In all cases, the synthesised MIP NPs exhibited size, specificity and solubility characteristics comparable to natural antibodies, thus making them suitable for use as direct antibodies replacements for *in vitro* applications, such as assay and sensor development, as well as potential *in vivo* applications, such as drug development and delivery, as well as imaging.

There are a number of reasons why MIP NPs, produced as described above, would have advantages over antibodies for diagnostic and potentially therapeutic applications (Table 5-1).

Table 5-1. Comparison of the properties of antibodies and MIP NPs.

	Antibodies	MIP NPs
Lifetime	6-12 months	Years
Storage	Freezer	From 4 °C to ambient temperature
Regeneration	Problematic, typically <10 times	Easy (e.g. using acid, solvent, surfactant)
Sterilisation	Problematic, typically using γ-irradiation	UV, autoclaving
Temperature stability	Denature at ~70 °C	Resistant up to 140 °C
Price	1-1000 $/mg	0.25-5 $/mg

Even at this early stage in the development of automated methods for the solid-phase synthesis of MIP NPs, it is clear that this major advance in MIP synthesis and in nanoscience has the potential to usher in a new era in the diagnostics and biotechnology sector in much the same way that solid-phase synthesis enabled combinatorial chemistry and the automation of DNA sequencing has sparked the genomics revolution.

Nevertheless, in order to realise the full scientific and commercial opportunities presented by the technology many more studies need to be performed (see *5.2 - Future work*).

5.2 Future work

At the time of writing a third prototype, combining both the automatic reactors described here, is being assembled and all system components will be integrated into a single case. This system should allow the execution of either photo or chemical polymerisation processes by the same machine, thus being suitable for preparing solid-phase MIP NPs for small or large molecular weight templates depending on the intended application.

To broaden the potential interest of commercial and industrial partners for this technology, it would be interesting to cover the following research topics in the future:

1) Alternative reactor formats: at the moment "column-like" reactor formats (either with packed or not packed solid-phase) have been tested. It would be interesting to investigate other possible formats in order to improve the penetration of the UV light during photopolymerisation and also the homogenisation of the solid-phase and its contact with the polymerisation mixture during the production process.

2) Different solid phases for template immobilisation: glass beads are cheap and convenient but the use of non-porous relatively large glass beads dramatically reduces the amount of template available for the imprinting process and hence the yield of the process itself. An ideal solid-phase should guarantee good flow properties and light penetration as well as being easy to derivatise and suspend in the polymerisation media. Possibly Merrifield-like resins or polymeric materials could present a better alternative to glass beads.

3) Optimisation of the template density: so far a large template excess was used during the immobilisation. However, it might not be the best strategy and currently a study is in progress to assess the optimum template density to obtain better yield, size and affinity of MIP NPs.

4) Different chain transfer agent for the photopolymerisation: it is plausible that other kinds of chain transfer agents, less functionalised with thiol groups, could allow better control over the polymerisation process (Odian, 2004).

5) Development of MIP NPs with integrated functionalities for diagnostic applications: for assays or sensors, the integration of recognition and signalling functionalities in the MIP NPs product is mandatory. Demonstrations of MIP NPs potential in these applications are being currently investigated with promising results.

6) Biological activity of MIP NPs: the final goal of the MIP NPs technology is the development of the first MIP NPs-based drug preparation. Due to their recognition properties, MIP NPs are ideal for being exploited either as targeting agents for drug-delivery systems or as drug delivery matrixes themselves, or both. Moreover, recent advances seem to address the possibility of producing MIP NPs with biological activity, hence their future use directly as drugs. Currently, enzyme-imprinted MIP NPs described in this thesis are being investigated for their biological activity with good results, and this last topic has been chosen as theme for a post-doc research to be undertaken in a UK institution by the author of this thesis.

References

Aghaei, A., Milani Hosseini, M.R., Najafi, M., 2010. A novel capacitive biosensor for cholesterol assay that uses an electropolymerized molecularly imprinted polymer. Electrochim. Acta. 55, 1503-1508

Ahrer, K., Buchacher, A., Iberer, G., Jungbauer, A., 2006. Thermodynamic stability and formation of aggregates of human immunoglobulin G characterised by differential scanning calorimetry and dynamic light scattering. J. Biochem. Biophys. Methods. 66, 73-86

Alexander, C., Andersson, H.S., Andersson, L.I., Ansell, R.J., Kirsch, N., Nicholls, I.A., O'Mahony, J., Whitcombe, M.J., 2006. Molecular imprinting science and technology: a survey of the literature for the years up to and including 2003. J. Mol. Recogn. 19, 106-180

Allender, C.J., Brain, K.R., Heard, C.M., 1997. Binding cross-reactivity of Boc-Phenylalanine enantiomers on molecularly imprinted polymers. Chirality. 9, 233-237

Andersson, L.I., Mosbach, K., 1990. Enantiomeric resolution on molecularly imprinted polymers prepared with only non-covalent and non-ionic interactions. J. Chromatogr. 516, 313-322

Ansell, R.J., 2004. Molecularly imprinted polymers in pseudoimmunoassay. J. Chromatogr. B Anal. Technol. Biomed. Life Sci. 804, 151-165

Ansell, R.J., Mosbach, K., 1998. Magnetic molecularly imprinted polymer beads for drug radioligand binding assay. Analyst. 123, 1611-1616

Arshady, R., Mosbach, K., 1981. Synthesis of substrate-selective polymers by host-guest polymerization. Die Makromolekulare Chemie. 182, 687-692

Arslan, G., Özmen, M., Gündüz, B., Zhang, X., Ersöz, M., 2006. Surface modification of glass beads with an aminosilane monolayer. Turk. J. Chem. 30, 203-210

Barral, S., Guerreiro, A., Villa-García, M.A., Rendueles, M., Díaz, M., Piletsky, S., 2010. Synthesis of 2-(diethylamino)ethyl methacrylate-based polymers: effect of cross-linking degree, porogen and solvent on the textural properties and protein adsorption performance. React. Funct. Polym. 70, 890-899

Barrett, A.M., Cullum, V.A., 1968. Lack of interaction between propranolol and mebanazine. J. Pharm. Pharmacol. 20, 911-915

BBC News, 2010. China dairy products found tainted with melamine. Bbc.co.uk (http://www.bbc.co.uk/news/10565838). Date accessed: 11th November 2012

Behnke, B., Johansson, J., Bayer, E., Nilsson, S., 2000. Fluorescence imaging of frit effects in capillary separations. Electrophoresis. 21, 3102-3108

Beil, J.B., Zimmerman, S.C., 2004. A monomolecularly imprinted dendrimer (MID) capable of selective binding with a tris(2-aminoethyl)amine guest through multiple functional group interactions. Chem. Commun., 488-489

Biffis, A., Graham, N.B., Siedlaczek, G., Stalberg, S., Wulff, G., 2001. The synthesis, characterization and molecular recognition properties of imprinted microgels. Macromol. Chem. Phys. 202, 163-171

Binz, H.K., Amstutz, P., Plückthun, A., 2005. Engineering novel binding proteins from nonimmunoglobulin domains. Nat. Biotechnol. 23, 1257-1268

Biocompare Surveys and Reports, 2009. 2009 Antibody report - Market overview and industry survey - Executive summary. Market Research.com, Rockville, USA, 1-32

Bompart, M., De Wilde, Y., Haupt, K., 2010. Chemical nanosensors based on composite molecularly imprinted polymer particles and surface-enhanced Raman scattering. Adv. Mater. 22, 2343-2348

Bompart, M., Gheber, L.A., De Wilde, Y., Haupt, K., 2009. Direct detection of analyte binding to single molecularly imprinted polymer particles by confocal Raman spectroscopy. Biosens. Bioelectron. 25, 568-571

Bompart, M., Haupt, K., 2009. Molecularly imprinted polymers and controlled/living radical polymerization. Aust. J. Chem. 62, 751-761

Bonini, F., Piletsky, S., Turner, A.P.F., Speghini, A., Bossi, A., 2007. Surface-imprinted beads for the recognition of human serum albumin. Biosens. Bioelectron. 22, 2322-2328

Borm, P.J.A., Robbins, D., Haubold, S., Kuhlbusch, T., Fissan, H., Donaldson, K., Schins, R., Stone, V., Kreyling, W., Lademann, J., Krutmann, J., Warheit, D.B., Oberdorster, E., 2006. The potential risks of nanomaterials: a review carried out for ECETOC. Part. Fibre Toxicol. 3, 1-35

Bossi, A., Piletsky, S.A., Piletska, E.V., Righetti, P.G., Turner, A.P.F., 2001. Surface-grafted molecularly imprinted polymers for protein recognition. Anal. Chem. 73, 5281-5286

Bossi, A., Whitcombe, M.J., Uludag, Y., Fowler, S., Chianella, I., Subrahmanyam, S., Sanchez, I., Piletsky, S.A., 2010. Synthesis of controlled polymeric cross-linked coatings via iniferter polymerisation in the presence of tetraethyl thiuram disulphide chain terminator. Biosens. Bioelectron. 25, 2149-2155

Brüggemann, O., Haupt, K., Ye, L., Yilmaz, E., Mosbach, K., 2000. New configurations and applications of molecularly imprinted polymers. J. Chromatogr. A. 889, 15-24

Butler, J.E., 2000. Solid supports in enzyme-linked immunosorbent assay and other solid-phase immunoassays. Methods. 22, 4-23

Byström, S.E., Börje, A., Akermark, B., 1993. Selective reduction of steroid 3- and 17-ketones using lithium aluminum hydride activated template polymers. J. Am. Chem. Soc. 115, 2081-2083

Cao, L., Zhou, X.C., Li, S.F.Y., 2001. Enantioselective sensor based on microgravimetric quartz crystal microbalance with molecularly imprinted polymer film. Analyst. 126, 184-188

Carboni, D., Flavin, K., Servant, A., Gouverneur, V., Resmini, M., 2008. The first example of molecularly imprinted nanogels with aldolase type I activity. Chem. Eur. J. 14, 7059-7065

Casella, C., Taglietti, V., 1993. Principi di fisiologia vol. 1. La Goliardica Pavese, Pavia, Italy, 1-937

Chan, E., Griffiths, S.M., Chan, C.W., 2008. Public-health risks of melamine in milk products. Lancet. 372, 1444-1445

Chen, Z., Hua, Z., Wang, J., Guan, Y., Zhao, M., Li, Y., 2007. Molecularly imprinted soluble nanogels as a peroxidase-like catalyst in the oxidation reaction of homovanillic acid under aqueous conditions. Appl. Catal. A Gen. 328, 252-258

Chen, Z., Xu, L., Liang, Y., Zhao, M., 2010. pH-sensitive water-soluble nanospheric imprinted hydrogels prepared as horseradish peroxidase mimetic enzymes. Adv. Mater. 22, 1488-1492

Choi, H.-Y., Yeu, S.-U., Han, C.-S., Cha, W.-S., 2002. Method of preparing latex for coating paper. Patent WO0250128

Choong, C.-L., Bendall, J.S., Milne, W.I., 2009. Carbon nanotube array: a new MIP platform. Biosens. Bioelectron. 25, 652-656

Chronakis, I.S., Jakob, A., Hagström, B., Ye, L., 2006. Encapsulation and selective recognition of molecularly imprinted theophylline and 17β-estradiol nanoparticles within electrospun polymer nanofibers. Langmuir. 22, 8960-8965

Ciardelli, G., Borrelli, C., Silvestri, D., Cristallini, C., Barbani, N., Giusti, P., 2006. Supported imprinted nanospheres for the selective recognition of cholesterol. Biosens. Bioelectron. 21, 2329-2338

Ciardelli, G., Cioni, B., Cristallini, C., Barbani, N., Silvestri, D., Giusti, P., 2004. Acrylic polymeric nanospheres for the release and recognition of molecules of clinical interest. Biosens. Bioelectron. 20, 1083-1090

Cirillo, G., Iemma, F., Puoci, F., Parisi, O.I., Curcio, M., Spizzirri, U.G., Picci, N., 2009. Imprinted hydrophilic nanospheres as drug delivery systems for 5-fluorouracil sustained release. J. Drug Targeting. 17, 72-77

Cramer, N.B., Reddy, S.K., O'Brien, A.K., Bowman, C.N., 2003. Thiol-ene photopolymerization mechanism and rate limiting step changes for various vinyl functional group chemistries. Macromolecules. 36, 7964-7969

Cunliffe, D., Kirby, A., Alexander, C., 2005. Molecularly imprinted drug delivery systems. Adv. Drug Deliv. Rev. 57, 1836-1853

Curcio, P., Zandanel, C., Wagner, A., Mioskowski, C., Baati, R., 2009. Semi-covalent surface molecular imprinting of polymers by one-stage mini-emulsion polymerization: glucopyranoside as a model analyte. Macromol. Biosci. 9, 596-604

Cutivet, A., Schembri, C., Kovensky, J., Haupt, K., 2009. Molecularly imprinted microgels as enzyme inhibitors. J. Am. Chem. Soc. 131, 14699-14702

Danielsson, B., 2007. Artificial receptors. Adv. Biochem. Eng. Biotechnol. 109, 97-122

Debord, J.D., Lyon, L.A., 2003. Synthesis and characterization of pH-responsive co-polymer microgels with tunable volume phase transition temperatures. Langmuir. 19, 7662-7664

Diltemiz, S.E., Say, R., Büyüktiryaki, S., Hür, D., Denizli, A., Ersöz, A., 2008. Quantum dot nanocrystals having guanosine imprinted nanoshell for DNA recognition. Talanta. 75, 890-896

Dvorakova, G., Haschick, R., Chiad, K., Klapper, M., Müllen, K., Biffis, A., 2010. Molecularly imprinted nanospheres by nonaqueous emulsion polymerization. Macromol. Rapid Commun. 31, 2035-2040

Esen, C., Andac, M., Bereli, N., Say, R., Henden, E., Denizli, A., 2009. Highly selective ion-imprinted particles for solid-phase extraction of Pb^{2+} ions. Mater. Sci. Eng. C. 29, 2464-2470

Espicom, 2011. Point of care diagnostics: players, products & future market prospects. Espicom, Chichester, UK, 1-396

Gao, D., Zhang, Z., Wu, M., Xie, C., Guan, G., Wang, D., 2007. A surface functional monomer-directing strategy for highly dense imprinting of TNT at surface of silica nanoparticles. J. Am. Chem. Soc. 129, 7859-7866

Gao, R., Zhang, J., He, X., Chen, L., Zhang, Y., 2010. Selective extraction of sulfonamides from food by use of silica-coated molecularly imprinted polymer nanospheres. Anal. Bioanal. Chem. 398, 451-461

Ge, Y., Turner, A.P.F., 2009. Molecularly imprinted sorbent assays: recent developments and applications. Chem. Eur. J. 15, 8100-8107

Ge, Y., Turner, A.P.F., 2008. Too large to fit? Recent developments in macromolecular imprinting. Trends Biotechnol. 26, 218-224

Giri, S., Trewyn, B.G., Stellmaker, M.P., Lin, V.S.-Y., 2005. Stimuli-responsive controlled-release delivery system based on mesoporous silica nanorods capped with magnetic nanoparticles. Angew. Chem. Int. Ed. 44, 5038-5044

Gonzato, C., Courty, M., Pasetto, P., Haupt, K., 2011. Magnetic molecularly imprinted polymer nanocomposites via surface-initiated RAFT polymerization. Adv. Funct. Mater. 21, 3947-3953

Göttlicher, B., Bächmann, K., 1997. Application of particles as pseudo-stationary phases in electrokinetic chromatography. J. Chromatogr. A. 780, 63-73

Grant, S.D., Porter, A.J., Harris, W.J., 1999. Comparative sensitivity of immunoassays for haptens using monomeric and dimeric antibody fragments. J. Agric. Food Chem. 47, 340-345

Grönwall, C., Ståhl, S., 2009. Engineered affinity proteins - Generation and applications. J. Biotechnol. 140, 254-269

Guerreiro, A.R., Chianella, I., Piletska, E., Whitcombe, M.J., Piletsky, S.A., 2009. Selection of imprinted nanoparticles by affinity chromatography. Biosens. Bioelectron. 24, 2740-2743

Hage, D.S., 1998. Chapter 13. Affinity chromatography, in: Katz, E., Eksteen, R., Schoenmakers, P., Miller, N. (Eds.), Handbook of HPLC. Marcel Dekker Inc., New York, USA, 483-498

Haginaka, J., Tabo, H., Kagawa, C., 2008. Uniformly sized molecularly imprinted polymers for d-chlorpheniramine: influence of a porogen on their morphology and enantioselectivity. J. Pharm. Biomed. Anal. 46, 877-881

Halliwell, C.M., Cass, A.E.G, 2001. A factorial analysis of silanization conditions for the immobilization of oligonucleotides on glass surfaces. Anal. Chem. 73, 2476-2483

Hansel, T.T., Kropshofer, H., Singer, T., Mitchell, J.A., George, A.J.T., 2010. The safety and side effects of monoclonal antibodies. Nat. Rev. Drug Discov. 9, 325-338

Haupt, K., 2012. Preface, in: Haupt, K. (Ed.), Molecular Imprinting. Springer-Verlag Berlin Heidelberg, London, UK, ix-xii

Haupt, K., 2003. Molecularly imprinted polymers: the next generation. Anal. Chem. 75, 376-383

Haupt, K., 1999. Molecularly imprinted sorbent assays and the use of non-related probes. React. Funct. Polym. 41, 125-131

Haupt, K., Dzgoev, A., Mosbach, K., 1998a. Assay system for the herbicide 2,4-dichlorophenoxyacetic acid using a molecularly imprinted polymer as an artificial recognition element. Anal. Chem. 70, 628-631

Haupt, K., Mayes, A.G., Mosbach, K., 1998b. Herbicide assay using an imprinted polymer-based system analogous to competitive fluoroimmunoassays. Anal. Chem. 70, 3936-3939

Haupt, K., Noworyta, K., Kutner, W., 1999. Imprinted polymer-based enantioselective acoustic sensor using a quartz crystal microbalance. Anal. Commun. 36, 391-393

Hayakawa, I., Atarashi, S., Yokohama, S., 1986. Synthesis and antibacterial activities of optically active ofloxacin. Antimicrob. Agents Chemother. 29, 163-164

Hey, T., Fiedler, E., Rudolph, R., Fiedler, M., 2005. Artificial, non-antibody binding proteins for pharmaceutical and industrial applications. Trends Biotechnol. 23, 514-522

Hock, B., Rahman, M., Rauchalles, S., Dankwardt, A., Seifert, M., Haindl, S., Kramer, K., 1999. Stabilisation of immunoassays and receptor assays. J. Mol. Catal. B Enzym. 7, 115-124

Horvath, S.J., Firca, J.R., Hunkapiller, T., Hunkapiller, M.W., Hood, L., 1987. [16] An automated DNA synthesizer employing deoxynucleoside 3′-phosphoramidites. Methods Enzymol. 154, 314-326

Hoshino, Y., Haberaecker III, W.W., Kodama, T., Zeng, Z., Okahata, Y., Shea, K.J., 2010a. Affinity purification of multifunctional polymer nanoparticles. J. Am. Chem. Soc. 132, 13648-13650

Hoshino, Y., Kodama, T., Okahata, Y., Shea, K.J., 2008. Peptide imprinted polymer nanoparticles: A plastic antibody. J. Am. Chem. Soc. 130, 15242-15243

Hoshino, Y., Koide, H., Urakami, T., Kanazawa, H., Kodama, T., Oku, N., Shea, K.J., 2010b. Recognition, neutralization, and clearance of target peptides in the bloodstream of living mice by molecularly imprinted polymer nanoparticles: a plastic antibody. J. Am. Chem. Soc. 132, 6644-6645

Hoshino, Y., Shea, K.J., 2011. The evolution of plastic antibodies. J. Mater. Chem. 21, 3517-3521

Hosoya, K., Yoshizako, K., Tanaka, N., Kimata, K., Araki, T., Haginaka, J., 1994. Uniform-size macroporous polymer-based stationary phase for HPLC prepared through molecular imprinting technique. Chem. Lett. 23, 1437-1438

Hoyle, C.E., Lee, T.Y., Roper, T., 2004. Thiol-enes: chemistry of the past with promise for the future. J. Polym. Sci. Part A. 42, 5301-5338

Huang, X., Liu, Y., Liang, K., Tang, Y., Liu, J., 2008. Construction of the active site of glutathione peroxidase on polymer-based nanoparticles. Biomacromolecules. 9, 1467-1473

Hunkapiller, M.W., Hood, L.E., 1980. New protein sequenator with increased sensitivity. Science. 207, 523-525

Ikegami, T., Lee, W.-S., Nariai, H., Takeuchi, T., 2004. Covalent molecular imprinting of bisphenol a using its diesters followed by the reductive cleavage with $LiAlH_4$. J. Chromatogr. B Anal. Technol. Biomed. Life Sci. 804, 197-201

Ivanova-Mitseva, P.K., Guerreiro, A., Piletska, E.V., Whitcombe, M.J., Zhou, Z., Mitsev, P.A., Davis, F., Piletsky, S.A., 2012. Cubic molecularly imprinted polymer nanoparticles with a fluorescent core. Angew. Chem. Int. Ed. 51, 5196-5199

Jantarat, C., Tangthong, N., Songkro, S., Martin, G.P., Suedee, R., 2008. *S*-Propranolol imprinted polymer nanoparticle-on-microsphere composite porous cellulose membrane for the enantioselectively controlled delivery of racemic propranolol. Int. J. Pharm. 349, 212-225

Jenik, M., Seifner, A., Krassnig, S., Seidler, K., Lieberzeit, P.A., Dickert, F.L., Jungbauer, C., 2009. Sensors for bioanalytes by imprinting-polymers mimicking both biological receptors and the corresponding bioparticles. Biosens. Bioelectron. 25, 9-14

Jiang, D., Tang, J., Liu, B., Yang, P., Shen, X., Kong, J., 2003. Covalently coupling the antibody on an amine-self-assembled gold surface to probe hyaluronan-binding protein with capacitance measurement. Biosens. Bioelectron. 18, 1183-1191

Johnson, K.R., Young, K.K., Weimin, F., 1999. Antagonistic interplay between antimitotic and G1-S arresting agents observed in experimental combination therapy. Clin. Canc. Res. 5, 2559-2565

Jones, C.F., Grainger, D.W., 2009. In vitro assessments of nanomaterial toxicity. Adv. Drug Deliv. Rev. 61, 438-456

Kambara, H., Nishikawa, T., Katayama, Y., Yamaguchi, T., 1988. Optimization of parameters in a DNA sequenator using fluorescence detection. Biotechnology. 6, 816-821

Kan, X., Liu, T., Zhou, H., Li, C., Fang, B., 2010. Molecular imprinting polymer electrosensor based on gold nanoparticles for theophylline recognition and determination. Microchim. Acta. 171, 423-429

Kandimalla, V.B., Ju, H., 2004. Molecular imprinting: a dynamic technique for diverse applications in analytical chemistry. Anal. Bioanal. Chem. 380, 587-605

Kannurpatti, A.R., Lu, S., Bunker, G.M., Bowman, C.N., 1996. Kinetic and mechanistic studies of iniferter photopolymerizations. Macromolecules. 29, 7310-7315

Kempe, H., Kempe, M., 2004. Novel method for the synthesis of molecularly imprinted polymer bead libraries. Macromol. Rapid Commun. 25, 315-320

Kent, S.H., Hood, L.E., Beilar, H., Meister, S., Geiser, T., 1984. High yield chemical synthesis of biologically active peptides on an automated peptide synthesizer of novel design, in: Ragnarsson, E. (Ed.), Peptides 1984: Proceedings of the 18th European Peptide Symposium. Almqvist and Wiksell, Stockholm, Sweden, 185-188

Kotrotsiou, O., Chaitidou, S., Kiparissides, C., 2009. Boc-L-tryptophan imprinted polymeric microparticles for bioanalytical applications. Mater. Sci. Eng. C. 29, 2141-2146

Kramer, K., 2002. Evolutionary affinity and selectivity optimization of a pesticide-selective antibody utilizing a hapten-selective immunoglobulin repertoire. Environ. Sci. Technol. 36, 4892-4898

Kryscio, D.R., Peppas, N.A., 2012. Critical review and perspective of macromolecularly imprinted polymers. Acta Biomater. 8, 461-473

Lai, J.-P., Yang, M.-L., Niessner, R., Knopp, D., 2007. Molecularly imprinted microspheres and nanospheres for di(2-ethylhexyl) phthalate prepared by precipitation polymerization. Anal. Bioanal. Chem. 389, 405-412

Lakshmi, D., Bossi, A., Whitcombe, M.J., Chianella, I., Fowler, S.A., Subrahmanyam, S., Piletska, E.V., Piletsky, S.A., 2009. Electrochemical sensor for catechol and dopamine based on a catalytic molecularly imprinted polymer-conducting polymer hybrid recognition element. Anal. Chem. 81, 3576-3584

Lavignac, N., Allender, C.J., Brain, K.R., 2004. Current status of molecularly imprinted polymers as alternatives to antibodies in sorbent assays. Anal. Chim. Acta. 510, 139-145

Lee, H., Dellatore, S.M., Miller, W.M., Messersmith, P.B., 2007. Mussel-inspired surface chemistry for multifunctional coatings. Science. 318, 426-430

Lehmann, M., Brunner, H., Tovar, G.E.M., 2002. Selective separations and hydrodynamic studies: a new approaoch using molecularly imprinted nanosphere composite membranes. Desalination. 149, 315-321

Lettau, K., Warsinke, A., Laschewsky, A., Mosbach, K., Yilmaz, E., Scheller, F.W., 2004. An esterolytic imprinted polymer prepared via a silica-supported transition state analogue. Chem. Mater. 16, 2745-2749

Li, J., Zu, B., Zhang, Y., Guo, X., Zhang, H., 2010a. One-pot synthesis of surface-functionalized molecularly imprinted polymer microspheres by iniferter-induced "Living" radical precipitation polymerization. J. Polym. Sci. Part A. 48, 3217-3228

Li, L., He, X., Chen, L., Zhang, Y., 2009. Preparation of novel bovine hemoglobin surface-imprinted polystyrene nanoparticles with magnetic susceptibility. Sci. China Ser. B Chem. 52, 1402-1411

Li, M., Zhang, L., Meng, Z., Wang, Z., Wu, H., 2010b. Molecularly-imprinted microspheres for selective extraction and determination of melamine in milk and feed using gas chromatography-mass spectrometry. J. Chromatogr. B Anal. Technol. Biomed. Life Sci. 878, 2333-2338

Li, P., Rong, F., Yuan, C., 2003. Morphologies and binding characteristics of molecularly imprinted polymers prepared by precipitation polymerization. Polym. Int. 52, 1799-1806

Li, Y., Dong, C., Chu, J., Qi, J., Li, X., 2011. Surface molecular imprinting onto fluorescein-coated magnetic nanoparticles via reversible addition fragmentation chain transfer polymerization: a facile three-in-one system for recognition and separation of endocrine disrupting chemicals. Nanoscale. 3, 280-287

Li, Y., Yang, H.-H., You, Q.-H., Zhuang, Z.-X., Wang, X.-R., 2006a. Protein recognition via surface molecularly imprinted polymer nanowires. Anal. Chem. 78, 317-320

Li, Z., Ding, J., Day, M., Tao, Y., 2006. Molecularly imprinted polymeric nanospheres by diblock co-polymer self-assembly. Macromolecules. 39, 2629-2636

Liu, F., Liu, X., Ng, S.-C., Chan, H.S.-O., 2006b. Enantioselective molecular imprinting polymer coated QCM for the recognition of L-tryptophan. Sens. Actuators, B Chem. 113, 234-240

Liu, L., Zheng, J., Fang, G., Xie, W., 2012. Improvement of the homogeneity of protein-imprinted polymer films by orientated immobilization of the template. Anal. Chim. Acta. 726, 85-92

Liu, X.D., Tokura, S., Haruki, M., Nishi, N., Sakairi, N., 2002. Surface modification of nonporous glass beads with chitosan and their adsorption property for transition metal ions. Carbohydr. Polym. 49, 103-108

Liu, Y., Hoshina, K., Haginaka, J., 2010. Monodispersed, molecularly imprinted polymers for cinchonidine by precipitation polymerization. Talanta. 80, 1713-1718

Lorenzo, R.A., Carro, A.M., Alvarez-Lorenzo, C., Concheiro, A., 2011. To remove or not to remove? The challenge of extracting the template to make the cavities available in molecularly imprinted polymers (MIPs). Int. J. Mol. Sci. 12, 4327-4347

Lu, C.-H., Wang, Y., Li, Y., Yang, H.-H., Chen, X., Wang, X.-R., 2009. Bifunctional superparamagnetic surface molecularly imprinted polymer core-shell nanoparticles. J. Mater. Chem. 19, 1077-1079

Lu, C.-H., Zhou, W.-H., Han, B., Yang, H.-H., Chen, X., Wang, X.-R., 2007. Surface-imprinted core-shell nanoparticles for sorbent assays. Anal. Chem. 79, 5457-5461

Maddock, S.C., Pasetto, P., Resmini, M., 2004. Novel imprinted soluble microgels with hydrolytic catalytic activity. Chem. Commun. 10, 536-537

Mairal, T., Cengiz Özalp, V., Lozano Sánchez, P., Mir, M., Katakis, I., O'Sullivan, C.K., 2008. Aptamers: molecular tools for analytical applications. Anal. Bioanal. Chem. 390, 989-1007

Markowitz, M.A., Kust, P.R., Deng, G., Schoen, P.E., Dordick, J.S., Clark, D.S., Gaber, B.P., 2000. Catalytic silica particles via template-directed molecular imprinting. Langmuir. 16, 1759-1765

Matsui, J., Miyoshi, Y., Doblhoff-Dier, O., Takeuchi, T., 1995. A molecularly imprinted synthetic polymer receptor selective for atrazine. Anal. Chem. 67, 4404-4408

Mayes, A.G., Mosbach, K., 1996. Molecularly imprinted polymer beads: suspension polymerization using a liquid perfluorocarbon as the dispersing phase. Anal. Chem. 68, 3769-3774

Mayes, A.G., Whitcombe, M.J., 2005. Synthetic strategies for the generation of molecularly imprinted organic polymers. Adv. Drug Deliv. Rev. 57, 1742-1778

Merrifield, B., 2012. Bruce Merrifield - Nobel Lecture: Solid Phase Synthesis. Nobelprize.org (http://www.nobelprize.org/nobel_prizes/chemistry/laureates/1984/merrifield-lecture.html). Date accessed: 9th August 2012

Mijangos, I., Navarro-Villoslada, F., Guerreiro, A., Piletska, E., Chianella, I., Karim, K., Turner, A., Piletsky, S., 2006. Influence of initiator and different polymerisation conditions on performance of molecularly imprinted polymers. Biosens. Bioelectron. 22, 381-387

Milja, T.E., Prathish, K.P., Prasada Rao, T., 2011. Synthesis of surface-imprinted nanospheres for selective removal of uranium from simulants of Sambhar salt lake and ground water. J. Hazard. Mater. 188, 384-390

Minko, S., 2008. Grafting on solid surfaces: "grafting to" and "grafting from" methods, in: Stamm, M. (Ed.), Polymer surfaces and interfaces - Characterization, modification and applications. Springer-Verlag Berlin Heidelberg, Berlin, Germany, 215-234

Missailidis, S., Hardy, A., 2009. Aptamers as inhibitors of target proteins. Expert Opin. Ther. Pat. 19, 1073-1082

Muldoon, M.T., Stanker, L.H., 1997. Molecularly imprinted solid phase extraction of atrazine from beef liver extracts. Anal. Chem. 69, 803-808

Muldoon, M.T., Stanker, L.H., 1995. Polymer synthesis and characterization of a molecularly imprinted sorbent assay for atrazine. J. Agric. Food Chem. 43, 1424-1427

Myers, P., Bartle, K.D. (Eds.), 2001. Capillary electrochromatography. The Royal Society of Chemistry, London, UK, 1-166

Nilsson, C., Birnbaum, S., Nilsson, S., 2007. Use of nanoparticles in capillary and microchip electrochromatography. J. Chromatogr. A. 1168, 212-224

Nilsson, C., Nilsson, S., 2006. Nanoparticle-based pseudostationary phases in capillary electrochromatography. Electrophoresis. 27, 76-83

Nilsson, C., Viberg, P., Spégel, P., Jömtén-Karlsson, M., Petersson, P., Nilsson, S., 2006. Nanoparticle-based continuous full filling capillary electrochromatography/electrospray ionization-mass spectrometry for separation of neutral compounds. Anal. Chem. 78, 6088-6095

Nilsson, J., Spégel, P., Nilsson, S., 2004. Molecularly imprinted polymer formats for capillary electrochromatography. J. Chromatogr. B Anal. Technol. Biomed. Life Sci. 804, 3-12

Nishino, H., Huang, C.-S., Shea, K.J., 2006. Selective protein capture by epitope imprinting. Angew. Chem. Int. Ed. 45, 2393-2396

Norrlöw, O., Glad, M., Mosbach, K., 1984. Acrylic polymer preparations containing recognition sites obtained by imprinting with substrates. J. Chromatogr. A. 299, 29-41

Oberdörster, G., Oberdörster, E., Oberdörster, J., 2005. Nanotoxicology: an emerging discipline evolving from studies of ultrafine particles. Environ. Health Perspect. 113, 823-839

Odian, G., 2004. Radical chain polymerization - Chain Transfer, in: Odian, G. (Ed.), Principles of polymerization. John Wiley & Sons, Inc., Hoboken, USA, 238-255

Ogiso, M., Minoura, N., Shinbo, T., Shimizu, T., 2007. DNA detection system using molecularly imprinted polymer as the gel matrix in electrophoresis. Biosens. Bioelectron. 22, 1974-1981

Omersel, J., Žager, U., Kveder, T., Božič, B., 2010. Alteration of antibody specificity during isolation and storage. J. Immunoassay Immunochem. 31, 45-59

O'Shannessy, D.J., Ekberg, B., Mosbach, K., 1989. Molecular imprinting of amino acid derivatives at low temperature (0 °C) using photolytic homolysis of azobisnitriles. Anal. Biochem. 177, 144-149

Otsu, T., 2000. Iniferter concept and living radical polymerization. J. Polym. Sci. Part A. 38, 2121-2136

Otsu, T., Matsunaga, T., Doi, T., Matsumoto, A., 1995. Features of living radical polymerization of vinyl monomers in homogeneous system using *N,N*-diethyldithiocarbamate derivatives as photoiniferters. Eur. Polym. J. 31, 67-78

Otsu, T., Matsunaga, T., Kuriyama, A., Yoshioka, M., 1989. Living radical polymerization through the use of iniferters: controlled synthesis of polymers. Eur. Polym. J. 25, 643-650

Paschke, M., 2006. Phage display systems and their applications. Appl. Microbiol. Biotechnol. 70, 2-11

Pasetto, P., Flavin, K., Resmini, M., 2009. Simple spectroscopic method for titration of binding sites in molecularly imprinted nanogels with hydrolase activity. Biosens. Bioelectron. 25, 572-578

Pasetto, P., Maddock, S.C., Resmini, M., 2005. Synthesis and characterisation of molecularly imprinted catalytic microgels for carbonate hydrolysis. Anal. Chim. Acta. 542, 66-75

Peng, Y., Xie, Y., Luo, J., Nie, L., Chen, Y., Chen, L., Du, S., Zhang, Z., 2010. Molecularly imprinted polymer layer-coated silica nanoparticles toward dispersive solid-phase extraction of trace sulfonylurea herbicides from soil and crop samples. Anal. Chim. Acta. 674, 190-200

Percival, C.J., Stanley, S., Galle, M., Braithwaite, A., Newton, M.I., McHale, G., Hayes, W., 2001. Molecular-imprinted, polymer-coated quartz crystal microbalances for the detection of terpenes. Anal. Chem. 73, 4225-4228

Pérez, N., Whitcombe, M.J., Vulfson, E.N., 2001. Surface-imprinting of cholesterol on submicrometer core-shell emulsion particles. Macromolecules. 34, 830-836

Pérez, N., Whitcombe, M.J., Vulfson, E.N., 2000. Molecularly imprinted nanoparticles prepared by core-shell emulsion polymerization. J. Appl. Polym. Sci. 77, 1851-1859

Pérez-Moral, N., Mayes, A.G., 2007. Molecularly imprinted multi-layer core-shell nanoparticles - A surface grafting approach. Macromol. Rapid Commun. 28, 2170-2175

Pérez-Moral, N., Mayes, A.G., 2006a. Direct rapid synthesis of MIP beads in SPE cartridges. Biosens. Bioelectron. 21, 1798-1803

Pérez-Moral, N., Mayes, A.G., 2006b. MIP formats for analytical applications, in: Piletsky, S.A., Turner, A. (Eds.), Molecular imprinting of polymers. Eurekah.com/Landes Bioscience, Georgetown, USA, 1-11

Pérez-Moral, N., Mayes, A.G., 2004. Noncovalent imprinting in the shell of core-shell nanoparticles. Langmuir. 20, 3775-3779

Pérez-Moral, N., Mayes, A.G., 2002. Molecular imprinting of polymeric core-shell nanoparticles. Mater. Res. Soc. Symp. Proc. 723, 61-66

Piacham, T., Josell, A., Arwin, H., Prachayasittikul, V., Ye, L., 2005. Molecularly imprinted polymer thin films on quartz crystal microbalance using a surface bound photo-radical initiator. Anal. Chim. Acta. 536, 191-196

Piletska, E.V., Guerreiro, A.R., Whitcombe, M.J., Piletsky, S.A., 2009. Influence of the polymerization conditions on the performance of molecularly imprinted polymers. Macromolecules. 42, 4921-4928

Piletska, E.V., Piletsky, S.A., 2010. Size matters: Influence of the size of nanoparticles on their interactions with ligands immobilized on the solid surface. Langmuir. 26, 3783-3785

Piletska, E.V., Piletsky, S.A., Subrahmanyam, S., Karim, K., Turner, A.P.F., 2001. A new reactive polymer suitable for covalent immobilisation and monitoring of primary amines. Polymer. 42, 3603-3608

Piletsky, S.A., Guerreiro, A., Piletska, E.V., Chianella, I., Karim, K., Turner, A.P.F., 2004. Polymer cookery. 2. Influence of polymerization pressure and polymer swelling on the performance of molecularly imprinted polymers. Macromolecules. 37, 5018-5022

Piletsky, S.A., Guerreiro, A.R.L., Whitcombe, M.J., 2011. Preparation of soluble and colloidal molecularly imprinted polymers. Patent WO2011067563

Piletsky, S.A., Mijangos, I., Guerreiro, A., Piletska, E.V., Chianella, I., Karim, K., Turner, A.P.F., 2005. Polymer cookery: influence of polymerization time and different initiation conditions on performance of molecularly imprinted polymers. Macromolecules. 38, 1410-1414

Piletsky, S.A., Piletska, E.V., Karim, K., Freebairn, K.W., Legge, C.H., Turner, A.P.F., 2002. Polymer cookery: influence of polymerization conditions on the performance of molecularly imprinted polymers. Macromolecules. 35, 7499-7504

Piletsky, S.A., Piletska, E.V., Sergeyeva, T.A., Nicholls, I.A., Weston, D., Turner, A.P.F., 2006. Synthesis of biologically active molecules by imprinting polymerisation. Biopolym. Cell. 22, 63-67

Piletsky, S.A., Turner, A., 2006. A new generation of chemical sensors based on MIPs, in: Piletsky, S.A., Turner, A. (Eds.), Molecular imprinting of polymers. Eurekah.com/Landes Bioscience, Georgetown, USA, 64-79

Piletsky, S.A., Turner, A.P.F., 2008. Imprinted polymers and their application in optical sensors, in: Ligler, F.S., Rowe Taitt, C.A. (Eds.), Optical biosensors: today and tomorrow. Elsevier Science, B.V., Hungary, 543-581

Piperno, S., Tse Sum Bui, B., Haupt, K., Gheber, L.A., 2011. Immobilization of molecularly imprinted polymer nanoparticles in electrospun poly(vinyl alcohol) nanofibers. Langmuir. 27, 1547-1550

Polyakov, M.V., 1931. Adsorption properties and structure of silica gel. Zhur. Fiz. Khim. 2, 799-805

Priego-Capote, F., Ye, L., Shakil, S., Shamsi, S.A., Nilsson, S., 2008. Monoclonal behavior of molecularly imprinted polymer nanoparticles in capillary electrochromatography. Anal. Chem. 80, 2881-2887

Puoci, F., Iemma, F., Muzzalupo, R., Spizzirri, U.G., Trombino, S., Cassano, R., Picci, N., 2004. Spherical molecularly imprinted polymers (SMIPs) via a novel precipitation polymerization in the controlled delivery of sulfasalazine. Macromol. Biosci. 4, 22-26

Qu, P., Lei, J., Zhang, L., Ouyang, R., Ju, H., 2010. Molecularly imprinted magnetic nanoparticles as tunable stationary phase located in microfluidic channel for enantioseparation. J. Chromatogr. A. 1217, 6115-6121

Reimhult, K., Yoshimatsu, K., Risveden, K., Chen, S., Ye, L., Krozer, A., 2008. Characterization of QCM sensor surfaces coated with molecularly imprinted nanoparticles. Biosens. Bioelectron. 23, 1908-1914

RNCOS, 2011. Global in vitro diagnostic market analysis. Rncos.com, Noida, India, 1-130

Rocha, C., Gonçalves, M.P., Teixeira, J.A., 2005. Trypsin immobilisation on zeolites, in: CHEMPOR 2005 – 9th International Chemical Engineering Conference. Coimbra, 972-8055

Roque, A.C.A., Lowe, C.R., Taipa, M.Â, 2004. Antibodies and genetically engineered related molecules: production and purification. Biotechnol. Prog. 20, 639-654

Rosengren-Holmberg, J.P., Karlsson, J.G., Svenson, J., Andersson, H.S., Nicholls, I.A., 2009. Synthesis and ligand recognition of paracetamol selective polymers: Semi-covalent versus non-covalent molecular imprinting. Org. Biomol. Chem. 7, 3148-3155

Rückert, B., Hall, A.J., Sellergren, B., 2002. Molecularly imprinted composite materials via iniferter-modified supports. J. Mater. Chem. 12, 2275-2280

Ruigrok, V.J.B., Levisson, M., Eppink, M.H.M., Smidt, H., Van Der Oost, J., 2011. Alternative affinity tools: more attractive than antibodies? Biochem. J. 436, 1-13

Schirhagl, R., Latif, U., Dickert, F.L., 2011. Atrazine detection based on antibody replicas. J. Mater. Chem. 21, 14594-14598

Schirhagl, R., Latif, U., Podlipna, D., Blumenstock, H., Dickert, F.L., 2012. Natural and biomimetic materials for the detection of insulin. Anal. Chem. 84, 3908-3913

Schirhagl, R., Lieberzeit, P.A., Dickert, F.L., 2010. Chemosensors for viruses based on artificial immunoglobulin copies. Adv. Mater. 22, 2078-2081

Schweitz, L., Spegel, P., Nilsson, S., 2000. Molecularly imprinted microparticles for capillary electrochromatographic enantiomer separation of propranolol. Analyst. 125, 1899-1901

Sellergren, B., Andersson, L., 1990. Molecular recognition in macroporous polymers prepared by a substrate analogue imprinting strategy. J. Org. Chem. 55, 3381-3383

Sellergren, B., Hall, A.J., 2000. Chapter 2 Fundamental aspects on the synthesis and characterisation of imprinted network polymers, in: Sellergren, B. (Ed.), Molecularly Imprinted Polymers: Man-Made Mimics of Antibodies and their Applications in Analytical Chemistry, Vol. 23. Elsevier, Amsterdam, Netherlands, 21-57

Sener, G., Ozgur, E., Yilmaz, E., Uzun, L., Say, R., Denizli, A., 2010. Quartz crystal microbalance based nanosensor for lysozyme detection with lysozyme imprinted nanoparticles. Biosens. Bioelectron. 26, 815-821

Sener, G., Uzun, L., Say, R., Denizli, A., 2011. Use of molecular imprinted nanoparticles as biorecognition element on surface plasmon resonance sensor. Sens. Actuators, B Chem. 160, 791-799

Sergeyeva, T.A., Slinchenko, O.A., Gorbach, L.A., Matyushov, V.F., Brovko, O.O., Piletsky, S.A., Sergeeva, L.M., Elska, G.V., 2010. Catalytic molecularly imprinted polymer membranes: development of the biomimetic sensor for phenols detection. Anal. Chim. Acta. 659, 274-279

Servant, A., Haupt, K., Resmini, M., 2011. Tuning molecular recognition in water-soluble nanogels with enzyme-like activity for the Kemp elimination. Chem. Eur. J. 17, 11052-11059

Shamsipur, M., Besharati-Seidani, A., Fasihi, J., Sharghi, H., 2010. Synthesis and characterization of novel ion-imprinted polymeric nanoparticles for very fast and highly selective recognition of copper(II) ions. Talanta. 83, 674-681

Shen, X., Ye, L., 2011. Interfacial molecular imprinting in nanoparticle-stabilized emulsions. Macromolecules. 44, 5631-5637

Sheng, H., Ye, B.-C., 2009. Different strategies of covalent attachment of oligonucleotide probe onto glass beads and the hybridization properties. Appl. Biochem. Biotechnol. 152, 54-65

Shiomi, T., Matsui, M., Mizukami, F., Sakaguchi, K., 2005. A method for the molecular imprinting of hemoglobin on silica surfaces using silanes. Biomaterials. 26, 5564-5571

Shukla, A.A., Thömmes, J., 2010. Recent advances in large-scale production of monoclonal antibodies and related proteins. Trends Biotechnol. 28, 253-261

Sidhu, S.S., Koide, S., 2007. Phage display for engineering and analyzing protein interaction interfaces. Curr. Opin. Struct. Biol. 17, 481-487

Silvestri, D., Borrelli, C., Giusti, P., Cristallini, C., Ciardelli, G., 2005. Polymeric devices containing imprinted nanospheres: A novel approach to improve recognition in water for clinical uses. Anal. Chim. Acta. 542, 3-13

Small, P.M., Chambers, H.F., 1990. Vancomycin for *Staphylococcus aureus* endocarditis in intravenous drug users. Antimicrob. Agents Chemother. 34, 1227-1231

Smith, P.K., Krohn, R.I., Hermanson, G.T., 1985. Measurement of protein using bicinchoninic acid. Anal. Biochem. 150, 76-85

Spégel, P., Nilsson, S., 2002. A new approach to capillary electrochromatography: disposable molecularly imprinted nanoparticles. Am. Lab. 34, 29-33

Spégel, P., Schweitz, L., Nilsson, S., 2003. Selectivity toward multiple predetermined targets in nanoparticle capillary electrochromatography. Anal. Chem. 75, 6608-6613

Steinmeyer, D.E., McCormick, E.L., 2008. The art of antibody process development. Drug Discov. Today. 13, 613-618

Stoltenburg, R., Reinemann, C., Strehlitz, B., 2007. SELEX-A (r)evolutionary method to generate high-affinity nucleic acid ligands. Biomol. Eng. 24, 381-403

Suedee, R., Jantarat, C., Lindner, W., Viernstein, H., Songkro, S., Srichana, T., 2010. Development of a pH-responsive drug delivery system for enantioselective-controlled delivery of racemic drugs. J. Control. Release. 142, 122-131

Sulitzky, C., Rückert, B., Hall, A.J., Lanza, F., Unger, K., Sellergren, B., 2002. Grafting of molecularly imprinted polymer films on silica supports containing surface-bound free radical initiators. Macromolecules. 35, 79-91

Sun, F., Ma, W., Xu, L., Zhu, Y., Liu, L., Peng, C., Wang, L., Kuang, H., Xu, C., 2010. Analytical methods and recent developments in the detection of melamine. TrAC Trends Anal. Chem. 29, 1239-1249

Suriyanarayanan, S., Cywinski, P.J., Moro, A.J., Mohr, G.J., Kutner, W., 2012. Chemosensors based on molecularly imprinted polymers, in: Haupt K. (Ed.), Molecular Imprinting. Springer-Verlag Berlin Heidelberg, London, UK, 165-266

Surugiu, I., Danielsson, B., Ye, L., Mosbach, K., Haupt, K., 2001. Chemiluminescence imaging ELISA using an imprinted polymer as the recognition element instead of an antibody. Anal. Chem. 73, 487-491

Surugiu, I., Ye, L., Yilmaz, E., Dzgoev, A., Danielsson, B., Mosbach, K., Haupt, K., 2000. An enzyme-linked molecularly imprinted sorbent assay. Analyst. 125, 13-16

Svenson, J., Nicholls, I.A., 2001. On the thermal and chemical stability of molecularly imprinted polymers. Anal. Chim. Acta. 435, 19-24

Sylvestre, P., Couture-Tosi, E., Mock, M., 2002. A collagen-like surface glycoprotein is a structural component of the Bacillus anthracis exosporium. Mol. Microbiol. 45, 169-178

Szenczi, A., Kardos, J., Medgyesi, G.A., Závodszky, P., 2006. The effect of solvent environment on the conformation and stability of human polyclonal IgG in solution. Biologicals. 34, 5-14

Tan, C.J., Tong, Y.W., 2007. Molecularly imprinted beads by surface-imprinting. Anal. Bioanal. Chem. 389, 369-376

Titirici, M.M., Hall, A.J., Sellergren, B., 2002. Hierarchically imprinted stationary phases: mesoporous polymer beads containing surface-confined binding sites for adenine. Chem. Mater. 14, 21-23

Titirici, M.M., Sellergren, B., 2004. Peptide recognition via hierarchical imprinting. Anal. Bioanal. Chem. 378, 1913-1921

Tokonami, S., Shiigi, H., Nagaoka, T., 2009. Review: micro- and nanosized molecularly imprinted polymers for high-throughput analytical applications. Anal. Chim. Acta. 641, 7-13

Umpleby II, R.J., Bode, M., Shimizu, K.D., 2000. Measurement of the continuous distribution of binding sites in molecularly imprinted polymers. Analyst. 125, 1261-1265

Urraca, J.L., Moreno-Bondi, M.C., Orellana, G., Sellergren, B., Hall, A.J., 2007. Molecularly imprinted polymers as antibody mimics in automated on-line fluorescent competitive assays. Anal. Chem. 79, 4915-4923

Vaihinger, D., Landfester, K., Kräuter, I., Brunner, H., Tovar, G.E.M., 2002. Molecularly imprinted polymer nanospheres as synthetic affinity receptors obtained by miniemulsion polymerisation. Macromol. Chem. Phys. 203, 1965-1973

Van Herk, A.M., Monteiro, M., 2003. Heterogeneous systems, in: Matyjaszewski, K., Davis, T.P. (Eds.), Handbook of radical polymerization. John Wiley & Sons, Inc., Hoboken, USA, 301-332

Wang, X., Ding, X., Zheng, Z., Hu, X., Cheng, X., Peng, Y., 2006. Magnetic molecularly imprinted polymer particles synthesized by suspension polymerization in silicone oil. Macromol. Rapid Commun. 27, 1180-1184

Wang, X., Wang, L., He, X., Zhang, Y., Chen, L., 2009. A molecularly imprinted polymer-coated nanocomposite of magnetic nanoparticles for estrone recognition. Talanta. 78, 327-332

Welhouse, G.J., Bleam, W.F., 1993. Cooperative hydrogen bonding of atrazine. Environ. Sci. Technol. 27, 500-505

Whitcombe, M.J., 2012. Database statistics – All Items. Mipdatabase.com (http://mipdatabase.com/all_items.php). Date accessed: 25th October 2012

Whitcombe, M.J., Chianella, I., Larcombe, L., Piletsky, S.A., Noble, J., Porter, R., Horgan, A., 2011. The rational development of molecularly imprinted polymer-based sensors for protein detection. Chem. Soc. Rev. 40, 1547-1571

Whitcombe, M.J., Rodriguez, M.E., Villar, P., Vulfson, E.N., 1995. A new method for the introduction of recognition site functionality into polymers prepared by molecular imprinting: synthesis and characterization of polymeric receptors for cholesterol. J. Am. Chem. Soc. 117, 7105-7111

Wu, N., Feng, L., Tan, Y., Hu, J., 2009. An optical reflected device using a molecularly imprinted polymer film sensor. Anal. Chim. Acta. 653, 103-108

Wulff, G., 1982. Selective binding to polymers via covalent bonds. The construction of chiral cavities as specific receptor sites. Pure Appl. Chem. 54, 2093-2102

Wulff, G., Chong, B.-O., Kolb, U., 2006. Soluble single-molecule nanogels of controlled structure as a matrix for efficient artificial enzymes. Angew. Chem. Int. Ed. 45, 2955-2958

Wulff, G., Sarhan, A., 1972. The use of polymers with enzyme-analogous structures for the resolution of racemates. Angew. Chem. Int. Ed. 11, 341

Yan, M., 2002. Molecularly imprinted polymers as antibody mimics: applications in immunoassays and recent developments. J. Clin. Ligand Assay. 25, 234-236

Yang, H.-H., Zhang, S.-Q., Tan, F., Zhuang, Z.-X., Wang, X.-R., 2005. Surface molecularly imprinted nanowires for biorecognition. J. Am. Chem. Soc. 127, 1378-1379

Yang, K., Berg, M.M., Zhao, C., Ye, L., 2009. One-pot synthesis of hydrophilic molecularly imprinted nanoparticles. Macromolecules. 42, 8739-8746

Yao, Q., Zhou, Y., 2009. Surface functional imprinting of bensulfuron-methyl at surface of silica nanoparticles linked by silane coupling agent. J. Inorg. Organomet. Polym. Mater. 19, 215-222

Yaqub, S., Latif, U., Dickert, F.L., 2011. Plastic antibodies as chemical sensor material for atrazine detection. Sens. Actuators, B Chem. 160, 227-233

Ye, L., Cormack, P.A.G., Mosbach, K., 2001. Molecular imprinting on microgel spheres. Anal. Chim. Acta. 435, 187-196

Ye, L., Cormack, P.A.G., Mosbach, K., 1999. Molecularly imprinted monodisperse microspheres for competitive radioassay. Anal. Commun. 36, 35-38

Ye, L., Mosbach, K., 2008. Molecular imprinting: synthetic materials as substitutes for biological antibodies and receptors. Chem. Mater. 20, 859-868

Ye, L., Mosbach, K., 2002. Molecularly imprinted materials: towards the next generation. Mater. Res. Soc. Symp. Proc. 723, 51-59

Ye, L., Mosbach, K., 2001. Polymers recognizing biomolecules based on a combination of molecular imprinting and proximity scintillation: a new sensor concept. J. Am. Chem. Soc. 123, 2901-2902

Ye, L., Surugiu, I., Haupt, K., 2002. Scintillation proximity assay using molecularly imprinted microspheres. Anal. Chem. 74, 959-964

Ye, L., Weiss, R., Mosbach, K., 2000. Synthesis and characterization of molecularly imprinted microspheres. Macromolecules. 33, 8239-8245

Ye, L., Yoshimatsu, K., Kolodziej, D., Da Cruz Francisco, J., Dey, E.S., 2006. Preparation of molecularly imprinted polymers in supercritical carbon dioxide. J Appl. Polym. Sci. 102, 2863-2867

Yilmaz, E., Haupt, K., Mosbach, K., 2000. The use of immobilized templates - A new approach in molecular imprinting. Angew. Chem. Int. Ed. 39, 2115-2118

Yoshimatsu, K., Reimhult, K., Krozer, A., Mosbach, K., Sode, K., Ye, L., 2010. Corrigendum to "Uniform molecularly imprinted microspheres and nanoparticles prepared by precipitation polymerization: the control of particle size suitable for different analytical applications" [Anal. Chim. Acta 584 (2007) 112-121] (DOI:10.1016/j.aca.2006.11.004). Anal. Chim. Acta. 657, 215

Yoshimatsu, K., Reimhult, K., Krozer, A., Mosbach, K., Sode, K., Ye, L., 2007. Uniform molecularly imprinted microspheres and nanoparticles prepared by precipitation polymerization: the control of particle size suitable for different analytical applications. Anal. Chim. Acta. 584, 112-121

Yoshimatsu, K., Ye, L., Lindberg, J., Chronakis, I.S., 2008. Selective molecular adsorption using electrospun nanofiber affinity membranes. Biosens. Bioelectron. 23, 1208-1215

Zeng, Z., Hoshino, Y., Rodriguez, A., Yoo, H., Shea, K., 2010. Synthetic polymer nanoparticles with antibody-like affinity for a hydrophilic peptide. ACS nano. 4, 199-204

Zheng, X., Tu, W., Fan, R., 2009. Preparation of molecularly imprinted polymer films on monodisperse macromolecular beads. J. Appl. Polym. Sci. 113, 2620-2627

Zhou, W.-H., Lu, C.-H., Guo, X.-C., Chen, F.-R., Yang, H.-H., Wang, X.-R., 2010. Mussel-inspired molecularly imprinted polymer coating superparamagnetic nanoparticles for protein recognition. J. Mater. Chem. 20, 880-883

Zhu, R., Zhao, W., Zhai, M., Wei, F., Cai, Z., Sheng, N., Hu, Q., 2010. Molecularly imprinted layer-coated silica nanoparticles for selective solid-phase extraction of bisphenol A from chemical cleansing and cosmetics samples. Anal. Chim. Acta. 658, 209-216

Zimmerman, S.C., Wendland, M.S., Rakow, N.A., Zharov, I., Suslick, K.S., 2002. Synthetic hosts by monomolecular imprinting inside dendrimers. Nature. 418, 399-403

Zourob, M., Mohr, S., Mayes, A.G., Macaskill, A., Pérez-Moral, N., Fielden, P.R., Goddard, N.J., 2006. A micro-reactor for preparing uniform molecularly imprinted polymer beads. Lab Chip Miniaturisation Chem. Biol. 6, 296-301